UNIVERSITY OF Hull

Identification and Functional Characterisation of Putative Mitochondrial Nucleotide Transporters from the Human Pathogen *Trypanosome brucei*

Thesis submitted for the Degree of Doctor of Philosophy
In biomedical sciences
The University of Hull

By,
Mohammed Alshegifi
201113497
Decamber 2018

Acknowledgement

Throughout the entire project, I have experienced many setbacks and problems, which I would not have been able to overcome without the help of many people. I would like to express my gratitude to them.

First, I would like to thank God (Allah) almighty for giving me the patience and ability to complete this thesis, for, without his help, I would not have been able to do it. I also extend my deepest thanks to my principle supervisor, Dr Frank Voncken, for the effort, assistance and advice he has done throughout my studies without getting bored of the many tasks. He is the one that brought me to this research, and he has all of my respect and appreciation. I also would like to express my thanks to my second supervisor, Professor John Greenman, for his help, advice and comments on the entire work. I also extend my thanks to both Dr Cordula, Fuli Zheng and Yahya Madkhali for assisting me in my research.

Also, thanks to my beloved family, who involves Dad and Mum, dear wife Hanan, three sons Mosa, Talal and Sami, and daughter Danah, for their support, assistance and patience throughout the study. They have all my love, appreciation and respect.

Last but not least, thanks to the Ministry of Education of the Kingdom of Saudi Arabia for financially supporting me to complete my study.

Abstract

Trypanosoma brucei is a medically important protozoan parasite that causes African sleeping sickness in humans. Although disease treatment is possible, it is hindered by the limited availability of effective drugs and the rapid emergence of drug resistance. It is, therefore, important to identify novel drug targets for the development of new, more effective drugs.

Mitochondrial carrier family (MCF) proteins transport a wide range of key metabolites across the mitochondrial inner membrane. They are important for the maintenance of key metabolic pathways in all eukaryotic cells. In particular, the MCF proteins that have been implicated in mitochondrial adenosine triphosphate (ATP) import appear to be essential for cell function and survival due to their roles in defence against oxidative stress and in the provision of the ATP required for mitochondrial electron transport and associated ATP production. Based on their important physiological roles, mitochondrial nucleotide transporters are potential novel drug targets.

The main aim of this thesis was to identify and functionally characterise the putative mitochondrial nucleotide transporters in *T. brucei*. Sequence analysis revealed that the *T. brucei* genome contains 5 MCF proteins: TbMCP1, TbMCP15, TbMCP16, TbMCP20 and TbMCP23. The proteins were predicted to have roles in mitochondrial nucleotide transport based on their homology to functionally characterised MCF proteins that transport nucleotides. Of these TbMCPs, TbMCP1 has the highest sequence similarity to functionally characterised mitochondrial flavin carriers and peroxisomal ATP/adenosine monophosphate carriers in other eukaryotes, such as Flx1 in *Saccharomyces cerevisiae*. Sequence analysis further predicted that TbMCP15 and TbMCP16 were closely related to mitochondrial adenosine diphosphate (ADP/ATP) transporters, such as AAC2 in *S. cerevisiae*, whereas TbMCP20 appeared to be closely related to mitochondrial S-adenosylmethionine transporters, such as SAM5 in *S. cerevisiae,* and TbMCP23 appeared to be closely related to mitochondrial pyrimidine transporters, such as *S. cerevisiae* RIM2.

Immunofluorescence microscopy was used to detect tagged recombinant TbMCP1, TbMCP15 and TbMCP20 and/or polyclonal antibodies were raised against these proteins. All of the putative nucleotide transporters localised exclusively to the *T. brucei* mitochondrion, which supported the hypothesis that they perform mitochondrial transport functions.

RNA interference was used to knock down the expression of the TbMCPs to investigate their effects on cell survival and growth. The expression of TbMCP1, TbMCP15, TbMCP16 and TbMCP20 was essential for trypanosome survival, whereas knockdown of TbMCP23 did not result in a growth phenotype in *T. brucei*. These results indicated that TbMCP1, TbMCP15, TbMCP16 and TbMCP20 fulfil key roles in the transport of essential metabolites, whereas TbMCP23 plays a less important transport role or is redundant with other MCF proteins.

The putative transport functions of the TbMCPs were investigated by (1) functional complementation studies using specific *S. cerevisiae* deletion strains lacking specific MCF proteins and (2) mitochondrial ATP production assays in mitochondria isolated from wildtype and MCF protein knockdown *T. brucei* cell lines. Functional complementation studies in the *S. cerevisiae* deletion strain Δ JL1 2 3u revealed that TbMCP15 expression restored the growth of the strain on the non-fermentable carbon source glycerol. In addition, mitochondrial ATP production assays revealed that TbMCP15-depleted *T. brucei* mitochondria was able to produce ATP from oxoglutarate. These results confirmed that TbMCP15 most likely functions as an ADP/ATP transporter in *T. brucei*.

A similar approach was used to investigate the function of TbMCP20. Functional complementation studies in the *S. cerevisiae* deletion strain ΔSAM5 revealed that TbMCP20 expression restored the growth of this strain, which confirmed that TbMCP20 most likely functions as a mitochondrial s-adenosylmethionine transporter in *T. brucei*.

Unfortunately, the same investigative approach was not feasible for TbMCP1 and TbMCP23. There are no suitable *S. cerevisiae* deletion strains with detectable phenotypes and both TbMCPs have extremely low or non-detectable expression levels. However, experiments revealed that metabolic flux measured as substrate (glucose and proline) consumption and product (acetate, succinate and pyruvate) formation, was substantially increased in the TbMCP1 knockdown compared to the WT *T. brucei* cell line. These results suggested that TbMCP1 plays a key role in *T. brucei* energy metabolism. The potential role of TbMCP1 in mitochondrial nucleotide transport remains to be determined. Five potential mitochondrial nucleotide transporters have been identified in *T. brucei*: TbMCP1, TbMCP15, TbMCP16,

TbMCP20 and TbMCP23. Of the identified transporters, TbMCP15 was confirmed to function as a mitochondrial ATP/ADP transporter and TbMCP20 was shown to function as a mitochondrial s-adenosylmethionine transporter, based on their abilities to restore the growth of transporter-deficient yeast strains on non-fermentative carbon sources. Further research will be required to determine the specific mitochondrial transport functions of the remaining candidates. These findings provide vital information about mitochondrial metabolite transport in *T. brucei* and provide a solid foundation for future novel drug development.

Table of Contents

Abbreviations

ADP	Adenosine Diphosphate
AMP	Adenosine Monophosphate
ASCT	Acetate: succinate CoA Transferase
ATP	Adenosine Triphosphate
BLA	Blasticidin
BSF	Bloodstream Form
PCF	Procyclic Form
CP I II III	Contact Points I,II and III
DAPI	4,6-diamidino-2-phenylindole
DIC	Dicarboxylate-Tricarboxylate Carrier
ECL	Enhanced Chemiluminiscence
FCS	Foetal Calf Serum
HAT	Human African Trypanosoma
HYG	Hygromycin
IB	Inclusion Bodies
IFA	Immunofluorescence Microscopy
IPTG	Isopropyl-beta-D-thiogalactopyranoside
KO	Knockout
LB	Luria-Bertani Medium
MCF	Mitochondria Carrier Family
MCP	Mitochondria Carrier Protein
MCS	Multiple Cloning Site
MEM-Pros	Minimum Essential Medium with P
mRNA	Messenger RNA

MTP	Mitochondrial Transition Pore
MW	Molecular Weight
mtDNA	Mitochondrial Deoxyribonucleic Acid
NAD+	Nicotinamide Adenine Dinucleotide
NADP+	Nicotinamide Adenine Dinucleotide Phosphate Oxidize
NADPH	Nicotinamide Adenine Dinucleotide Phosphate Reduced
Ni-NTA	Nickel-Nitiloacetic Acid
OD	Optical Density
ORF	Open Reading Frame
PBS	Phosphate Buffer Saline
PCR	Polymerase Chain Reaction
PEP	Phosphoenolpyruvate
RNAi	Ribonucleic Acid Interference
SDS	Sodium Dodecyl Sulphate
SDS-PAGE	Polyacrylamide Gel Electrophoresis
SoTE	Sorbitol Tris EDTA buffer
TCA	Tricarboxylic Acid
TET	Tetracycline
VSG	Variant Surface Protein
WT	Wild Type
WB	Western Blot

Chapter 1: Introduction

1.1 *Trypanosoma brucei* and African sleeping sickness

The parasite *Trypanosoma brucei* belongs to the order Kinetoplastida in the phylum Protozoa (Moreira *et al*., 2004; Alvar *et al*., 2012). The kinetoplast, a large network of specialised mitochondrial DNA, is the characteristic feature of the organism (Stuart *et al*., 2008). Mammals can be infected by three subspecies of *T. brucei* (Sutherland *et al*., 2015): *T. b. gambiense*, which causes a chronic disorder that mostly affects individuals in Central and West Africa; *T. b. rhodesiense*, which causes East African sleeping sickness, a more acute disorder with greater virulence (Sutherland *et al*., 2015); and *T. b. brucei,* the subspecies present in most of sub-Saharan Africa, which cannot infect humans because it is susceptible to lysis by trypanosome lytic factor in the serum. *T. b. brucei* typically causes a wasting disease in vertebrate animals (Sutherland *et al*., 2015). The three subspecies of *T. brucei* are transmitted by the tsetse fly, which is commonly found in savannah and woodland regions. Around 50,000–70,000 infections occurred annually in Africa until 2005. However, the number of new cases dropped to fewer than 10,000 in 2010, then to 2,804 cases in 2015, due to the efforts of the World Health Organization (WHO), which now provides anti-trypanosoma medicines free of charge in endemic countries (WHO, 2017).

Human African trypanosomiasis (HAT), or sleeping sickness, can be divided into two stages or phases: the haemolymphatic stage, followed by meningoencephalitis. The first phase involves the multiplication of the parasite in the spinal fluid, lymph and blood, thereby causing extreme fatigue, muscle and joint pain, headache and fever (Barrett *et al*., 2003; Rodgers, 2009). The second phase involves the invasion of the central nervous system by the parasite after it crosses the blood–brain barrier. Patients experience extreme disturbances in their circadian rhythms, characterised by increased somnolence, which can lead to unconsciousness and coma. The disease can cause death in the absence of the necessary treatment (Stich *et al*., 2002; Kennedy, 2006; Jamonneau *et al*., 2012).

1.2 Morphology of *T. brucei*

T. brucei is a motile, unicellular, eukaryotic organism. As shown in Figure 1.1, *T. brucei* contain the main organelles found in eukaryotic cells, such as mitochondria, Golgi bodies, endoplasmic reticulum and a nucleus (Engstler *et al*, 2004). A single flagellum, linked to the body of the cell via an undulating membrane, is responsible for its motility. The flagellum originates from the flagellar pocket, which is located near the kinetoplast. The kinetoplast, a unique structure comprising mitochondrial DNA, is a characteristic feature of the organisms

of the order Kinetoplastida (Engstler *et al* , 2004). *T. brucei* also contain a glycosome, which is a peroxisome-like microbody responsible for the glycolytic and pentose phosphate pathways, β-oxidation of fatty acids, purine salvage and the biosynthesis of pyrimidines (Parsons *et al*., 2001). Furthermore, the mitochondria of trypanosomatids possess extraordinary features (van Hellemond *et al*., 2005). Firstly, despite the fact that classically studied cells have 5 to 10,000 mitochondria per cell, trypanosomatids have only a single, large mitochondrion. Secondly, the DNA in a trypanosomatid has an atypical, highly concatenated structure because it is stored in kinetoplasts. The replication of kinetoplast DNA and mitochondrial division are linked to cell division (Gull, 2003). Another feature of *T. brucei* is the expression of variant surface glycoprotein (VSG) on the cell surface, which enables *T. brucei* to protect itself by antigenic variation. *T. brucei* can switch the type of VSG on its surface via the selective expression of VSG genes and pseudogenes (Hall *et al*., 2013). The parasites make use of VSG to prolong their circulation in the blood, thereby increasing the likelihood of transmission. VSG proteins are attached to the plasma membrane by glycosylphosphatidylinositol (GPI) (Hall *et al*., 2013). In insect vectors, the *T. brucei* surface coat includes procyclin (EP/GPEET), which provides protection against the hostile insect intestinal environment. In addition, transcription in kinetoplastid protoctista, accomplished via the trans-splicing of mRNA, differs from the paradigms of eukaryotic gene expression. *T. brucei* undergoes polycistronic transcription and its pre-mRNA molecules are spliced into individual mRNAs (Hall *et al*., 2013). Trans-splicing is a special form of RNA processing in which the ends of two primary RNA transcripts are joined. Trans-splicing was discovered by comparing the nucleotide sequences of the 5′ ends of VSG mRNAs with the corresponding coding genes. A 39-bp-long spliced leader RNA sequence (SL RNA) has been found in the first exon of the 5′ ends of mRNA molecules; it is processed by RNA polymerase II (Hall *et al*., 2013).

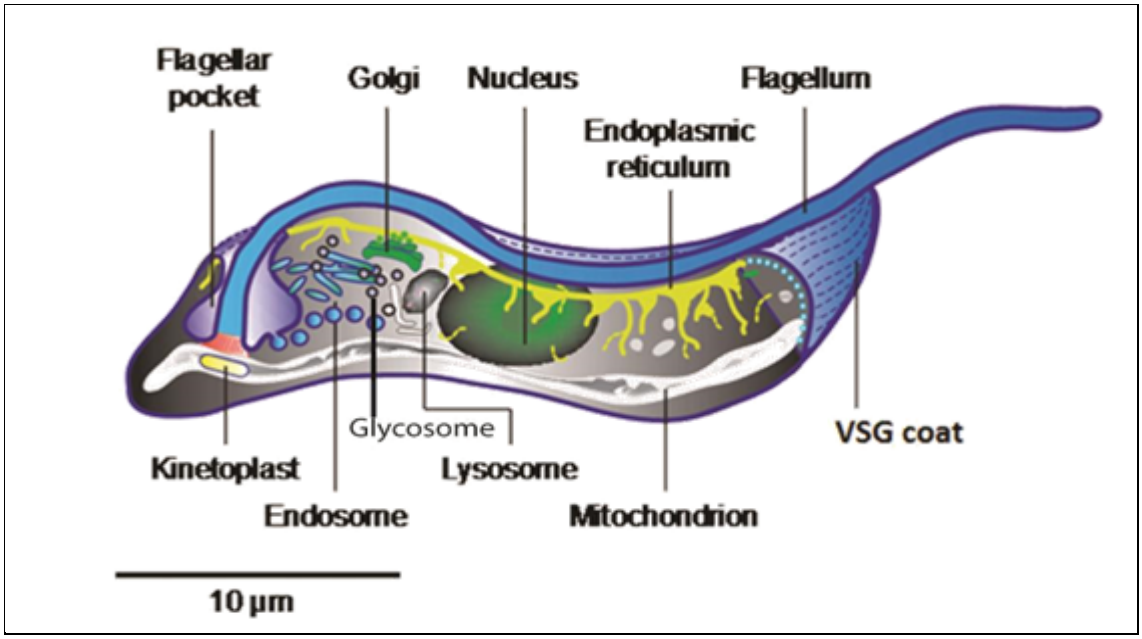

Figure 1.1. Schematic of the main organelles of *T. brucei.* (Engstler *et al,* 2004)

1.3 The life cycle of *T. brucei*

T. brucei has a complex life cycle during which it adapts to different environments in its hosts and vectors by adopting two replicative forms (Matthews *et al*., 2004; Vickerman, 1985). The bloodstream form (BSF) is found in mammalian blood and tissue fluids, whereas the procyclic form (PCF) is found in the midgut of the tsetse fly. *T. brucei* first infects the midgut of its vector in its dividing midgut form through a blood meal. Then, it migrates via the proventriculus to the salivary glands (Figure 1.2). This stage of its life cycle is known as the epimastigote. A fraction of the parasites differentiates into the infective metacyclic form, ready to be transferred upon insect bite into the bloodstream of mammalian species. The parasite undergoes a series of adaptations, from slender to intermediate to stumpy form, resulting in a stumpy form that is able to re-infect the fly vector after a blood meal (Figure 1.2). The slender form of *T. brucei*, but not the stumpy form, is able to proliferate (Matthews *et al*., 2004). At later stages of the infection, the parasite can infect the lymph and cerebrospinal fluid of mammalian hosts. Although uncommon, *T. brucei* can also be transmitted via the exchange of body fluids or blood. Some factors, like *cis*-aconitase (Matthews *et al*., 2004), can trigger the differentiation of trypanosomes from their BSF into their PCF *in vitro*.

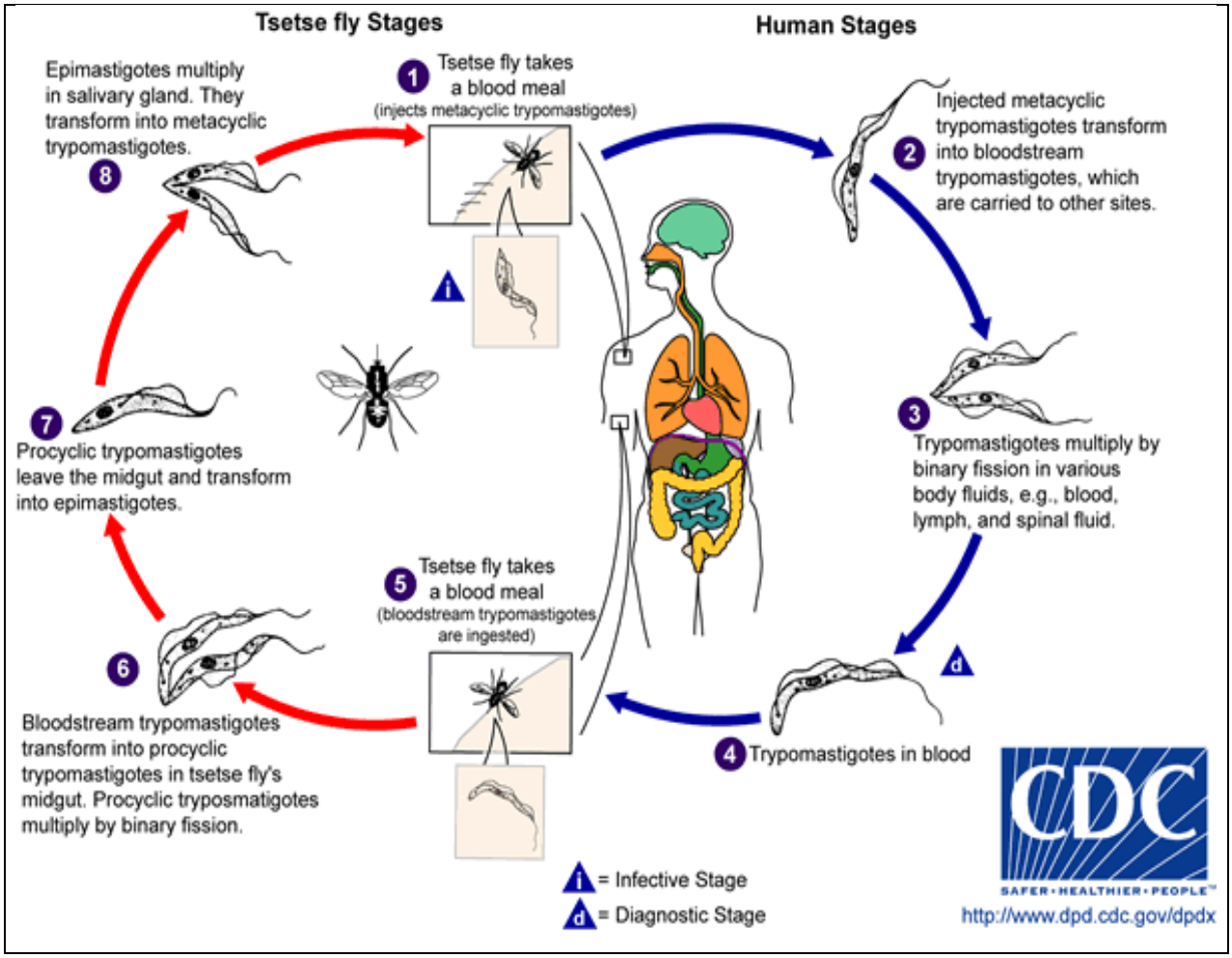

Figure 1.2. Life cycle of *T. brucei*. The cycle starts when an individual is bitten by an infected tsetse fly, allowing the metacyclic trypomastigote form of the parasite to enter the human blood. The non-dividing metacyclic forms differentiate into dividing trypomastigotes, which are taken up by another vector. Inside the midgut of the vector, the trypomastigotes differentiate into dividing procyclic trypomastigotes. These, in turn, convert to epimastigotes that travel to the salivary gland of the insect vector. Finally, the epimastigotes replicate and give rise to metacyclic trypomastigotes, which can be transmitted to human hosts (Centers for Disease Control and Prevention [CDC]: http://www.cdc.gov/parasites/sleepingsickness/biology.html).

1.4 Treatment of sleeping sickness

The strategy for treating sleeping sickness is determined by the infectious agent (i.e., *T. b. gambiense* or *T. b. rhodesiense*) and the stage of the disease (i.e., the haemolymphatic or neurological phase) (Kennedy, 2004; Barrett *et al.*, 2007; Rodgers, 2009). Eflornithine, nifurtimox, suramin, melarsoprol and pentamidine are currently used to treat the disease (Simarro *et al*., 2012). These drugs act against specific subspecies of the parasite in specific phases. Suramin has been utilised since the 1920s for treating acute East African sleeping sickness caused by *T. b. rhodesiense* (Simarro *et al.*, 2012). Pentamidine is effective against *T. b. gambiense*; it has been used since 1941 for the treatment of the first phase of West African sleeping sickness (Steverding., 2010). Although pentamidine can destroy *T. b. gambiense*, it has been associated with cases of intense, adverse neurological events (Simarro *et al*., 2012).

Melarsoprol can be used to treat the second phase of sleeping sickness caused by *T. b. rhodesiense* or *T. b. gambiense* as it is the only *T. brucei*-specific drug capable of crossing the blood–brain barrier. This organic arsenical-based drug has been used since 1949. However, it is also associated with intense adverse reactions, including tachycardia, convulsions, coma and heart failure, leading to a 5% mortality rate (Rodger *et al*., 2009; Steverding, 2010). The second phase of sleeping sickness caused by *T. b. gambiense* can be treated with eflornithine. However, the parasite is less susceptible to this drug than nifurtimox as eflornithine inhibits the ornithine carboxylase enzyme in the parasite and in humans. Furthermore, in humans, the turnover rate for eflornithine is greater than that in the parasite (Matovu *et al*., 2003). Nifurtimox can also be used to treat the second phase of *T. b. gambiense*-related sleeping sickness, but has been associated with adverse reactions in some cases. A combination of eflornithine and nifurtimox is effective against the second phase of *T. b. gambiense*-related disease (Alirol *et al*., 2013). However, the development of drug resistance by *T. brucei* has been reported (Matovu *et al*., 2003).Therefore, it is important and urgent to find new drug targets and drugs to continue the effective treatment of sleeping sickness.

1.5 *T. brucei* energy metabolism

Energy metabolism in trypanosomatids involves multiple subcellular compartments, including the glycosome, the mitochondrion and the cytosol. Glycosomes are found only in members of Kinetoplastea and *Diplonema* (Matthews *et al*., 2004) . They are microbody-like organelles that contain the majority of enzymes in the glycolytic pathway (Figure 1.3 and Table 1.1). Via 10 steps, glycolysis converts one molecule of glucose into two molecules of pyruvate, two molecules of adenosine triphosphate (ATP) and two molecules of reduced nicotinamide adenine dinucleotide (NADH). The compartmentalisation of glycolysis in glycosomes prevents metabolic interference by separating enzymes from cofactors, such as ATP and NADH (Matthews *et al*., 2004). Net ATP is not generated in the glycosome, but in the cytosol, when phosphoenolpyruvate is converted into pyruvate. Purine salvage also occurs in glycosomes.

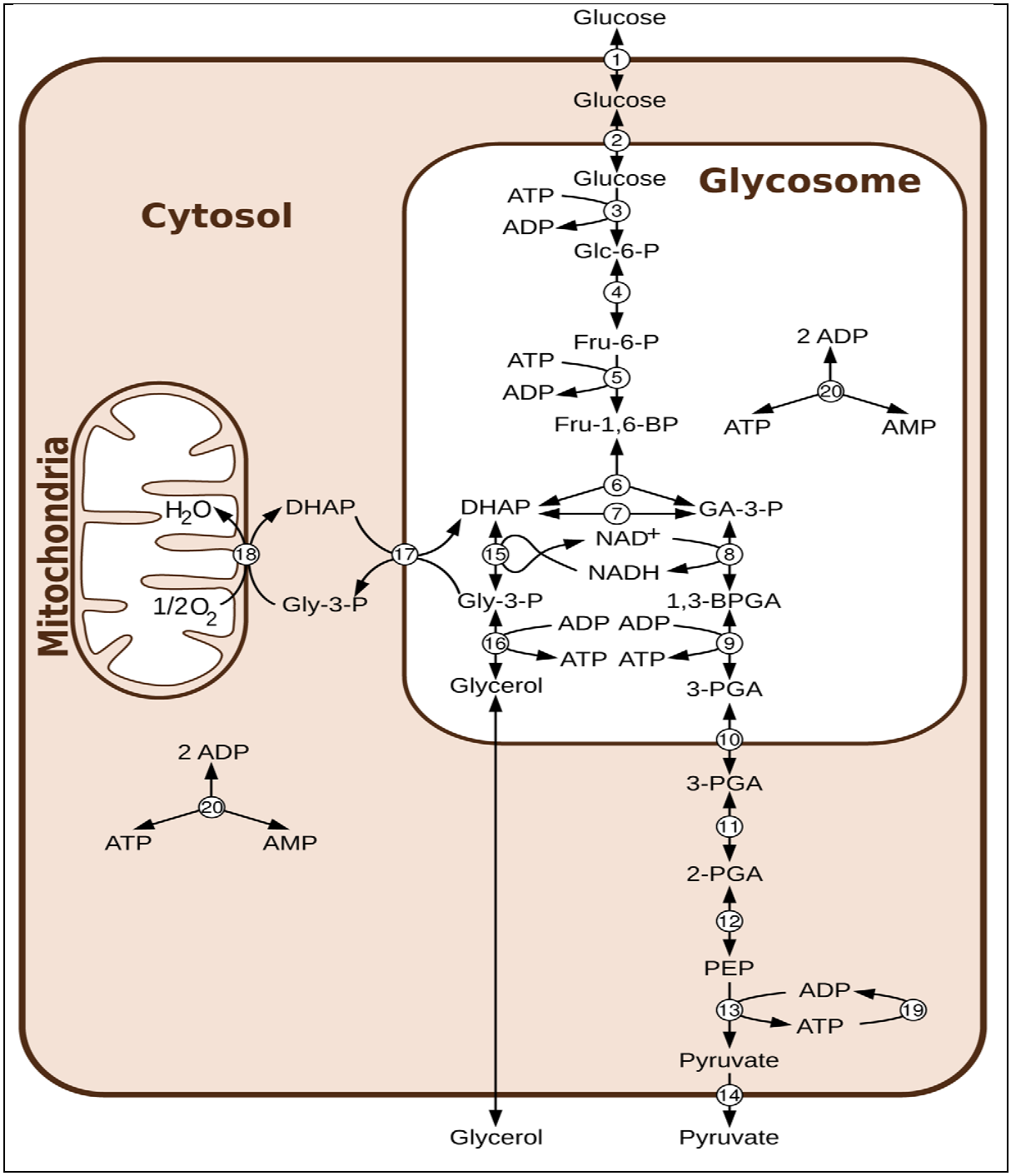

Figure 1.3. Energy metabolism in the BSF of *T. brucei*. Glc, glucose; TbHK, *T. brucei* hexokinase; G-6-P, glucose 6-phosphate; PGI, glucose-6-phosphate isomerase; F-6-P, Fructose-6-phosphate; PFK, phosphofructokinase; FBP, fructose 1,6-bisphosphate; ALD, aldolase; DHAP, dihydroxyacetone phosphate; GPDH, glycerol-3-phosphate dehydrogenase; GK, glycerol kinase; Gly-3-p, glycerol-3-phosphate; G-3-P, glyceraldehyde-3-phosphate; GAPDH, glyceraldehyde-3-phosphate dehydrogenase; 1,3-BPGA, 1,3-bisphosphoglycerate; PGK, phosphoglycerate kinase; 3-PGA, 3-phosphoglycerate; PGM, phosphoglycerate mutase; 2-PGA, 2-phosphoglycerate; ENO, enolase; PEP, phosphoenolpyruvate; PK, pyruvate kinase; PYR, pyruvate; TAO, trypanosome alternative oxidase; UQ, ubiquinone; GPD, glycerol-3-phosphate dehydrogenase (Vonder *et al*., 2009)

Table 1.1. The changes in metabolism during the life cycle of *T. brucei*. The PCF and BSF comprise the two stages of the T. brucei life cycle.

	PCF	**BSF**
Preferred nutrients	Proline and glucose	Glucose
Main secreted end products	Alanine, acetate and succinate	Pyruvate,Glycerol
Main pathways of ATP production	Oxidative phosphorylation and glycolysis	Glycolysis
Respiratory chain	Active	Inactive

There are multiple differences in the metabolic pathways utilised by the PCF and the BSF. In the transition between the forms, the parasite adapts its morphology, surface composition and metabolism (Matthews *et al*., 2004). In the *T. brucei* BSF, glucose is primarily metabolised to 3-phosphoglycerate (3-PGA) in glycosomes, then further degraded into the end product pyruvate in the cytosol (Gull, 2003). In the BSF, ATP is obtained only by substrate-level phosphorylation; mitochondria are notably smaller than in the PCF and lack key enzymes and components of the Krebs cycle (Opperdoes *et al*., 1977;; Clayton & Michels, 1996 Michels *et al*., 2000).

The *T. brucei* PCF has a more elaborate, net-like mitochondrion that can generate ATP both from the substrate level and via oxidative phosphorylation (Michels *et al*., 2000; Coustou *et al*., 2003; van Weelden *et al*., 2005). The NADH balance is maintained by the conversion of oxaloacetate into succinate in the glycosomes of PCF trypanosomes (Besteiro *et al*., 2002; Coustou *et al*., 2005). Nicotinamide adenine dinucleotide phosphate, on the other hand, is produced by the PCF from both malic enzymes and via the pentose phosphate pathway (Coustou *et al*., 2005). In the PCF, pyruvate, the end product of glycolysis, is not excreted but further metabolised in the mitochondrion, where it is degraded to acetate or succinate as ATP is generated (van Hellemond *et al*., 1998; Rivière *et al*., 2004). Testing the intracellular levels of components of the glycolytic and Krebs cycles in an aconitase-mutant strain revealed that Krebs cycle enzymes are present in the PCF; however, they are not used in the full cycle for energy generation, but for energy transduction (van Weelden *et al*., 2003).

The mitochondrial respiratory chain is essential for survival and growth (Figure 1.4 and Table 1.1). In addition to carbohydrate degradation, it is responsible for ATP generation via the oxidation of amino acids, especially proline and threonine (Lamour *et al*., 2005).

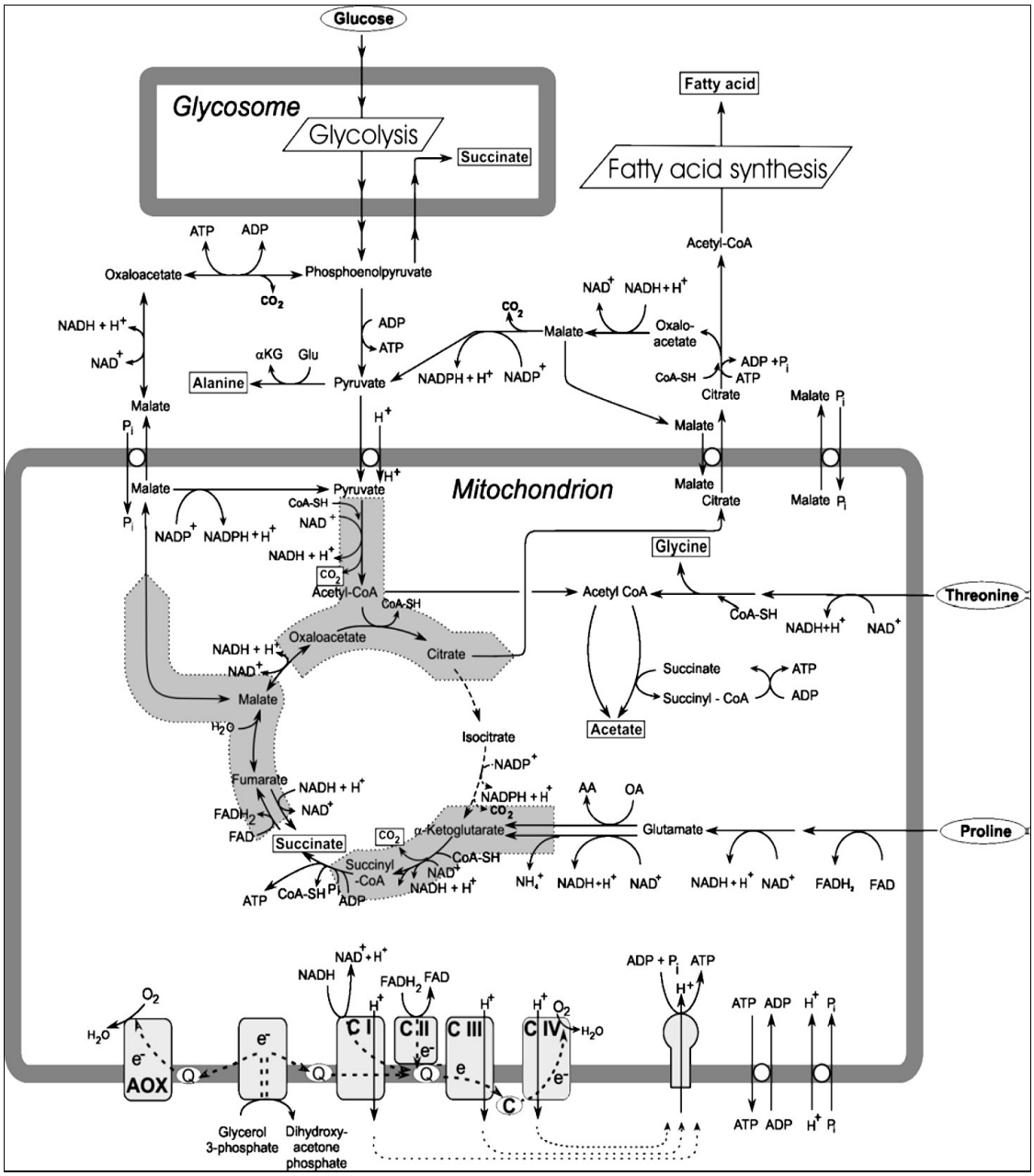

Figure 1.4. A schematic diagram of energy metabolism in the *T. brucei* PCF. Substrates are shown in ovals and end products in boxes. The broad, shaded arrows in the background of the citric acid cycle are active in the PCF. The broad, shaded arrow from pyruvate and oxaloacetate to citrate indicates the flux in this part of the citric acid cycle, which is used in the transport of acetyl-CoA units from the mitochondrion to the cytosol. The broad, shaded arrow from α-ketoglutarate to succinate represents the part of the cycle that degrades proline and glutamate to succinate. The broad, shaded arrow from succinate to malate indicates the part of the cycle that is used during gluconeogenesis. Abbreviations: AA, amino acid; CI, II, III and IV, complex I, II, III and IV of the respiratory chain; c, cytochrome c; Glu, glutamate; α-KG, α-ketoglutarate; OA, oxoacid; Q, ubiquinone (van Hellemond *et al*., 2005)

1.6 The mitochondria of *T. brucei*

Although the structure and function of the mitochondria in the PCF of *T. brucei* have been studied, the mitochondria of the BSF of the parasite are still under investigation (Rivière & Coustou, 2006; Schneider *et al.*, 2007; Stephens *et al.*, 2007; Panigrahi *et al.*, 2009). As it performs oxidative and substrate-level phosphorylation to produce ATP via the transfer of a phosphate ($-PO_3$) group to adenosine diphosphate (ADP), the mitochondrion of the procyclic parasite is a major supplier of ATP to the cell (Bringaud, Rivière & Coustou, 2006; Schneider *et al.*, 2007; Zikova *et al*., 2009). In addition to ATP generation, the mitochondria are responsible for carbohydrate metabolism, the pentose phosphate pathway and maintenance of the cellular redox balance (Bringaud, Barrett & Zilberstein, 2012). The mitochondrion in *T. brucei* is structurally identical to the mitochondria of other eukaryotes; it contains a mitochondrial outer membrane (MOM), a mitochondrial intermembrane space (IMS), a matrix and a mitochondrial inner membrane (MIM) (Panigrahi *et al*., 2008). The only difference is that there is only one tubular mitochondrion in each *T. brucei,* which resides along the whole length of the parasite. This elongated mitochondrion can change both structurally and functionally, depending on the environmental conditions in different hosts and on the presence of different substrates in each environment (Matthews, 2005; Bringaud, Rivière & Coustou, 2006; Fenn & Matthews, 2007). The *T. brucei* mitochondrion can form branches, leading to the formation of a cellular network. This process is dependent on the phase of the parasite life cycle (Schneider, 2001). In the case of the PCF of the parasite, most of its ATP is obtained from proline degradation and substrate-level and oxidative phosphorylation in the mitochondrion (Bochud-Allemann & Schneider, 2002; Schneider *et al.*, 2007; Bringaud, Barrett & Zilberstein, 2012). Van Hellemond *et al*. (2005) reported the existence of a functional respiratory chain, which includes complexes I to IV, in the mitochondrion; the chain sustains the cellular redox balance and produces ATP using ATP synthase. The cytochrome-independent oxidase of the mitochondrion electron transport chain (trypanosome alternative oxidase, or TAO) and the ATP synthase cooperate to sustain the redox balance inside the BCF (Deramchia *et al*., 2014). These are the only known functions of the mitochondrion in the BSF. It has been suggested that cytochrome c, the respiratory chain and the Krebs cycle are absent from the BSF mitochondrion and have no role in ATP generation (van Hellemond *et al*., 2005).

1.7 Mitochondrial carrier family proteins

Since the inner membrane of the mitochondrion is impermeable, specific transporters are needed to transfer metabolites across the membrane (Schneider *et al*., 2007). The majority of the transporters expressed in the inner membranes of mitochondria belong to the mitochondrial carrier family (MCF) (Nury *et al*., 2006). These proteins transport various metabolites, such as iron, protons, amino acids, carboxylic acids, phosphate and nucleotides (Palmieri, 2004; Palmieri *et al*., 2006; Kunji & Robinson, 2006; Colasante *et al*., 2009). Therefore, these proteins participate in the majority of mitochondrial metabolic processes and constitute a metabolic bridge between the cell and the mitochondrion (Palmieri, 2008; Kunji, 2004). MCF proteins have a characteristic, highly conserved structure comprising repeats of three homologous sequences. Their molecular masses range from 30–35 kDa (Millar & Heazlewood, 2003; Palmieri *et al*., 2006; Picault *et al*., 2004). Figure 1.5 shows the conserved structure of an MCF protein, which consists of six transmembrane (TM) helices that are linked to the two TM domains through a hydrophilic loop (Palmieri, 2004). Each odd-numbered hydrophilic loop (M1b, M2b and M3bA) contains the conserved MCF signature sequence motif PX[D/E]XX[K/R]X[K/R][20–30 residues][D/E]G[4–5 residues][W/F/Y][K/R]G, in which 'X' refers to any amino acid (Palmieri, 2004). Another conserved canonical motif is present at different substrate contact points downstream of the signature motifs (CPI, CPII and CPII; Figure 1.5).

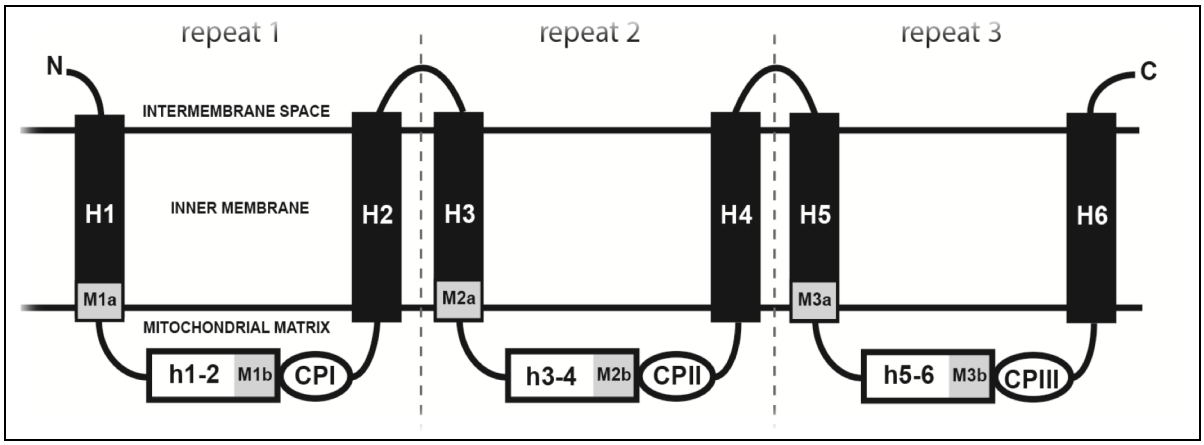

Figure 1.5. Schematic presentation of the conserved structure of MCF proteins. C, C-terminal; N, N-terminal; h, hydrophilic loop; H, transmembrane domain; M1-3a, first part of canonical signature sequence motif (PX[D/E]XX[K/R]X[K/R]); M1-3b, second part of canonical signature sequence motif ([D/E]G[4–5 residues][W/F/Y][K/R]G). (Adapted from Colasante *et al*., 2009)

To date, researchers have discovered more than 50 MCF proteins in plants and humans and approximately 30 MCF proteins in yeast (Palmieri *et al*., 2000; Picault *et al*., 2004; Wohlrab, 2006; Haferkamp *et al*., 2012). Functional studies have revealed their roles in various cellular mechanisms, such as DNA replication in mitochondria, the formation and degradation of amino acids and energy generation. MCF proteins transport the pyruvate formed through glycolysis to the mitochondrion, where it is converted to acetyl-CoA. The Krebs cycle then consumes acetyl-CoA as a substrate (Hildyard & Halestrap, 2003). Similarly, two MCF proteins, the phosphate carrier and the ADP/ATP carrier, transport inorganic phosphate and ADP, respectively, from the cytosol into the mitochondrion. These two substrates are required for ATP generation in the mitochondrion (Deramchia *et al*., 2014). Numerous MCF proteins are essential for the exchange of Krebs cycle intermediates between the cytosol and the mitochondrion, including the dicarboxylate carrier, which exchanges malate and succinate for inorganic phosphate, sulphate and thiosulphate (Palmieri *et al*., 2009); the tricarboxylate carrier, which transports citrate in exchange for malate or other anionic metabolites; and the oxoglutarate/malate carrier, which exchanges 2-oxoglutarate for malate or other dicarboxylic acids (Palmieri *et al*., 2009). Similarly, mitochondrial biosynthesis and the degradation of amino acids are dependent on different MCF proteins for the transportation of substrates and intermediates (Figure 1.6) (Kunji, 2004), including the citrulline/ornithine carrier, which exchanges ornithine for citrulline (Fiermonte *et al*., 2003); the aspartate/glutamate exchanger, which exchanges glutamate for aspartate (Fiermonte *et al*., 2002; Palmieri *et al*., 2006); and the oxoglutarate carrier, which transports oxoglutarate in exchange for oxoadipate derived from cytosolic lysine and tryptophan degradation (Fiermonte *et al*., 2001). In addition, mitochondrial DNA replication is dependent on MCF proteins, such as the deoxynucleotide carrier, which exchanges deoxynucleotides, and the S-adenosylmethionine carrier, which is required for the methylation of mitochondrial DNA (Dolce *et al*., 2001; Marobbio *et al*., 2003). Amino acid biosynthesis, as well as degradation inside the mitochondrion, requires several MCF proteins for the transport of various intermediates and substrates (Kunji, 2004). For instance, the oxoglutarate carrier exchanges oxoglutarate for oxoadipate, which is generated by the cytosolic degradation of tryptophan and lysine. Glutamate is exchanged for aspartate by the aspartate/glutamate exchanger (Fiermonte *et al*., 2002; Palmieri *et al*., 2006).

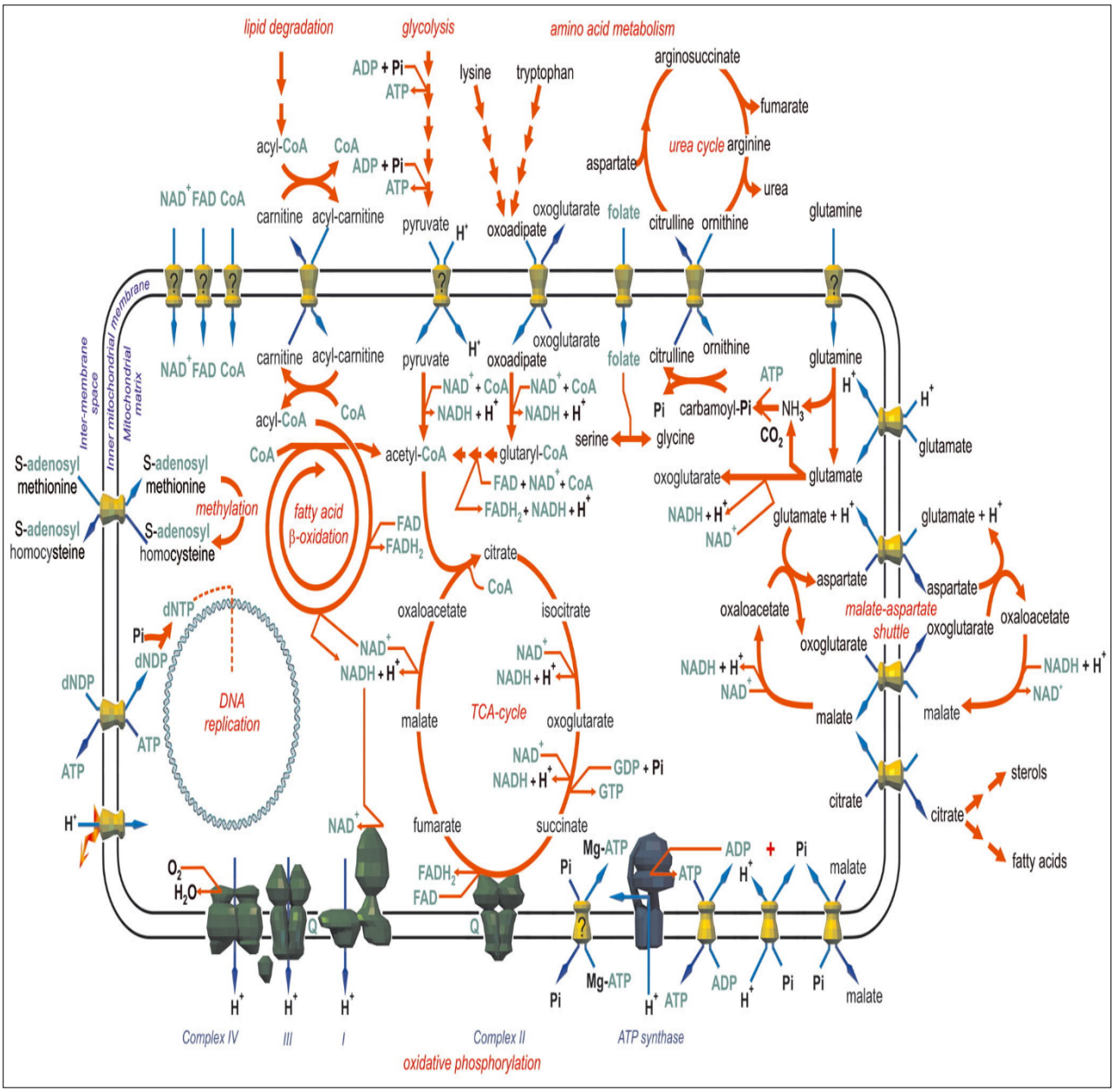

Figure 1.6. Schematic diagram of the probable roles of MCF proteins in the metabolic pathways of the cell and mitochondrion. Red arrows indicate metabolic pathways, blue arrows indicate the direction of transportation and green indicates energy-rich intermediates and cofactors. (Kunji, 2004)

Researchers have employed three strategies for studying MCF proteins and their roles in the transportation of molecules. The first, extensively employed strategy is the reconstitution of MCF proteins in synthetic liposomes, followed by analysis of the transportation of radiolabelled substrates into proteoliposomes (Palmieri *et al*., 2006b; Palmieri, 2004; Picault *et al*., 2002; Hoyos *et al*., 2003). However, this strategy is problematic as many reconstituted proteins are unable or only poorly able to transport molecules due to issues related to heterologous expression, purification, renaturation and refolding. Furthermore, correctly

inserting and orienting the reconstituted protein in the liposome is difficult (Palmieri *et al*., 2006b; Rigaud *et al*., 1995; Rigaud, 2006). In order to deal with these issues, certain MCF proteins have been produced in prokaryotic cells, such as *Escherichia coli*, in which their ability to transport radiolabelled substrates has been studied (Haferkamp *et al*., 2002; Tjaden *et al*., 2004; Leroch *et al*., 2005). Numerous studies have proven that MCF proteins are not post-translationally modified and are consequently capable of folding and integrating correctly into the plasma membrane of *E. coli* (Geigenberger *et al*., 2001; Haferkamp *et al*., 2002; Leroch *et al*., 2005; Tjaden *et al*., 2004;). A considerable limitation of this strategy is that it can only be used to study the transporters of metabolites that are not transported by any native transporters in *E. coli*. For instance, an ADP/ATP carrier can be studied using this strategy (Colasante *et al*., 2009). Utilisation of *Saccharomyces cerevisiae* knockout strains that lack particular MCF proteins has proven to be a more useful strategy (Palmieri *et al*., 2004). A majority of the knockout yeast strains lacking MCF proteins can be grown on a fermentable source of carbon, such as glucose, but are unable to grow on non-fermentable sources of carbon, such as lactate or glycerol (Clemencon *et al*., 2008; Palmieri *et al*., 2006). However, the complementation allows growth on non-fermentable carbon sources (Clemencon *et al*., 2008; Babot *et al*., 2012). However, functional complementation cannot be employed for all MCF proteins because all knockouts do not give rise to an analysable growth defect (Babot *et al*., 2012). In comparison to transport function in wild types, function may not be fully complemented in a yeast strain lacking an MCF protein (Mayr *et al*., 2011; De Marcos Lousa *et al*., 2002). Heterologous MCF proteins lack functional or yeast-specific mitochondrial targeting signals, leading to problems with protein expression and targeting to the mitochondrion (Palmieri *al*., 2006).

1.8 The MCF protein inventory of *T. brucei*

The genome of *T. brucei* (www.genedb.org) contains 26 genes that encode 24 MCF proteins. These proteins are called TbMCP1–24 (Colasante *et al*., 2009). Sequence analysis and reciprocal database searches have revealed that the *T. brucei* proteins are genuine MCF proteins. Notable amino acid similarity has been found between all 24 TbMCPs and those from *S. cerevisiae* and human (SLC25A). Moreover, all TbMCPs contain three semi-conserved 100-amino-acid protein domains that are essential for protein function. Each domain consists of the conserved MCF signature sequence motif, with conserved amino acid residues located at a specific distance from each other (Figure 1.5), and a pair of TM helices (Colasante *et al*., 2009).

Immunolocalisation studies have revealed that all TbMCPs localise to the mitochondria (Colasante *et al*., 2006a; Colasante *et al*., 2009). Phylogenetic reconstruction (Chapter 2: Materials and Methods) and reciprocal Basic Local Alignment Search Tool (BLAST) database searches have illuminated the possible roles of TbMCPs. In MCF proteins, there are numerous conserved amino acids downstream of the signature sequence. These amino acid residues have been reported to play a part in the recognition of and binding with particular substrates (Kunji & Robinson, 2006). As shown in Figure 1.5, these residues are mostly found in CPI–III. The first amino acid of each CP appears six residues downstream of the conserved glycine. CPI–III are conserved in MCF proteins that are responsible for transporting similar substrates. CPII, which may be involved in the discrimination between different substrates, contains the amino acid sequence 'G(IVLM)' in nucleotide carriers, '(R/K)Q' in phosphate carriers, 'R(QHNT)' in dicarboxylic acid carriers, 'R(D/E)' in amino acid carriers and 'MN' in iron carriers (Kunji & Robinson, 2006). The identification and comparison of CPI–III to previously characterised sequences from higher eukaryotic organisms has allowed a more specific definition of their putative functions (Colasante *et al*., 2006; Colasante *et al*., 2009). TbMCP6 has been studied in the greatest detail. The function of TbMCP6 as an ADP/ATP or ATP-Mg/Pi exchanger was suggested by phylogenetic reconstruction and sequence analysis (Colasante *et al*., 2006; Colasante *et al*., 2009). When TbMCP6 was reconstituted in *E. coli* and exposed to α^{32}P-tagged substrates, such as ADP, ATP and Mg, it did not transport the substrates. However, in knockdown experiments, TbMCP6 was found to be essential for the *T. brucei* PCF. TbMCP6 deficiency negatively affects cytokinesis and kinetoplast division (Colasante *et al*., 2006). Thus, TbMCP6 may be a mitochondrial nucleotide carrier similar to ATP-Mg/Pi and ADP/ATP carriers (Colasante *et al*., 2006; Colasante *et al*., 2009). TbMCP5 and TbMCP15 have also been proposed to participate in ADP/ATP exchange in mitochondria. They may be essential for PCF *T. brucei* energy metabolism (Colasante *et al*., 2009), which relies on mitochondria for ATP generation at the substrate level, oxidative phosphorylation and proline degradation (Bringaud *et al*., 2006; Schneider *et al*., 2007; Bochud-Allemann & Schneider, 2002). Importantly, one or more phosphate carriers is required for ADP/ATP carrier function to ensure that the Pi used for mitochondrial ATP generation is replenished (Palmieri *et al*., 2006). In *T. brucei*, TbMCP8 and TbMCP11 have been proposed as the required mitochondrial phosphate carriers (Colasante *et al*., 2009).

MCF protein sequence analysis can aid in determining the role of a protein in transportation. This functional analysis can be performed by: (1) determining the sequence similarity between

the MCF proteins of *T. brucei* and previously studied yeast and human MCF proteins, (2) assessing the phylogenetic relationship between a TbMCP sequence and other studied MCF proteins, and (3) analysing substrate-specific CPs. CPs comprise conserved amino acid sequences and may be involved in discrimination between different substrates. The determination of substrate specificity based on these conserved sequences has proven difficult. Given the great diversity of MCF proteins, the most helpful strategies for the functional characterisation of MCF proteins include the metabolic analysis of knockout strains and the reconstitution of proteins in artificial liposomes (Colasante *et al*., 2009). The present study will focus on nucleotide carriers, which are the most abundant carriers in the mitochondria (Liu & Chen, 2013). According to Liu and Chen (2013), MCF mitochondrial nucleotide transporters (ANT) constitute the most abundant group of mitochondrial proteins. Nury *et al*. (2006) found that the genes for ANTs reside in the nuclear DNA. Moreover, the proteins are produced in the cytosol, then transferred to mitochondria and inserted into the mitochondrial membrane. Brand *et al*. (2005) reported that catalysis of ADP/ATP exchange is the major function of ANTs. The ATP produced as a result of oxidative phosphorylation is sent to the cytosol to mediate various functions. On the other hand, ADP is sent to the mitochondrial matrix to produce ATP. ANTs exchange ADP for ATP. Moreover, ANTs participate in protein leakage. ANTs play a fatty acid-dependent role in the protein leakage pathway and are responsible for half to two-thirds of basal protein conductance (Brand *et al*., 2005). However, the mechanisms of conductance are still unknown. Consequently, ANT can be responsible for low levels of uncoupling protein and for reduced ATP generation (Desquiret *et al*., 2006). A number of isoforms of ANTs have been identified in yeasts, plants and humans; the majority are well studied (Brand *et al*., 2005). Analysis of the genome of *T. brucei* strain TREU92 (http://www.genedb.org) revealed that the sequences of genes encoding MCF proteins bore considerable resemblance to those for nucleotide carrier proteins in the mitochondria of higher eukaryotes, such as humans (Table 1.2).

Table 1.2. Genomic and functional homology between the MCF proteins of *T. brucei*, yeasts and humans. Gene sequences for *T. brucei* MCF proteins were obtained from www.genedb.org and gene sequences for human (SLC25A) and *S. cerevisiae* MCF proteins were obtained from www.ncbi.nlm.nih.go. (Colasante *et al*., 2009)

TbMCP	Gene ID	Human homology	Yeast homology	Transport function
1	Tb09.211.3200	SLC25A17	Y1A6	FAD carrier
4	Tb10.70.2290	Grave's disease carrier	LEU5	Unclear
5	Tb10.61.1810	AAC1	ANT1	ADP/ATP
6	Tb.927.4.1660	AAC1	ANT2	Unclear
8	Tb.10.406.0470	PTP	PIC2	Phosphate carrier
11	Tb.09.211.1750	PTP	PIC2	Phosphate carrier
15	Tb.927.8.1310	AAC2	ANT2	ADP/ATP
16	Tb.927.7.3940	AAC4	ANT2	Unclear
20	Tb.10.61.2510	SAMC	PET8 (SAM5)	S-Adenosylmethionine
23	Tb.927.5.1550	PNC	RIM2	Pyrimidine nucleotide carrier

1.9 The mitochondrial ADP/ATP carrier

The ADP/ATP carrier is one of the best-studied MCF proteins. It is abundantly expressed in the MIM (Trezeguet *et al*., 2008; Klingenberg, 2008). The carrier is required for energy metabolism in eukaryotic cells as it exports mitochondrial-generated ATP to the cytosol and, in return, imports ADP from the cytosol to the mitochondrion. Thus, it supplies ADP to the mitochondrion to maintain ATP generation (Klingenberg, 2008; Palmieri *et al*., 2006). Cardiolipin, a lipid molecule exclusively present in the MIM, is required for the exchange of ADP and ATP (Trezeguet *et al*., 2008). According to Palmieri *et al*. (2006), the ADP/ATP carrier is also a component of the mitochondrial transition pore (MTP), which is required for

the apoptotic pathway mediated by cytochrome c. The importance of the ADP/ATP carrier for energy metabolism in eukaryotic cells is obvious in humans, as disruption of MCF protein function results in severe diseases, such as cardiomyopathy and mitochondrial myopathy. The lack of isoform 1 of the ADP/ATP carrier results in the deletion of large quantities of mitochondrial DNA, as well as exercise intolerance, ptosis and progressive external ophthalmoplegia (Kaukonen *et al*., 2000; Napoli *et al*., 2001). In addition to mutations of the gene for the ADP/ATP carrier, disruptions in gene transcription or transference of the carrier to the mitochondrion can cause Sengers syndrome and other problems, such as lactic acidaemia, hypertrophic cardiomyopathy and exercise intolerance (Palmieri, 2004). Generally, tissues with altered ADP/ATP carrier function demonstrate diminished energy generation and oxidative phosphorylation (Dahout-Gonzalez *et al*., 2006; Palmieri, 2004). X-ray crystallography has been used to study the structure of ATP/ADP carriers from different organisms, such as *Bos taurus* ANT1 (Pebay-Peyroula *et al*., 2003) and *S. cerevisiae* AAC3 (Kunji & Harding., 2003). This structural analysis is also employed to predict the structures of new MCF proteins (Palmieri *et al*., 2011).

A number of conserved amino acids are present in CPI–III of MCF proteins, where they are responsible for selective binding to the substrates to be transported (Kunji & Robinson, 2006). The carriers of similar proteins have similar CPs (Kunji & Robinson, 2006; Klingenberg *et al*., 2008). In the ADP/ATP carrier, three conserved amino acids comprise CPI: arginine, threonine and asparagine. Glycine and isoleucine constitute CPII, whereas CPIII contains only arginine (Kunji & Robinson, 2006). Mutations in any of these CPs limit or prevent the function of the carrier (Kunji & Robinson, 2006). In addition to the repeat sequences and conserved sequences, the canonical hexapeptide sequence 'RRRMMM' is also present in the carrier, where it is required for binding with ADP (Nury *et al*., 2006; Clemencon *et al*., 2011).

At least one gene that encodes a mitochondrial ADP/ATP carrier is present in the genomes of all eukaryotes studied to date (Colasante *et al*., 2009). The genomes of higher eukaryotes generally contain additional genes for different isoforms of the ADP/ATP carrier (Traba *et al*., 2011; Loytynoja & Milinkovitch, 2001). A high degree of sequence similarity has been found among these isoforms, which suggests they have been formed through gene duplication events during evolution (Loytynoja & Milinkovitch, 2001). The human genome contains genes for four isoforms of the carrier (Battini *et al*., 1987; Houldsworth & Attardi, 1988; Dolce *et al*., 2005), as does the *B. taurus* genome (Powell *et al*., 1989). Three isoforms are present in the *S. cerevisiae* genome (Kolarov *et al*., 1990b; Lawson & Douglas, 1988; Adrian *et al*., 1986).

However, the genomes of protozoans generally contain only one isoform of the ADP/ATP carrier (Tjaden *et al*., 2004; Williams *et al*., 2008; Chang *et al*., 2005). In higher eukaryotes, gene expression of the different isoforms is tissue dependent (Powell *et al*., 1989; Dahout-Gonzalez *et al*., 2006). The ADP/ATP carrier isoform 1 is found in skeletal muscle, the heart, and, to a lesser extent, the brain (Stepien *et al*., 1992; Dolce *et al*., 2005); isoform 2 is found in developing and differentiating tissues; isoform 3 is found in all tissues, but at varying levels of expression; and isoform 4 is found only in the brain, testes and liver. In contrast to multicellular eukaryotes, unicellular eukaryotes demonstrate simple ADP/ATP carrier gene expression, as it is the only carrier encoded in the genome (Traba *et al*., 2011). Moreover, the expression of the carrier isoforms is determined by environmental factors, such as the presence of substrates and the types of metabolism linked to the substrates (Klingenberg, 2008). However, *S. cerevisiae* has a different pattern of ADP/ATP carrier expression than other unicellular eukaryotes as it has genes for three different isoforms, called ScAnc1–3 (Palmieri, 2004). The expression and function of the ScAnc1–3 isoforms are affected by environmental factors and the availability of metabolic substrates (Palmieri, 2004). ScAnc1p expression is down-regulated in a haem-independent fashion in an anaerobic environment (Gavurnikova *et al*., 1996). In contrast, ScAnc2p and ScAnc3p expression are dependent on haem availability. ScAnc2p is required for aerobic yeast growth on non-fermentable sources, such as glycerol and lactate, and ScAnc3p is needed for growth in anaerobic or fermentative environments (Betina *et al*., 1995; Sabova *et al*., 1993; Palmieri *et al*., 2006). Thus, it can be postulated that different isoforms of ScAncp have developed during evolution to allow the organism to adapt to varying energy requirements in different environmental conditions by generating ATP from various substrates through multiple mechanisms (Klingenberg *et al*., 2008). *T. brucei* also demonstrates adaptive energy metabolism in response to changes in substrates and environmental conditions, particularly in response to the life cycles of its two hosts (Matthews, 2005; Bringaud *et al*., 2006; Michels *et al*., 2006). The MCF protein inventory of *T. brucei* (Table 1.2) includes TbMCP5 and TbMCP15. These two ADP/ATP carriers demonstrate considerable sequence similarity to well-researched eukaryotic ADP/ATP carriers (Colasante *et al*., 2009).

1.10 The mitochondrial pyrimidine nucleotide carrier

According to Franzolin *et al*. (2012), the pyrimidine nucleotide carrier is a multi-copy suppressor in mitochondria. It can partly compensate for the growth defects in PIFI-null mutants. PIFIp is a DNA helicase that is required to maintain mitochondrial DNA (Agrimi *et*

al., 2014). The deletion of pyrimidine nucleotide carrier gene (RIM2) in yeast causes reduced growth on non-fermentable carbon sources as a result of the loss of mitochondrial DNA (Van Dyck *et al*., 1995). Numerous reports have suggested that pyrimidine (deoxy)nucleotides may be transported by Pyt1p. Pyrimidine nucleoside diphosphates are produced in *S. cerevisiae* outside the mitochondria (Palmieri *et al*., 2009). Ribonucleotide reductases (Rnr1p-4p) and nucleoside diphosphate kinase (Ynk1p) are also found exterior to the MIM (Amutha *et al*., 2003; Yao *et al*., 2003). RNA and DNA formation in mitochondria involve the incorporation of pyrimidine (deoxy)nucleoside triphosphates (Py(d)NTPs). Py(d)NTPs are also essential for the formation of the RNA primers that are required for the initiation of DNA repair and replication. Thus, there must be a mechanism by which these molecules are transferred into mitochondria. Numerous purine nucleotide carriers have been detected in mitochondria (Froschauer *et al*., 2009), but they do not transport pyrimidine nucleotides. Pyrimidine nucleotides are transported by Pyt1p (Marobbio *et al*., 2006). Pyt1p is responsible for the hetero- and homo-exchange of all pyrimidine (deoxy)nucleotides and (deoxy)nucleosides. Diphosphates and triphosphates are transported more quickly than monophosphates. However, the transportation of pyrimidine deoxynucleotides occurs at a similar rate to that of the corresponding nucleotides (Agrimi *et al*., 2014). Among the mitochondrial family proteins, SL25A33 and SLC25A36 have been characterised as human pyrimidine nucleotide carriers, whereas only one has been identified in *S. cerevisiae* (Agrimi *et al*., 2014; Palmieri *et al*., 2003). The MCF protein inventory of *T. brucei* (Table 1.2) includes a single pyrimidine nucleotide carrier: TbMCP23. It also includes TbMCP6 and TbMCP1, which are carriers with considerable sequence similarity to the pyrimidine nucleotide carriers of the extensively studied higher eukaryotes (Colasante *et al*., 2009).

1.11 The mitochondrial S-adenosylmethionine carrier

S-Adenosylmethionine (SAM) is a methyl group donor involved in almost all methylation mechanisms in cells. SAM is required for protein, RNA and DNA methylation (Palmieri *et al*., 2003). It is also involved in the formation of the biotin in yeast (Marquet *et al*., 2001; Kumar *et al*., 2002), ubiquinone (Bringaud, 2015) and lipoic acid (Sulo *et al*., 1993). The enzyme required for the production of SAM, methionine adenosyltransferase, is found only in the cytosol, not in the mitochondria (Palmieri *et al*., 2003). However, mitochondria contain ample SAM .Thus, SAM must be transported from the cytosol into mitochondria through a carrier Palmieri *et al*., 2003).

Purohit *et al*. (2008) studied the biochemical characteristics of SAM in the mitochondria of rat livers. Mitochondria were found to be capable of storing SAM, the uptake of which can be prevented by structural analogues of SAM, such as adenosyl-ornithine and S-adenosylhomocysteine (SAHC). However, this carrier system has not been found in mammalian cells. S-adenosylmethionine carrier (SAMC), on the other hand, is present in human cells. Its kinetic properties, subcellular localisation and transport mechanisms indicate that SAMC is comparable to the SAM carrier in the mitochondria of rat livers. SAMC appears to transfer SAM into mitochondria. The transportation of SAM by carriers requires the efflux of another substrate because SAMC works only through a counter-exchange mechanism. SAHC, which is generated through a methylation reaction and subjected to hydrolysis in the cytosol (Marobbio *et al*., 2003), can behave as a counter-substrate for SAM. This evidence supports the conclusion that SAMC transports SAM into mitochondria in exchange for SAHC. Prohibitin (PHB1) and subunits I and II of cytochrome c oxidase are post-translationally down-regulated in mice lacking hepatic SAM synthetase (*MAT1A−/−*). This effect has also been observed in rat hepatocytes grown in media lacking methionine or containing cycloleucine (a MAT1 inhibitor). The effects are known to be post-translational as there is no reduction in the number of mRNA copies in these experiments (Santamaria *et al*., 2003). The lower levels of PHB1 were linked with reduced mitochondrial function (Santamaria *et al*., 2003). Since SAMC is required for metabolism in mitochondria, it is present in all human tissues studied to date and is widely present in eukaryotic cells (Palmieri *et al*., 2016). The SAM5 (PET8) gene in yeast encodes the carrier of adenosylmethionine and renders yeast incapable of growing on non-fermentable carbon sources, such as acetate and glycerol (Palmieri *et al*., 2006). Yeast cells deficient in this gene cannot grow on minimal synthetic media containing fermentable substrates, such as glucose or galactose, even if biotin is absent or the biotin precursor dethiobiotin is present (Palmieri *et al*., 2003). Based on this observation, the role of SAM5 was thought to be (Bio2p) converted dethiobiotin to biotin and Bio2p inside the mitochondria, (Kumar *et al*., 2002). Researchers postulated that SAM5 was required for the export of biotin or import of dethiobiotin. However, this possibility was eliminated through direct transport assays using artificial liposomes. The likely reason for the biotin auxotrophy of SAM5 is the lack of SAM in mitochondria, which results in disruption of the conversion of dethiobiotin to biotin. The MCF protein inventory (Table 1.2) of *T. brucei* includes TbMCP20, an S-adenosylmethionine carrier, which has considerable sequence similarity to the S-adenosylmethionine carrier of other eukaryotic cells (Colasante *et al*., 2009).

1.12 Aims of the project

MCF proteins play important roles in cellular energy metabolism. The mitochondria of *T. brucei* play a crucial role in providing energy, in the form of ATP, to the cells. ATP is generated in the mitochondria by oxidative and substrate-level phosphorylation, using inorganic phosphate and ADP. ATP generated in the mitochondria of the pathogen must be exported from the mitochondrial matrix to the rest of the cell and ADP and Pi must be imported from the cytosol. This balance is required to maintain energy provision in the cells (Thompson *et al*., 2011).

The focus of the present study was on nucleotide carriers, which are the most abundant carriers in the mitochondria (Liu & Chen, 2013). The aim of the study was to functionally characterise the mitochondrial ANTs of *T. brucei*: TbMCP1 (homologue of FAD, chapter 3), TbMCP15 and TbMCP16 (homologue of ADP/ATP, chapter 4), TbMCP20 (homologue of SAM5, chapter 5),and TbMCP23 (homologue of RIM2, chapter 6).

The sequences of the genes were first aligned with known mitochondrial carriers at the DNA and protein levels and subjected to phylogenetic reconstruction. Protein localisation was studied using immunofluorescence microscopy followed by western blotting. The phenotypes of knockdown cell lines, generated by RNAi, and overexpressing cell lines were characterised *in vitro*. Finally, the functions of the proteins of interest were examined using functional complementation assays in yeast.

Chapter 2: Materials and Methods

2.1 Materials

Cell lines of *T. brucei*

T. brucei PCF449 and BSF449 were provided by Dr F Voncken.

Scientific Laboratory Suppliers

27-°C incubator

CO_2 incubator

Sigma -Aldrich Chemical Company, Poole, UK

Agar

Agarose gel

Ammonium persulfate

Antibiotic solution (Penicillin − Streptomycin − Neomycin Solution)

Bovine serum albumin (BSA)

Carboxyatractyloside

Coomassie Brilliant Blue R-250

4′,6-Diamidino-2-phenylindole dihydrochloride (DAPI)

Electrophoresis power supply

Fish gelatin

Formaldehyde powder

Laemmli Lysis-buffer (2×)

LB broth medium

MEM-Pros medium

Phosphate-buffered saline (PBS)

Proline powder

RNAzol®

Saline sodium citrate buffer

Sarkosyl

Tris base–acetic acid–ethylenediaminetetraacetic acid (EDTA) buffer

Triton™ X-100

TWEEN® 20

UVP, Cambridge, UK

UV transilluminator

Roche Applied Science, Burgess Hill, UK

Complete™ EDTA-free Protease Inhibitor Cocktail

Crysalon: Norton Company, London, UK

Silicon carbide

Stratagene, USA

Prime-It Random Primer Labeling Kit

EUROSCARF resource centre, Frankfurt, Germany

Yeast *S. cerevisiae* strains BY4741 (MATa his3Δ1 leu2Δ0 met15Δ0 ura3Δ0); YNL003c (ΔSam-5: MATa his3Δ1 leu2Δ0 met15Δ0 ura3Δ0); ANC2 (J1-3U^{-}Δ); MATa his3-Δ1 leu2-3 leu2-112 ura3-52 trp1-289)

Promega, Southampton, UK

Luciferase assay substrate (luciferin)

Luminescent Cell Viability Assay kits

NucleoSpin® Gel and PCR Clean-up

pET28 cloning vector

pGEM-T Easy Vector System

pHD767 cloning vector

Tris-borate EDTA buffer (10×)

New England Biolabs, Hertfordshire, UK

Taq polymerase

T4 DNA ligase

Eurofins MWG, Wolverhampton, UK

Primers (Appendix 3)

Carl Zeiss, Welwyn Garden City, UK

Laser scanning microscope

Bio-Rad, Hemel Hempstead, Hertfordshire, UK

Polymerase chain reaction (PCR) thermal cycler

Electroporator

Electroporation cuvettes

Nitrocellulose membranes

Hybond™-N nylon membrane

Abcam, Cambridge, UK

Acetate assay kit

Rabbit polyclonal anti-goat (IgG) horseradish peroxidase (HRP)-conjugated antibody

Mouse polyclonal anti-goat (IgG) HRP-conjugated antibody

Tubulin monoclonal anti-rat antibody

Succinate assay kit

Rat polyclonal anti-goat antibody

His-tag monoclonal anti-mouse antibody

Pyruvate assay kit

EZ Biolabs, Carmel, IN, USA

polyclonal anti-rabbit TbMCP20 antibody

Thermo Fisher Scientific, Paisley, UK

cDNA synthesis kit

Competent *E. coli* strain DH10B-T1

DNA ladder

DNA loading dye

DNase I

Enhanced chemiluminescence (ECL) detection kit

EDTA

Ethidium bromide

Glycerol solution

Magnesium chloride

Poly-lysine

QuantiTect® SYBR® Green RT-PCR kit

Sodium acetate

Sodium dodecyl sulphate (SDS)

Sodium hydroxide

Fisher Scientific, Loughborough, Leicestershire, UK

Glycine

NaCl

Dithiothreitol (DTT) buffer

Tris base

Trichloroacetic Acid (TCA)

24-well culture plates

25-cm^2 tissue culture flasks

75-cm^2 tissue culture flasks

Haemocytometer chamber

MitoTracker™ Red CMXRos

Fast Digest enzymes

2.2 Methods

2.2.1 Phylogenetic reconstruction and sequence analysis

Phylogenetic reconstruction was performed using phylogeny.fr software (available at http//www.phylogeny.fr). Multiple sequence alignments were generated using Clustal Omega (ClustalO) .Motif structures were added manually to protein sequence alignments using Adobe Illustrator®. Phylogenetic trees were constructed using PhyML and visualised using TreeDyn. BLASTP (http://blast.ncbi.nlm.nih.gov/Blast.cgi?PAGE=Proteins) was employed to retrieve similar protein sequences from trypanosomatids, plants, insects, fungi and mammals. The retrieved protein sequences were then imported into ClustalO and aligned. Using the neighbour joining method , a phylogenetic tree was drawn with the bootstrap set to 1000. Only bootstrap values above 50% were shown (Colasante *et al*., 2009). After the phylogenetic tree was generated, the groups were manually labelled using Adobe Illustrator®.

2.2.2 Plasmid construction

Plasmids were constructed by cloning specific genes into a number of different vectors using standard molecular biology protocols (Appendix 4). For the growth experiments using RNAi, the plasmids included pHD676 + TbMCP1 RNAi, pHD676 + TbMCP15 RNAi, pHD676 + TbMCP16 RNAi, pHD676 + TbMCP20 RNAi and pHD676 + TbMCP23 RNAi. For the protein expression studies, the plasmids included pET28 + TbMCP15, pET28 + TbMCP16, pET28 + TbMCP20 and pET28 + TbMCP23. For the mitochondrial localisation experiments, the plasmids included pHD1484+TbMCP1-cmyc^{ti}, pHD1484+TbMCP15-cmyc^{ti} and pHD1484+TbMCP20-cmyc^{ti}. For the yeast complementation experiments, the plasmids included pCM190 + TbMCP5, pCM190 + TbMCP15, pCM190 + TbMCP16, pCM190 + TbMCP20 and pCM190 + SAM-5.

2.2.2.1 PCR and primer design

The full-length sequences of the target genes were obtained from NCBI GenBank. The forward and reverse primers (Appendix 4) were designed according to the target sequences and synthesised by Eurofins MWG. A standard 50-µl PCR amplification reaction contained 10× Taq buffer (5 µl), dNTP mix (5 µl; 2 mM each), and 0.1–1 µM forward and reverse primers (Appendix 3), 1–4 µl $MgCl_2$ (25 mM stock), 10 pg–1 µg template DNA, 1.25 units of Taq DNA polymerase and dH_2O (to adjust the total volume to 50 µl). All components were assembled on ice. After mixing the reactions for 10 seconds, the PCR tubes were transferred

to a thermal cycler with a preheated 95 °C block. The thermocycling conditions for routine reactions were initial denaturation at 95 °C for 5 minutes, followed by 30 to 35 cycles of denaturation for 30 seconds at 95 °C, annealing for 1 minute at the appropriate annealing temperature (Appendix 4), followed by primer extension for 1 minute at 72 °C. The reactions were then completed by extension for 10 minutes at 72 °C and a final hold at 4 °C. When the PCR reactions were complete, the DNA products were electrophoresed on a 1% (w/v) agarose gel for size assessment or DNA purification.

2.2.2.2 Restriction enzyme digestion, ligation and transformation of *E. coli*

For restriction enzyme analysis or the creation of sticky DNA ends for ligation, restriction enzymes and Fast Digest enzymes were used for digestion. The digested vectors or inserts were purified by gel extraction and processed with a PCR clean-up kit. T4 ligase was used for sticky-end ligation and PCR products were inserted directly into different cloning, including pGEM-T Easy (for sequencing), and specific *T. brucei* and *E. coli* expression vectors. The ligation products were transformed into chemically treated competent *E. coli* DH10. Tubes of DH10 competent *E. coli* cells were placed on ice and gently mixed for 10 seconds, then the cells were carefully pipetted into transformation tubes on ice. Plasmid DNA (1–5 µl) or ligation product (1 pg–100 ng DNA) was added to each tube of competent cells and carefully flicked 4–5 times to mix the cells and DNA. The mixtures were incubated on ice for 30 minutes, then heat-shocked for 90 seconds at exactly 42 °C. The heat-treated mixtures were left on ice for a further 2 minutes, then LB medium (450 µl; containing 10 g/l tryptone, 5 g/l yeast extract, and 5 g/l NaCl) (Bertani, 2004) was added. After incubation at 37 °C for 30 minutes, the mixtures were spread on LB plates with selection antibiotics (100 µg/ml ampicillin and 50 µg/ml kanamycin) and incubated overnight at 37 °C.

2.2.3 Down-regulation of the expression of a specific gene using RNAi

Parts of the open reading frames (ORFs) of the genes of interest were amplified from *T. brucei* Lister 449 genomic DNA using forward and reverse primers (Appendix 4). The amplified DNA sequences were inserted into pHD676 and pHD1484 (Appendix 4). RNAi was used to down-regulate the expression of specific genes. The antisense and sense transcripts of the target genes were amplified using primers (Appendix 4) with restriction enzyme sites added at both ends, then cloned into the transfection vectors pHD676 and pHD1484.

2.2.4 *T. brucei* cell subculture and growth assessment

The parental *T. brucei* PCF449 cell line and derived mutant cell lines were cultured in MEM-Pros medium (Appendix 1) supplemented with 10% heat-inactivated FBS, haem (2.5 mg/ml in 100 mM NaOH) and penicillin/streptomycin (final concentration, 100 units/ml penicillin and 10 µg/ml streptomycin). The MEM-Pros medium (500 ml) was further supplemented with 0.5 M proline (5 ml). Strain BSF449 was cultured in HMI-9 medium (Appendix 2) supplemented with 10% serum, penicillin/streptomycin (final concentration, 100 units/ml penicillin and 10 µg/ml streptomycin), 50 mM L-cysteine·HCl·H_2O and 20 mM β-mercaptoethanol. The appropriate antibiotics were added depending on the different cell lines and the various plasmids used for transfection (see section 2.2.2.2). The PCF449 cell lines were cultured in a 27-°C incubator, whereas the BSF449 cell lines were cultured at 37 °C in a 5.0%-CO_2 incubator. The cells were subcultured (split) every 48 to 72 hours. The growth experiments were performed by inoculating samples of *T. brucei* from the stock cultures into 25-cm^2 culture flasks containing 10 mL culture medium supplemented with the corresponding antibiotics. All growth experiments were performed in triplicate and as independent experiments. The cell density of each flask was measured every 24 hours for at least five days using a haemocytometer. The data collected were analysed using Microsoft® Excel.

2.2.5 *T. brucei* transfection

Before transfection, the RNAi plasmids were linearized by *Not* I digestion and DNA purified and concentrated by precipitation using 70% (v/v) final concentration ethanol. The *T. brucei* cells (2×10^7) were subjected to centrifugation at 2,000 *g* for 10 minutes. The culture supernatants of grown *T. brucei* cultures were used as conditioned media to promote trypanosome growth during recovery after transfection. The recovery media contained conditioned medium (5 ml), fresh medium (5 ml), 5 mM glucose and maintenance antibiotics. After centrifugation, the cell pellets were washed in approximately an equal volume of filter-sterilised ZPFM or Cytomix (Appendix 5), then resuspended in ZPFM/Cytomix (500 µl). The DNA (20 µl) and cells (500 µl) were transferred into 4-mm electroporation cuvettes and mixed briefly. Subsequently, the samples were electroporated (capacitance, 25 µFD; resistance, 400 Ω; and voltage, 1.7 kV). Then, the mixtures were transferred into culture media and incubated overnight under normal culture conditions. On the second day post-transfection, the selective antibiotics were added and the cultures were serially diluted in 24-well plates to select potential clones. In the culture flasks, the selection antibiotics (Hygromycin and Blastidicin) were

added and fresh media supplemented with selection antibiotics were prepared. For the dilutions, transfected cells (1 ml) were added to the wells in the first row of each plate. Fresh medium (0.5 ml) was added to the remaining 3 wells in each column. Then, in each column, cells (0.5 ml) from the first row were mixed with the medium in the second row, then diluted cells (0.5 ml) from the second row were mixed with the medium in the third row. Finally, diluted cells (0.5 ml) from the third row were added to the last row of the plate. After serial dilution, the 24-well plates were incubated for seven to ten days and checked for growth every 48-72 hours using the microscope. The wells containing viable after one week of antibiotic treatment were considered positive and the cells were grown in tissue culture flasks for further study (Colasante *et al*., 2009).

2.2.6 Analysis of mitochondrial subcellular localisation by immunofluorescence microscopy

Microscopy coverslips were treated with poly-lysine (0.5 ml; 0.1 mg/ml) for 30 minutes at room temperature without shaking. After three washes with an excess of water, the slides were air-dried. Aliquots of *T. brucei* cultures (approximately 1×10^7 cells) were collected in 2.0-ml Eppendorf tubes. For BSF449 cells, MitoTracker™ Red CMXRos was added at a final concentration of 0.05 μM, then the cells were incubated in an open tube at 37 °C in a gassed incubator (5% CO_2) for 10 minutes. For PCF449 cells, MitoTracker™ Red CMXRos was added at a final concentration of 0.5 μM and the cells were incubated in a tightly capped tube at 27 °C for 10 minutes. Next, the cells were subjected to centrifugation at 2,000 *g* for 10 minutes, washed with the appropriate pre-warmed culture medium (10 ml) to remove residual dye and incubated for 20 minutes with pre-warmed culture medium (without dye; 5 ml) to incorporate the remaining dye in the cytosol into the mitochondria. Then, the cells were pelleted, washed with PBS and fixed in freshly made 4% (w/v) paraformaldehyde. The tubes were inverted three times and the cells were incubated for exactly 18 minutes without shaking. After fixation, the cells were washed three times with excess PBS to remove the residual paraformaldehyde. Then, the cells were resuspended in PBS, aliquoted onto treated coverslips in 24-well plates and incubated overnight at 4 °C. The following day, the supernatants were removed and the coverslips were incubated with 0.2% (w/v) Triton™ X-100 for 20 minutes at room temperature to permeabilise the cells. After three washes with PBS, each coverslip was covered in 0.5% (w/v) PBS and incubated for 20 minutes. Then, the coverslips were treated with anti-myc primary antibody (1:500), incubated for 60 minutes on a shaker and washed twice. The coverslips were incubated with the secondary antibody for 60 minutes. One drop

of glycerol-based mounting medium with DAPI was applied to each slide, then the coverslips with the cells were mounted on the slides and fixed with nail polish. The slides were stored in the dark at 4 °C and analysed using a laser scanning confocal microscope within 2–3 days.

2.2.7 Analysis of mitochondrial subcellular fractionation

The *T. brucei* PCF449 cell line was grown to 5×10^6 cells/ml and harvested by centrifugation at 2,000 *g* for 10 minutes. The cells were washed once in TEDS (50 ml; 25 mM Tris, 1 mM EDTA, 1 mM DTT and 250 mM sucrose; pH 7.8). After centrifugation as above, the cell pellets were resuspended in 1 volume of TEDS supplemented with Complete™ EDTA-free Protease Inhibitor Cocktail and ground in a pre-chilled mortar with 1 volume of silicon carbide. The cell lysates were subjected to centrifugation at 1,000 *g* for 10 minutes to remove the nuclei. The supernatants were subjected to centrifugation at 5,000 *g* for 10 minutes to yield the 'large organelle' fraction and the resulting supernatants were subjected to centrifugation at 33,000 *g* for 25 minutes to yield the 'small organelle' fraction. Each organelle fraction was pooled, diluted with TEDS, layered onto a 30%–60% (w/v) sucrose step gradient in 10 mM Tris-HCl buffer (pH 7.5) with 1 mM EDTA and applied to a 70% (w/v) sucrose cushion. Centrifugation was performed at 33,000 *g* for 1 hour at 4 °C. Aliquots (1 ml) were collected from the bottom of the tubes by puncture. Samples (equal volumes) of each fraction were concentrated by TCA precipitation and the precipitates were resuspended in denaturing SDS-polyacrylamide gel electrophoresis (PAGE) buffer, then separated on a 12%-SDS-polyacrylamide gel. The proteins were transferred to a Hybond™-P nylon membrane and detected with an antibody against GIM5 (glucosome integral membrane protein number 5) (Lorenz, 1998) for the identification of glycosome-enriched fractions, an antibody against LPDH (lipoamide dehydrogenase) (Schoneck, 1997) for the identification of mitochondria-enriched fractions.

2.2.8 SDS-PAGE and western blotting

SDS-PAGE was performed according to the Laemmli method (Laemmli, 1970). Briefly, samples were prepared in Laemmli sample buffer (0.0625 M Tris-HCl [pH 6.8], 0.1% [v/v] β-mercaptoethanol, 0.1% [w/v] EDTA and 0.1% [v/v] glycerol) and heated at 95 °C for 5 minutes. The samples were run on 12% denaturing polyacrylamide gels (running gel: 0.375 M Tris-HCl [pH 8.0], 0.1% [w/v] SDS and 0.1% [w/v] ammonium persulfate; stacking gel: 0.125 M Tris-HCl [pH 6.8], 0.1% [w/v] SDS, 0.1% [w/v] ammonium persulfate and 4% polyacrylamide). The gels were run at 200 V until the fronts reached the ends of the gels. For western blotting, samples were separated by SDS-PAGE and transferred to nitrocellulose or polyvinylidene fluoride (PVDF) membranes at 100 V for 50 minutes in Towbin buffer (48 mM Tris, 39 mM glycine and 20% [v/v] methanol; pH 8.3). The membranes were blocked under shaking conditions in Tris-buffered saline with 0.1% TWEEN® 20 (TBST) and 5% (w/v) skimmed milk at room temperature for 1 hour. Subsequently, the membranes were incubated with the primary antibody in TBST containing 5% milk for 1 hour at room temperature or overnight at 4 ºC to improve the signal. After incubation, the membranes were washed three times with excess TBST buffer (10 minutes/wash). The secondary antibody incubations and washes were performed in conditions similar to those for the primary antibodies. Proteins were detected with an ECL kit.

2.2.9 Heterologous protein expression, purification in *E. coli* and antibody generation

2.2.9.1 Expression vector cloning and isopropyl-β-D-thiogalactopyranoside induction

PCR was used to amplify the ORFs of the genes of interest, which were then cloned into the pGEM T-easy vector for sequencing and later sub-cloned into the expression vectors pTrcHis A or pET28a.To enable inducible expression upon isopropyl-β-D-thiogalactopyranoside (IPTG) treatment, the plasmid constructs were transformed into the *E. coli* Rosetta™ 2(DE3)pLysS and Lemo21(DE3) strains. Single colonies were inoculated into LB medium containing ampicillin (100 μg/ml) and chloramphenicol (25 μg/ml) to form precultures. The precultures were grown overnight at 37 °C, then diluted 1:20 dilution in LB medium and cultured with constant shaking at 37 °C. When the absorbance of the samples at 600 nm reached 0.48–0.5, they were treated for 4–6 hours with IPTG (final concentration, 0.4 mM) to induce protein expression. Following induction, aliquots (1 ml) were collected every hour to establish a growth curve.

2.2.9.2 Purification of inclusion bodies

After the induction of protein expression for 4 hours, the cultures were harvested by centrifugation at 4,000 *g* for 10–20 minutes at 4 °C. One gram (wet weight) of cell pellet was resuspended in 5 ml native resuspension buffer (50 mM Na_3PO_4 [pH 8.0], 300 mM NaCl and 0.01% TWEEN® 20) supplemented with Complete™ EDTA-free Protease Inhibitor Cocktail, 0.2 mg/ml lysozyme and 5 unit/µl DNase, followed by incubation on ice for 30 minutes. The cell lysates were passed twice through a French press (University of Hull) until the solutions were clarified. Inclusion bodies were pelleted by centrifugation at 13,000 *g* for 30 minutes. The supernatants and pellets were collected for SDS-PAGE. The inclusion bodies were resuspended in resuspension buffer containing 2% Sarkosyl. Ni-NTA agarose (1 ml) was added to the solubilised proteins (20 ml), the mixtures were stirred for 60 minutes at room temperature or until the solutions had become translucent, then the solutions were applied to a Ni-NTA column at 4 °C for protein binding. The supernatants containing unbound proteins or contaminants were removed by centrifugation at 500 *g* for 5 minutes. Then, the Ni-NTA agarose was washed twice to remove potential contaminants with a wash buffer (8 mM Na_2HPO_4, 286 mM NaCl, 1.4 mM KH_2PO_4, 2.6 mM KCl and 0.1% [w/v] sarkosyl; pH 7.4). Finally, protein was eluted from the Ni-NTA with an elution buffer (8 mM Na_2HPO_4, 286 mM NaCl, 1.4 mM KH_2PO_4, 2.6 mM KCl, 500 mM imidazole and 0.1% [w/v] sarkosyl; pH 7.4). The purified protein (3 mg) was loaded onto a prep gel, which was stained with Coomassie Brilliant Blue R-250, then the bands were cut from the prep gel and sent to Thermo Fisher Scientific for polyclonal antibody generation. The resultant antiserum was diluted 1:250 in 5% [w/v] skimmed milk and used as a primary antibody for western blotting.

2.2.10 *S. cerevisiae* functional complementation

2.2.10.1 *S. cerevisiae* subculture media

S. cerevisiae strains were maintained on standard yeast extract peptone dextrose/glucose (YPD) medium (1% [w/v] yeast extract, 2% [w/v] peptone, 2% [w/v] glucose and 2% [w/v] agar). In order to test cell growth on different carbon sources, the glucose in YPD was replaced with 3% [v/v] glycerol (resulting in YPG). Synthetic complete medium without uracil (0.67% [v/v] yeast nitrogen base without amino acids and 1.4% [w/v] dropout medium supplements (without histidine, leucine, tryptophan and uracil) supplemented with 60 mg/l leucine, 20 mg/l tryptophan, 20 mg/l histidine, 2% [w/v] agar and 2% [w/v] dextrose) was used for clone selection after transfection. The plasmids containing the target genes were transformed into the functional corresponding knockout strains using the $C_2H_3LiO_2$/single-stranded carrier

DNA method described by Gietz and Woods (2002). The yeast clones were maintained on synthetic complete dextrose (glucose) medium without uracil.

2.2.10.2 *S. cerevisiae* growth complementation

Single colony was inoculated into starter cultures (5 ml YPD) and grown at 28°C–30°C with shaking overnight. The next day, aliquots (1 ml) of the starter cultures were placed in cuvettes and the absorbance of the cells at 600 nm was measured. Then, appropriate volumes of the starter cultures were inoculated into the main cultures (20 ml appropriate medium) to achieve an absorbance of 0.1 or 0.2, depending to the medium; the main cultures were performed in triplicate for each experimental group. The absorbance of the cultures were measured every 3–4 hours until the cells reached stationary phase (absorbance values at 600 nm >1.5). The absorbance data were analysed using Microsoft Excel. For the plate-based experiments on solid media, the four dots of each culture had absorbance values at 600 nm of 1, 0.1, 0.01 and 0.001. The plate experiments were performed in triplicate.

2.2.11 Real-time reverse transcription PCR

2.2.11.1 Isolation of total RNA from *T. brucei*

T. brucei (5×10^7 cells) were collected by centrifugation at 12,000 *g* and lysed in RNAzol® (1 ml). Then, RNase-free water (0.4 ml) was added and the mixtures were shaken vigorously for 15 seconds. After standing at room temperature for 10 minutes, the supernatants containing RNA were separated by centrifugation at 12,000 *g* for 15 minutes and transferred into RNase-free 2.0-ml Eppendorf tubes. Then, 75% [v/v] ethanol (0.4 ml) was added to each to tube to precipitate the RNA. The samples were subjected to centrifugation at 12,000 *g* for 8 minutes. The white pellets on the sides and bottoms of the tubes that contained the RNA were washed twice with 75% ethanol (0.5 ml) and subjected to centrifugation at 8,000 *g* for 3 minutes at room temperature. The alcohol solution was removed completely with a pipette tip. Finally, the RNA was solubilised in RNase-free water (30 µl) by vortexing for 2–5 minutes and the RNA concentration was assessed with a spectrophotometer as the absorbance at 260 nm.

2.2.11.2 First-Strand cDNA synthesis

Before cDNA synthesis, genomic DNA was removed by DNase I treatment. The RNA (2 µg) was treated with 1 unit of DNase I (2 µl) in 10× reaction buffer with $MgCl_2$ (2 µl) and RNase-free water (to achieve a total volume of 18 µl) at 37 °C for 30 minutes. The reaction was terminated by adding 50 mM EDTA (2 µl) and incubating at 65 °C for 10 minutes. Then, an equal volume of $MgCl_2$ was added to inactivate the EDTA. Next, First-Strand cDNA synthesis reactions (total volume, 20 µl: 10 µl template RNA after genomic DNA removal, 1 µl random primers, 4 µl 5× reaction buffer, 1 µl RiboLock RNase Inhibitor, 2 µl 10 mM dNTP and 2 µl M-MuLV reverse transcriptase) were mixed. DNA synthesis was performed at 25 °C for 5 minutes, followed by 37 °C for 60 minutes. The reactions were terminated by incubation at 70 °C for 5 minutes.

2.2.11.3 Real-time reverse transcription-PCR

The mRNA samples were subjected to one-step real-time reverse transcription (RT)-PCR with the QuantiTect® SYBR® Green RT-PCR Kit. The RNA isolation and genomic DNA removal steps (sections 2.2.11.1 and 2.2.11.2) were followed by quantitative RT-PCR (0.5 µg RNA/12.5 µl reaction). The RT-PCR primers (Appendix 3) designed for use at 55 °C yielded the expected PCR product of 150 bp. The C_T values for the experimental samples (in triplicate) were compared with those for the WT after normalising to the C_T for housekeeping genes (tubulin or TERT) and the fold-changes in expression were calculated.

2.2.12 Northern blot analysis of TbMCP1 gene expression

Total RNA (20 µg) and mRNA (4 µg) were separated on a 1% denaturing formaldehyde-agarose gel and blotted onto a Hybond™-N nylon membrane. The DNA probe for the complete ORF of TbMCP1 was labelled with α^{32}P-dCTP using the Prime-It® Random Primer Labeling Kit. The membranes were pre-hybridised for 30 minutes at 60 °C in hybridisation buffer (5× SSC, 0.1% [w/v] SDS, 5× Denhardt's solution and 100 µg/ml denatured and sheared salmon sperm DNA). After hybridisation at 60 °C overnight, the blots were washed for 30 minutes in 10× SSC with 0.1% [w/v] SDS at room temperature, then for 45 minutes in 1× SSC with 0.5% [w/v] SDS at 42 °C, and for 30 minutes in 0.1× SSC with 0.2% [w/v] SDS at 42 °C. Finally, the blots were exposed to X-ray film.

2.2.13 Determination of substrate consumption and end product formation

T. brucei cells were cultured for 96 hours and cell density was determined every 24 hours. A 3-ml culture sample was collected to determine substrate (proline and glucose) consumption and metabolic end product (acetate, succinate and pyruvate) formation. Prior to the assays, the samples (3 ml) were deproteinated by adding 35% [v/v] perchloric acid (PCA; 100 µl). After incubation on ice for 10 minutes, the samples were neutralised by the addition of neutralisation solution (134 µl; 5 M KOH and 0.2 M MOPS). The protein precipitates were removed by centrifugation at 11,000 *g* for 10 minutes and the protein-free supernatants were collected for analysis. Glucose levels were determined using a glucose oxidase-based method (Bergmeyer & Gawehn, 1974): the precipitated samples (100 µl) and glucose standard (100 µl; 91 mg/l) were mixed with glucose detection reagent (2.5 ml; 100 mM phosphate buffer [pH 7.0], 1 mg/ml HRP, 10 units/ml glucose oxidase and 1 mg/ml 2,2′-azino-bis[3-ethylbenzthiazoline-6-sulphonic acid]). The absorbance at 660 nm was determined after incubation at room temperature for 30 minutes. The glucose concentrations in the samples were calculated using a glucose calibration curve. The proline concentrations were determined using a standard method (Shabnam *et al*., 2015). For the proline assay, the following solution was prepared: cell culture sample (5 µl), water (95 µl), 3% [v/v] sulfosalicylic acid (100 µl), ninhydrin reagent (200 µl; 125 mg ninhydrin, 3 ml 99% acetic acid and 2 ml 6 M phosphoric acid) and glacial acetic acid (200 µl). The reaction was incubated for 1 hour at 95 °C. Then, the reaction was incubated for 10 minutes on ice before toluene (400 µl) was added and the reaction mixture was vortexed vigorously. The reaction mixtures (300 µl) were diluted with toluene (700 µl) and their absorbances read at 520 nm. The proline concentrations of the samples were calculated using a corresponding proline calibration curve.

The concentrations of the metabolic consumption and metabolic end product acetate, pyruvate and succinate were measured according to the manufacturer's protocol using acetate, pyruvate and succinate determination kits (Abcam).

2.2.14 Raising TbMCP1 polyclonal antiserum

The Protean program, included in the 'Lasergene' program package (DNASTAR), was used to select the immunogenic peptide sequence in TbMCP1, e.g. the N-terminal amino acid residues 6 to 25 (HDKSTRQNTAPTSLSKAETK). The peptide (2 mg) was synthesised and coupled to Keyhole Limpet Haemocyanin (KLH). Two guinea pigs were immunised with the peptide (150 ng) in complete Freund's adjuvant and received three individual boosts at three-week intervals in incomplete Freund's adjuvant (150 ng peptide/boost). Finally, the guinea pigs were bled by heart puncture. The peptide synthesis, KLH coupling and guinea pig immunisation were performed by PEPTID.DE (Heidelberg, Germany). The specificity of the generated antiserum was tested by western blot analysis.

2.2.15 Measurement of mitochondrial ATP production

Trypanosomes (1×10^8 cells) were collected by centrifugation at 1,500 *g* for 10 minutes. Then, the cells were washed once with an equal volume of SoTE buffer (20 mM Tris-HCl (pH 7.5), 2 mM EDTA and 0.6 M sorbitol), resuspended in the same buffer (0.5 ml) and transferred to 1.5-ml Eppendorf tubes. The plasma membranes were permeabilised by adding pre-warmed, room-temperature SoTE buffer with 0.016% digitonin (0.5 ml) to the cell suspensions and inverting once. The reactions were incubated for exactly 5 minutes on ice, then immediately subjected to centrifugation for 3 minutes at 8,000 *g* at 4 °C. After centrifugation, the supernatants were removed and the pellets were washed twice with SoTE buffer (1 ml). The pellets containing the mitochondrial fractions were resuspended in assay buffer (0.5 ml; 20 mM Tris-HCl [pH 7.4], 15 mM KH_2PO_4, 0.6 M sorbitol and 5 mM $MgSO_4$) to assess mitochondrial ATP production. Each mitochondrial ATP production assay consisted of a mitochondria-enriched fraction (25 µl) in assay buffer (25 µl) with 20 µmol ADP and 2 mM α-ketoglutarate. Three negative control groups were included: (1) a group treated with carboxyatractyloside (final concentration, 5.2 µM), a highly selective inhibitor of cytosolic-specific mitochondrial ADP/ATP carriers (Vignais *et al*., 1973), for 5 minutes at 30 °C prior to the addition of the substrate; (2) an ADP group with ADP in the absence of the substrate); and (3) a group without ADP or substrate to monitor background ATP. The mitochondrial ATP production reaction was initiated by the addition of substrate. After incubation for 30 minutes at 30 °C, the mitochondrial ATP production reaction was terminated by adding 10 mM Tris-HCl and 1 mM disodium EDTA (pH 8.0; 10 µl) with 0.2% Triton™ X-100. The ATP concentration was measured after adding the luminescent reagent (60 µl) of the Luminescent

Cell Viability Assay. An ATP standard curve, ranging from 0 to 1,000 nM, was prepared using the ATP assay buffer.

Chapter 3: Sequence analysis and functional characterisation of TbMCP1, a putative mitochondrial FAD carrier

3.1 Introduction

Mitochondria play important roles in almost all aspects of the cell, including growth, apoptosis, differentiation, the production of complex cellular substances, the regulation of cellular signalling, and most importantly, the generation of cellular energy in the form of ATP (Stephen and Douglas., 2012).

Similar to the mitochondria from other eukaryotes, also the *T. brucei* mitochondrion requires different cofactors and coenzymes for the functioning of its metabolic pathways. One of these cofactors, e.g. flavin adenine dinucleotide (FAD), is required for the functioning of various mitochondrial pathways in *T. brucei.* Next to being a coenzyme for the mitochondrial acyl-CoA dehydrogenase during β-oxidation, it also functions as a cofactor for pyruvate dehydrogenase (E3), a redox carrier in mitochondrial oxidative phosphorylation (FADH2), and as a prosthetic group in succinate dehydrogenase (Colasante *et al.,* 2009).

FAD must be imported into the mitochondrion from the cytosol, since the mitochondrial inner membrane is impermeable for charged molecules. This transport is facilitated by members of the mitochondrial carrier family (MCF), which are located in the mitochondrial inner membrane (Palmieri *et al*., 2009). Mitochondrial FAD (flavin) transporters have been identified and functionally characterised for different eukaryotes, including the yeast *Saccharomyces cerevisiae* (FLX1) and *Homo sapiens* (SLC25A17) (Palmieri *et al*., 2009)

The *T. brucei* genome contains 26 genes which encode for 24 different MCF proteins (TbMCP1–24; Colasante *et al*., 2009). The identified *T. brucei* MCF proteins have been confirmed as part of this family by sequence analysis and reciprocal database searches (BLASTP). Moreover, these TbMCPs share significant (~39%–78%) amino acid sequence similarity with previously characterised MCF proteins in *S. cerevisiae* and *Homo sapiens* (Colasante *et al.*, 2006; Colasante *et al.*, 2009). A previously published study indicated that one of the identified TbMCPs, e.g.TbMCP1, shows significant similarity to the functionally characterised mitochondrial flavin transporters FLX1 and SLC25A17 (Colasante *et al.*, 2006; Colasante *et al.*, 2009).

This chapter will address the results of the identification and functional characterisation of TbMCP1, a putative mitochondrial FAD transporter of *T. brucei*. First, the protein sequence of TbMCP1 was analysed and compared to known and functionally characterised mitochondrial carrier family proteins from other eukaryotes. The protein sequence was also subjected to phylogenetic reconstruction. Second, immunofluorescence microscopy and subcellular fractionation was used to confirm the exclusive mitochondrial localisation of TbMCP1.

Northern blotting was performed to assess TbMCP1 expression in two of the main life cycle stages of *T. brucei*, e.g. the bloodstream form (BSF449) and the procyclic (insect) form (PCF449) of *T. brucei*. The importance of TbMCP1 was assessed by down-regulating the expression of TbMCP1 by RNAi and the analysis of *T. brucei* growth under different culture conditions. Finally, the consumption of metabolic substrates and the production of various metabolic intermediates and end products was measured to determine if TbMCP1 does play a role in the energy generation in *T. brucei*.

3.2 Results

3.2.1 Phylogenetic reconstruction and sequence alignment of TbMCP1

Various approaches have been used to identify the putative transport functions of TbMCPs. Phylogenetic reconstruction and reciprocal BLAST analysis revealed the similarities between TbMCPs and the MCP proteins that have been functionally characterised in other eukaryotes (Colasante *et al*., 2009). Human (SLC25A) and *S. cerevisiae* MCF proteins were functionally characterised by physiological or genetic experiments focused on subgroups of substrates or in *in vitro* proteoliposome-based transport assays (Palmieri *et al.*, 2004; Palmieri *et al.*, 2006). The transport function of a carrier can be deducted from the conserved substrate contact points CPI CPII and CPIII, which were previously shown to be essential for binding and transport of the different substrates (Robinson and Kunji., 2006). Among the different substrate contact points, CPIII is the most defining and conserved one in terms of substrate recognition, whereas CPI and CPII can be more variable between MCF proteins transporting similar substrates (Colasanate *et al*., 2018). MCF proteins require particular amino acids in the right position in the substrate binding pockets in order to recognise a specific substrate (Robinson and Kunji., 2006). The BLAST comparisons of yeast and human MCF proteins with TbMCP1 suggested that the *T. brucei* protein is homologous to the FAD carrier. In addition, the BLAST analysis of TbMCP1 against the eukaryotic protein database (http:/www.ncbi.nlm.nih.gov) retrieved potential mitochondrial flavin transporters from multiple species, such as FLX1 from *S. cerevisiae* and PMP34 from mammals like *Homo sapiens* and *Mus musculus*. The predicted function of TbMCP1 as a mitochondrial flavin transporter was further assessed by phylogenetic reconstruction (Saitou & Nei, 1987; Figure 3.1). The resulting of the phylogenetic tree revealed that TbMCP1 and homologous sequences from the trypanosomatids *T. cruzi* and *L. major* formed a separate clade, which was supported by high(>0.90%) bootstrap values.

Figure 3.1 also shows that TbMCP1 clustered within a group of sequences that encompasses the two flavin carriers from *S. cerevisiae* and *S. pombe* (bootstrap value: 0.94%) and the different peroxisomal ATP carriers found in mammals, *Xenopus laevis* and *Candida boidinii* (bootstrap value: 0.99%). Bootstrapping involves repeating the phylogenetic analysis on a random subset of the data; the reported value is the percentage of bootstrap replicates in which the node appeared (Harrison., 2006). Thus, a bootstrap value of 0.99 means that the node is well supported as it appeared in all bootstrap replicates. This essentially means that more than 0.99% of the 1000 different trees show the same node. The branching at this point is consistent and reliable

Moreover, BLAST analysis of the TbMCP1 sequence against the genome databases of the related kinetoplastids *T. cruzi* and *L. major* (accessible at http://www.genedb.org) revealed the genes with high amino acid sequence similarity to TbMCP1. These genes also appeared in equivalent positions in a three-way alignment of the relevant *T. brucei*, *T. cruzi* and *L. major* chromosomes (El-Sayed *et al*., 2005).

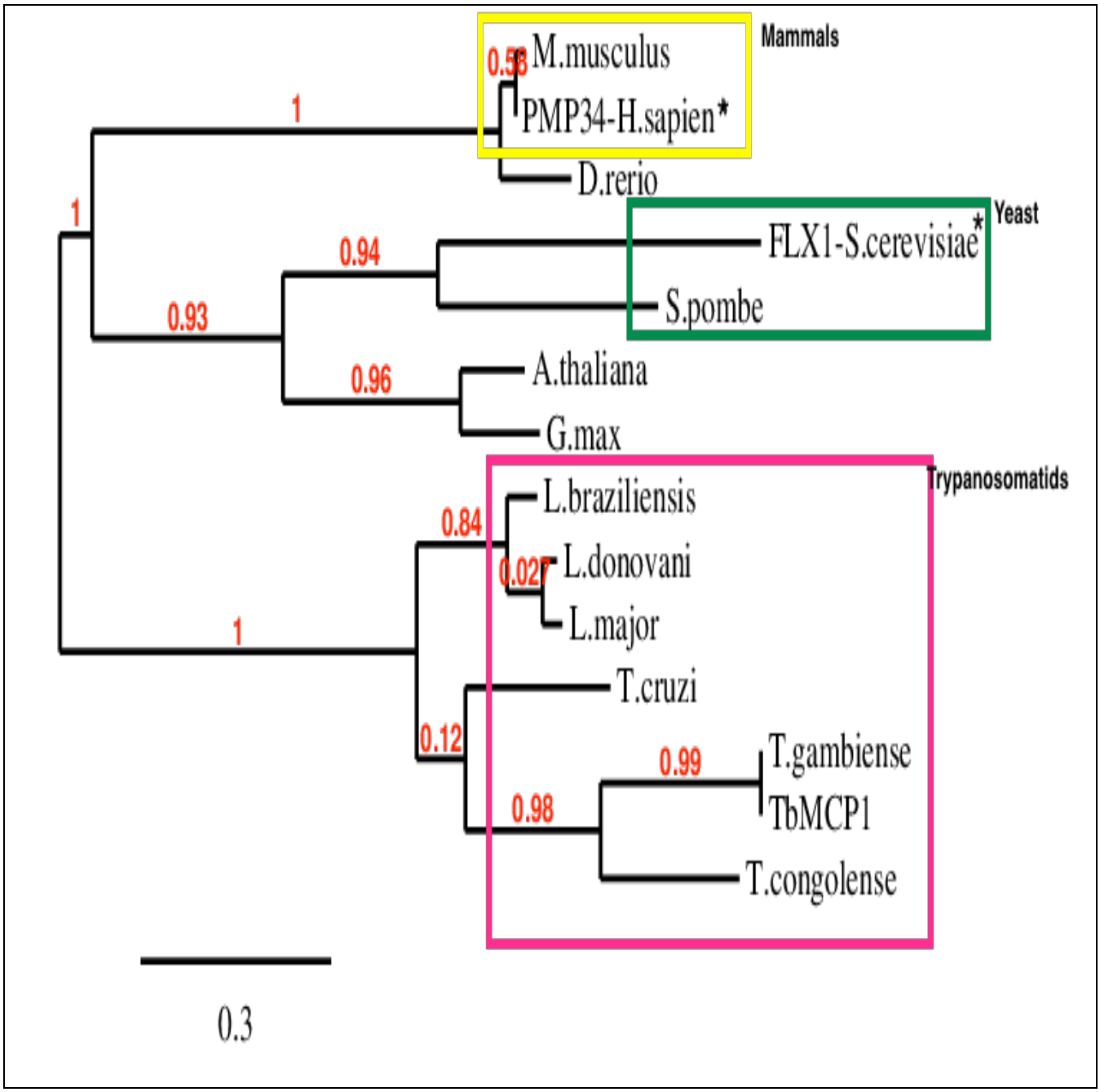

Figure 3.1. A phylogenetic tree depicting the relationship of TbMCP1 to other MCF proteins. The maximum likelihood tree shows the evolutionary relationship between TbMCP1 in mammals (yellow), yeast (green) and trypanosomatids (pink). The colours indicate the clustering of carriers with the same transport function. The bootstrap values, located at each node, represent the percentages after resampling analysis of 1,000 iterations. Functionally characterised FAD transporters (*H.sapien* (PMP34) and *S.cerevisiae* (FLX1) are labelled with '*'.

TbMCP1 exhibits all of the conserved sequence and structural features characteristic of MCF proteins (Figure 3.2). Its sequence consists of three conserved, repetitive, domains of approximately 100 amino acids and each domain contains two transmembrane (TM) α-helices and a canonical MCF protein signature sequence (Palmieri *et al* , 2004; Colasante *et al*., 2009). The MCF protein signature sequence is the hallmark of all MCF proteins: it comprises the amino acid sequence 'PX[D/E]XX[K/R]X[K/R][20–30 residues][D/E]G[4–5 residues][W/F/Y][K/R]G', where 'X' represents any amino acid residue (Palmieri *et al.*, 2012). The first part of the motif, 'PX[D/E]XX[K/R]X[K/R]', is located at the C-terminal end of the odd-numbered TM helices H1, H3 and H5, whereas the second part of the sequence, '[D/E]G[45 residues][W/F/Y][K/R]G' is located after the amphipathic helices h1–2, h3–4 and h5–6 (Figure 3.2). The conservation of the signature sequence in TbMCP1 was analysed by comparing it with the corresponding signature sequences from *S. cerevisiae* and *H. sapiens* (Figure 3.2). The majority of the amino acid residues in the first part of the signature sequence (M1, M2 and M3) appeared to be conserved, including (1) the highly conserved proline (P) found at the start of the M1, M2 and M3 motifs; (2) the conserved acidic amino acid residue, either an aspartic acid (D) or glutamic acid (E), at position 3 of the same motifs; and (3) the positively charged amino acid, either a lysine (K) or an arginine (R) (Figure 3.2A, B). In contrast to the first part of the sequence signature, the second part of the signature sequence was less conserved (Figure 3.2). The first two amino acids of the motif, '[D/E]G', were not well conserved and the number of amino acids (X) between '[D/E]G' and '[W/F/Y][K/R]G' also varied. The final glycine (G) of the motif, which confers flexibility to the loop that links the two helices, was highly conserved in nucleotide carriers (Palmieri *et al.*, 2012). In MCF proteins, the groups of conserved amino acids located downstream of each signature motif participate in substrate discrimination, recognition and binding. The well-conserved CPI, CPII and CPIII have been extrapolated for all MCF proteins that transport similar substrates (Kunji & Robinson, 2006; Palmieri *et al.*, 2011). The protein sequence alignments revealed that CPI (SAY) and CPII (IV) of the mitochondrial flavin carriers were conserved (Figure 3.2). Apart from the signature features described above, additional amino acids were found to be conserved, such as the glutamic acid (E) and histidine (H) located in helix 1 before M1a, as well as the glycine (G) in CPI. In addition, the arginine (R) immediately before CPIII was conserved in all species tested. In 2006, Kunji and Robinson identified two clusters of conserved, highly symmetric residues in the MCF transporter proteins, which form salt bridge networks. These salt bridge networks can open or close the passage to mediate substrate

transport. The first clusters were found on H1, H3 and H5 on the matrix side of the transporter, which consists of the PX[DE]XX[RK] motif, whereas the second cluster, which consists of the [FY][DE]XX[RK] motif, is located on the cytoplasmic side of H2, H4 and H6. The matrix and cytoplasmic networks can open or close the passage to mediate substrate transport (King *et al* ., 2016). The salt bridge networks were highly conserved among the aligned sequences (Figure 3.2).

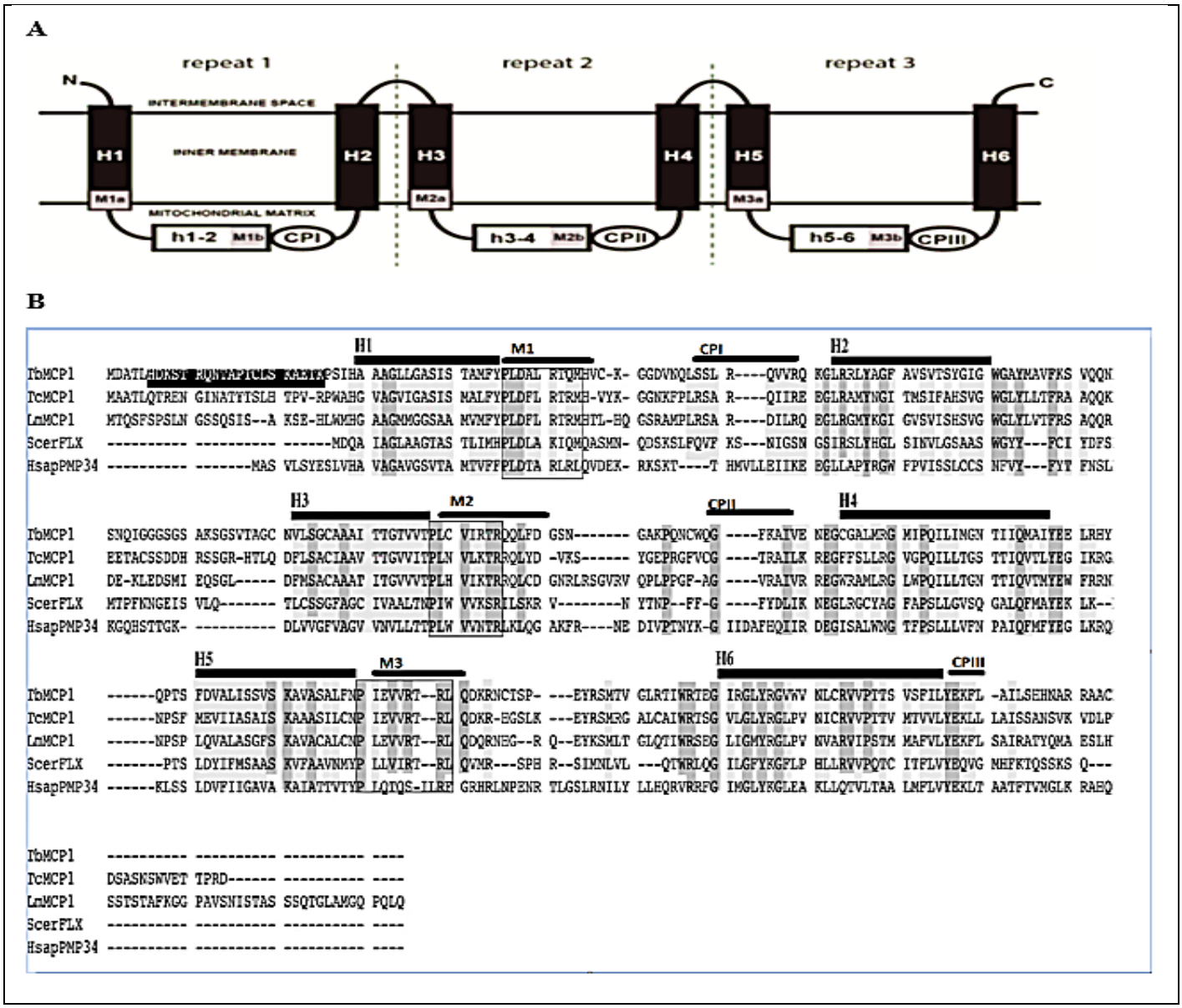

Figure 3.2. TbMCP1 contains the characteristic amino acid sequence features of conventional MCF carriers and the functional residues conserved in FAD carriers. **A**: Schematic representation of MCPs. The protein structure consists of six TM helices (H1–6) linked by hydrophilic loops (h1–2, h3–4 and h5–6). M1a, M2a and M3a comprise the first segment of the signature sequence motif, PX[D/E]XX[K/R]X[K/R], which is located at the end of the odd-numbered TM helices. M1b, M2b and M3b comprise the second part of the motif, [D/E]G[*n* residues][K/R]G, which is located at the end of each hydrophilic loop. **B**: Multiple sequence alignment of TbMCP1 and the corresponding human and yeast sequences. The amino acid sequences were aligned using Clustal Omega. H1–H6 represent the six TM helices. CPI, CPII and CPIII are located next to TM H1, H3 and H6, respectively. Grey bands indicate similar conserved amino acid residues.

3.2.2 Knockdown of TbMCP1 caused a growth defect in *T.brucei*

Various approaches, including gene knockout or knockdown, can be used to study the effects of the TbMCP1 gene on the growth of *T. brucei* PCF449. In this experiment, the TbMCP1 gene was knocked down using RNAi. RNA interference (RNAi) was used to determine whether expression of TbMCP1 is essential for the growth and survival of *T. brucei*. The resulting growth phenotype can further give valuable information regarding the respective physiological functions of TbMCP1. The expression of TbMCP1 in *T. brucei* was down-regulated ("knocked-down") by using an RNAi-approach (section 2.2.3). It was previously reported that the introduction of single-stranded antisense RNA is not appropriate for the modification of *T. brucei* as the parasite can destroy the RNA during its growth phase (10 to 14 days) (Ngô *et al.*, 1998). Thus, in this experiment, RNAi-approach is based on the expression of double-stranded (sense + antisense) RNA molecules for TbMCP1, respectively, leading to a reduced or depleted expression of the targeted protein in *T. brucei*.

3.2.2.1 Knockdown-related plasmid construction

RNAi was performed by the simultaneous expression of the sense and corresponding antisense RNA molecules of the targeted gene sequences (Appendix 4) (Bringaud *et al.*, 2000). Primers were designed to PCR amplify a 990 bp sense and an antisense version of the open reading frames of TbMCP1. The primers included the unique restriction sites *Bam*HI, *Apa*I, and *Hind*III, allowing the site-directed cloning of the sense and antisense DNA products in the *T. brucei* expression vector pHD676 (Appendix 5, section 5.1). The antisense primer for TbMCP1 gene was designed to include the *Bam*HI and *Apa*I restriction sites, whereas the primer for the sense DNA fragment was designed to include the *Apa*I and *Hind*III restriction sites. The sense and antisense DNA PCR products were cloned in tandem and joined at the *Apa*I site behind an inducible *T. brucei* promotor in the vector pHD676. Expression from the pHD676 vector will lead to the formation of a double-stranded RNA molecule connected by a short single stranded loop at the 3' end. Such a structure was shown to be more stable and more effective than a single-stranded antisense RNA molecule for the down-regulation of expression in *T. brucei* (Ngô *et al.*, 1998).

The resulting pHD676+TbMCP1(sense + antisense) RNAi construct was analysed by using PCR, restriction enzyme digestion and gel electrophoresis to determine whether it contained the correct DNA fragments in the right order. Positive clone was further sent for sequencing (Eurofins MWG). The sequencing results confirmed that the used construct was indeed correct.

The verified pHD676+TbMCP1 RNAi construct was used to transfect the *T. brucei* cell line PCF449 (section 2.2.5) and positive clonal cell lines were isolated. For comparison (same genetic background), a *T.brucei* PCF449 cell line was generated containing an empty (no insert) version of plasmid pHD676. Growth of the generated TbMCP1 RNAi and PCF449+pHD676 cell lines was analysed in MEM-Pros medium (Appendix 1) containing 5 mM proline and 0.12 mM glucose as carbon sources. RNAi was induced by the addition of tetracycline to the culture medium (section 2.2.4.2). Growth curves were plotted using Microsoft® Excel (Figures 3.3).

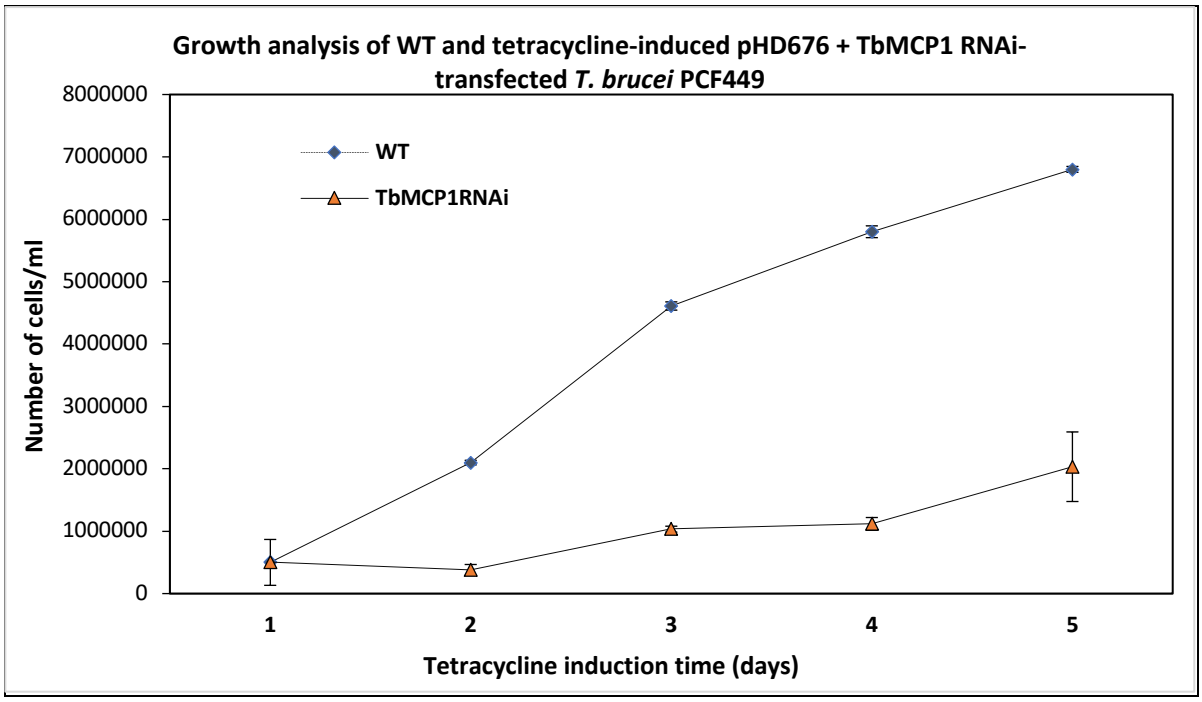

Figure 3.3. Comparison of the growth phenotypes of "wildtype" *T. brucei* PCF449 (WT) and tetracycline-induced pHD676+TbMCP1 RNAi cell lines in standard MEM-Pros medium containing 5 mM proline and 0.12 mM glucose. Cultures were started with 1×10^6 cells/ml and counted every 24 hours for five days. The data points represent the mean and standard deviation of three independent experimental replicates.

Upon induction with tetracycline, the TbMCP1 RNAi cell line presented a significant reduction in growth when compared to the 'wildtype" *T. brucei* PCF449 cell line, suggesting that TbMCP1 protein is essential for growth and thus the survival of T. *brucei*.

3.2.3 TbMCP1 is predominantly expressed in the PCF of *T. brucei*

It was unknown if the life cycle stages of *T. brucei* determined the expression of TbMCP1. Colasante *et al*. (2006 & 2012) reported that the expression of some TbMCPs is dependent on the life cycle stage of the parasite. Northern blot analysis (Section 2.2.12) with the TbMCP1 ORF, produced a single hybridising band of approximately 2.0 kb, indicated that the levels of TbMCP1 mRNA were similar in the BSF449 and PCF449 of *T. brucei* (Figure 3.4A). Hybridisation with total RNA (20 μg) produced a weak signal (Figure 3.4A, lane 1), but a stronger band was produced with poly(A)$^+$-enriched RNA (4 μg; Figure 3.4A, lane 2). Based on the rules for the prediction of mRNA processing in *T. brucei* (Benz *et al.*, 2005) and assuming that the current annotation of the downstream ORF is correct, *trans*-splicing is predicted at the AG dinucleotide at position 36 with a 3' untranslated region of 750 nucleotides. This would produce a predicted polyadenylated RNA of approximately 2 kb, in agreement with the measured size (Figure 3.4A).

The up-regulation of the expression of TbMCP1 in the PCF449 was confirmed at the protein level by western blotting (Figure 3.4 B). An antibody against the N-terminus of TbMCP1 (Section 2.2.14) detected a band of the predicted size (35 kDa) in the PCF449 but not the BSF449. However, the TbMCP1 antiserum also detected bands other than that for the TbMCP1 protein (Figure 3.5B), suggesting that the antiserum is not specific for TbMCP1. Therefore, apart from the expected (specific) 35kDa band, two other HMW bands reacted with the antibody suggested that the raised antibody is not specific enough. Hence it cannot be used for immunofluorescence microscopy(section 3.2.4). The expression in the two different life cycle stages follows the same trend as seen for the mRNA (much higher in PCF449, suggesting an important function in this life cycle stage).

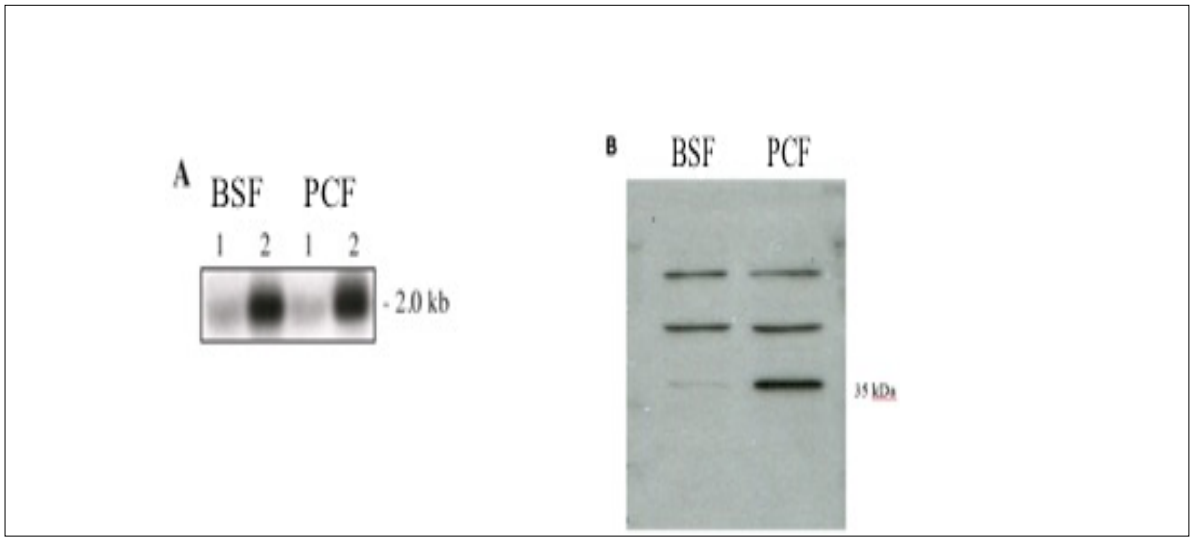

Figure 3.4. TbMCP1 protein expression. **A**: Northern blot analysis of total RNA (20 µg; lane 1) and enriched mRNA (4 µg; lane 2) from *T. brucei* BSF449 and PCF449 probed with dCTP-labelled TbMCP1 DNA. **B**: Western blot of *T. brucei* PCF449 and BSF449 samples with TbMCP1 antiserum. Each lane was loaded with an equal number of cell equivalents (2×10^6). The results represent five independent experiments.

3.2.4 TbMCP1 localised to the mitochondrion of *T. brucei* PCF449

The subcellular localisation of TbMCP1 in the PCF449 of *T. brucei* was investigated using immunofluorescence microscopy. Since the raised TbMCP1 antisera detected protein bands other than that for TbMCP1, it could not be used to determine the localisation of TbMCP1. Therefore, a recombinant myc-tagged version of TbMCP1 was expressed instead, allowing the use of the commercially available myc antibodies.

3.2.4.1 Plasmid construction

The ORF of TbMCP1 was amplified by PCR using primers with added unique *Hind*III and *Bam*HI restriction sites. The PCR product was cloned into the pGEM®-T Easy vector and the construct (10 µl) was sequenced (Eurofins MWG). Then, the ORF of TbMCP1 was subsequently cloned into the *T. brucei* expression vector pHD1484 vector using the *Hind*III and *Bam*HI restriction enzyme sites resulting in the pHD1484-TbMCP1-cmyc^{ti} construct. The tetracycline inducible expression from pHD1484 will add a double myc-tag to the c-terminal of TbMCP1.

3.2.4.2 Subcellular localisation

The *T. brucei* PCF449 cell line was transfected with pHD1484-TbMCP1-cmyc^{ti} and expression of the myc-tagged version of TbMCP1 was induced by addition of tetracycline (section 2.2.6). Immunofluorescence microscopy was performed using a commercial available myc antibody (Figure 3.5A). The immunofluorescence microscopy results showed a specific tubular shaped staining of PCF 449 *T. brucei* when using the myc antibody, which recognises myc-tagged TbMCP1. This staining pattern was identical to the one obtained for MitoTracker, which is

used as a mitochondrial marker for *T. brucei*. This result confirmed the mitochondrial localisation of TbMCP1 in *T. brucei* PCF449.

The localisation of TbMCP1 was further investigated by subcellular fractionation of *T. brucei* PCF449, followed by western blotting. TbMCP1 cofractionated with the mitochondrial marker α-LPHD (Figure 3.5B, fractions 8–12) (Schonek, 1997). No TbMCP1 was detected in fractions 13–16 (Figure 3.5B), which contained the glycosome marker αGIM5 (Lorenz, 1998). These findings suggested that TbMCP1 exclusively localises to the mitochondria of *T. brucei* PCF449.

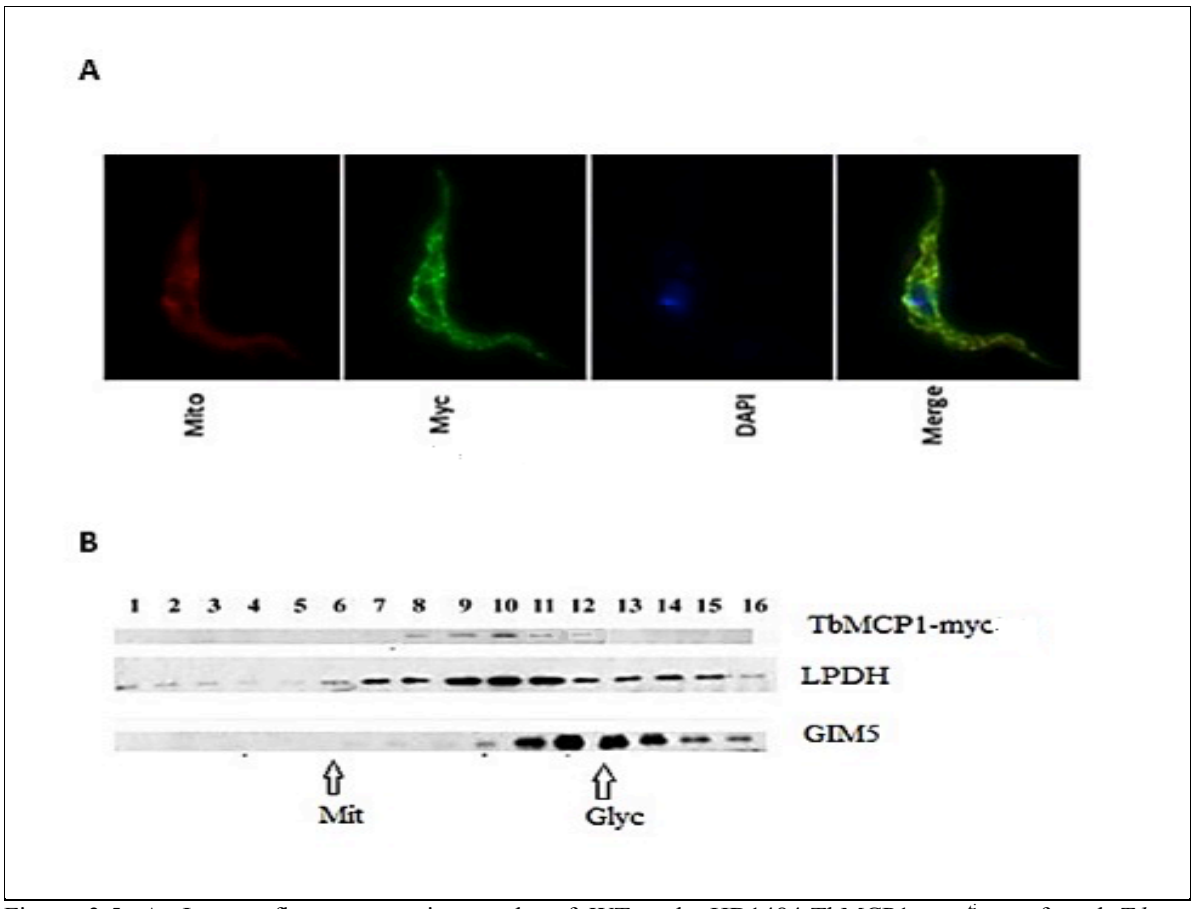

Figure 3.5. **A**: Immunofluorescent micrographs of WT and pHD1484-TbMCP1cmyc^{ti}-transfected *T.brucei* PCF449 cell lines. The MitoTracker (Mito; red), TbMCP1-myc antibody (green) and DAPI (blue) signals were merged to form the overlay. The images represent three independent experiments. **B**: Western blot analysis of *T. brucei* PCF449 cell lysate fractions (15 µg/lane) separated on an iodixanol-sucrose gradient. The anti-LPDH antibody was used to detect fractions containing mitochondria (Mito). The anti-GIM5 antibody detected fractions containing glycosome (Glyc). TbMCP1 was detected using the commercial anti-myc antibody. Fraction 1 is at the top of the gradient and fraction 16 is at the bottom. The results are representative of seven independent experiments.

3.2.5 TbMCP1 over-expression increased metabolic flux

The phylogenetic reconstruction and sequences analysis (Section 3.2.1) suggested that TbMCP1 is likely to be a FAD transporter. FAD is involved in energy generation as a cofactor or prosthetic group for succinate dehydrogenase and pyruvate dehydrogenase and as a redox carrier in mitochondrial oxidative phosphorylation (Besteiro *et al*., 2005). *T. brucei* uses glucose, proline or a combination as its main substrate for ATP generation, during which succinate, acetate, pyruvate, lactate and glycerol are formed as metabolic intermediates and end products (Besteiro *et al*., 2005). Therefore, in this study, substrate consumption and the concentrations of metabolic intermediates and end products were quantified in *T. brucei* PCF449 and tetracycline-induced TbMCP1 cells to investigate if the over-expression of TbMCP1 altered trypanosome metabolism. The concentrations were measured in WT(cloned in empty vector) and TbMCP1-over-expressing cells cultured in low- and high-glucose MEM-Pros medium.

Therefore, the *T.brucei* PCF449 WT and TbMCP1-over-expressing strains grown in low- and high-glucose media, the concentrations of proline and glucose that were consumed and the concentrations of succinate, pyruvate and acetate that were formed were measured after 60 hours (Figure 3.6). In the high-glucose medium, the proline flux was slightly lower over time for both strains than in the low-glucose medium (Figure 3.6A). Trypanosomes prefer to use glucose rather than proline to produce energy; the presence of glucose represses proline metabolism (Lamou *et al*., 2005). However, in the same medium, the TbMCP1-over-expressing strain consumed almost 2.5 times more glucose than the WT cells. In contrast, in the low-glucose medium supplemented with 10 mM proline, proline flux increased for the TbMCP1-over-expressing strain but decreased for the WT over time (Figure 3.6B). Analysis of the main metabolic end products suggested that the types of metabolic pathways used did not change in the TbMCP1-over-expressing trypanosomes, but that the rate of metabolism was higher upon TbMCP1 over-expression (Figure 3.6A, B). In the high-glucose medium, the production of acetate was approximately 2.6-fold higher by the TbMCP1-over-expressing cells than by the WT cells, which paralleled the increase in glucose consumption. The results for the other metabolites were similar (Figure 3.6A). In the low-glucose medium, a similar increase in the specific flux of proline and its metabolites was observed. These results suggested that TbMCP1 over-expression did not affect the pattern of metabolism, but resulted in the uncoupling of growth and metabolism.

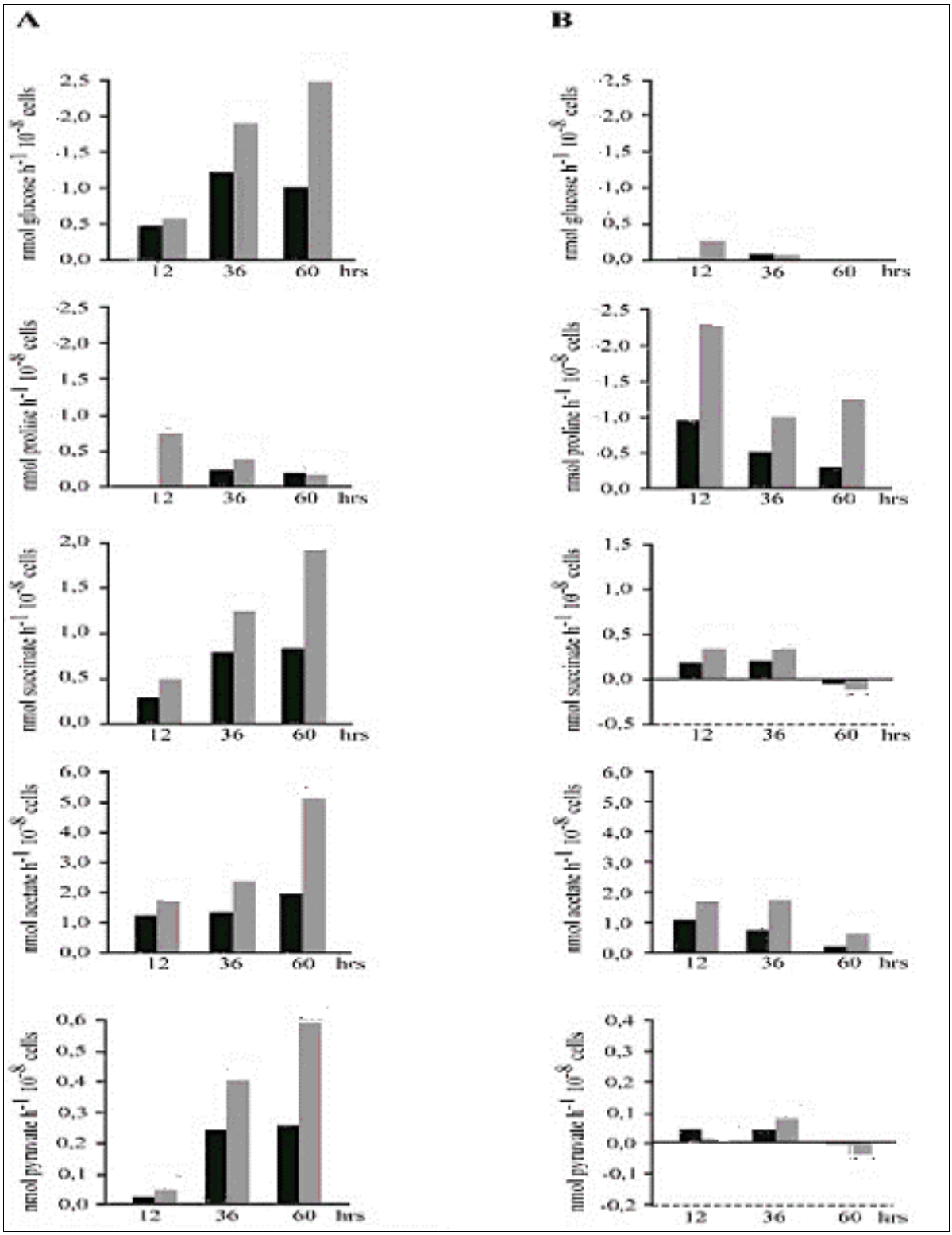

Figure 3.6. The concentrations of the substrates consumed (glucose and proline) and the metabolic end products (pyruvate, succinate and acetate) in cultures of WT (black) and TbMCP1-over-expressing (grey) *T. brucei*. **A:** Cultures in high-glucose MEM-Pros medium. **B:** Cultures in low-glucose/high-proline MEM-Pros medium. The results are representative of two independents experiments.

3.3 Discussion and Conclusion

TbMCP1 is an MCF protein in *T. brucei*. Its transportation of substrates across the mitochondrial membrane still remains to be determined. Previous phylogenetic reconstruction studies have suggested that TbMCP1 is a putative carrier for either ATP/AMP or mitochondrial flavin (Colasante *et al.*, 2006). The peroxisomal ATP/AMP carrier in humans has been proposed to play an important role in supplying ATP for peroxisomal β-oxidation in mitochondria via exchange for AMP (Palmieri *et al.*, 2001; Lasorsa *et al.*, 2004). In yeast, the FAD transporter have an important role in maintaining the normal activity of mitochondrial FAD binding enzymes, including succinate dehydrogenase and lipoamide dehydrogenase (Giancaspero *et al.*, 2008). In this study, BLAST analysis suggested that TbMCP1 is more closely related to the yeast(FLX1) than the human (PMP34) FAD carrier, which was supported by a high bootstrap value. In addition, the in-depth TbMCP1 amino acid sequence alignment with yeast molecules indicated that the first of the signature motif were almost entirely conserved, suggesting that TbMCP1 is more likely FAD transporter.

The classification of TbMCP1 as a possible mitochondrial flavin carrier is partially based on its similarity to yeast FLX proteins. FLX proteins play important roles in cellular flavin homeostasis (Giancaspero *et al.*, 2015). However, TbMCP1 precise transport function is not clear at this point and need further experiments such as transport assay experiment.
Nearly all functionally characterised MCF proteins localise to mitochondria however, a few do localise to other cellular compartments. The *Ant1p* gene in yeast localises to peroxisomes although it has all of the conserved features of mitochondrial MCF proteins (Palmieri *et al*., 2001; Lasorsa *et al*., 2004). In addition, the *Ant1p* gene plays an important role in the transport of ATP into the peroxisome via exchange for cytosolic AMP; it may also play a role in lipid biosynthesis (Palmieri *et al*., 2001; Lasorsa *et al*., 2004).

On the other hand, TbMCP6 has been identified as a putative ATP/Mg-Pi carrier in the mitochondria of the BSF449 and PCF449 of *T. brucei*. Thus, regardless of the presence of conserved sequences, it is essential to experimentally determine the localisation of each MCF protein in *T. brucei*. In this study, TbMCP1 was found to localise exclusively to the mitochondria of the PCF449 of the trypanosome using immunofluorescence microscopy and western blotting of *T. brucei* subcellular fractions. A surplus of ATP is generated in mitochondria by substrate-level or oxidative phosphorylation and ATP, ADP and AMP levels

are equilibrated by adenylate kinases (Allemann *et al*., 2000; Coustou *et al.*, 2005; Lamour *et al.*, 2005; van Weelden *et al.,* 2005).

The expression of TbMCP1 mRNA and protein in different forms of the trypanosomes varied dramatically. These findings are consistent with polycistronic transcription in trypanosomes, which necessitates the regulation of gene expression at the post-transcriptional level (Daniels *et al.*, 2010). The observed variation in TbMCP1 expression in the BSF449 and PCF449 further supported the substantial differences in the methods of ATP production in *T. brucei* at its various life cycle stages. The BSF depends mainly on glycolysis to generate ATP, whereas the PCF449 uses a complex mechanism dependent on proline degradation through oxidative and substrate-level phosphorylation (Tielens & van Hellemond, 1998; Hannaert *et al.*, 2003a; Chaudhuri *et al.*, 2006; Michels *et al.*, 2006; Tielens & van Hellemond, 2009).

TbMCP1 gene replacement and RNAi studies revealed that ΔTbMCP1 trypanosomes have impaired growth compared to that of WT cells at high cell densities. This finding suggests that TbMCP1 is essential for the survival of the PCF449 of *T. brucei*, with a possible role in *T. brucei* kinetoplast division (Voncken *et al.*, 2006). Knockout of the FLX1-encoding gene (flavin transporter) in yeast resulted in respiratory deficiency under normal growth on fermentable carbon sources but very poor growth on non-fermentable substrates (Turcotte *et al*., 2009). The low concentration level of mitochondrial FAD in FLX1 knockout strains suggested that FLX1 is included in flavin transporting (Turcotte *et al*., 2009).

The metabolites measurements, in the knock down strain revealed that, there is a change in flux (2.5 times more substrate consumed and end product formed) but no differences in concentration of different formed end products. This suggest that the metabolic pathways themselves are not affected, but that most probably the linked energy production is affected. The cells try to compensate for the lower energy production efficiency by pushing more substrate through the metabolism, which will not help since there is not enough FAD in the mitochondrion. That a knock down of an FAD carrier affects energy production is not surprising at all as , FAD is an essential cofactor/coenzyme of enzymes/proteins involved in the electron transport chain/OXPHOS and is an important electron carrier in the mitochondrion. Less FAD suggests to the cell that there is a problem with energy production and by ramping up the metabolic flux and it tries to compensate .

So, in contrast to the FLX1 deficiency in yeast, TbMCP1 deficiency seemed to accelerate the mitochondrial pathways in which flavin-dependent enzymes were involved. In yeast and mammals, flavin mononucleotide (FMN) and FAD are synthesised from riboflavin. Both flavins are essential cofactors of dehydrogenases and oxidases, which play a crucial role in cellular bioenergetics. The homeostasis of flavin is regulated by a mitochondrial riboflavin/FAD cycle, which includes the uptake of riboflavin into the mitochondria, its conversion to FMN and FAD, and the recovery of riboflavin in flavoprotein degradation (Giancaspero *et al.*, 2015 *et al*). Moreover, FAD has different functions in metabolic pathways , this include nucleotide biosynthesis , amino acid catabolism, DNA repair , electron transport, beta oxidation of fatty acid and as synthesis of the cofactors such as CoA. In TCA cycle, FAD bound the succinate dehydrogenase (complex II in the electron transport chain) to catalyse the oxidation of succinate to fumarate (Kim *et al*., 2013)

Close analysis of the *T. brucei* genome (http://www.genedb.org; Berriman *et al.,* 2005) indicates that it contains a mitochondrial riboflavin kinase (*Tb*09.211.3420) that enables the production of FMN from riboflavin, but lacks other enzymes of the mitochondrial riboflavin/FAD cycle, such as FAD synthase, FAD pyrophosphatase and FMN phosphohydrolase. Thus, riboflavin and FAD must be imported from the environment. The MEM-Pros culture medium for the PCF449 of trypanosomes (Overath, 1986) contains 300 nM riboflavin, which is comparable to the concentration in human serum (Hustad *et al.*, 1999; Hustad *et al.,* 2000). The other flavins, FAD (up to 26 nM) and FMN (up to 3 nM), must be derived from the supplemented serum.

ΔFLX1 yeast have a respiratory defect ,they undergo normal growth on fermentable carbon sources, but very poor growth on non-fermentable substrates (Bafunno *et al.,* 2004). Isolated ΔFLX1 mitochondria can import riboflavin, FMN and FAD, but are unable to export FAD. The mutants had lower mitochondrial FAD-dependent enzyme activities than the WT strain (Bafunno *et al.*, 2004).

In conclusion, the results of this study suggested that TbMCP1 is a flavin carrier that is essential for *T. brucei* survival. The over-expression of TbMCP1 did not affect overall metabolism patterns, but appeared to enhance flux through specific pathways. The role of TbMCP1 as a flavin carrier will further investigate using functional reconstitution experiments in the following chapters. In particular, yeast functional complementation was used to determine if TbMCP1 could rescue the growth of ΔFLX1 yeast.

Chapter 4: Sequence analysis and functional characterisation of TbMCP15 and TbMCP16, putative mitochondrial ADP/ATP carriers

4.1 Introduction

The ADP/ATP carrier is one of the most abundant proteins in the mitochondrial inner membrane (Kunji *et al*., 2016). This carrier plays an essential role in the cellular energy metabolism by exporting ATP from the cytosol in exchange for ADP, an exchange that is vital for the eukaryote energy metabolism (Palmieri *et al*., 2006). In all eukaryotes, the mitochondrial ADP/ATP carrier exists as different isoforms, which have arisen by gene duplication (Traba *et al*., 2011). In the yeast *Saccharomyces cerevisiae*, three different isoforms (AAC1, AAC2 and AAC3) exist, whereas in *Homo sapiens* four different isoforms are present (hANT1, hANT2, hANT3 and hANT4) (Palmieri *et al*., 2009). These different AAC isoforms were shown to play different physiological roles (Palmieri *et al*., 2016).

Reciprocal BLASTP analysis against sequences of known and functionally characterised ADP/ATP carrier proteins from *H. sapiens* and *S. cerevisiae* revealed that the genome of *T. brucei* contains 3 putative ADP/ATP carrier-encoding genes, e.g. TbMCP5, TbMCP15 and TbMCP16. One of these genes, here TbCMP5, was previously functionally characterised (Colasante *et al*., 2009). Its gene product was shown to function as an ADP/ATP carrier, and subsequent gene knockout studies revealed that TbMCP5 is essential for the survival of *T. brucei* under specific cell culture conditions, e.g. with no glucose, but mainly proline as a carbon source in the cell culture medium (Colasante *et al*., 2009). When grown in the absence of glucose, *T. brucei* is only capable of generating ATP through the degradation of proline by oxidative phosphorylation, a process which exclusively takes place in the trypanosome mitochondrion (Lamour *et al*., 2005; Coustou *et al*., 2008; Ebikeme *et al*., 2010). This process requires the expression and full functionality of an ADP/ATP carrier in the mitochondrial inner membrane in order to sustain the supply of ADP in exchange of ATP formed in the mitochondrial matrix (Colasante *et al*., 2012). The aim of this chapter was to functionally characterise the other two putative ADP/ATP carriers, e.g. TbMCP15 and TbMCP16, using an approach similar to the one used in Chapter 3.

4.2 Results

4.2.1 Phylogenetic reconstruction and sequence alignment of TbMCP15 and TbMCP16

Sequence analysis of *T. brucei* TbMCP15 revealed considerable sequence similarity to prototypical AACs from higher eukaryotic organisms. Its sequence similarities with *S. cerevisiae* and *H. sapiens* AACs was 45% and 47%, respectively. These are considered to be high values for *T. brucei* since MCF protein proteins, in evolutionary terms, are highly divergent and only the few amino acids required for transport and substrate recognition are conserved across most eukaryotes (Boudko *et al*., 2012). Other amino acids are far less conserved apart from their role in maintaining the conserved secondary protein structure of the transporter, including its 6 hydrophobic TM domains and the hydrophilic loops extending into the mitochondrial matrix and inner membrane space.

The transport function of MCF proteins can be deducted from the conserved substrate contact points CPI, CPII and CPIII, which were previously shown to be essential for binding and transport of the different substrates (Robinson and Kunji., 2006). Among the different substrate contact points, CPIII is the most defined and conserved one in terms of substrate recognition, whereas CPI and CPII can be more variable (Colasante *et al*., 2018). Substrate recogntion requires particular amino acids in the right position in the substrate binding pockets in order to bind a specific substrate.

Detailed sequence analysis using the *S, cerevisiae* and *H. sapiens* AAC protein sequences for comparison, showed that the substrate contact points CPI, CPII and CPIII, which are involved in the binding of the substrates ADP and ATP, were partly conserved in TbMCP15 (Figure 4.1). All previously characterised AACs contain the conserved CPI sequence motif 'RXXXTXXXN', where X indicates any amino acid. However, TbMCP15 possesses an 'SXXXVXXXH' motif. Similarly, CPII from TbMCP15 was partly conserved. In all characterised AACs, the 'GI' amino acid duet in CPII is believed to constitute the hydrophobic binding pocket. However, in TbMCP15, a semi-conserved 'GS' sequence motif replaced this duet. Unlike the variants seen in CPI and CPII, CPIII was entirely conserved in TbMCP15 (Figure 4.2). The CPIII substrate-binding site is characterised by the presence of the positively charged arginine (R) residue. Outside the substrate-binding sites, the 'RRRMMM' motif in the M3 motif of TbMCP15 has been replaced by 'RRRMMI'. The 'RRRMMM' motif has been recognised as a hallmark of all previously characterised AAC proteins. Hence, the 'RRRMMI' motif in TbMCP15 may behave similarly to the 'RRRMMM' motif in other prototypical AACs

because the amino acid exchange is conservative; both the isoleucine (I) residue and the methionine (M) are hydrophobic. The relative conservation of the prototypical AAC sequences and the substantial sequence similarity between TbMCP15 and TbMCP5 suggested that TbMCP15 may function as an AAC.

In comparison to TbMCP15, TbMCP16 diverges to a greater extent from the sequences of the prototypical AACs found in other organisms. As shown in Figure 4.1, TbMCP16 shares only 32% sequence similarity with *S. cerevisiae* and *H. sapiens* AACs. Regarding CPIII, TbMCP16 possesses a 'SRRMQL' motif instead of the typical 'RRRMMM' motif, meaning that the uncharged but polar serine (S) residue has replaced the positively charged arginine (R) residue at the first position. In addition, the positively charged glutamine (Q) has replaced the hydrophobic methionine (M) residue at the fifth position. The 'SRRMQL' motif of TbMCP16 contains three positively charged amino acids as does the 'RRRMMM' motif (Figure 4.2). Considerable disparities were found for the CPI and CPII substrate-binding sites of TbMCP16 and those of previously characterised AACs. In place of the conserved 'RXXXTXXXN' CPI motif, TbMCP16 contains the 'LXXXAXXXE' motif. However, a conservative substitution has been identified in CPII. Prototypical, functionally characterised AACs contain the conserved 'GI' duet. In TbMCP16, these amino acids have been replaced by alanine (A) and valine (V), respectively (Figure 4.2). The substituted amino acids are hydrophobic, as are those they replaced. However, the characteristic, positively charged arginine (R) residue of CPIII has been replaced by the hydrophobic valine (V) residue in TbMCP16.

Considering the disparities in the substrate-binding sites and the low level of sequence similarity between TbMCP16 and the other functionally characterised AAC proteins, TbMCP16 was deemed unlikely to function as an AAC.

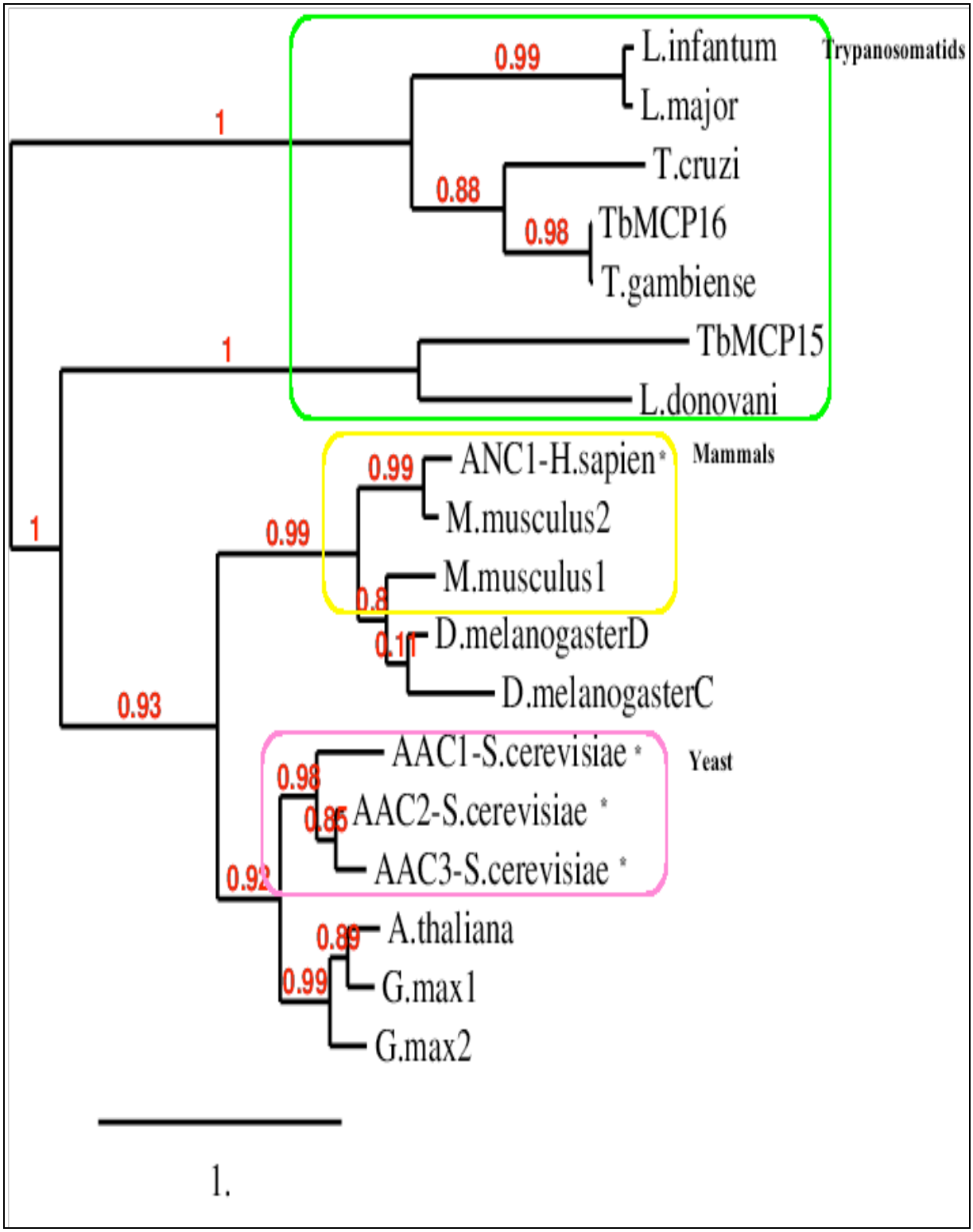

Figure 4.1. The phylogenetic maximum likelihood tree of TbMCP15, TbMCP16 and related MCF proteins with separate clade clustering. The maximum likelihood tree depicts the evolutionary relationship between TbMCP15 and TbMCP16 in mammals (yellow), yeast (pink) and trypanosomatids (green). TbMCP15 is obviously clustring with the ADP/ATP transporters from other organisms, whereas TbMCP16 sits on the out the group. The coloured boxes indicate the clustering of carriers with the same transport function. The bootstrap values located at the nodes represent the percentages obtained after resampling analysis of 1000 iterative data sets. Functionally characterised mitochondrial ADP/ATP transporters (ANC "*H.sapien*" and AAC1-3 "*S.cerevisiae*" are labelled with '*'.

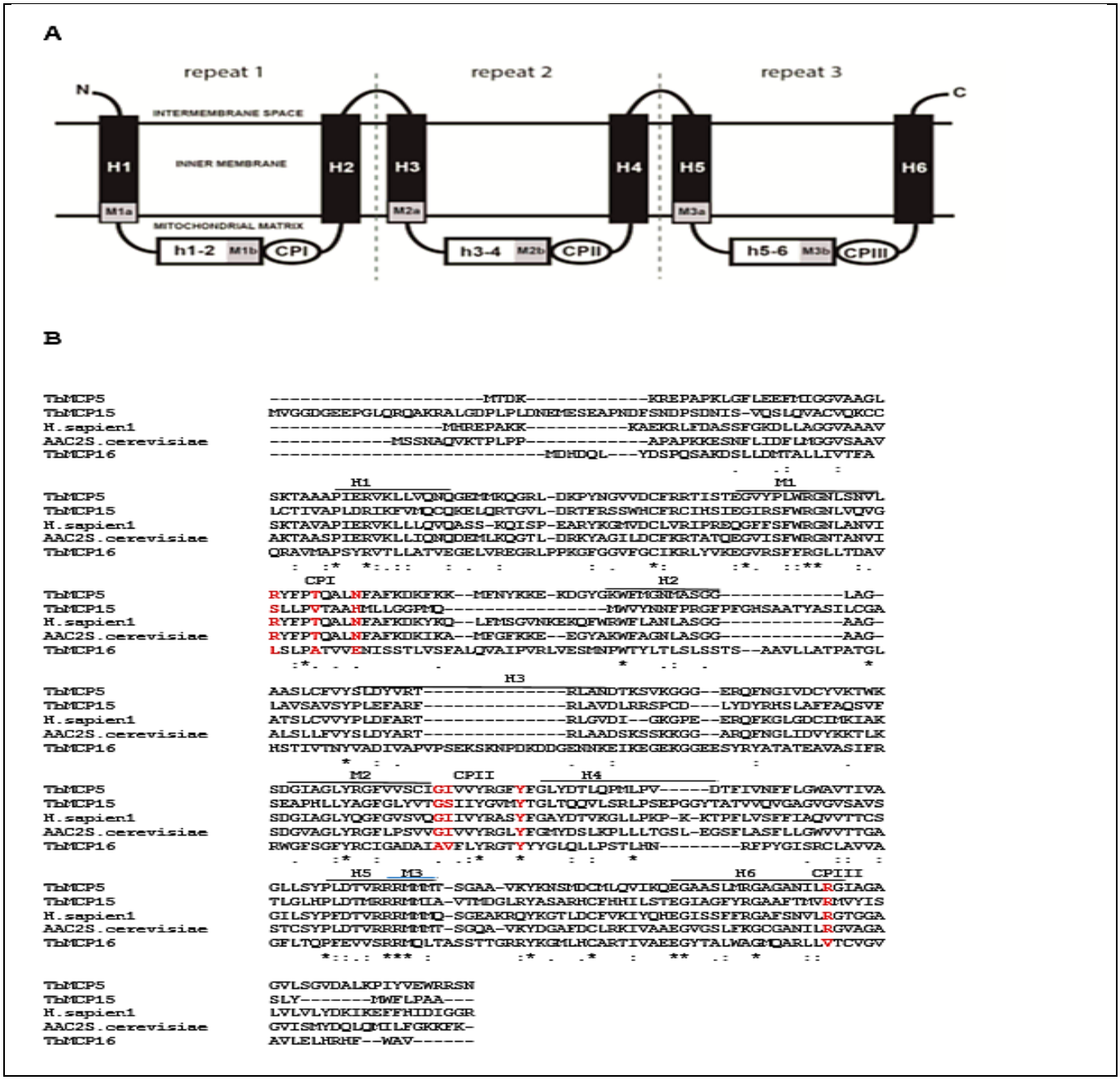

Figure 4.2. Alignment of the TbMCP15 and TbMCP16 deduced protein sequences with comparable sequences from *H. sapiens* and *S. cerevisiae* (AAC2). **A**: Schematic representation of the conserved structure of MCF proteins. The protein structures consist of six TM helices (H1–6) linked by hydrophilic loops (h1-2, h3-4 and h5-6). M1a, M2a and M3a represent the first segment of the signature sequence motif, PX[D/E]XX[K/R]X[K/R], located at the end of the odd-numbered TM helices while M1b, M2b and M3b represent the second part of the motif, [D/E]G[*n* residues][K/R]G, located at the end of each hydrophilic loop. **B**: Multiple sequence alignment of TbMCP15 and TbMCP16 with the human and yeast sequences. The amino acid sequences were aligned using ClustalO. The substrate contact points CPI, CPII and CPIII are located next to H1, H3 and H6, respectively. An asterisk (*) indicates positions with a single, fully conserved residue. A colon (:) signifies conservative substitutions of similar amino acids. A period (.) indicates substitutions of weakly similar amino acids.

4.2.2 Expression of TbMCP15 rescued the growth of the *S. cerevisiae* deletion strain Δ JL1 2 3u on a non-fermentative carbon source

The *S. cerevisiae* gene deletion strain ΔJL1 2 3u lacks all genes coding for mitochondrial ADP/ATP carriers (Clemencon *et al*., 2008). As a consequence, this AAC-deficient yeast strain is not able to grow on media containing non-fermentable (mitochondrial) carbon sources such as glycerol or lactate, but instead can only grow on fermentative carbon sources such as glucose (Clemencon *et al*., 2008). Growth of *S. cerevisiae* ΔJL1 2 3u on a non-fermentable carbon source such as glycerol can be restored (rescued) by the expression of a functional ADP/ATP carrier (Clemencon *et al*., 2008). In order to test whether TbMCP15 or TbMCP16 could function as an ADP/ATP carrier, both *T. brucei* MCF proteins were heterologous expressed in the *S. cerevisiae* deletion strain ΔJL1 2 3u, followed by the analysis of the resulting growth phenotype on different fermentable (glucose) and non-fermentable (glycerol) carbon sources (section 2.2.10).

4.2.2.1 Plasmid construction using the yeast expression vector pCM190

The ORFs of TbMCP5, TbMCP15 and TbMCP16 were amplified by PCR (section 2.2.2.1). The restriction sites for *Bam*HI and *Not*I were incorporated into the relevant primers to facilitate the site-directed cloning of the PCR products. The PCR products were initially cloned into the pGEM®-T Easy TA cloning vector, which was used for sequencing (Eurofins MWG). From the constructs verified as correct (no deviations in DNA sequence), the ORFs of TbMCP5, TbMCP15 and TbMCP16 were subsequently cloned into the yeast expression vector pCM190, using the *Bam*HI and *Not*I restriction enzyme sites to generate the plasmids pCM190 +TbMCP5, pCM190+TbMCP15 and pCM190+TbMCP16.

4.2.2.2 Growth complementation experiment

The plasmids pCM190+TbMCP5, pCM190+TbMCP15 and pCM190+TbMCP16 were transfected into the *S. cerevisiae* gene deletion strain ΔJL1 2 3u (section 2.2.10.2). In addition, the empty pCM190 plasmid without insert was transfected into both the *S. cerevisiae* deletion strain ΔJL1 2 3u and the parental *S. cerevisiae* strain BY4741 (section 2.2.10.2). The resulting yeast strain ΔJL1 2 3u transfected with TbMCP5+pCM190 was used as a positive control (Colasante *et al.*, 2012), while the parental strain *S. cerevisiae* BY4741 transfected with the empty plasmid pCM190 was used as the “wildtype” (WT) strain.

The resultant yeast strains were grown on different carbon sources to examine the effects of the gene complementation. On glucose medium (YPD), all of the yeast strains showed the same growth as the WT strains (Figure 4.3). This was expected since under these conditions growth is fermentative (glucose as carbon source) and not dependent on mitochondrial function. However, in glycerol medium (YPG) where growth is reliant on mitochondrial function (Palmieri *et al*., 2003), only pCM190+TbMCP5 (positive control) and pCM190+TbMCP15 were able to rescue growth to levels comparable to those of the WT *S.cerevisiae* BY4741 strain containing the empty pCM190 plasmid. This in contrast to pCM190+TbMCP16, which was not able to rescue growth of the *S. cerevisiae* gene deletion strain ΔJL1 2 3u on the non-fermentable carbon source glycerol, suggesting that TbMCP16 most probably does not function as a mitochondrial ADP/ATP exchanger (Figure 4.3).

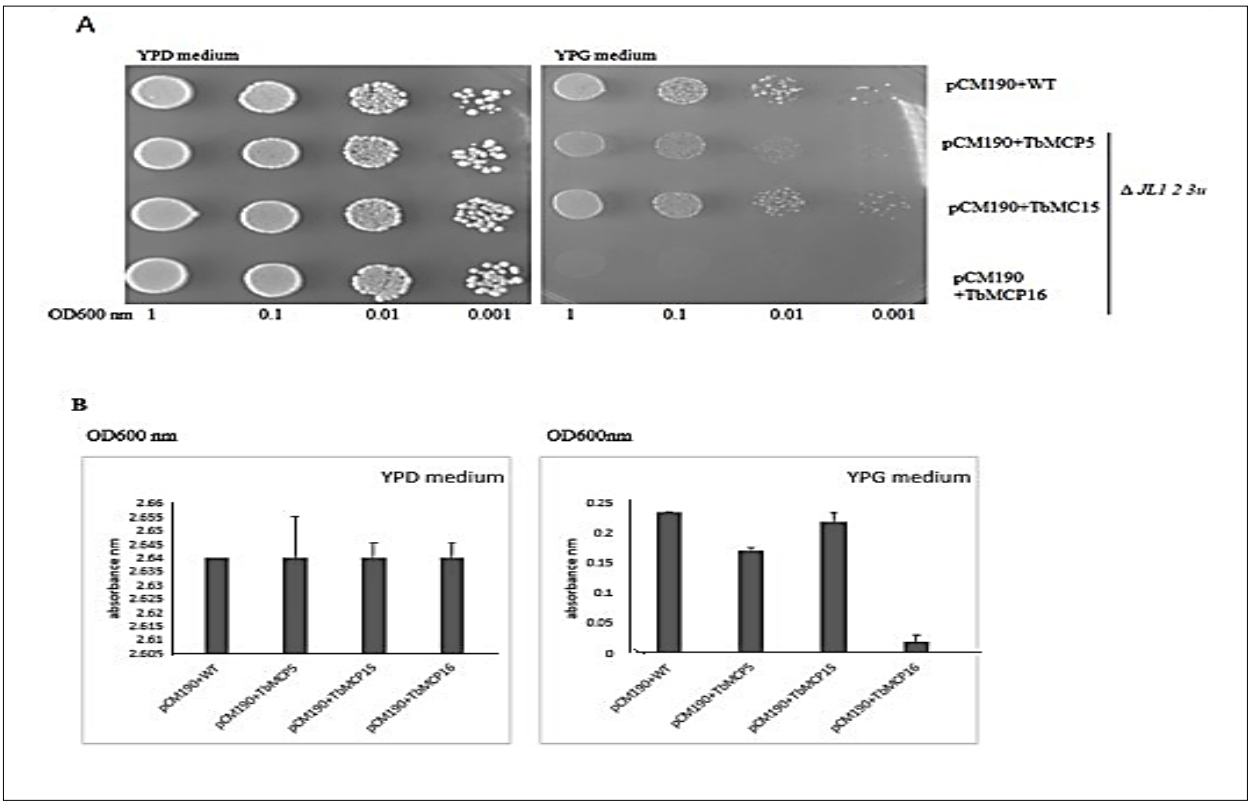

Figure 4.3. The growth of the wildtype strain *S. cerevisiae* BY4741 (WT, containing empty pCM190 plasmid) and the ADP/ATP carrier deficient *S. cerevisiae* strain ΔJL1 2 3u containing respectively pCM190+TbMCP5, pCM190+TbMCP15 and pCM190+TbMCP16, was analysed on different YPD (glucose) and YPG (glycerol) culture media. **A**: Cells of the different *S. cerevisiae* strains were grown on solid YPD and YPG culture media by spotting 10 ul of four sequential 10-fold dilutions of a starter culture with an OD_{600nm} of 1. **B**: Growth of the same *S. cerevisiae* strains in liquid YPD and YPG culture media. Single colonies of the different strains were used to inoculate 10 ml of liquid YPD and YPG medium. The liquid culture growth graphs represent the mean and standard deviation of six independent experimental replicates.

4.2.3 Knockdown of TbMCP15 and TbMCP16 caused growth defects in *T. brucei*

RNA interference (RNAi) was used to determine whether expression of TbMCP15 and TbMCP16 is essential for the growth and survival of *T. brucei*. The resulting growth phenotype can further give valuable information regarding the respective physiological functions of TbMCP15 and TbMCP16. The expression of TbMCP15 and TbMCP16 in *T. brucei* was down-regulated ("knocked-down") by using an RNAi-approach as described in chapter 3 (section 2.2.3). This RNAi-approach is based on the expression of double-stranded (sense+antisense) RNA molecules for TbMCP15 and TbMCP16, respectively, leading to a reduced or depleted expression of the targeted proteins in *T. brucei*.

4.2.3.1 Knockdown-related plasmid construction

RNAi was performed by the simultaneous expression of the sense and corresponding antisense RNA molecules of the targeted gene sequences (Appendix 4) (Bringaud *et al.*, 2000). Primers were designed to PCR amplify a 1050bp sense and an antisense version of the open reading frames of TbMCP15 and TbMCP16, respectively. The primers included the unique restriction sites *Bam*HI, *Apa*I, and *Hind*III, allowing the site-directed cloning of the sense and antisense DNA products in the *T. brucei* expression vector pHD676 (Appendix 5, section 5.1). The antisense primers for TbMCP15 and TbMCP16 genes were designed to include the *Bam*HI and *Apa*I restriction sites, whereas the primers for the sense DNA fragments were designed to include the *Apa*I and *Hind*III restriction sites. The sense and antisense DNA PCR products were cloned *in tandem* and joined at the *Apa*I site behind an inducible *T. brucei* promotor in the vector pHD676. Expression from the pHD676 vector will lead to the formation of a double-stranded RNA molecule connected by a short single stranded loop at the 3' end. Such a structure was shown to be more stable and more effective than a single-stranded antisense RNA molecule for the down-regulation of expression in *T. brucei* (Ngô *et al*., 1998).

The resulting pHD676+TbMCP15 RNAi and pHD676+TbMCP16 RNAi constructs were analysed by using PCR, restriction enzyme digestion and gel electrophoresis to determine whether they contained the correct DNA fragments in the right order. Positive clones were further sent for sequencing (Eurofins MWG). The sequencing results confirmed that the used constructs were indeed correct.

The verified pHD676+TbMCP15 RNAi and pHD676+TbMCP16 RNAi constructs were used to transfect the *T. brucei* cell line PCF449 (section 2.2.5) and positive clonal cell lines were

isolated. For comparison, and to maintain the same genetic background, a *T. brucei* PCF449 cell line was generated containing an empty (no insert) version of plasmid pHD676. Growth of the generated TbMCP15 RNAi, TbMCP16 RNAi, and PCF449+pHD676 (empty vector control) cell lines were analysed in MEM-Pros medium (Appendix 1) containing 5 mM proline and 0.12 mM glucose as carbon sources. RNAi was induced by the addition of tetracycline (0.5µg/ml) to the culture medium (section 2.2.4.2). Growth curves were plotted using Microsoft® Excel (Figures 4.4 and 4.5).

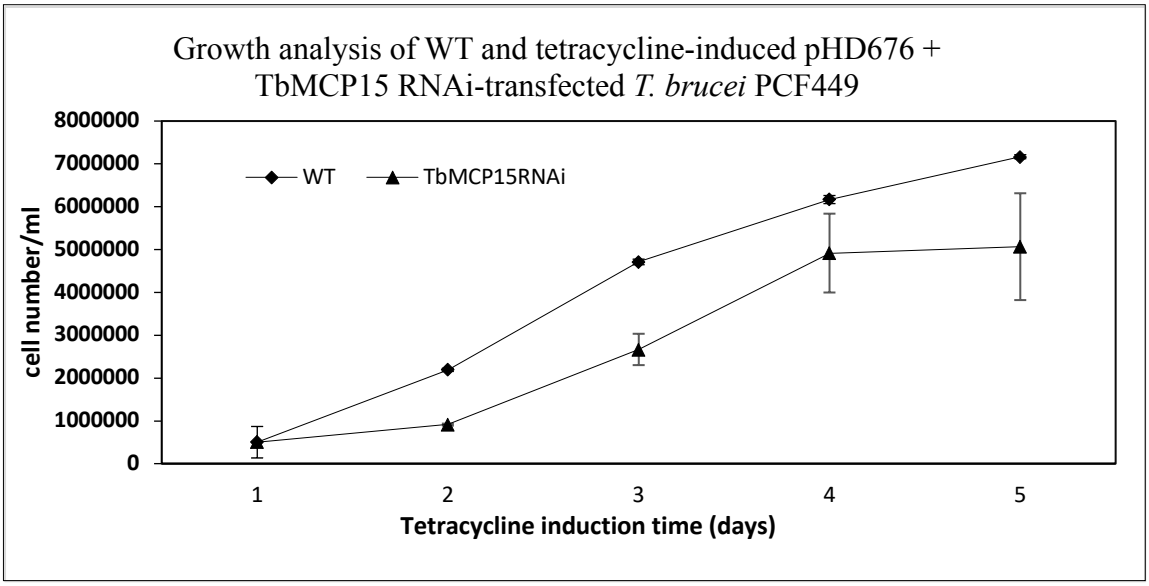

Figure 4.4. Comparison of the growth phenotypes of "wildtype" *T. brucei* PCF449 (WT) and tetracycline-induced pHD676+TbMCP15 RNAi cell lines in standard MEM-Pros medium containing 5 mM proline and 0.12 mM glucose. Cultures were started with 1×10^6 cells/ml and counted every 24 hours for five days. The tetracycline was added to the medium at the start of the experiment.The data points represent the mean and standard deviation of three independent experimental replicates.

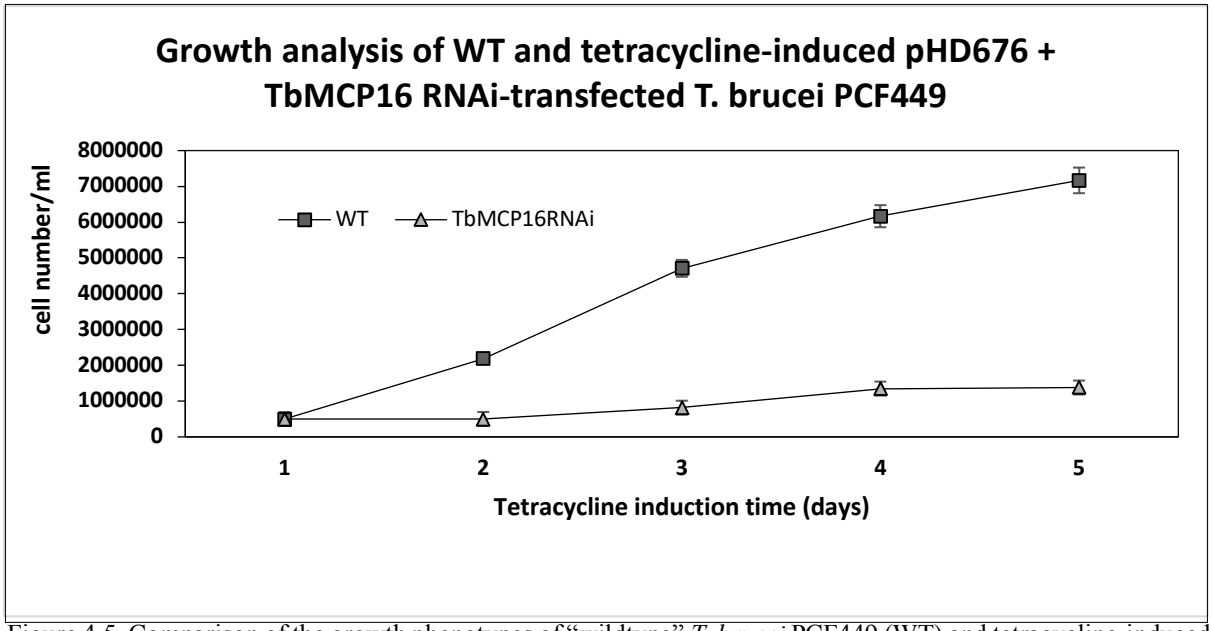

Figure 4.5. Comparison of the growth phenotypes of "wildtype" *T. brucei* PCF449 (WT) and tetracycline-induced pHD676+TbMCP16 RNAi cell lines in standard MEM-Pros medium with 5 mM proline and 0.12 mM glucose. Cultures were started with 1×10^6 cells/ml and counted every 24 hours for five days. The tetracycline was added to the medium at the start of the experiment The data points represent the mean and standard deviation of six independent experimental replicates.

Upon induction with tetracycline, both the TbMCP15 RNAi and TbMCP16 RNAi cell lines presented a significant reduction in growth when compared to the 'wildtype" (parental) *T. brucei* PCF449 cell line, suggesting that both TbMCP15 and TbMCP16 proteins are essential for growth and thus the survival of T. *brucei*. Growth of the induced *T.brucei* TbMCP16 RNAi cell line appeared to be more affected than growth of the induced TbMCP15 RNAi cell line.

Unfortunately, no antibodies could be generated for the detection of TbMCP15 and TbMCP16 protein in *T. brucei* (see below, section 4.2.4). The depletion of TbMCP15 and TbMCP16 in the respective *T. brucei* RNAi cell lines was therefore examined by quantitative RT PCR. It is expected that after the depletion of TbMCP15 or TbMCP16 mRNA a similar depletion will follow at the protein level, taking into account the reduction of existing TbMCP15 and TbMCP16 protein through ongoing cell division and protein turnover/degradation. The quantitative RT PCR results revealed that the TbMCP15 and TbMCP16 mRNA levels were approximately100-fold lower in the respective *T. brucei* RNAi cell lines when compared to the parental PCF449 cell line (wildtype control). This result confirmed an effective down-regulation of TbMCP15 and TbMCP16 expression in the different *T. brucei* RNAi cell lines (Figure 4.6), and a corresponding depletion of TbMCP15 and TbMCP16 protein was inferred.

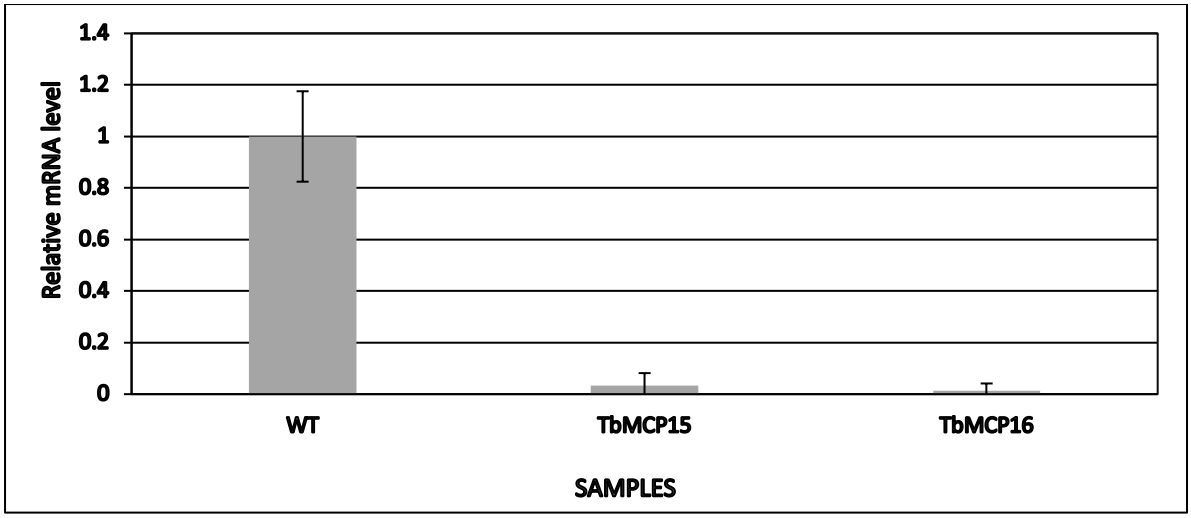

Figure 4.6. Relative mRNA levels of TbMCP15 and TbMCP16 in *T. brucei* PCF449 WT and tetracycline-induced RNAi cell lines. The level of TbMCP15 and TbMCP16 mRNA in the WT cell line was set as 1. The results represent the mean and standard deviation of six independent experimental replicates each.

4.2.4 Protein expression and antibody generation

In order to detect TbMCP15 and TbMCP16 expression at the protein level, and to better analysis the proposed function of these proteins, TbMCP15 and TbMCP16 were both expressed in *E. coli* using the inducible protein expression vector pET28. The resulting recombinant proteins were expected to contain an N-terminal His-tag, which can be used for protein detection and purification. The purified protein will be used for antibody generation.

4.2.4.1 Plasmid construction

The ORFs of TbMCP15 and TbMCP16 were amplified by PCR and the products were digested with the restriction enzymes *Eco*RI (forward primer) and *Xho*I (reverse primer). Then, the PCR products were initially cloned into the pGEM®-T Easy TA cloning vector and aliquots (10 µl) were sent for sequencing (Eurofins MWG). Subsequently, the TbMCP15 and TbMCP16 ORFs were cloned into the *E. coli* expression vector pET28 using *Eco*RI and *Xho*I, resulting in pET28+TbMCP15 and pET28+TbMCP16.

4.2.4.2 Protein expression

In order to produce adequate quantities of the proteins, the plasmids pET28+TbMCP15 and pET28+TbMCP16 were transformed into the *E. coli* strain Lemo21 (DE3) (section 2.2.9). Protein expression was induced with IPTG (0.4 mM final concentration)) Figures 4.7 and 4.8).

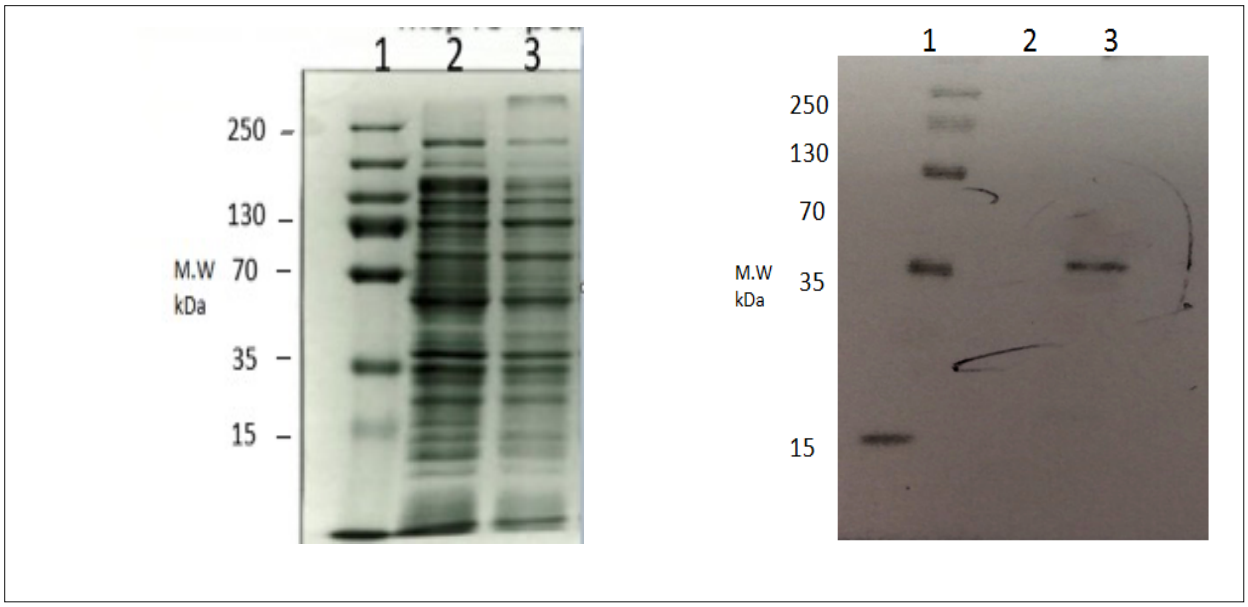

Figure 4.7. TbMCP15 western blots probed with commercially available anti-His antibody (right) or stained with Coomassie blue (left) to analyse protein expression. Cells were treated with IPTG (0.4 mM final concentration) for 4 hours to induce the expression of TbMCP15 (calculated MW is 40 kDa). The protein ladder is shown in lane 1. Lane 2 contained a transformed cell sample prior to induction. Lane 3 shows protein expression after four of induction. Each lane was loaded with 10 µg protein sample (10 µl) and the results represent seven individual attempts at inducing expression of the recombinant his-tagged TbMCP15 .

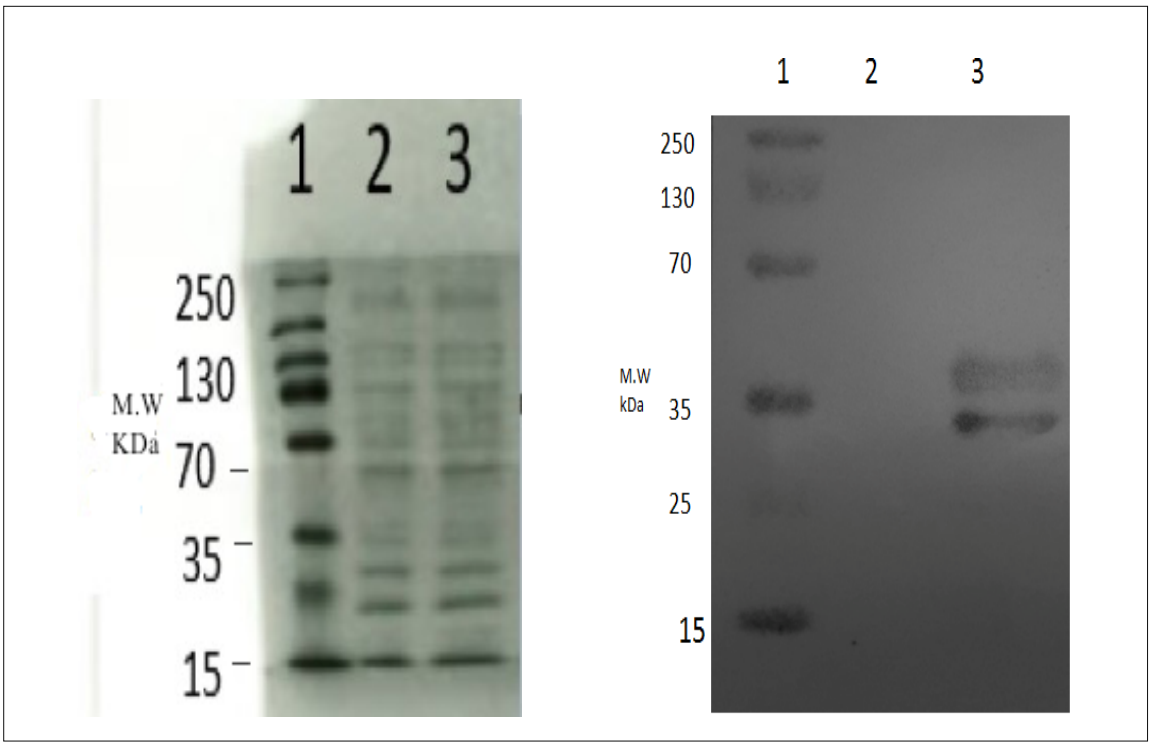

Figure 4.8. TbMCP16 western blots probed with commercially available anti-His antibody (right) or stained with Coomassie blue (left) to analyse protein expression. Cells were treated with IPTG (final concentration, 0.4 mM) for 4 hours to induce the expression of TbMCP16 (calculated MW is 39 kDa). The protein ladder is shown in lane 1. Lane 2 contained a transformed cell sample prior to induction. Lane 3 shows protein expression four hours after induction. Each lane was loaded with 10 µg protein. The results represent seven individual experiments attempts at inducing expression of the recombinant his-tagged TbMCP16.

As Figures 4.7 and 4.8 clearly show, protein bands with the expected molecular weight size were detected by western blotting for both TbMCP15 (predicted: 40 kDa) and TbMCP16 (predicted 39 kDa) the induction of expression in *E. coli* Lemo21 (DE3). Next to the expected 39 kDa band, an unexpected double protein band with a higher molecular weight (HMW) was observed for TbMCP16 . This HMW proteins apparently contain a His-tag since they are recognised by the anti-His antibody. The composition of the observed HMW double band is however unclear. When comparing the western blot results to the corresponding CBB stained SDS-PAGE gels, the by western blotting detectable TbMCP15 and TbMCP16 protein bands are not discernible from other proteins, suggesting that their expression level is rather low.

Heterologous over-expressed membrane proteins have previously been shown to exist in the cell as insoluble, inactive protein aggregates, also called inclusion bodies (Wingfield *et al.*, 2001; Rosano & Ceccarelli, 2014). A good initial step for the isolation of relatively "pure" recombinant protein could be to isolate inclusion bodies after over-expression of the protein. Therefore, the formation of inclusion bodies was assessed after the expression of the recombinant TbMCP15 and TbMCP16 proteins in *E. coli* Lemo21 (DE3) (section 2.2.9).

However, no TbMCP15/TbMCP16 containing inclusion bodies could be isolated suggesting that, under the standard conditions used for expressing His-tagged TbMP15 and TbMCP16, the proteins are not sufficiently over-expressed in the first place.

The enable a better detection of these apparently low-expressed proteins, and to reduce possible aggregation of membrane proteins (with protein aggregates stuck in the gel and not being transferred to the membrane), experiments were repeated using different sample preparation conditions, such as the treatment (denaturation) of samples at a lower temperature (85 °C instead of 95 °C) prior to loading, the use of cell lysis buffers containing higher concentrations of SDS, and the use of larger sample volumes (20–35 µl) containing an overall lower protein concentration (improved protein to SDS ratio). Unfortunately, the observed protein expression levels were still not sufficient to allow protein isolation in large enough quantities for immunisation.

Next to pET28, other protein expression vectors, such as for example pTrcHisA, were used to investigate if the used expression vectors had any effect on TbMCP15 and TbMCP16 expression. IPTG-inducible expression from pTrcHisA is driven by the Ptrc promoter and will lead to the addition of a 6xHis-tag to the N-terminal end of the expressed protein. Unfortunately, none of the tested expression vectors did improve the expression levels of either TbMCP15 or TbMCP16.

The failure to expressed sufficient TbMCP15 and TbMCP16 protein suggested that the problem could maybe be related to the use of the full-length genes. It was observed that soon after induction of protein expression the growth of the *E. coli* cells stopped, followed by some cell lysis. Expression of full-length gene products could potentially have a deleterious effect on the host cell if the protein and/or its function is toxic for the host cell. Therefore, expression experiments were repeated, but now only expressing the N-terminal half of the full-length ORFs of TbMCP15 and TbMCP16. Unfortunately, protein expression levels did not improve and were still found to be not sufficient for immunisation.

Overall, our experiments suggest that *E. coli* is unable to express TbMCP15 and TbMCP16 under the standard conditions that were successfully used for the bacterial expression of MCF proteins from other eukaryotes (Klingenberg, 2009).

4.2.5 TbMCP15 localised to the mitochondria of *T. brucei* PCF449

The subcellular localisation of TbMCP15 in the *T. brucei* PCF449 cell line was investigated by immunofluorescence microscopy. Since there are no specific antibodies available for TbMCP15, a recombinant myc-tagged version of TbMCP15 was expressed instead, allowing the use of commercially available myc antibodies. TbMCP16 was excluded from this analysis because it failed to complement the growth of the yeast deletion AAC ΔJL1 2 3u strain (section 4.2.2), which suggested that TbMCP16 does not function as an AAC.

4.2.5.1 Plasmid construction

The ORF of TbMCP15 was PCR amplified using primers with added unique *Bam*HI and *Hind*III restriction sites. The PCR product was cloned into the pGEM®-T Easy vector and the resulting construct was sequenced (Eurofins MWG). The ORF of TbMCP15 was subsequently cloned into the *T. brucei* expression vector pHD1484 using the unique *Bam*HI and *Hind*III restriction enzyme sites and resulting in the pHD1484-TbMCP15-cmyc^{ti} construct. The tetracycline-inducible expression from pHD1484 will add a double myc-tag to the c-terminus of TbMCP15.

4.2.5.2 Subcellular localisation

The *T. brucei* PCF449 cell line was transfected with pHD1484-TbMCP15-cmyc^{ti} and expression of the myc-tagged version of TbMCP15 was induced by addition of tetracycline (section 2.2.6). Immunofluorescence microscopy was performed using a commercial available myc antibody (Figure 4.9).

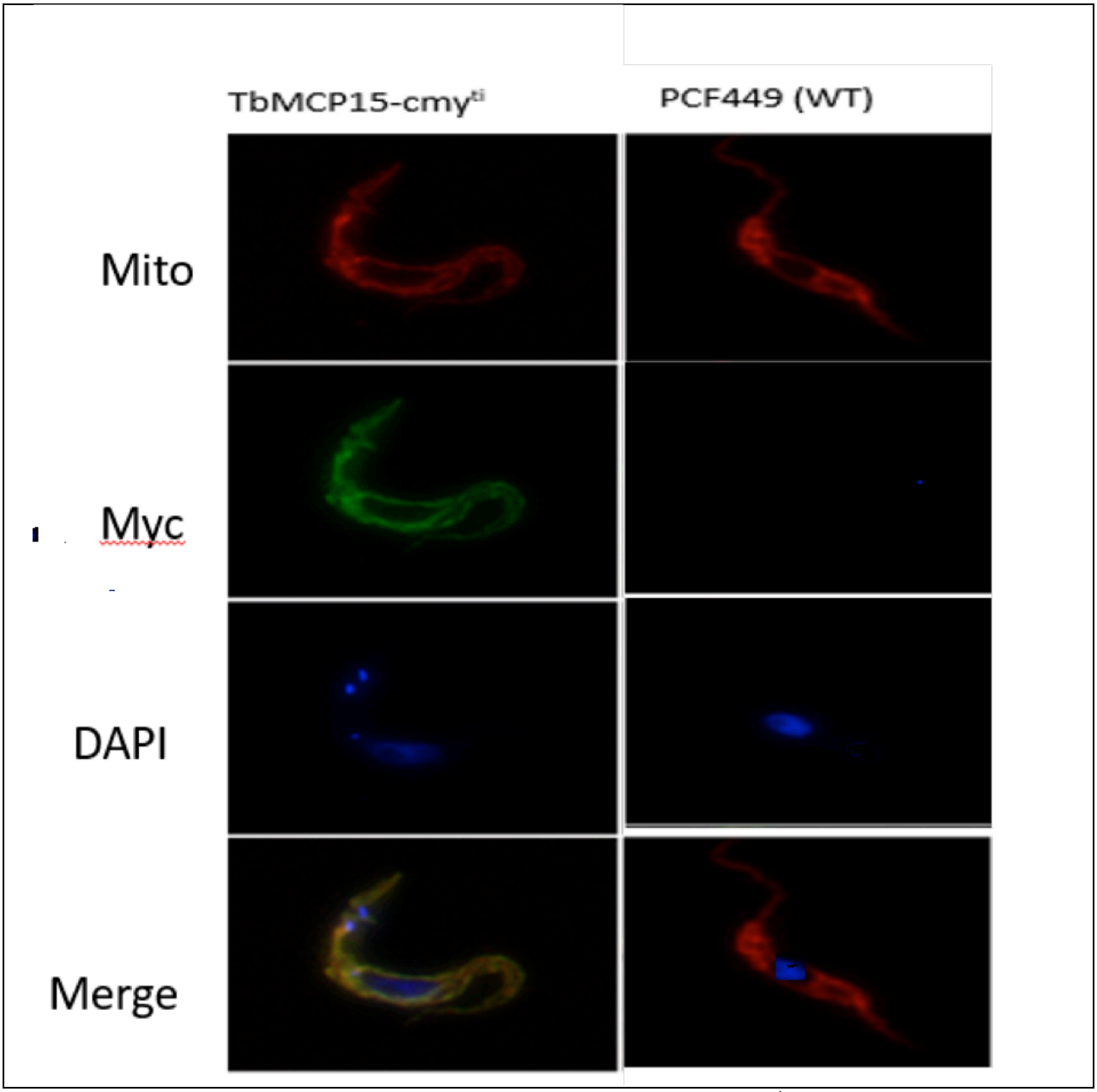

Figure 4.9. Immunofluorescent micrographs of WT and pHD1484-TbMCP15cmyc^{ti}-transfected *T.brucei* PCF449 cell lines. The MitoTracker (Mito; red), myc antibody (green) and DAPI (blue) signals were merged to form the overlay. The images represent three independent experiments.

The immunofluorescence results showed a specific tubular shaped staining pattern of PCF 449 *T. brucei* when using the TbMCP15 myc-tagged antibody. This staining pattern was identical to the one obtained for MitoTracker, which is used as a mitochondrial marker (Colsanate *et al*., 2006). Therefore, this result confirmed the mitochondrial localisation of TbMCP15 in *T. brucei* PCF449.

4.2.6 TbMCP15 aided mitochondrial ATP production in the presence of ADP

To determine whether TbMCP15 is fully or partially responsible for mitochondrial ADP/ATP exchange in *T. brucei,* a mitochondrial ATP production assay was performed. The classical approach to determine the metabolite exchange function of MCF proteins is the *in vitro* reconstitution of natural or affinity-tagged purified carrier proteins in liposomes, followed by transport assays using radiolabelled metabolites. This approach has been successful for the functional characterisation of a large number of MCF proteins from mammals, yeasts and plants (Picault *et al*., 2004; Palmieri *et al*., 2004; Palmieri *et al*., 2011). However, after numerous attempts, this classical approach proved to be unsuccessful for MCF proteins from *T. brucei* (Diaz *et al.*, 2009). Therefore, an alternative approach was used to assess the putative transport function of TbMCP15. This alternative approach is based on a well-established, previously published mitochondrial ATP production assay using *T. brucei* mitochondria which were enriched via digitonin fractionation (Schneider *et al*., 2007; Bochud-Allemann & Schneider, 2002). The obtained mitochondrial fraction is metabolically active and is able to synthesise ATP upon the addition of ADP and mitochondrial metabolic substrates such as the Krebs cycle intermediate oxoglutarate (α-ketoglutarate) (Allemann & Schneider, 2007). The mitochondrial ATP production is further dependent on the presence of mitochondrial metabolite transporters such as MCF proteins, which are responsible for mitochondrial ADP/ATP exchange (ADP import and ATP export) and the exchange of other metabolic substrates and end products across the semipermeable MIM (Besteiro *et al*., 2005).

4.2.6.1 ATP production assay

T. brucei cells were grown in standard MEM-Pros medium prior to the enrichment of mitochondria by digitonin-mediated cellular permeabilisation. ATP production by mitochondrial fractions (section 2.2.15) derived from *T. brucei* PCF449 cells (WT) and tetracycline-induced TbMCP15 RNAi cells was assessed in the presence of different combinations of metabolic substrates and inhibitor. The Krebs cycle metabolic intermediate α-ketoglutarate (alternatively called oxoglutarate) was added as a substrate to the isolated mitochondria in order to initiate oxidative phosphorylation via the Krebs cycle (Schneider *et al*., 2007). ADP was added as a phosphorylation substrate for mitochondrial ATP production, whilst the required inorganic phosphate was provided in the used assay buffer. Carboxyactractyloside (CATR) was added to specifically inhibit the mitochondrial ADP/ATP carrier (Peyroula et al., 2003). The inhibitor and the metabolic substrate used, allow the

discrimination between ATP produced by substrate-level phosphorylation or oxidative phosphorylation in the *T. brucei* mitochondrion (Schneider *et al*., 2007). The production of ATP was measured using a luciferase-based ATP detection kit (section 2.2.15).

4.2.6.2 Assessment of ATP production

In the control experiment, both ADP and oxoglutarate were added to the mitochondria-enriched fraction obtained from the wildtype *T. brucei* PCF449 cell line. As expected, ATP was produced (Figure 3.10). This ATP production was ablated when either ADP or oxoglutarate were omitted from the assay or the specific AAC inhibitor CATR was added in the presence of both substrates (Figure 3.10). These results indicated that the isolated mitochondria are functional and that the mitochondrial ATP production is dependent on the presence of both ADP and oxoglutarate as the metabolic substrates, as well as the presence of a functional ADP/ATP carrier. Addition of only oxoglutarate resulted in no ATP production, which is expected since mitochondrial ATP production is dependent on the constant provision of new ADP via the ADP/ATP exchanger. Addition of only ADP during the control experiment resulted in the detection of only small amounts of ATP, which is probably derived from residual ATP present in the isolated mitochondria. Similar experiments were performed for mitochondrial fractions obtained from the TbMCP15-depleted *T. brucei* cell line. The results revealed that mitochondria from the TbMCP15-depleted *T. brucei* cell line produced significantly less ATP (about 75%) compared to the mitochondria from the parental (wildtype) *T. brucei* PCF449 cell line (Figure 3.10). This result suggested that TbMCP15 is likely to be responsible for about 25% of the observed ADP/ATP exchange activity in *T. brucei* PCF449. The remaining ADP/ATP exchange activity is probably the resulting from TbMCP5, which has previously been reported to function as the major ADP/ATP exchanger in the *T. brucei* mitochondrion (Colasanate *et al*., 2009).

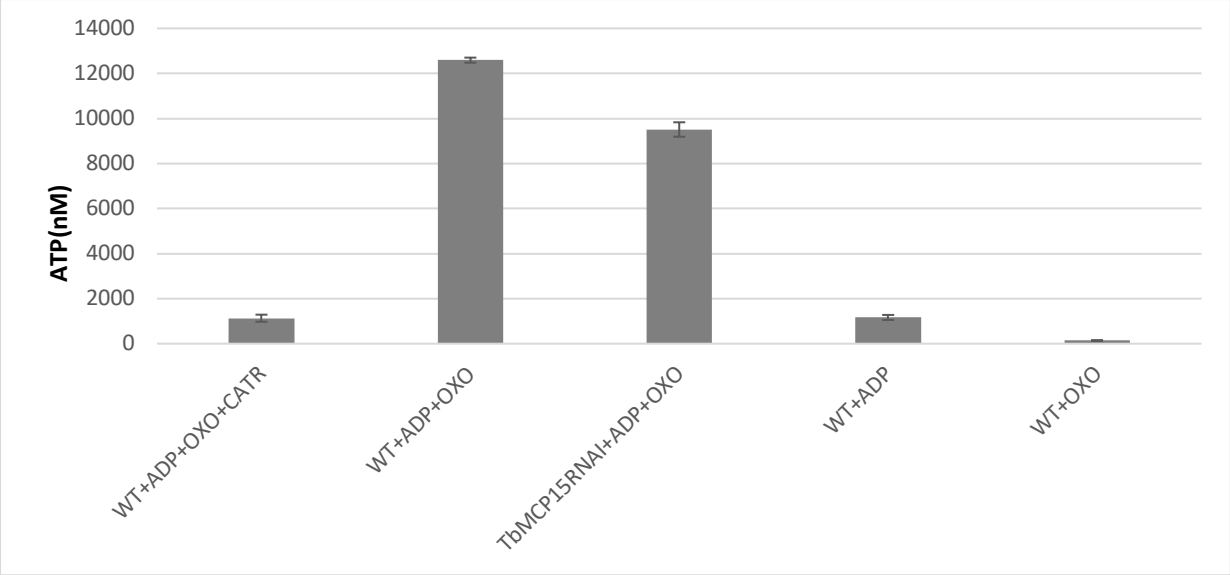

Figure 4.10. ATP generation by mitochondria isolated from WT PCF449 and TbMCP15 RNAi-expressing cells lines grown in standard MEM-Pros medium with α-ketoglutarate (OXO) as a substrate. WT mitochondria were able to generate ATP from α-ketoglutarate in the presence of ADP. The addition of carboxyatractyloside (CATR) inhibited ATP generation. The results represent the mean and standard deviation of six independent experimental done in duplicate.

4.3 Discussion and Conclusion

BLASTP analysis and phylogenetic reconstruction revealed that TbMCP15 and TbMCP16 had similar amino acid sequences to human and yeast AACs. AACs supplies ADP to maintain the oxidative phosphorylation (Kim *et al*., 2010) .AACs play an important roles in the metabolic processes which provide energy to the cells in the form of ATP (Haferkamp *et al*., 2002) . *T.brucei* contains a single gene coding for the TbMCP15 and TbMCP16. However, the sequence alignments of TbMCP15 and TbMCP16 with the human and yeast transporters revealed that only TbMCP15 contained the conserved motifs and transport-specific contact points associated with AACs. TbMCP15 contained relatively conserved CPI and CPIII sequences (Kunji & Robinson, 2006; Colasante *et al*., 2009), which bind with ADP and neutralise its charge (Heidkamper *et al*., 1996; Kunji & Robinson, 2006). CPII, which comprises the G[I/V/L/M] amino acid duet, has been found to be highly conserved in all AAC proteins. Moreover, the "RRRMMM" sequence motif , which is conserved in all most AAC proteins, was appeared to be modified in TbMCP15, revealing a "RRRMMI" motif instead. The methionine (M) residue at position 6 of "RRRMMM" was replaced by isoleucine (I), which they all are hydrophobic. Suggesting that the RRRMMI sequence motif in TbMCP15 possibly functions in the identical way as the RRRMMM sequence motif found on prototypical AAC proteins. Therefore, based on the above described and also its significant homology to TbMCP5, it can be said that TbMCP15 appeared to be functions as an AAC in *T. brucei* . In addition, TbMCP15 localised to the mitochondria of PCF449 *T. brucei,* where a surplus of ATP is generated by substrate-level or oxidative phosphorylation and where ATP and ADP are equilibrated by adenylate kinases (Allemann *et al*., 2000; Coustou *et al*., 2005; Lamour *et al*., 2005; van Weelden *et al*., 2005). Thus, TbMCP15 appeared likely to have a mitochondrial transport function.

The amino acid sequence of TbMCP16 shared a lower degree of similarity to the human and yeast AAC proteins. In particular, 3 out of 6 amino acids of the RRRMMM motifs are conserved . TbMCP16 contained the 'SRRMQL' motif instead of the conserved 'RRRMMM' motif. The positively charged (R) arginine at position one of this sequence motif has replaced by serine (S) uncharged, whereas the methionine at position five replaced by glutamine which is positively charged. Therefore, based on its dissimilar sequence motif and the different amino acids substitution in the substrate contact points , TbMCP16 unlikely to function as an AAC protein. In addition to that , because TbMCP16 was clustering within the nucleotide carriers as

shown by the phylogenetic tree, suggesting that, TbMCP16 is most possibly involved in the carrying of nucleotides or nucleotides-related substrate.

The non-conservative nature of the modifications suggested that they would influence the role of the molecule in oxidative phosphorylation (Schneider *et al*., 2007). The oxidative phosphorylation activity of a yeast AAC was diminished to less than half after the mutation of the first amino acid in the 'RRRMMM' motif (Heidkamper *et al*., 1996; Schneider *et al*., 2007). During ADP/ATP exchange, the three negative charges of ADP are neutralised by the three positive charges of the amino acids in the 'RRRMMM' motif (Heidkamper *et al*.,1996; Schneider *et al*., 2007).

The functions of TbMCP15 and TbMCP16 were analysed in functional complementation experiments. A yeast AAC -deficient cell line (ΔJL1 2 3u) was induced to heterologously express TbMCP15 or TbMCP16. Only TbMCP15 restored its growth on glycerol, as non-fermentative carbon source. This finding indicated that TbMCP15 is capable of rescuing mitochondrial ADP/ATP carrier deficiency of yeast, as TbMCP5 did (Colasanate *et al.*, 2009); suggesting that TbMCP15, like TbMCP5, acts as an ADP/ATP transporter. TbMCP16 did not restore the growth of the deficient strain. Unfortunately, there was no specific antibody available for TbMCP16, which can prove the presence of TbMCP16 protein mitochondria. The inability of TbMCP16 to restore ADP/ATP transport in the ΔJL1 2 3u cell line could be for many reasons, such as, the heterologousely expressed TbMCP16 protein is not sufficiently targeted to the yeast mitochondrion or may be TbMCP16 protein is too divergent to be used for heterologous complementation studies in the yeast. Therefore, TbMCP16 was consistent with its structural dissimilarity to ADP/ATP transporters and suggested the hypothesis that it is not function as an AAC proteins. Interestingly, the down-regulation of either TbMCP15 or TbMCP16 caused a growth defect, which indicated that both proteins are essential for the survival of the PCF449 of *T. brucei*.

The expression of His-tagged TbMCP15 and TbMCP16 differed in different heterologous systems. When expression was induced via IPTG, the protein level in the cell determined the expression of TbMCP15 and TbMCP16 proteins in *E. coli* Rossetta2 (DE3)-plysS and *E. coli* Lemo21 strains. Their expression was analysed by Coomassie blue staining and western blotting and. TbMCP15 formed a distinct band, which was detected with the His-tag antibody, of approximately 40 kDa. However, TbMCP16 was detected as two bands, this could be due to incomplete processing or alternative post-translational modification in *E.coli*

(Rosano *et al.,* 2014). However, the exact reason of appearing double band is still not known at this stage. Western blotting revealed that extremely small quantities of TbMCP15 and TbMCP16, just over the limit of detection, were formed within 4 hours of IPTG induction. Interestingly, the standard conditions that supported the expression of TbMCP15 and TbMCP16 in other eukaryotic cells were unsuitable for expression in *E. coli* Lemo21 and *E. coli* Rosetta cells, which were unable to survive the formation of these *T. brucei* MCF proteins. Thus, the expression of *T. brucei* TbMCP15 and TbMCP16 may be toxic for *E. coli* cells. The experiments demonstrated that His-tagged TbMCP15 and TbMCP16 are formed after IPTG induction, but at very low levels. After IPTG-induced expression of the proteins, the bacterial cells producing the proteins lost the ability to grow. Therefore, the two proteins could be toxic to *E. coli* cells, which prevented the expression of sufficient protein for analysis in several experiments. However, the exact reason for this failure is still unclear. The failure of the TbMCP15 and TbMCP16 proteins to be expressed in *E. coli* under the various conditions led to the hypothesis that the genes contain DNA codons that are rarely used in *E. coli* Lemo21 (DE3) and Rosetta strains, which hampered their expression (Sharp & Li, 1987). TbMCP15 and TbMCP16 may also be toxic to *E. coli*. The protein expression results for TbMCP15 and TbMCP16 varied substantially from the mRNA expression results. This finding was suggested the important role of these proteins in PCF449 *T.brucei.* the structural changes occur in the PCF, compare to BSF, of *T.brucei* play an important role in the formation of its membrane and these membranes are of paramount importance in the reconstitution of the carriers into liposomes. Therefore, due to the requirement for an isolated purified protein. Changes in the methodological approach is necessary to facilitate a successful analysis. Many factors play a role in the process of reconstitution and varying results have been achieved experimenting with different strains of the E.coli (Seddon *et al*., 2004). According to Gebert *et al*. (2011), some factors, like the redox state of the proteins or the phospholipids, play substantial roles in the functional incorporation of proteins into the membrane of the *T. brucei* mitochondrion. The essential factors that dictate the incorporation of *T. brucei* proteins into the mitochondrial membrane have not been established and must be further analysed.

The transport function of TbMCP15 was examined in a mitochondrial ATP production assay. In order to interpret the ATP production results, it is essential to understand the criteria for ATP production in this assay. First, AACs are essential for importing ADP into the

mitochondria and exporting ATP. Substrate transporters must be functional to import the exogenous metabolites into the mitochondria. Furthermore, if the carrier is functional as a cotransporter or counter-transporter, the cofactor or counter-transport metabolite must be available (i.e., it must be generated in the mitochondrial pathways from the added substrate). In addition, the enzymes that generate ATP must be active. If ATP is produced by oxidative phosphorylation through the electron transport chain, mitochondrial membrane potential is required. ATP generated through substrate level phosphorylation must be catalysed by either succinyl-CoA synthetase or acetate/succinate CoA transferase (the ASCT cycle). Finally, if ATP is generated through the ASCT cycle, succinate must be provided in addition to the testing substrate. Upon addition of α-ketoglutarate to the mitochondrial fractions, the majority of ATP production was generated by substrate phosphorylation that converted succinyl-CoA to succinate (Schenider *et al.*, 2007). In this study, TbMCP15-depleted *T. brucei* generated less levels of ATP compared to PCF449 *T.brucei* . This finding was similar to the previously published TbMCP5 (Colasanate *et al*., 2009). However, the slightly lower production of ATP by the TbMCP15-depleted cells could be explained by the residue TbMCP15 or alternatively some ATP could be transporter by other *T.brucei* mitochondrial proteins. It can be stated that next to TbMCP5, TbMCP15 plays an essential role in the PCF449 *T.brucei* energy metabolism (Colasanate *et al*., 2009), when the proline is the main sources for the ATP production in the mitochondria. TbMCP15 and TbMCP5 (Colasanate *et al*., 2009) are both an ADP/ATP transporters in *T.brucei*, while, TbMCP16 function as third type of ADP/ATP is not clear at this point, as its assumed ADP/ATP transport function is supported by BLASTP analysis but not phylogenetic reconstruction. The function of TbMCP16 is more likely to be a specific to the PCF449 of *T. brucei*. Further research into metabolic pathway regulation and signalling in all stages of the parasite lifecycle and in the PCF449, in particular, is required to understand the role of TbMCP16 in *T.brucei*.

In conclusion, evidence in this chapter shows that TbMCP15 is an ADP/ATP transporter, as indicated by phylogenetic reconstruction and its ability to restore the growth of the ΔJL1 2 3u cell. TbMCP15 is more likely to be responsible for the ADP/ATP exchange activity in *T.brucei* as indicated by mitochondria ATP transport assay. However, further functional assays would provide additional insight into the functions of TbMCP15 and TbMCP16, as would the measurement of TbMCP15 and TbMCP16 expression at the protein level.

Chapter 5: Sequence analysis and functional characterisation of TbMCP20, a putative SAMC

5.1 Introduction

S-adenosylmethionine (SAM), a methyl group donor, is involved in almost all cellular methylation processes occurring in eukaryotic cells, including the methylation of protein, RNA and DNA (Palmieri *et al*., 2003). In addition to the methylation function, SAM also acts as a metabolic intermediary required for the biosynthesis of biotin (Marquet *et al*., 2001; Kumar *et al*., 2002), ubiquinone (Bringaud, 2015) and lipoic acid (Sulo *et al*., 1993) in the yeast *Saccharomyces cerevisiae*. One of the enzymes required for the production of SAM, e.g. methionine adenosyltransferases, does not exist in mitochondria and is found only in the cytosol (Palmieri *et al*., 2006; Haferkamp *et al*., 2013). However, SAM can be bound in significant quantities in mitochondria, suggesting that it has to be imported from the cytosol into mitochondria through a carrier (Agrimi *et al*., 2003).

In human, SAMC was found to be expressed in all human tissues and also was shown to be located in the mitochondria . The functional role of SAMC was shown to be the exchange of cytosolic SAM for mitochondrial s-adenosylhomocysteine (Agrimi *et al*., 2004). Purohit *et al.* (2008) showed that rat liver mitochondria are capable of storing SAM, and that the mitochondria uptake of SAM can be stopped through the addition of structural analogues of SAM, i.e. adenosylornithine and S-adenosylhomocysteine (SAH). The kinetic properties, subcellular localisation and transport mechanisms of human SAMC indicated that it is comparable to the SAMC in rat liver mitochondria (Agrimi *et al.*, 2003; King *et al.*, 2016).

The yeast genome contains the gene SAM5 (PET8), which encodes the yeast s-adenosylmethionine carrier (SAM5). SAM5 yeast was overexpressed in bacteria and reconstituted into liposomes and identified as a SAM transporter through transport experiments using radiolabelled SAM (Agrimi *et al*., 2003). SAM5 was also found to be targeted to the yeast mitochondria as a fusion protein with green fluorescent protein. Moreover, SAM5 (PET8) was shown to be essential for yeast growth on media containing glycerol, acetate or other non-fermentable carbon sources (Palmieri *et al*., 2006). In the absence of this gene, yeast cannot be grown on a minimal synthetic medium with added galactose, glucose or other fermentable sources of carbon in the absence of biotin or in the presence of the biotin precursor dethiobiotin (Froschauer *et al*., 2013). Based on this finding, SAM5 was initially presumed to function as a biotin synthetase (Bio2p), which is responsible for the conversion of dethiobiotin to biotin (Kumar *et al*., 2002). The exchange of dethiobiotin for biotin was postulated to require

SAM. However, this hypothesis was disproven by performing specific transport assays using liposomes and radiolabelled SAM (Palmieri *et al.*, 2006).

Sequence analysis of the TbMCP inventory of *T. brucei* revealed a significant amino acid sequence homology between SAM5 from *S. cerevisiae* and TbMCP20 (Colasante *et al*., 2009), suggesting that TbMCP20 maybe functions as a mitochondrial s-adenosylmethionine transporter in *T. brucei*. Therefore, this chapter will address the results of the identification and functional characterisation of TbMCP20, using a similar approach as in the previous chapters.

5.2 Results

5.2.1 Phylogenetic reconstruction and sequence alignment of TbMCP20

Of the 24 MCF proteins that have been identified in *T. brucei* (TbMCP1–24), TbMCP20 has been identified as a homologue of the mitochondrial SAM transporters found in humans and yeast (Colasante *et al*., 2009). The transport function of a mitochondrial carrier family protein can be deducted from the conserved substrate contact points CPI CPII and CPIII, which were previously shown to be essential for binding and transport of the different substrates (Robinson and Kunji., 2006). Among the different substrate contact points, CPIII is the most defining and conserved one in terms of substrate recognition, whereas CPI and CPII can be more variable between MCF proteins transporting similar substrates (Colasanate *et al*., 2018). MCF proteins require particular amino acids in the right position in the substrate binding pockets in order to recognise a specific substrate (Boudko *et al*., 2012)

The TbMCP20 protein sequence was analysed by BLASTP analysis against mitochondrial carrier family proteins from other eukaryotes (http://blast.ncbi.nlm.nih.gov/). BLASTP analysis not only retrieved similar TbMCP20-related sequences from other Kinetoplastida species such as *T. b. gambiense*, *Trypanosoma equiperdum*, *Trypanosoma congolense* and *Leishmania donovani*, but also result TbMCP20 also demonstrated a similarity with the mammalian homologue SLC25 in *M. musculus* and *H. sapiens*. Based on these findings, the sequence of the TbMCP20 protein was analysed against genome databases for *H. sapiens* and *S. cerevisiae* . When compared against the *H. sapiens* genome database, the TbMC20 protein demonstrated the greatest similarity (0.97%) to the mitochondrial SAMC. This is considered to be high values for *T. brucei* since MCF proteins, in evolutionary terms, are highly divergent and only the few amino acids required for transport and substrate recognition are conserved across most eukaryotes (Boudko *et al*., 2012). Other amino acids are far less conserved apart from maintaining the MCF protein structure, including its 6 hydrophobic TM domains and the hydrophilic loops in between. Details sequence analysis using the *S.cerevisiae* SAMC protein sequences revealed that the TbMCP20 protein is homologous to the Pet8p (SAM5) transporter of *S. cerevisiae*. After all related sequences were collected and aligned, a phylogenetic tree was constructed with phylogeny.fr (Figure 5.1). phylogenetic analysis showed that TbMCP20 clustered with similar SAM transporters from other eukaryotes, such as SAMC from *H.sapien* and SAM5 *S.cerevisiae* proteins, supported by high bootstrap values at the nodes (Palmieri *et al*., 2006). These findings suggest that TbMCP20 could be a mitochondrial SAM transporter.

For a more in-depth sequence analysis, the amino acid sequence of TbMCP20 was aligned with functionally characterised SAM transporters from yeast (SAM5), *H. sapiens (*SAMC*)* and *Arabidopsis thaliana* (Palmieri *et al*., 2003; Palmieri *et al*., 2006). The results (Figure 5.2) showed that TbMCP20 is clearly a MCF protein because of its conserved the structural characteristics and conserved of MCF protein sequences and motives. Sequencing of TbMCP20 revealed that it comprised 310 amino acids, resulting in a 34-kDa protein. SIX TM domains were found in TbMCP20. The protein structure includes six TM α-helices (H1–6), similar to other MCF proteins (Colasante *et al*., 2009). The signature motif 'PX[D/E]XX[K/R]X[K/R]', where X represents any amino acid, is found in three out of six TM domain (Aquila *et al*., 1987; Saraste & Walker, 1982). This motif is located at the ends of H1, H3 and H5 (illustrated as M1, M2 and M3, respectively). Kunji and Robinson (2006) have reported a group of conserved amino acids resides downstream of each MCF protein signature motif. These conserved amino acids are involved in recognising and binding of substrates. CPI, CPII and CPIII, the three highly conserved substrate contact points in MCF proteins, are responsible for the transportation of similar substrates. When the sequences of mitochondrial SAM transporters were aligned, it was evident that the three amino acids in CPI are conserved 'YGL' (Figure 5.2). In CPIII, the first amino acid is an arginine (R). The CPIII substrate-binding site is characterised by the presence of a positively charged arginine (R) residue which is also entirely conserved in TbMCP20. The relative conservation of the prototypical SAMC sequences and the substantial sequence similarity between TbMCP20 ,SAMC from *H.sapien* and *S.cerevisiae* suggested that TbMCP20 may function as an SAM transporter.

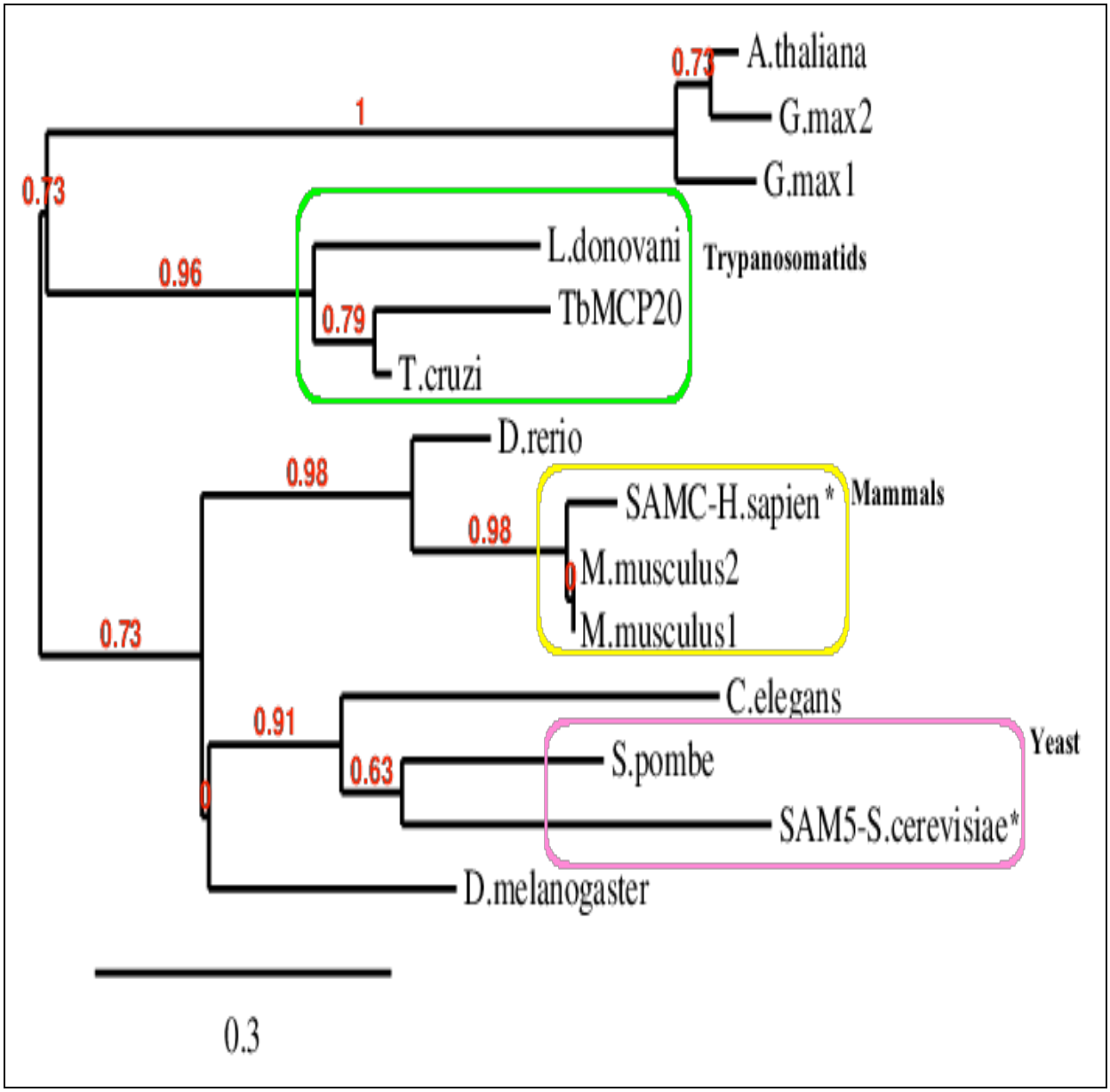

Figure 5.1. The phylogenetic maximum likelihood tree of TbMCP20 and related MCF proteins with separate clade clustering. The maximum likelihood tree depicts the evolutionary relationship between TbMCP20 in mammals (yellow), yeast (pink) and trypanosomatids (green). The colours boxes indicate the clustering of carriers with the same transport function. The bootstrap values located at the nodes represent the percentages obtained after resampling analysis of 1000 iterative data sets. Functionally characterised SAM transporters (*H.sapien* 'SAMC' and *S.cerevisiae* 'SAM5') are labelled with "*".

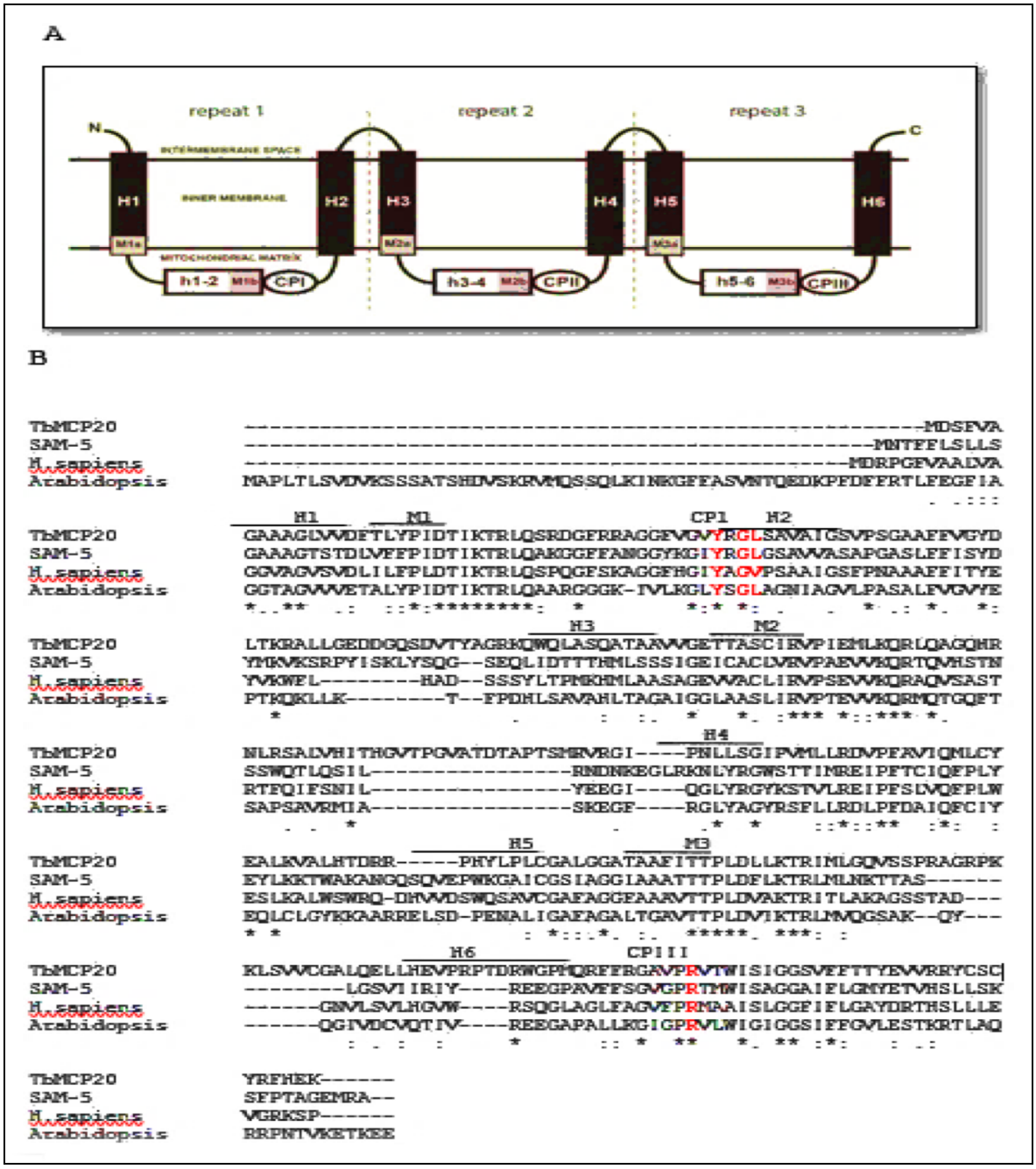

Figure 5.2. Alignment of the *T. brucei* TbMCP20 sequence with comparable sequences from *H. sapiens*, *S. cerevisiae* (SAM5) and *A. thaliana.* **A**: Schematic representation of the conserved structure of MCF proteins. The protein structure consists of six TM helices (H1–6) linked by hydrophilic loops (h1-2, h3-4 and h5-6). M1a, M2a and M3a indicate the first segment of the signature sequence motif, PX[D/E]XX[K/R]X[K/R], located at the ends of the odd-numbered TM helices, whereas M1b, M2b and M3b indicate the second part of the motif, [D/E]G[*n* residues][K/R]G, located at the end of each hydrophilic loop. **B**: Multiple sequence alignment of TbMCP20 with the human and yeast sequences. The amino acid sequences were aligned using ClustalO. The substrate contact points CPI, CPII and CPIII are located next to H1, H3 and H6, respectively. An asterisk (*) indicates positions with a single, fully conserved residue. A colon (:) signifies conservative substitutions of similar amino acids. A period (.) indicates substitutions of weakly similar amino acids.

5.2.2 Expression of TbMCP20 rescued the growth defect of the *S. cerevisiae* deletion strain ΔSAM5 on non-fermentative carbon sources

The *S. cerevisiae* gene deletion strain ΔSAM5 lacks the gene coding for the mitochondrial SAM carriers SAM5(Palmieri *et al*., 2003). As a consequence, this yeast deletion strain is not able to grow on media containing non-fermentable (mitochondrial) carbon sources such as glycerol or lactate, but instead can only grow on fermentative carbon sources such as glucose (Palmieri *et al*., 2003). Growth of *S. cerevisiae* ΔSAM5 on a non-fermentative carbon source such as glycerol can be restored by the expression of a functional mitochondrial SAM carrier (Palmieri *et al*., 2003). In order to test whether *T.brucei* TbMCP20 could function as a SAM carrier, TbMCP20 protein was heterologous expressed in the *S. cerevisiae* deletion strain ΔSAM5, followed by the analysis of the resulting growth phenotype on different fermentable (glucose) and non-fermentable (glycerol) carbon sources (section 2.2.10).

5.2.2.1 Plasmid construction using the yeast expression vector pCM190

The ORFs of TbMCP20 (*T. brucei*) and SAM5 (*S. cerevisiae*) were amplified by PCR (section 2.2.2.1). The restriction sites for *Bam*HI and *Not*I were incorporated into the relevant primers to facilitate the site directed cloning of the PCR products. The PCR products were initially cloned into the pGEM®-T Easy TA cloning vector, which was used for sequencing (Eurofins MWG). From the constructs verified as correct (no deviation in DNA sequence), the ORFs of TbMCP20 and SAM5 were subsequently cloned into the yeast expression vector pCM190, using *Bam*HI and *Not*I restriction enzyme sites to generate the plasmids , pCM190+TbMCP20 and pCM190+SAM5.

5.2.2.2 Growth complementation experiment

The plasmids pCM190+TbMCP20 and pCM190+SAM5 were transfected into the *S. cerevisiae* gene deletion strain ΔSAM5 (section 2.2.10.2). In addition, the empty pCM190 plasmid without insert was transfected into both the parental *S. cerevisiae* BY4741 and the *S. cerevisiae* deletion strain ΔSAM5 strain (section 2.2.10.2). The resulting yeast strain ΔSAM5 transformed with SAM5+pCM190 was used as a positive control (Palmieri *et al*., 2003), while the parental strain *S. cerevisiae* BY4741 transformed with the empty plasmid pCM190 was used as the "wildtype" (WT) strain.

The resultant yeast strains were grown on different carbon sources to examine the growth effects of the gene complementation. On glucose medium (YPD), all of the yeast strains

showed the same growth as the WT strain (figure 5.3). This was expected since under this condition growth is fermentative and not dependent on mitochondrial function. However, in the glycerol medium (YPG) where cell growth is more reliant on mitochondrial function (Palmieri *et al*., 2003), recombinant TbMCP20 gene expression was able to rescue 45% of the growth levels comparable to those of the WT *S. cerevisiae* BY4741 strain containing the empty pCM190 plasmid. The introduction of SAM5 into the ΔSAM5 strain restored only 50% of growth of the WT *S. cerevisiae* BY4741 strain containing the empty pCM190 plasmid (figure 5.3). This ability of heterologous expressed TbMCP20 to rescue the growth defect in the ΔSAM5 yeast strain suggested that expression of TbMCP20 gene complemented the transport function of SAM5.

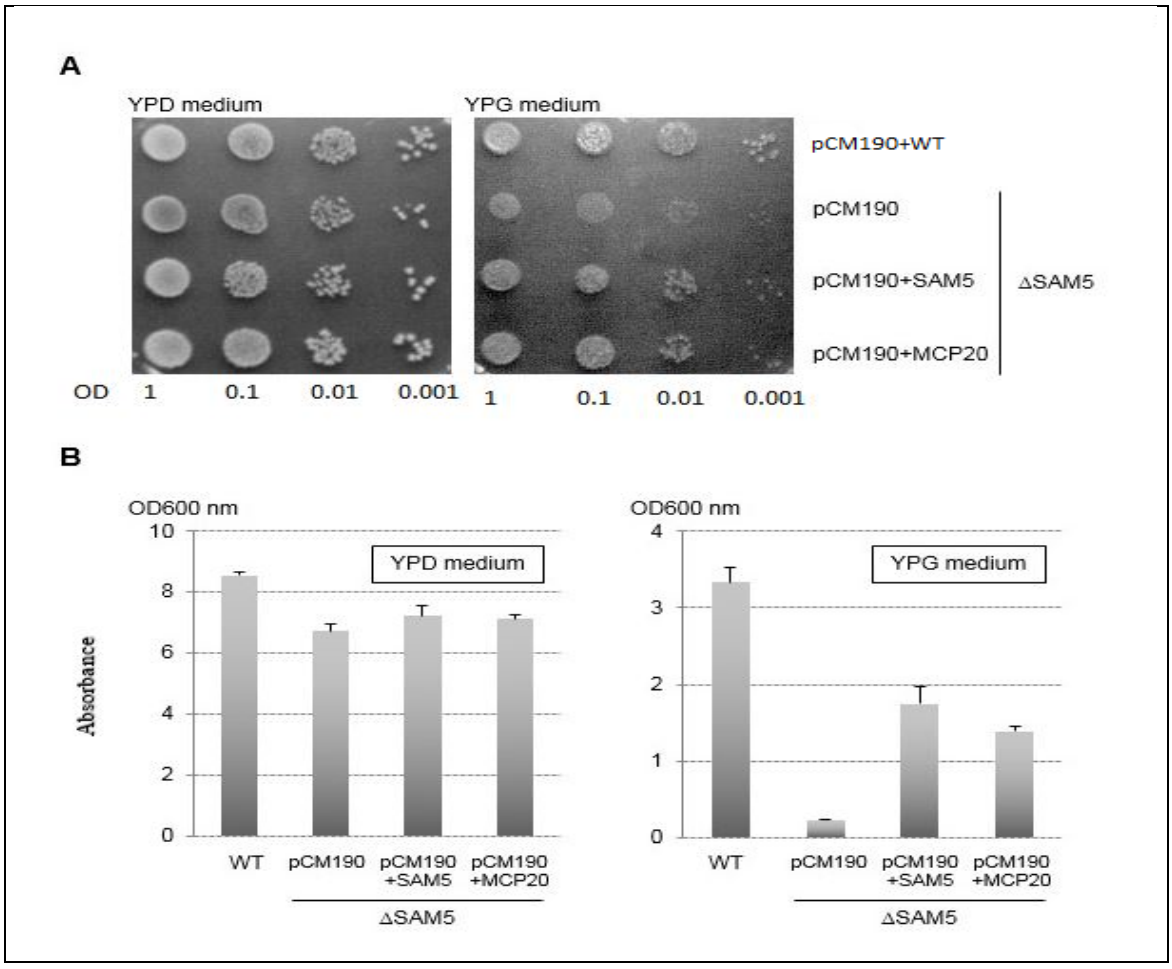

Figure 5.3. Growth of WT *S. cerevisiae* and ΔSAM5 on YPD and YPG media. **A**: YPG plates and YPD media were inoculated with four dot dilutions of WT BY4741 cells and ΔSAM5 cells transfected with empty pCM190, pCM190 + TbMCP20 or pCM190 + SAM5. The results represent five independent experiments. **B**: Growth analysis of the cells in YPD and YPG liquid media. Single colonies from all cells lines were cultured in liquid media and the rates of growth were recorded and plotted. The results represent the mean and standard deviation of six independent experimental replicates.

5.2.3 Knockdown of TbMCP20 caused a growth defect in *T. brucei*

Similar to the previous chapters, TbMCP20 was knocked down using RNAi approach by expression of double-stranded RNA containing both sense and antisense RNA sequences of TbMCP20, leading to a reduced or depleted expression of the targeted protein in *T. brucei*. The resulting growth phenotype can further give valuable information regarding the respective physiological function(s) of TbMCP20.

5.2.3.1 Knockdown-related plasmid construction

RNAi was performed by the simultaneous expression of the sense and corresponding antisense RNA molecules of the targeted gene sequences (Appendix 4) (Bringaud *et al.*, 2000). Primers were designed to PCR amplify a 1100 bp sense and an antisense version of the open reading frame of TbMCP20. The primer included the unique restriction sites *Bam*HI, *Apa*I, and *Hind*III, allowing the site-directed cloning of the sense and antisense DNA products in the *T. brucei* expression vector pHD676 (Appendix 5, section 5.1). The antisense primer for TbMCP20 gene was designed to include the *Bam*HI and *Apa*I restriction sites, whereas the primer for the sense DNA fragment was designed to include the *Apa*I and *Hind*III restriction sites. The sense and antisense DNA PCR products were cloned in tandem and joined at the *Apa*I site behind an inducible *T. brucei* promotor in the vector pHD676. Expression from the pHD676 vector will lead to the formation of a double-stranded RNA molecule connected by a short single stranded loop at the 3' end. Such a structure was shown to be more stable and more effective than a single-stranded antisense RNA molecule for the down-regulation of expression in *T. brucei* (Ngô *et al.*, 1998).

The resulting pHD676+TbMCP20 (sense+antisense) RNAi construct was analysed by using PCR, restriction enzyme digestion and gel electrophoresis to determine whether it contained the correct DNA fragment in the right order. A positive clone was further sent for sequencing (Eurofins MWG). The sequencing results confirmed that the used construct was indeed correct. The verified pHD676+TbMCP20 RNAi construct was used to transfect the *T. brucei* cell line PCF449 (section 2.2.5) and positive clonal cell lines were isolated. For comparison (same genetic background), a *T.brucei* PCF449 cell line was generated containing an empty (no insert) version of plasmid pHD676. Growth of the generated TbMCP20 RNAi and PCF449+pHD676 cell lines was analysed in MEM-Pros medium (Appendix 1) containing 5

mM proline and 0.12 mM glucose as carbon sources. RNAi was induced by the addition of tetracycline to the culture medium (section 2.2.4.2). Growth curves were plotted using Microsoft® Excel (Figures 5.4).

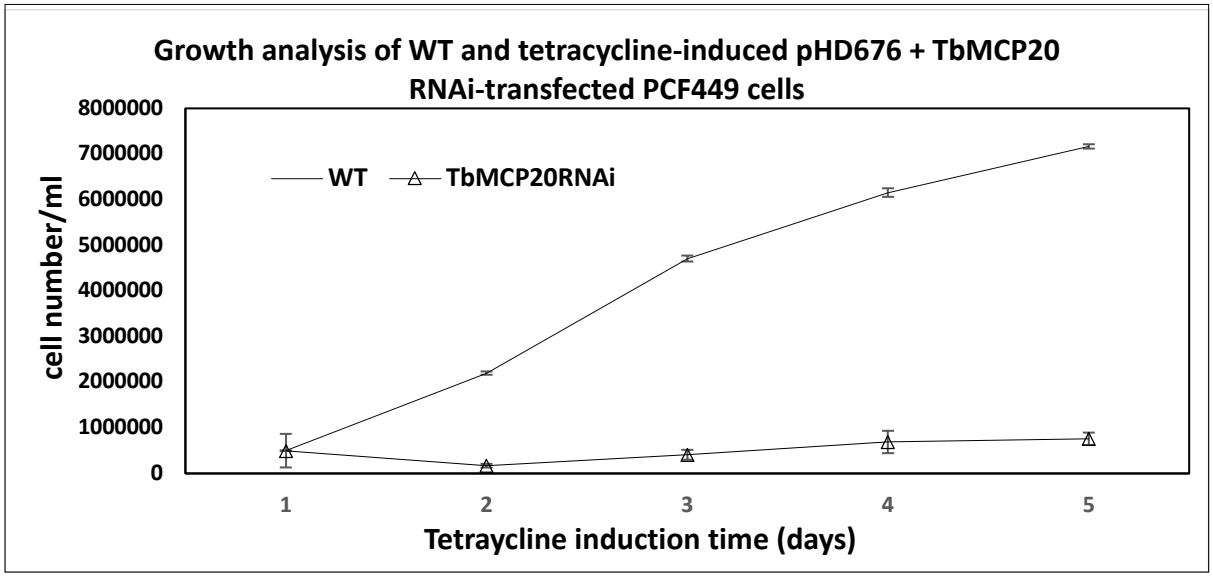

Figure 5.4. Comparison of the growth phenotypes of "wildtype" *T. brucei* PCF449 (WT) and tetracycline-induced pHD676+TbMCP20 RNAi cell lines in standard MEM-Pros medium containing 5 mM proline and 0.12 mM glucose. Cultures were started with 1×10^6 cells/ml and counted every 24 hours for five days. The data points represent the mean and standard deviation of three independent experimental replicates.

Upon induction with tetracycline, the TbMCP20 RNAi cell line presented a significant reduction in growth when compared to the 'wildtype" *T. brucei* PCF449 cell line, suggesting that TbMCP20 is essential for growth and thus the survival of T. *brucei*.

Unfortunately, no antibodies could be generated for the detection of TbMCP20 protein in *T. brucei* (see below, section 5.2.4). The depletion of TbMCP20 in the respective RNAi cell line was therefore examined by quantitative RT PCR. It is expected that after the depletion of TbMCP20 mRNA a similar depletion will follow at the protein level, taking into account a reduction of protein levels through ongoing cell division and protein turnover/degradation. The quantitative RT PCR results revealed that the TbMCP20 mRNA level was approximately100-fold lower in the respective RNAi cell line when compared to the parental PCF449 cell line (wildtype control).This result confirmed an effective down-regulation of TbMCP20 expression in the *T. brucei* RNAi cell line (Figure 5.5), and a corresponding depletion of TbMCP20 protein was inferred.

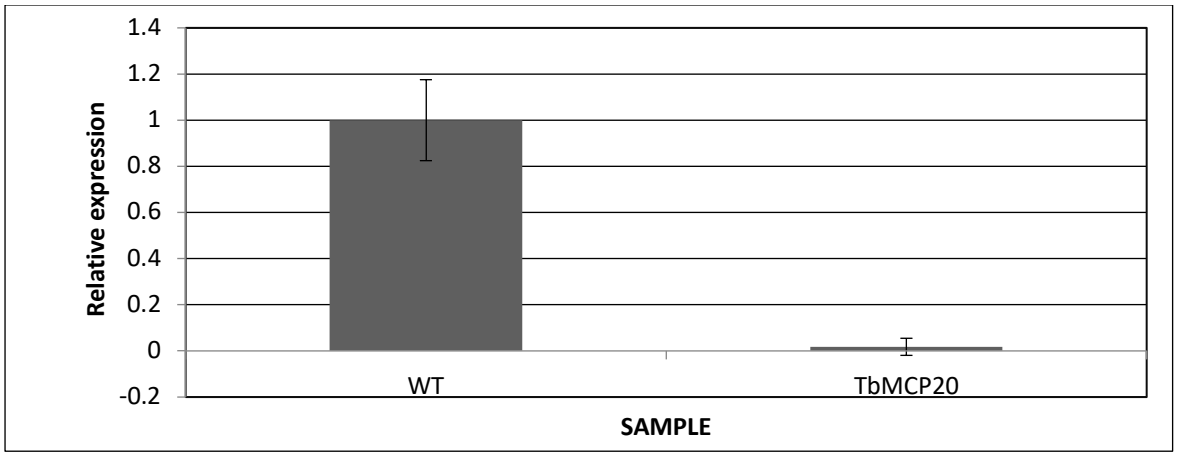

Figure 5.5. Relative mRNA levels of TbMCP20 in *T. brucei* PCF449 WT and tetracycline-induced RNAi cell lines. The level of TbMCP20 mRNA in the WT cell line was set as 1. The results represent the mean and standard deviation of six independent experimental replicates each.

5.2.4 Protein expression and antibody generation

In order to detect TbMCP20 expression at the protein level and to better analysis the propose function of this protein, TbMCP20 protein was expressed in and purified from *E. coli* using the inducible expression vector pET28. The resulting recombinant protein was expected to contain an N-terminal His-tag, which can be used for protein detection and purification. The purified protein will be used for antibody generation.

The ORF of TbMCP20 was amplified by PCR and the product was digested with the restriction enzymes of *Bam*HI (forward primer) and *Hind*III (reverse primer). Then, the PCR product was initially cloned into the pGEM®-T Easy TA cloning vector and the resulting clones were sent for sequencing (Eurofins MWG). Subsequentely, the verified TbMCP20 ORF was cloned into the *E. coli* expression vector pET28 using *Bam*HI and *Hind*III, resulting in pET28 + TbMCP20.

5.2.4.1 Protein expression

In order to produce adequate quantities of the protein, the plasmid pET28 + TbMCP20 was transformed into the *E. coli* strain Lemo21 (DE3 (section 2.2.9). Protein expression was induced with IPTG (final concentration; 0.4 mM; Figure 5.6).

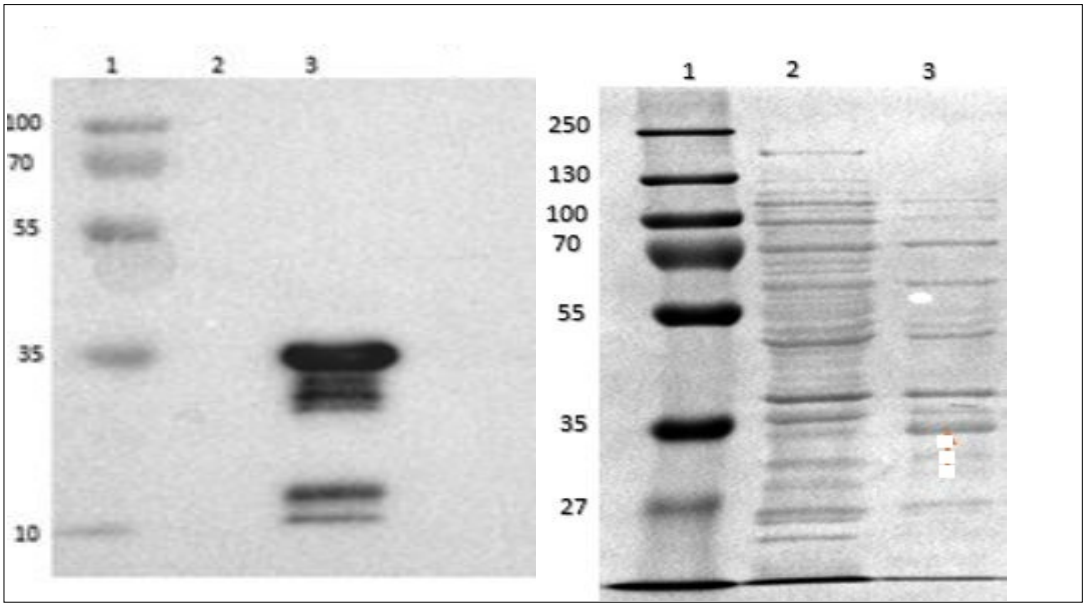

Figure 5.6. Western blots probed with commercially available anti-His-antibody (left) or stained with Coomassie blue (right) to analyse protein expression after induction of TbMCP20 (35 kDa) with IPTG (final concentration, 0.4 mM) for 4 hours. The protein ladder is shown in lane 1. Lane 2 contained a transformed cell sample prior to induction. Lane 3 shows protein expression after four hours induction. Each lane was loaded with 10 µg protein sample and the results are representative of three individual attempts at inducing expression of the recombinant his-tagged TbMCP20.

The heterologous expression of proteins in *E. coli* can generate insoluble, inactive protein aggregates called inclusion bodies (Rosano & Ceccarelli, 2014; Wingfield *et al.*, 2001). A good initial step for the isolation of "pure" recombinant protein could be to isolate inclusion bodies after the recombinant expression of the TbMCP proteins. Therefore, the formation of inclusion bodies was assessed after the expression of the recombinant TbMCP20 protein in *E. coli* strain Lemo21 (DE3) (section 2.2.9). As shown in Figure 5.7, TbMCP20-His expression was successfully induced and the protein was purified using Ni-NTA beads. However, both TbMCP20-His and unbound proteins passed through the column and were collected in the effluent (Figure 5.7). The Ni-NTA was washed three times to remove any residue, then eluted three times with buffer that contained detergents to free His-tagged proteins from the column. Only very limited amounts of protein were detected in the CL and the three wash samples, which indicated that the protein binding step was efficient (Figure 5.7). In the three elution samples, His-tagged protein was observed along with some degraded products. Approximately one-third of the His-tagged protein remained in the Ni-NTA beads.

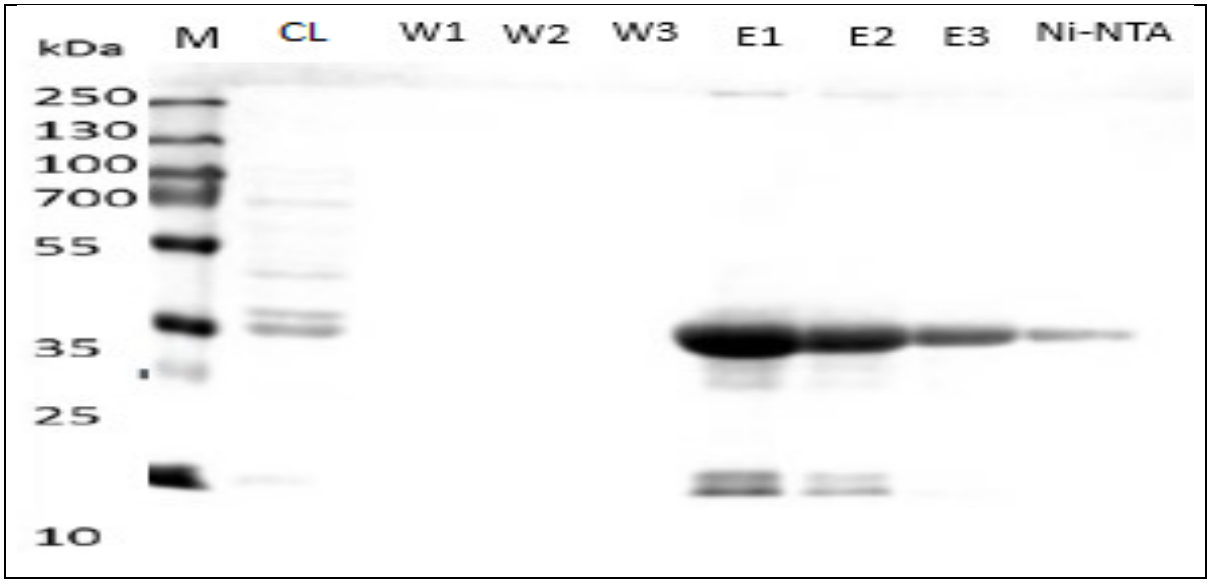

Figure 5.7. TbMCP20 protein purification using a Ni-NTA column. Samples were collected at the various stages of protein purification and loaded onto a Coomassie Brilliant Blue gel. Lane M: protein markers; CL: cell lysate prior to loading on Ni-NTA agarose; W1, W2 and W3: proteins obtained after first, second and third washes, respectively; E1, E2 and E3: proteins obtained after first, second and third elutions, respectively; Ni-NTA: proteins obtained from the agarose following elution. The results represent two independent experiments.

The proteins were next quantified using standard protein quantification methods, like the BCA protein assay. BSA was run at various concentrations as a standard alongside the protein samples (figure 5.8) ; the densities of the target protein bands were compared against the BSA bands on the Coomassie gel. The concentration of His-tagged protein in the 1:5 dilution of the elution sample (fraction E1) exceeded 375 μg/ml and the concentration in the 1:10 dilution of the elution sample was approximately 250 μg/ml (Figure 5.8). Approximately 3 mg of protein (0.5 ml) was loaded on a gel and the gel slice containing the protein was sent to EZBiolab (Carmel, IN, USA) for antibody generation in rabbits.

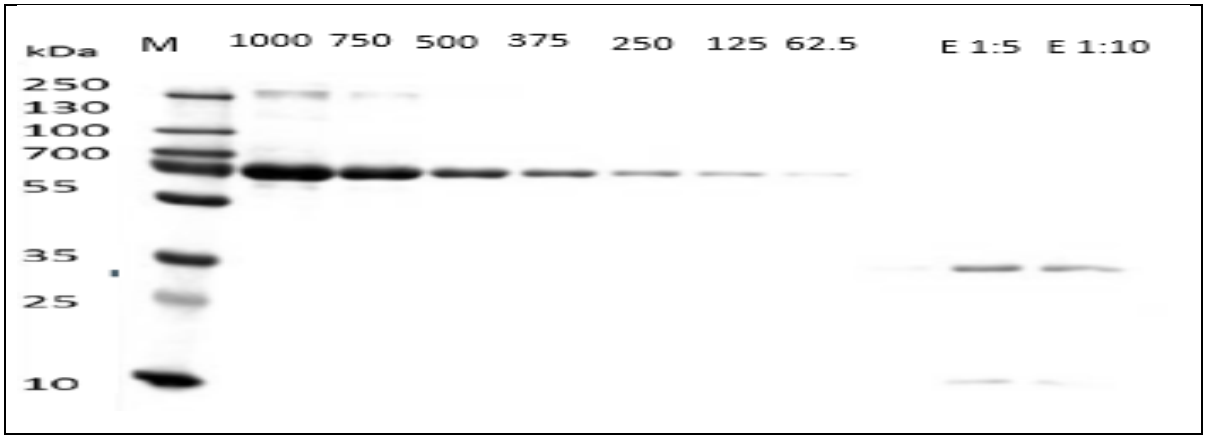

Figure 5.8. Quantification of the TbMCP20 protein concentration in the Ni-NTA elution fraction. BSA standards (62.5 µg/ml to 1000 µg/ml) and the elution fraction were subjected to SDS-PAGE and stained with Coomassie blue. The elutions containing TbMCP20-His were diluted 1:5 or 1:10 (E1:5 and E1:10). The gel represents three independent experiments.

The antisera generated from two rabbits challenged with TbMCP20-His were tested in the PCF449 and BSF449 *T. brucei* cell lines. The TbMCP20 antisera did not detect any bands in either the PCF449 or BSF449 cell lines (Figure 5.9). Furthermore, no protein bands were detected after testing different dilutions of the obtained TbMCP20 antisera. Moreover, we also tested different variations including loading more protein/sample, reducing the denaturation temperature in case this causes aggregation.

Figure 5.9. Western blot of the *T. brucei* PCF449 and BSF449 cell lines with TbMCP20 antisera (dilution 1:100). Each lane was loaded with 2×10^6 cells. The results are representative of three independent experimental replicates. Lane M, protein markers

5.2.5 TbMCP20 localised to the mitochondria of *T. brucei* PCF449

The subcellular localisation of TbMCP20 in the PCF449 of *T. brucei* was investigated using immunofluorescence microscopy. Since the raised TbMCP20 antisera was unable to detect TbMCP20 protein, a recombinant myc-tagged version of TbMCP20 was expressed instead, allowing the use of commercially available myc antibodies.

5.2.5.1 Plasmid construction

The ORF of TbMCP20 was PCR amplified using primers with added unique *Bam*HI and *Hind*III restriction sites. The PCR product was cloned into the pGEM®-T Easy vector and the construct (10 µl) was sequenced (Eurofins MWG). Then, the ORF of TbMCP20 was subsequently cloned into the *T. brucei* expression vector pHD1484 using the *Bam*HI and *Hind*III restriction enzyme sites and resulting in the pHD1484-TbMCP20-cmyc^{ti} construct. The tetracycline inducible expression from pHD1484 will add a double myc-tag to the c-terminus of TbMCP20.

5.2.5.2 Subcellular localisation

The *T. brucei* PCF 449 cell line was transfected with pHD1484-TbMCP20-myc^{ti}and expression of the myc-tagged version of TbMCP20 was induced by addition tetracycline (section 2.2.6). Immunofluorescence microscopy was performed using a commercial available myc antibody (Figure 5.10).

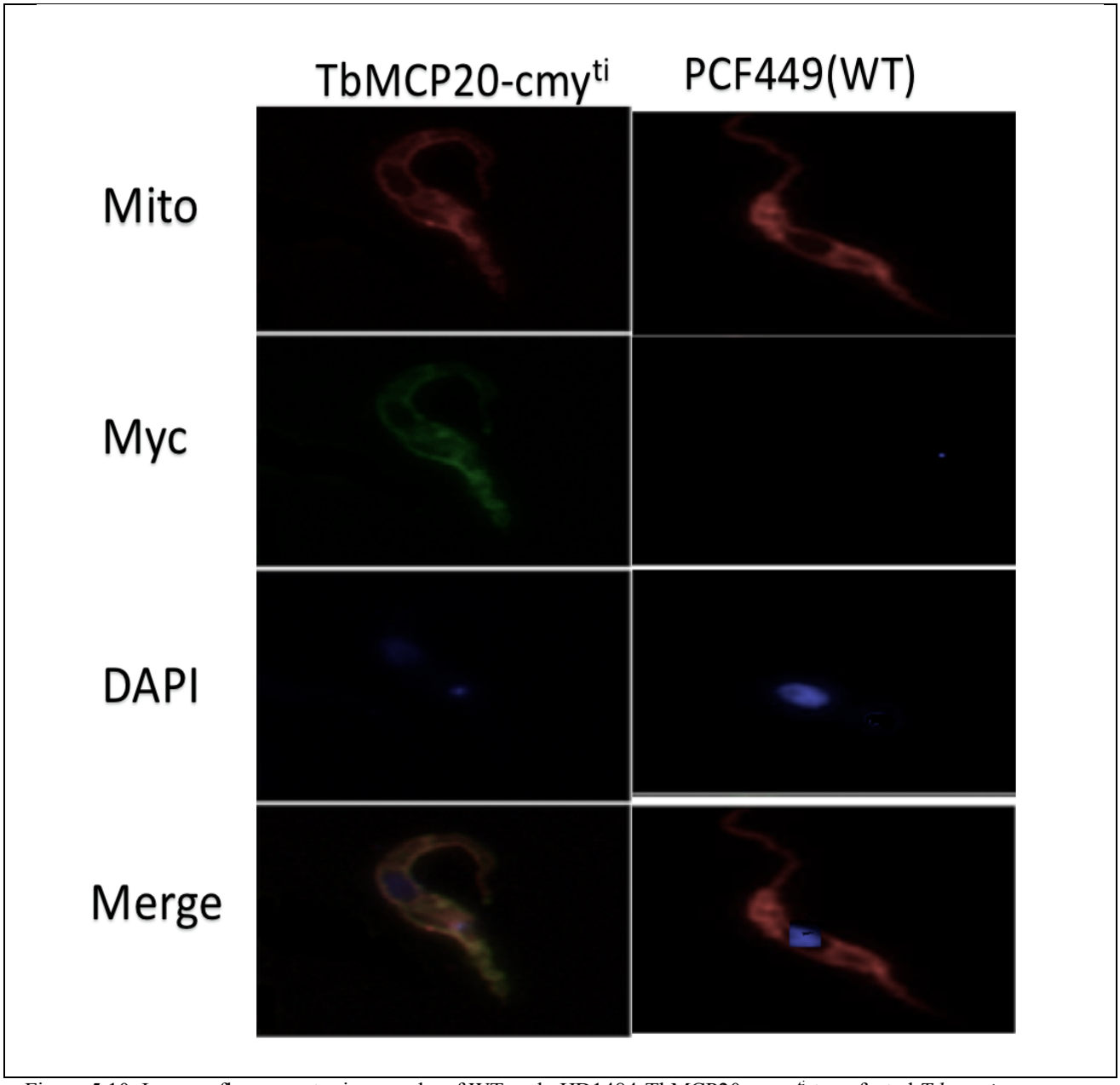

Figure 5.10. Immunofluorescent micrographs of WT and pHD1484-TbMCP20-cmyc^{ti}-transfected *T.brucei* PCF449 cell lines .The MitoTracker (Mito; red), TbMCP20-myc (green) and DAPI (blue) signals were merged to form the overlay. The results represent three independent experiments.

The immunofluorescence results showed a specific tubular shaped staining of PCF 449 *T. brucei* when using the myc antibody, which recognises myc-tagged TbMCP20. This staining pattern was identical to the one obtained for MitoTracker, which is used as a mitochondrial marker for *T. brucei* .This result confirmed the mitochondrial localisation of TbMCP20 in PCF449 *T. brucei*.

5.3 Discussion and Conclusion

In yeast and humans, SAM is required as a substrate for the production of polyamines (Takahashi *et al*., 2010). In addition, SAM also functions as a methyl donor for nearly all methylation reactions taking place in the mitochondrion (King *et al*., 2016). To fulfil this function, SAM must be transported across the mitochondrial membrane from the cytosol to sustain energy metabolism (Palmieri *et al*., 2009). In yeast and humans, SAM was shown to transported into the mitochondrial matrix by the MCF proteins SAM5 and SAMC, respectively (Palmieri *et al*., 2016).

In African trypanosomes, SAM is either formed from methionine via the s-adenosylmethionine synthetase reaction or it can be imported directly from the host serum (Marobbio *et al*., 2003). Either way, SAM needs to be imported into the *T. brucei* mitochondrion. Colasante *et al*. (2006) previously identified 24 mitochondrial carrier family proteins, e.g. TbMCP1–24, which catalyse the transport of various metabolites across the mitochondrial membrane in *T. brucei.* Of these *T. brucei* MCF proteins, only TbMCP20 was found to be significantly homologous to SAMCs found in humans/mammals and SAM5 yeast (Colasante *et al*., 2009). Therefore, sequence aanalysis indicated that TbMCP20 could be a s-adenosylmethyoinine transporter in *T. brucei*.

It is essential to experimentally determine the localisation of each MCF proteins in *T. brucei*. Here therefore, TbMCP20 was found to localise exclusively to the mitochondria of the PCF449 *T.brucei* , where it appears to perform a mitochondrial transport function.

The function of TbMCP20 was also examined by functional complementation studies in yeast using the SAM deletion strain ΔSAM5. The ΔSAM5 *S. cerevisiae* strain was induced to express heterologous TbMCP20, which restored its growth on glycerol as a non-fermentative carbon source. This finding indicated that TbMCP20 is capable of rescuing mitochondrial SAM5 carrier deficiency of yeast. Therefore, the successful complementation of the growth defect caused by SAM5 deficiency (Palmieri *et al*., 2003) strongly supported the hypothesis that TbMCP20 is probably fulfils a similar function as SAMC. Notably, the control experiment, which involved the re-introduction of SAM5 into the ΔSAM5 strain, did not result in the complete rescue of *S. cerevisiae* growth. This could be due to lower than endogenous expression of the SAM5 gene from the plasmid or detrimental SAM5 over-expression (Agrimi *et al*., 2003; Palmieri *et al.*, 2006). Our results on the complementation study of the TbMCP20

on fermentative and non-fermentative carbon sources substrate suggested that SAM plays an important role in the mitochondria for the cell life and also essential for respiratory growth (Diaz *et al*., 2012).

DNA methylation, a type of epigenetic modification, is performed by DNA methyltransferases. DNA methylation has been extensively studied in plants and mammals (Chen *et al*., 2011). However, information about this phenomenon in lower eukaryotes is incomplete as these organisms pass through numerous lifecycle stages, which makes it difficult to reliably determine their methylation status at any specific stage (Moore *et al*., 2012). In mammals, most methylated cytosine is found in cytosine–phosphate–guanine, or CpG, dinucleotides (Li *et al*., 2014). Relatively few studies about DNA methylation in eukaryotes like *T. brucei* have been published compared to the number of studies published on that process in mammals and plants (Leeuwen *et al*., 2000). Methylcytosine has only been found in mammals, but Heino *et al*. (2005) hypothesised that unicellular organisms contain methylcytosine. methylcytosine in *T. brucei* was suggested to be involved in the silence of the transcriptional genes repression. However, other possibilities role of the methylcytosine in *T. brucei* require attention as well (Militello et al., 2008). In *T. brucei* the modified DNA base is named Base J (Militello *et al*., 2008). Base J, or β-D-glucosyl-hydroxymethyluracil, is a modified DNA base that can be substituted for thymine in the nuclear DNA of kinetoplastid parasites such as *T. brucei*. Its role in silencing specific genes in *T. brucei* is reminiscent of the role of methylated cytosine in higher eukaryotes (Leeuwen *et al*., 2000).
TbMCP20 gene replacement and RNAi studies revealed that ΔTbMCP20 trypanosomes have impaired growth compared to that of PCF449 *T.brucei* cells at high cell densities. This finding suggests that TbMCP20 is essential for the survival of the PCF449 of *T. brucei*, with a possible detrimental effect role in *T. brucei* cytokinesis and kinetoplast division (Voncken *et al.*, 2006).

TbMCP20 antibody generation and immunoblotting were performed. However, the generated antisera did not detect the TbMCP20 protein in *T. brucei* BSF449 or PCF449. The failure of the antisera to bind could be due to: (1) the short boost times in the host rabbits or (2) insufficient binding affinities of the TbMCP20 antisera. Protein expression of *T. brucei* genes is developmentally regulated at the mRNA level (Kramer., 2012). The expression of the tagged TbMCP20 protein is consistent with post-transcriptional regulation of TbMCP20 at the mRNA level, which is common in trypanosomatids due to their reliance on polycistronic transcription, trans- dsplicing and polyadenylation (Liang *et al*, 2003). However, the depletion of mRNA did

not necessarily imply down-regulation at the protein level since low mRNA copy number can be sufficient to promote protein expression.

In conclusion, TbMCP20 is the only homologue among the *T. brucei* MCF proteins to a mitochondrial SAM transporter. It proved to be essential for *T. brucei* growth. The introduction of TbMCP20 into yeast ΔSAM-5 cells restored their growth defect. For future studies , the following experiments are suggested to be included. First of all, concerning antibody generation, more elution steps or larger volume of elution buffer should be applied. If the same problem turns up again, more powerful detergent or higher concentrations should be tested. Also SAM transport assays, should be conducted to elucidate the function of TbMCP20.

Chapter 6: Sequence analysis and functional characterisation of TbMCP23: a putative pyrimidine nucleotide carrier

6.1 Introduction

Kinetoplastida parasites, including important pathogens such as *Trypanosoma* and *Leishmania* species, they both have pyrimidine biosynthesis and salvage mechanisms (De Koning *et al*., 2005). The pyrimidine nucleotide carrier has been reported to be a multi-copy mitochondrial suppressor (Marobbio *et al*., 2006).

Deoxyuridine 5′-triphosphate (dUTP) nucleotidohydrolase has also been confirmed as a drug target in the pyrimidine pathway. Inhibition of the enzyme through RNAi-mediated knockdown diminishes the growth rate of the organism. It also results in the toxic accumulation of dUTP in cells, leading to DNA breaks (Castillo-Acosta *et al*., 2008). Sienkiewicz *et al*. (2008) reported lethal effects of dihydrofolate reductase-thymidylate synthase knockdown in *T. brucei*, except in the presence of high levels of thymidine *in vitro*. In another study, when an enzyme from the pyrimidine biosynthesis pathway, dihydroorotate dehydrogenase, was knocked down using RNAi and cells were grown with limited scope for pyrimidine salvage, the BSF of the parasite demonstrated extremely reduced growth (Arakaki *et al*., 2008). In pyrimidine-insufficient conditions *in vitro*, *L. donovani* requires uridine monophosphate (French *et al*., 2011).

Some of the *T. brucei* enzymes that are involved with the pyrimidine interconversion pathways (salvage and de novo pathways) have proven to be promising drug targets (Leija *et al*., 2016). Thus, several drug targets have been identified in the pyrimidine metabolic system of African trypanosomes. Although researchers have discovered high-affinity transporter molecules for uridine (TbU2) and uracil (TbU1) in the PCF of the parasite (Gudin *et al*., 2006), knowledge about pyrimidine transporters in the BSF remains scarce. The shortage of data related to the transportation of pyrimidine in the BSF prevents the development of chemotherapies that target the pyrimidine pathways.

T. brucei TbMCP23 shares conserved sequences with the yeast mitochondrial pyrimidine carrier Rim2 (Yoon *et al*., 2011). In this chapter, due to time constraints, preliminary experiments on TbMCP23 were performed, including sequence analysis, TbMCP23 RNAi cell line generation and growth phenotype detection. The protein was also heterologous expressed in *E. coli* to facilitate antibody generation.

6.2 Results

6.2.1 Phylogenetic reconstruction and sequence alignment of TbMCP23

Among the 24 MCF proteins identified in *T. brucei* (TbMCP1–24) ,TbMCP23 is a homologue of the previously characterised pyrimidine carrier SLC25 in human mitochondria (Colasante *et al*., 2009). The protein sequence of TbMCP23 was subjected to BLAST analysis (http://blast.ncbi.nlm.nih.gov/) against the genome database. The greatest sequence similarity was found with sequences belonging to species of Kinetoplastida, such as *T. b. gambiense* and *T. b. cruzi*. The protein also demonstrated similarity to mammalian SLC25, including that of *M. musculus.* The sequence of the TbMCP23 protein was also analysed against the genome databases of *H. sapiens* and *S. cerevisiae.* When compared against the *H. sapiens* genome database, the TbMCP23 protein demonstrated the greatest similarity with the mitochondrial pyrimidine transporter SLC25A33. Results from the BLAST analysis also showed that TbMCP23 demonstrated homology to the yeast Rim2 protein .After the related sequences were collected and aligned, phylogeny.fr was used to form a phylogenetic tree (Figure 6.1). Due to their highly conserved sequences, the trypanosomes formed a distinct clade. This clade was closely related to the mammalian SLC25 and yeast Rim2 proteins, which have been characterised as mitochondrial pyrimidine transporters (Hildyard & Halestrap, 2003; Van Dyck *et al*., 1995; Marobbio *et al*., 2006; Da-Rè *et al*., 2014). These results implied that TbMCP23 could be a mitochondrial pyrimidine transporter.

As TbMCP23 appeared to be a potential pyrimidine transporter, its sequence was aligned with PNC1, Rim2 and homologues from *Leishmania.* Furthermore, the structural sequence features of TbMCP23 were analysed. Sequence alignment of TbMCP23 with homologues from *L. major, S. cerevisiae* Rim2 and *H. sapiens* PNC1 showed that TbMCP23 contained all of the conserved sequences and structural features of MCF proteins (Figure 6.2). TbMCP23 consists of 310 amino acids and has a predicted protein size of 34 kDa. TbMCP23, like other MCF proteins, comprises of three repetitive domains and each domain contains two TM α-helices. The signature sequence motif 'PX[D/E]XX[K/R]X[K/R]', where 'X' represents any amino acid residue (Aquila *et al*., 1987; Saraste & Walker, 1982), can be found at the ends of H1, H3 and H5 (labelled M1, M2 and M3). There were four exceptions to the conservation of the signature sequence motif. First, the [D/E] in M2 was replaced by a nonpolar phenylalanine (F; see TbMCP23 and *L. major* homologue) or tryptophan (W; see Rim2 and PNC1). This polar mutation is known to result in a different pyrimidine transport mechanism (Palmieri *et*

al., 2016). In addition, in the M3 of trypanosomatids (represented by *T. brucei* and *L. major*), the [D/E] was replaced by asparagine (N), the first [K/R] was replaced by methionine (M) and the second [K/R] was replaced by histidine (H), which falls in the positively charged amino acid group. Similarly, the second signature motif '[D/E]G[4–5 residues][W/F/Y][K/R]G' (labelled M1, M2 and M3) was also conserved, except for the first two amino acids in M1.

In MCF proteins, the groups of conserved amino acids located downstream of each signature motif participate in substrate discrimination, recognition and binding. The three well-conserved substrate contact points CPI, CPII and CPIII are shared by MCF proteins that transport similar substrates (Kunji & Robinson, 2006). As shown by the protein sequence alignments of the mitochondrial pyrimidine carriers (Figure 6.2), the three amino acids of CPI are relatively conserved. The first amino acid in CPI was either a hydrophobic alanine (A) in trypanosomatids or a hydrophobic glycine (G) in yeast and human, the second amino acid was a hydrophilic serine (S) or hydrophobic alanine (A) in yeast, and the third amino acid was either a tyrosine (Y) in trypanosomatids or asparagine (N) in yeast. For CPII, the first glycine (G) was conserved in all four sequences, as Kunji predicted. The second amino acid varied as a positively charged arginine (R), hydrophilic serine (S) or hydrophobic isoleucine (I). The positively charged arginine (R) in CPIII is involved in phosphate binding (Kunji & Robinson, 2006).

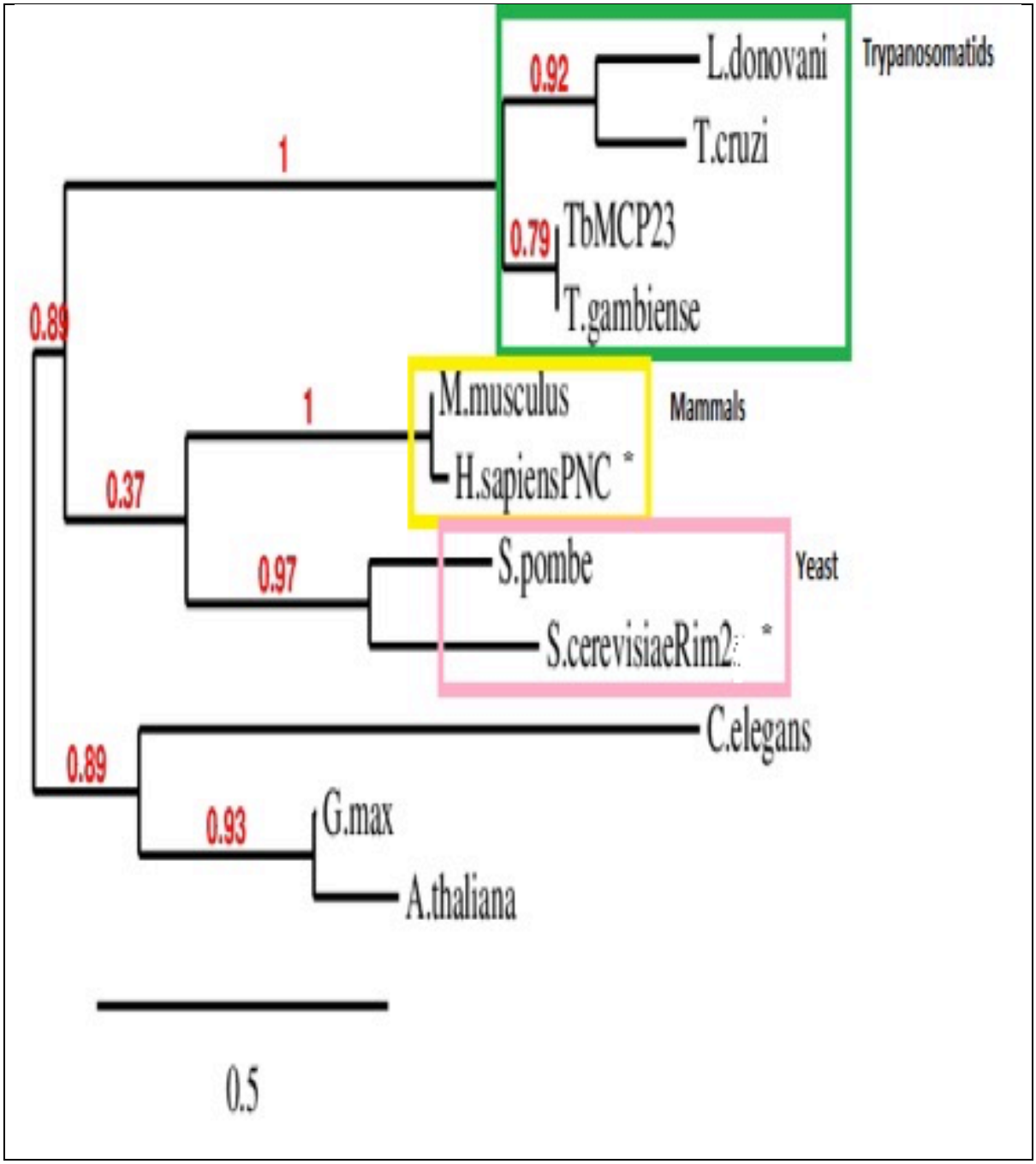

Figure 6.1. The phylogenetic tree of TbMCP23 and related MCF proteins, which clustered in separate clades. The maximum likelihood tree shows the evolutionary relationship between TbMCP23 in mammals (yellow), yeast (pink) and trypanosomatids (green). The colours indicate the clustering of the carriers with the same transport function. The bootstrap values located at the nodes represent the percentages obtained after resampling analysis of 100 iterative data sets.

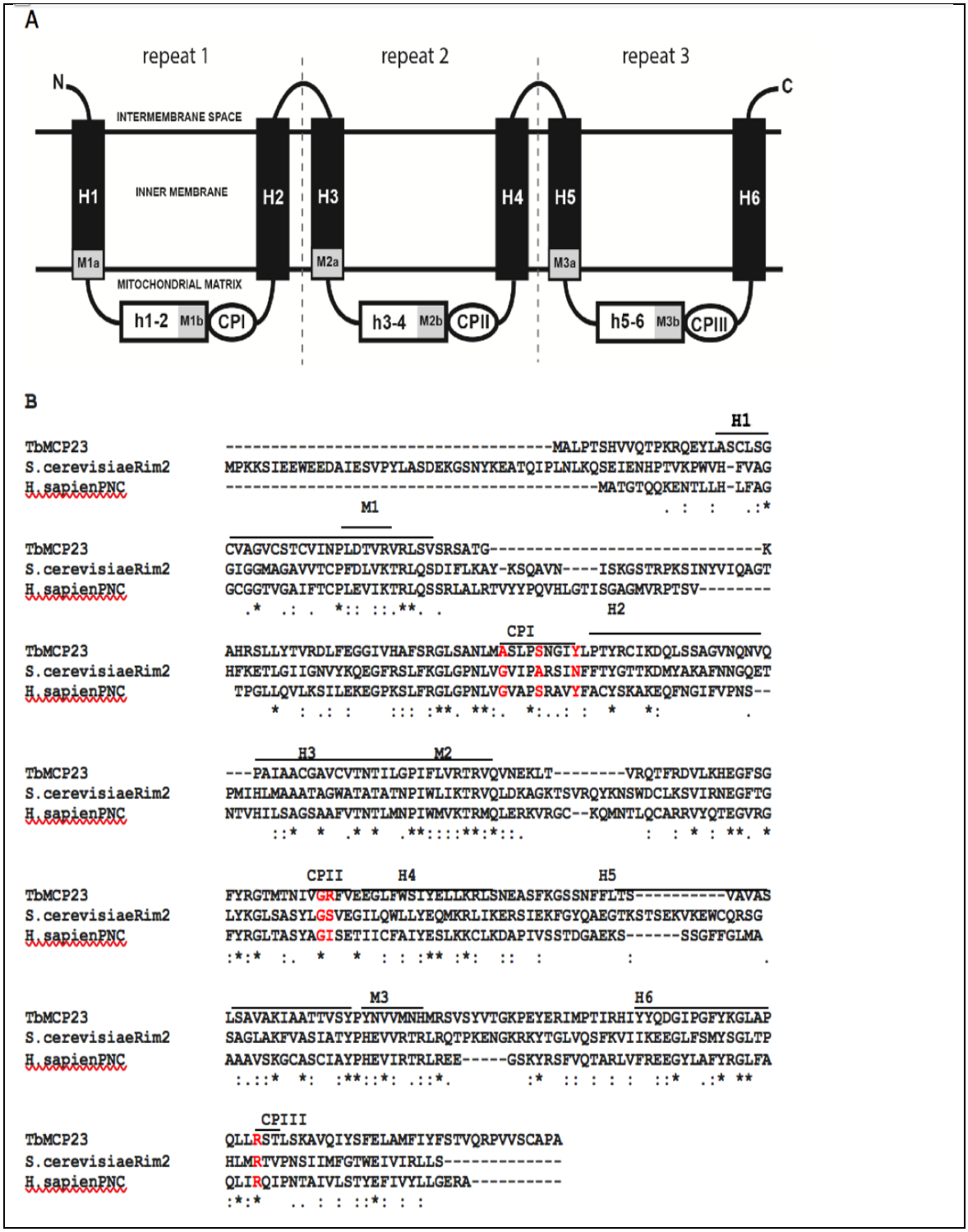

Figure 6.2. Alignment of the TbMCP23 sequence with comparable sequences from *L. major, S. cerevisiae* Rim2 and *H. sapiens* PNC1. **A**: Schematic representation of MCPs. The protein structure consists of six TM helices (H1–6) linked by hydrophilic loops (h1-2, h3-4 and h5-6). M1a, M2a and M3a indicate the first segment of the signature sequence motif, PX[D/E]XX[K/R]X[K/R], located at the end of the odd-numbered TM helices, whereas M1b, M2b and M3b indicate the second part of the motif, [D/E]G[*n* residues][K/R]G, located at the end of each hydrophilic loop. **B**: Multiple sequence alignment of TbMCP23 with related human and yeast proteins. Amino acid sequences were aligned using ClustalO. The substrate contact points (CPI, CPII and CPIII) are located next to TM H1, H3 and H6, respectively. An asterisk (*) indicates positions which have a single, fully conserved residue. Colon (:) signifies conservation between groups of strongly similar residues. Period (.) stands for conservation between groups of weakly similar residues.

6.2.2 Knockdown of TbMCP23 slightly increased growth compared to *T. brucei*

As described on the previous chapters, RNAi approach was used to Knockdown TbMCP23. RNA interference (RNAi) was used to determine whether expression of TbMCP23 is essential for the growth and survival of *T. brucei*. The resulting growth phenotype can further give valuable information regarding the respective physiological functions of TbMCP23.The expression of TbMCP23 in *T. brucei* was down-regulated ("knocked-down") by using an RNAi-approach as described in the previous chapters (section 2.2.3). This RNAi-approach is based on the expression of double-stranded (sense+antisense) RNA molecules for TbMCP23, leading to a reduced or depleted expression of the targeted protein in *T. brucei*.

6.2.2.1 Knockdown-related plasmid construction

RNAi was performed by the simultaneous expression of the sense and corresponding antisense RNA molecules of the targeted gene sequences (Appendix 4) (Bringaud *et al.*, 2000). Primers were designed to PCR amplify a 1000 bp sense and an antisense version of the open reading frames of TbMCP23.The primer included the unique restriction sites *Bam*HI, *Apa*I, and *Hind*III, allowing the site-directed cloning of the sense and antisense DNA products in the *T. brucei* expression vector pHD676 (Appendix 5, section 5.1). The antisense primer for TbMCP23 gene was designed to include the *Bam*HI and *Apa*I restriction sites, whereas the primer for the sense DNA fragment was designed to include the *Apa*I and *Hind*III restriction sites. The sense and antisense DNA PCR products were cloned in tandem and joined at the *Apa*I site behind an inducible *T. brucei* promotor in the vector pHD676. Expression from the pHD676 vector will lead to the formation of a double-stranded RNA molecule connected by a short single stranded loop at the 3' end. Such a structure was shown to be more stable and more effective than a single-stranded antisense RNA molecule for the down-regulation of expression in *T. brucei* (Ngô *et al*., 1998).

The resulting pHD676+TbMCP23 (sense+antisense) RNAi construct was analysed by using PCR, restriction enzyme digestion and gel electrophoresis to determine whether they contained the correct DNA fragments in the right order. Positive clones were further sent for sequencing (Eurofins MWG). The sequencing results confirmed that the used constructs were indeed correct.

The verified pHD676 +TbMCP23RNAi construct was transfected into the *T. brucei* cell line PCF449 (section 2.2.5) and positive clonal cell line was isolated. For comparison (same genetic background), a *T.brucei* PCF449 cell line was generated containing an empty (no insert) version of plasmid pHD676. The growth of the TbMCP23 RNAi cell line was analysed in MEM-Pros medium (Appendix 1) containing 5 mM proline and 0.12 mM glucose after treatment with tetracycline (section 2.2.4.2). The growth phenotype outcomes were plotted on graph using Microsoft® Excel software (Figure 6.3).

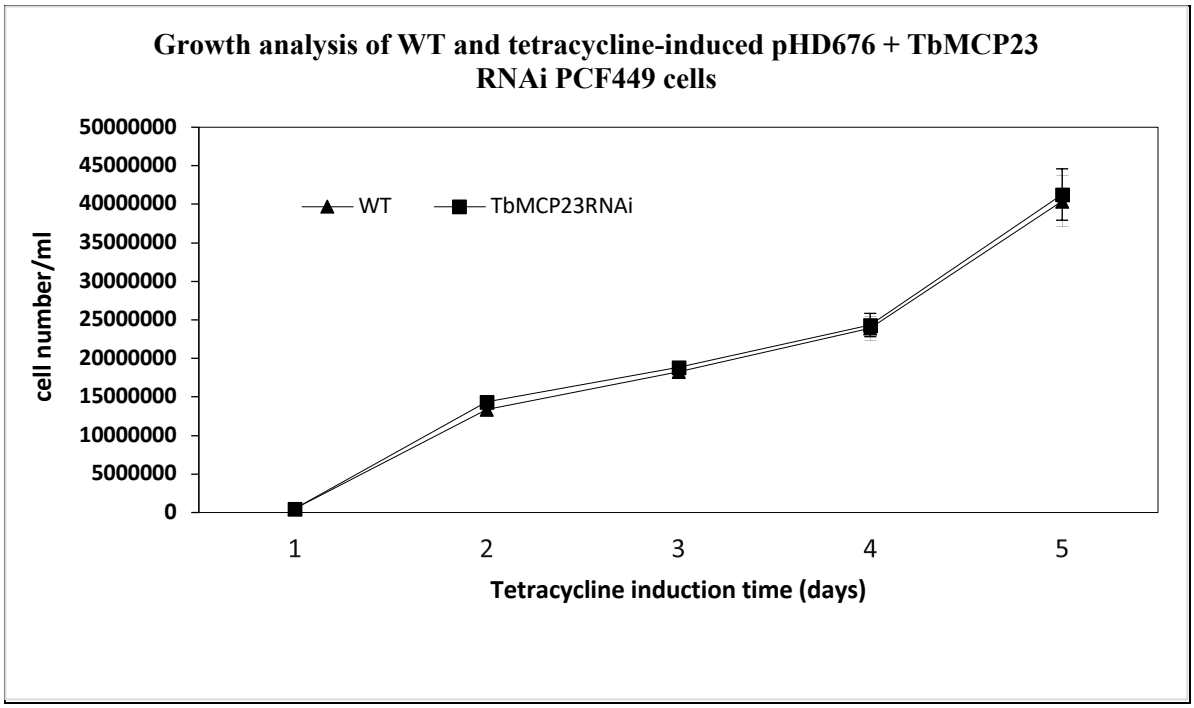

Figure 6.3. Comparison of the growth phenotypes of the WT *T. brucei* PCF449 and tetracycline-induced TbMCP23 RNAi-transfected cell line in standard MEM-Pros medium with 5 mM proline and 0.12 mM glucose. Cultures were started with 5×10^5 cells/ml and counted every 24 hours for five days. The values represent the mean and standard deviation of six independent experimental replicates.

Therefore, the TbMCP23 RNAi cell line grew at a slightly higher cell density than the WT *T. brucei* PCF449, which suggested that TbMCP23 is not essential for *T. brucei* survival at this stage. However, this need to be confirmed by doing quantitative RT-PCR to show that there is no TbMCP23RNA left or an antibody against TbMCP23.

6.2.3 Protein expression and antibody generation

In order to detect TbMCP23 expression at the protein level, and to better characterise the proposed function of this protein, TbMCP23 was expressed in *E. coli* using the inducible expression vector pET28. The resulting recombinant protein were expected to contain an N-terminal His-tag, which can be used for protein detection and purification. The purified protein will be used for antibody generation.

6.2.3.1 Protein expression

The isolated pET28+TbMCP23 construct was transformed into Lemo21 *E. coli* cells, in which protein expression was induced. As shown in Figure 6.4, a band of the predicted size for TbMCP23-His (~34 kDa) was observed after Coomassie blue staining and confirmed by blotting with the anti-His antibody.The result indicated that TbMCP23 was successfully expressed after IPTG induction.

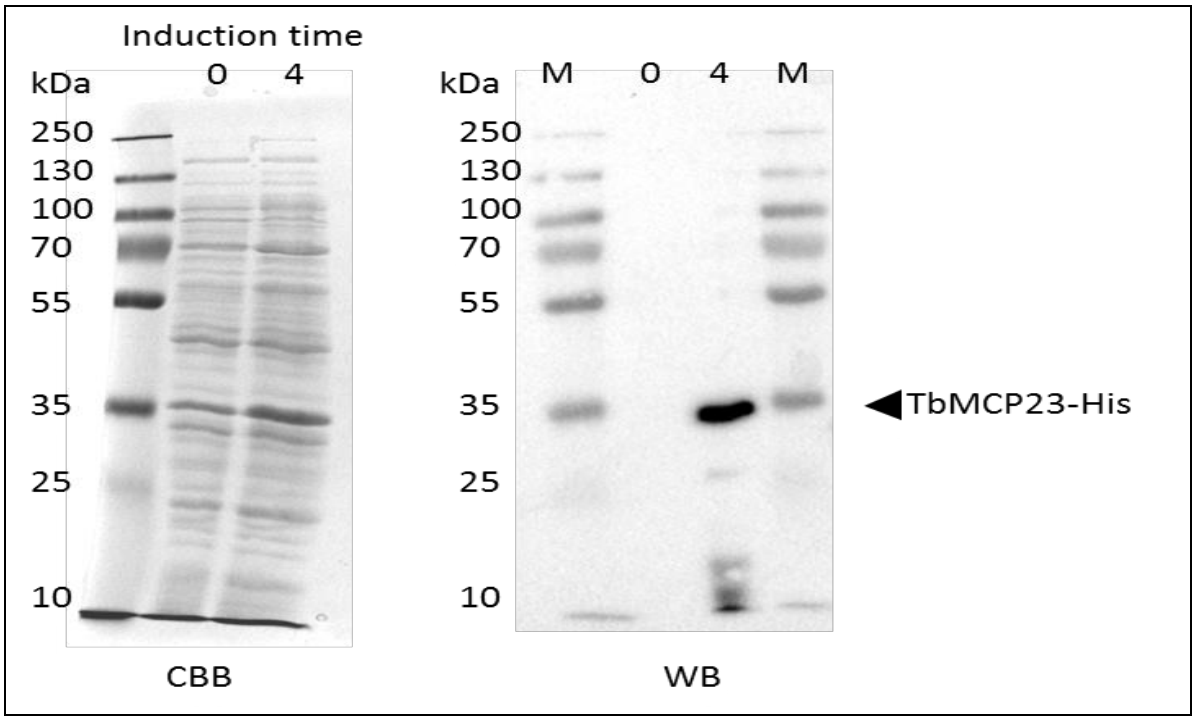

Figure 6.4. Western blots probed with a commercially available anti-His antibody (WB) or stained with Coomassie blue (CBB) to analyse protein expression after induction of TbMCP23 (34 kDa) expression with IPTG (final concentration, 0.4 mM) for four hours. The protein ladder is shown in lane M. Lane 0 contained a protein sample prior to induction. Lane 4 contained a protein sample after four hours of induction. Each lane was loaded with 10 µg protein. The results represent four individual experiments.

6.2.3.2 Protein purification

TbMCP23 was heterologously expressed in and isolated from *E. coli* cells and purified using Ni-NTA beads. In this study, TbMCP23-His and unbound proteins passed through the column and were collected in the flow-through (FT) sample. After the application of the cell lysate, the Ni-NTA was washed three times to remove possible impurities, then eluted twice using elution buffer with detergents to remove His-tagged proteins from the column. As shown in Figure 6.5A, no protein was detected by western blotting of the FT or three wash samples, which indicated that the protein binding step was efficient. This finding was also supported by the Coomassie Brilliant Blue staining results, which revealed multiple bands in the FT samples and suggested the successful removal of the majority of impurities (Figure 6.5B). After two elutions, sufficient protein for assessment was released along with some degraded products, but approximately one-third of the protein remained in the Ni-NTA beads. These results may be due to an insufficient volume of elution buffer or low elution buffer efficiency.

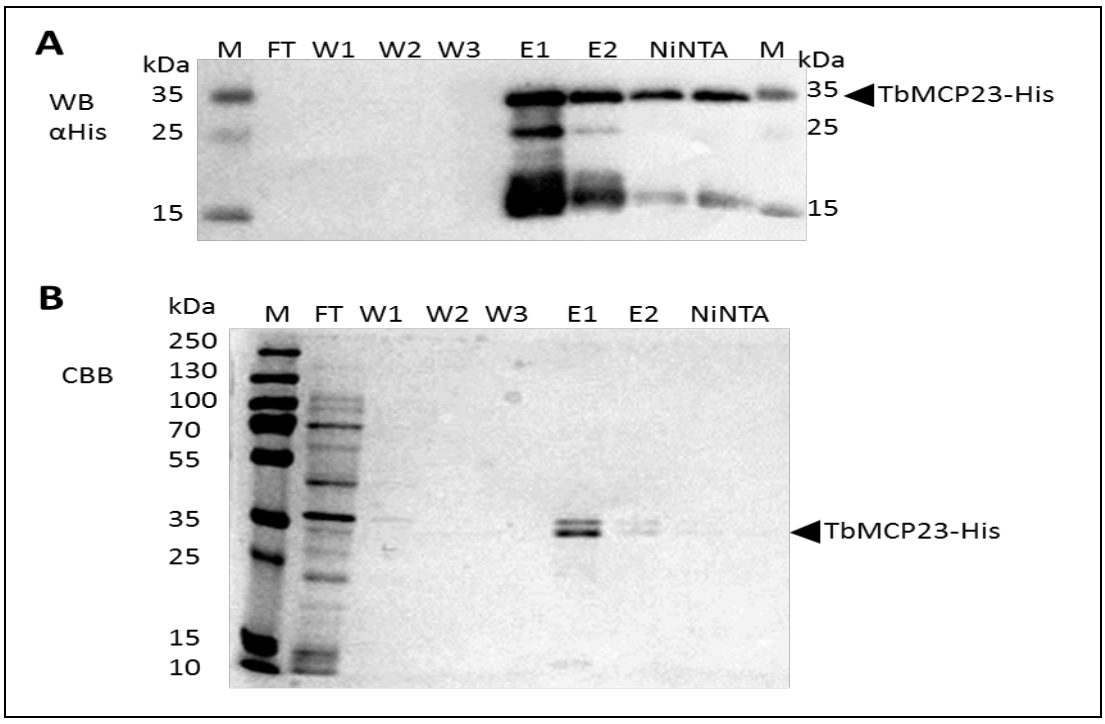

Figure 6.5. TbMCP23-His protein purification using a NiNTA column. The protein was purified using a standard Ni-NTA column procedure. The samples from the various steps were collected and probed by western blotting (**A**; WB) and Coomassie Brilliant Blue staining (**B**; CBB). M: protein markers; FT: flow-through sample; W1, W2 and W3: three continuous washes; E1 and E2: elutions one and two; Ni-NTA: Ni-NTA bead slurry. For western blotting, the anti-His antibody was used to detect the target protein. The Coomassie stain was used to demonstrate the purity of the samples from the different steps.

6.3 Discussion and Conclusion

In this chapter, the preliminary steps for the identification and characterisation of TbMCP23 were performed. Sequence alignment of TbMCP23 with the mitochondrial pyrimidine transporters from other species and the resultant phylogenetic tree indicated that TbMCP23 is a potential nucleotide transporter, likely for pyrimidines. In this study, TbMCP23 knockdown via RNAi did not cause a growth defect. In *Drosophila*, however, the TbMCP23 homologue drim2 double knockout presented some growth defects at the larval stage, a marked defect at the pupal stage and was unable to survive at the adult stage, but no growth defects were observed when only one of the gene copies was depleted (Da-Rè *et al*., 2014). A similar growth defect was found in yeast (Van Dyck *et al*., 1995). These contradictory results suggest that either a small percentage of the TbMCP23 mRNA is sufficient for cell growth or that TbMCP23 is not essential for cell growth, which further implies the expression of alternative transporters in *T. brucei.* However, the depletion of mRNA is not necessarily related to the down-regulation of the protein, since low copy numbers of mRNA can be sufficient for protein expression. Thus, a His-tagged protein/anti-His antibody system for the detection of the TbMCP23 protein was developed. The system was validated by the heterologous expression of TbMCP23-His protein in *E. coli* and successful detection of the protein after binding to a Ni-NTA column.

In future studies, the method can be optimised to facilitate the generation of an anti-TbMCP23 antibody, a greater proportion of the protein could be retrieved from the beads by adding elution steps or using a larger volume of elution buffer. If the protein still remained bound to the Ni-NTA beads, a more powerful detergent or higher concentration of the current detergent should be tested. To resolve the discrepancy with the growth defects in the gene knockouts from other species, conventional gene double-knockout *T. brucei* lines could be generated to achieve 100% gene deficiency. Furthermore, the generation of a TbMCP23-over-expressing, myc-tagged cell line is recommended. The over-expressing cell line could be used to determine the cellular localisation of TbMCP23 by immunofluorescence microscopy and to examine potential growth phenotypes. Functional experiments, such as nucleotide production assessment or pyrimidine transport assays, could be conducted to reveal the function of TbMCP23.

Chapter 7 : General discussion and conclusion

7.1 Discussion

MCF proteins are crucial for cells as they play an important role in the maintenance of the ADP/ATP balance and are involved in the regulation of the the mitochondrial–cytoplasmic redox state. These proteins are also required to transport the essential metabolic intermediates produced by the Krebs cycle in the mitochondria to the rest of the cell. The flux control exerted by these proteins on several metabolic pathways has been well studied (Palmieri *et al*., 2014).

Mitochondria play important roles in almost all aspects of the cell, including growth, apoptosis, differentiation, the production of complex cellular substances, the regulation of cellular signalling, and most importantly, the generation of cellular energy in the form of ATP (Stephen and Douglas*.,* 2012). The same is true in *T. brucei*, although mitochondrial ATP generation seems to be occurs only in the PCF of the organism (Schneider *et al*., 2007). The Krebs cycle does not supply ATP in *T. brucei* as it does in other organisms (van Weelden *et al*., 2003). Moreover, ATP is generated in mitochondria mostly through oxidative and substrate-level phosphorylation, for which proline is used as the substrate for degradation (Bochud-Allemann & Schneider, 2002; Bringaud *et al*., 2012). In the mitochondrion of the PCF of the parasite, oxidative phosphorylation occurs due to the proton-motive force via a mechanism that involves a proton-pumping ATP synthase complex, TAO and the electron transport chain (functional complexes I–IV) (Deramchia *et al*., 2014).

The genome of *T. brucei* contains 26 genes that encode 24 distinct MCF proteins: TbMCP1–24 (Colasante *et al*., 2009). Sequence analysis and reciprocal database searches have demonstrated that these *T. brucei* proteins belong to the mitochondrial carrier family. Sequence similarity (39%–78%) has been observed between MCF proteins from *T. brucei* and other eukaryotes, such as *S. cerevisiae* yeast and humans. Moreover, all TbMCPs contain three semi-conserved protein domains comprising 100 amino acids each. A conserved MCF signature sequence motif and a pair of TM helices are present in each domain (Colasante *et al*., 2009). Therefore, to gain better understanding of the unique *T.brucei* metabolism, this study was aimed to functionally characterise the putative mitochondrial nucleotide transporters TbMCP1, TbMCP15, TbMCP16, TbMCP20 and TbMCP23.

BLASTP analysis and phylogenetic reconstruction showed that the TbMCPs in this study were homologous to the carriers that have been characterised in humans and yeast.
Sequence analysis of TbMCP1 suggested that this MCF protein is homologous to previously functionally characterised flavin adenine dinucleotide (FAD) carriers from multiple species,

such as FLX1 from *S. cerevisiae* and PMP34 from mammals like *Homo sapiens (*Palmieri *et al.,*2009*).* FLX1 of the yeast was showed that it transports riboflavin, as well as FAD. In yeast and human, FAD is essential cofactors of dehydrogenases and oxidases, which play a crucial role in cellular bioenergetics (Giancaspero *et al.*, 2009). The homeostasis of flavin is regulated by a mitochondrial riboflavin/FAD cycle, which involves the uptake of riboflavin into the mitochondria and conversion to FAD, and the recovery of riboflavin in flavoprotein degradation (Bafunno *et al*., 2004). Knockout of the FLX1-encoding gene (flavin transporter) in yeast resulted in respiratory deficiency under normal growth on fermentable carbon sources but very poor growth on non-fermentable substrates (Turcotte *et al*., 2010). TbMCP1 gene replacement and RNAi studies revealed that ΔTbMCP1 trypanosomes have impaired growth compared to that of WT cells at high cell densities. This finding suggests that TbMCP1 is essential for the survival of the PCF449 of *T. brucei.* In contrast to the FLX1 deficiency in yeast, TbMCP1 deficiency seemed to accelerate the mitochondrial pathways in which flavin-dependent enzymes are involved.

FAD is suggested to play various roles in *T. brucei;* it is act as a coenzyme for mitochondrial acyl-CoA dehydrogenase during β-oxidation, a cofactor for pyruvate dehydrogenase (E3), a redox transporter in mitochondrial oxidative phosphorylation (FADH2) and a prosthetic group in succinate dehydrogenase (Colasante *et al.,* 2009).

The expression level of TbMCP1 protein is higher in PCF than BSF which. The various mRNA and protein expression levels of FAD carrier are also found in human tissues: high in liver, pancreas and kidney but low in brain, heart, skeletal muscle and lungs (Agrimi *et al,*. 2012). On the other hand, many mitochondrial-related proteins (Colasante et al. 2006; Saas et al. 2000; Peña-Diaz et al. 2012) have presented a life-cycle regulatory expression pattern: highly expressed in PCF and low expression level or absent in BSF in *T. Brucei,* which is related to the repressed mitochondrial function in BSF (Bringaud et al. 2015).

The potential role of TbMCP1 in energy metabolism was assessed by measuring glucose and proline consumption and succinate, acetate and pyruvate production. The results were consistent with previous findings in the field that (1) glucose, when present, is the preferred carbon source for *T. brucei* PCF449 compared with proline (Lamour *et al*., 2005) and (2) succinate is not the end product in *T. brucei* PCF449 and can be converted to acetate or fed into gluconeogenesis after glucose has been completely depleted through the pathway (from

fumarate to malate, pyruvate, phosphoenolpyruvate and glyceraldehyde 3-phosphate) (van Weelden *et al*., 2005; van Hellemond *et al*., 2005). The results of this study indicated a considerable increase in specific metabolic flux during the metabolism of proline or glucose. This implied that TbMCP1 gene knockdown caused uncoupling of cellular growth and catabolism and up-regulation of flux via various metabolic mechanisms, thereby allowing cells to survive.

TbMCP15 and TbMCP16 are homologous to mitochondrial ADP/ATP carrier. Sequence analysis indicated that TbMCP15 of *T. brucei* has considerable sequence similarity with prototypical AACs in higher eukaryotic organisms. Its considerable amino acid sequences similarities with yeast and human AACs were 45% and 47%, respectively. MCF protein sequence analysis can aid in determining the role of a protein in transportation. This functional analysis can be performed by: (1) determining the sequence similarity between the MCF proteins of *T. brucei* and previously studied yeast and human MCF proteins, (2) assessing the phylogenetic relationship between a TbMCP sequence and other studied MCF proteins, and (3) analysing substrate-specific CPs. CPs comprise conserved amino acid sequences and may be involved in discrimination between different substrates. Detailed sequence analysis based on human and yeast AACs showed that CPI, CPII and CPIII, which are conserved in all AACs were partly conserved in TbMCP15. The 'RRRMMM' hallmark, which is conserved in AACs, was modified in TbMCP15 to 'RRRMMI. The methionine at position 6 of 'RRRMMM' is replaced by isoleucine, which are both hydrophobic, it can be assumed that they have the same function. Therefore, the findings of this study suggest that TbMCP15 is more likely to be functions as a *T. brucei* AAC. However, TbMCP16 shared fewer conserved motifs with known AACs; it contained the 'SRRMQL' motif in place of the conserved 'RRRMMM' motif. Mutation of the first amino acid in the 'RRRMMM' motif of a yeast AAC limited the oxidative phosphorylation activity of the AAC to less than half that of proteins with the WT sequence (Müller *et al*., 1996; Heidkamper *et al*., 1996; Colasante *et al*., 2009). Given the disparities in their substrate binding sites and the low degree of sequence similarity between TbMCP16 and other functionally characterised AAC proteins, TbMCP16 is unlikely to function as an AAC.

AACs supply ADP to the mitochondrion in order to sustain oxidative phosphorylation (Kim *et al*., 2010). *S. cerevisiae* has three AAC isoforms (AAC1, AAC2 and AAC3) with substantial homology to *T. brucei* proteins . Just as the yeast genome encodes multiple AAC isoforms, the human genome contains four paralogous genes that encode different isoforms of AAC

proteins (Kim *et al*., 2010). These isoforms are termed hANT1, hANT2, hANT3 and hANT4. In humans, the different AAC isoforms are expressed at varying levels in different tissues. hANT3, for instance, is expressed in all tissues at differing levels. Heart and skeletal muscle express hANT1 and differentiating and developing tissues express hANT2. However, hANT4 is expressed only in the liver, testis and brain (Stephen *et al*., 1992; Dolce *et al*., 2005; Kim *et al*., 2010).

In yeast and humans the ADP/ATP carriers cannot function without the phosphate carrier (Pi) and are further part of the important mitochondrial permeability transition pore complex (Dolce *et al*., 2005).AAC in *T.brucei* is not stable component of the respiratory supercomplex III+IV or the ATP synthases but its function as a physical separate entity in this organism(van Hellemond *et al*., 2005). The transport function of TbMCP15 was further examined using a mitochondrial ATP production assay. In order to facilitate the interpretation of the ATP production results, the criteria for ATP production using this assay are described. First, AACs are essential for importing ADP into and exporting ATP from the mitochondria. Next, a substrate transporter must be functional to import metabolites into mitochondria. Furthermore, if the carrier is functional as a cotransporter or counter-transporter, the cofactors or counter-transport metabolites must be available after generation from the exogenously added substrate via mitochondrial pathways. The activities of enzymes that generate ATP are also required. In addition, if ATP is produced by oxidative phosphorylation through the electron transport chain, mitochondrial membrane potential is required. On the other hand, ATP generation through substrate-level phosphorylation must be catalysed by either succinyl-CoA synthetase or the ASCT cycle. Finally, if ATP is generated through the ASCT cycle, succinate must be provided in addition to the test substrate. Upon the addition of α-ketoglutarate to mitochondrial fractions, the majority of ATP production occurs through substrate-level phosphorylation to convert succinyl-CoA to succinate (Schneider *et al*., 2007). In this study, the levels of ATP produced by ΔTbMCP15 mitochondria was less than those produced by PCF449 *T. brucei*. However, the slight decrease in ATP production by ΔTbMCP15 cells could be interpreted as the result of (1) the depletion of a transporter for α-ketoglutarate (TbMCP15) or (2) down-regulation of the activities of the required enzymes by TbMCP15 knockdown. Also this result suggested that TbMCP15 is likely to be responsible for about 25% of the observed ADP/ATP exchange activity in *T. brucei* PCF449. The remaining ADP/ATP exchange activity is probably the

resulting from TbMCP5, which has previously been reported to function as the major ADP/ATP exchanger in the *T. brucei* mitochondrion (Colasanate *et al*., 2009).

In yeast and humans, AACs play vital roles in the metabolic processes that provide energy to cells and in mechanisms like apoptosis and programmed cell death (Trindade *et al*., 2016). According to Kühlbrandt (2015), these phenomena occur in the membrane of a large mitochondrion where microdomains are responsible for the formation of channels by proteins. This is enables the dispersal of substrates, which, in turn, ablates prompt metabolic shifts.

According to Silvester *et al*. (2017), cell membranes contain microenvironments that include AACs and other proteins, which can form channels and in which the proteins interact. Irrespective of its activity, structural changes in an AAC like TbMCP15 may occur upon the addition of a myc tag, which could result in inadequate recognition of other proteins and, ultimately, affect signalling. Thus, tagging a protein can affect the transportation of metabolites and intermediates (Claypool, 2009). Many protein complexes include AACs, which interact with other proteins and lipids. Therefore, the ways to avoid these complications or the best method to interpret findings that have these caveats, by using various methods, like mitochondrial assays, have been applied to study carrier activity. The mitochondrial assay is the gold standard for the analysis of the activity of a carrier like TbMCP15; however, an isolated purified protein is required for the assay. The structural changes that occur in the PCF, compared to the BSF, of *T. brucei* play an essential role in the formation of its membranes. These membranes are of paramount importance in the reconstitution of the carriers into liposomes. Due to the requirement for an isolated purified protein, a change in the methodological approach is necessary to facilitate a successful analysis. According to Klingenberg (2001), there were many hurdles to expressing AACs from *Neurospora crassa* in *E. coli*. Many factors play a role in the process of reconstitution and varying results have been achieved experimenting with different strains of the same bacterium. Some of the critical factors for protein production have been studied. According to Madeo *et al.* (2009), insect cells can be used to express eukaryotic membrane proteins, including mitochondrial carrier proteins. However, since the formation and composition of the microdomains that contain AACs in *T. brucei* have not been previously studied, the expression of *T. brucei* proteins in insect cells has been unsuccessful. According to Gebert *et al*. (2011), some factors, like the redox state of the proteins or the phospholipids, play substantial roles in the functional incorporation of proteins into the membrane of the *T.*

brucei mitochondrion. The essential factors that dictate the incorporation of *T. brucei* proteins into the mitochondrial membrane have not been established and must be further analysed.

A great deal of research into the mitochondrial membranes of *T. brucei* remains to be done, so the materials extracted in this study can be of great value. Utilising the extracted mitochondrial fractions in alternative assays would add to the existing evidence on TbMCP15. This can be achieved via the following methods: Firstly, Reconstitution with the mitochondrial-enriched portions using the "fused membranes" approach (van der Giezen *et al.*, 2002). After separating the mitochondrial-enriched fractions by disparity centrifugation, the fractions could be subjected to constant or alternating isopycnic gradient centrifugation.

Secondly, purification of sufficient amounts of the protein for reconstitution. Natural protein purification is a difficult, sensitive technique that will require time to perfect. Wang *et al.* (2008) used various procedures to isolate AACs from beef heart mitochondria. Natural conditions have been used for the purification of the natural protein. *T. brucei* mitochondrial-enriched fractions have been used for the purification of natural proteins (Claypool *et al.*, 2009). Other procedures, like hydrophobic (phenyl or octyl sepharose) chromatography in combination with gel filtration chromatography, may also be used for protein isolation from this parasite.

Many studies have investigated how AACs work and their roles in various cellular processes. AACs participate in the respiratory chain and the mitochondrial transition pore and have a relationship with the phospholipid cardiolipin. Thus, the possibility that TbMCP15 interacts with other MCF proteins should be investigated, as should its possible role in *T. brucei* metabolism. The organelles of *T. brucei* differ from those of other species and only the relationship with the phosphate carrier has been studied in yeast (Traba *et al*., 2009).

The function of TbMCP16 is not yet clear. TbMCP16 appears to differ from the classical AACs, so its role in a broader array of metabolic pathways, beyond those associated with classical AACs, should be investigated to identify its specific role. The function of TbMCP16 is likely to be specific to the PCF449 of *T. brucei*. Further research into metabolic pathway regulation and signalling in all stages of the parasite lifecycle and in the PCF449, in particular, is required to understand the role of TbMCP16 and other proteins with uncharacterised functions.

TbMCP20 is the only *T. brucei* gene that showed sequence similarity to SAMCs from other eukaryotes. It shared the greatest similarity with sequences from Kinetoplastida species such as *T. b. gambiense*, *Trypanosoma equiperdum*, *Trypanosoma congolense* and *Leishmania donovani*. TbMCP20 also demonstrated similarity with the mammalian homologue SLC25 in *M. musculus* and *H. sapiens.* Moreover, TbMC20 protein demonstrated the greatest similarity to the mitochondrial SAM-5 transporter in *S. cerevisiae*. These findings implied that TbMCP20 could be a mitochondrial SAM transporter.

SAM carriers act as methyl donors for all methylation mechanisms in the mitochondria and must be transported through the mitochondrial membrane from the cytosol for energy metabolism (Palmieri *et al*., 2009). In yeast and humans, SAM is required as a substrate for the production of polyamines . In addition, SAM also functions as a methyl donor for nearly all methylation reactions taking place in the mitochondrion (Takahashi *et al*., 2010). To fulfil this function, SAM must be transported across the mitochondrial membrane from the cytosol to sustain energy metabolism (Palmieri *et al*., 2009). In yeast and humans, SAM was shown to transported into the mitochondrial matrix by the MCF proteins SAM5 and SAMC, respectively (Palmieri *et al*., 2016).

SAM5 in yeast, renders the organism capable of growth on media containing glycerol, acetate or other non-fermentable carbon sources (Palmieri *et al*., 2006). In the absence of this gene, the yeast cannot be cultured on a minimal synthetic medium with added galactose, glucose or other fermentable sources of carbon in the absence of biotin or in the presence of the biotin precursor dethiobiotin (Froschauer *et al*., 2013). Based on this finding, SAM5 was presumed to function as a biotin synthetase (Bio2p), which is responsible for the conversion of dethiobiotin to biotin (Kumar *et al*., 2002). In trypanosomes, SAM is obtained from methionine by synthesis using SAM synthetases (Marobbio *et al*., 2003). SAMC appears to transfer SAM into mitochondria. The transportation of SAM by carriers requires the efflux of another substrate because SAMC works only through a counter-exchange mechanism. SAHC in rat for example, which is generated through a methylation reaction and subjected to hydrolysis in the cytosol can behave as a counter-substrate for SAM (Marobbio *et al*., 2003). This evidence supports the conclusion that TbMCP20 transports SAM into mitochondria in exchange for SAHC.

Sequence analysis indicated that TbMCP23 is a potential pyrimidine carrier in the *T. brucei* mitochondrion. The homologous yeast pyrimidine transporter RIM2 has been found to cotransport nucleotides with iron (Yoon *et al*., 2011; Froschauer *et al*., 2013). No growth defect was observed for the TbMCP23 RNAi-transfected cells.Suggesting that TbMCP23 is not essential for PCF 449 *T.brucei* survival. The requirement for TbMCP1, TbMCP15, TbMCP16, TbMCP20 and TbMCP23 for parasite growth in standard MEM-Pros medium was tested in knockdown cells generated via RNAi. TbMCP1, TbMCP15, TbMCP16 and TbMCP20 were essential for the growth of *T. brucei* PCF449*,* as indicated by growth defects in the knockdown cell lines. The growth defects caused by these genes suggested that these proteins play a critical role in the parasite. Therefore, as these proteins are essential for the parasite survival , they could be a potential drug targets for human African trypanosomiasis. Problems is however that the host (humans) also have such carriers. The advantage could be that they are highly divergent which maybe could help to find specific inhibitors.. Therefore, further modifications should be made to existing drugs to facilitate specific targeting.

Unexpectedly, knockdown of TbMCP23 did not cause a growth defect. Interestingly, knockdown of the *Drosophila* TbMCP23 homologue drim2 caused some growth defects at the larval stage, significant defects at the pupal stage and prevented survival at the adult stage (Da-Rè *et al*., 2014). Alternatively, TbMCP23 may not be essential for PCF449 *T. brucei* cell growth, which would imply that *T. brucei* expresses alternative transporters. To address the lack of correspondence between mRNA and protein expression, antibodies were raised for the detection of TbMCP15, TbMCP16, TbMCP20 and TbMCP23.

In addition to *in silico* gene identification and *in vitro* functional characterisation, antibody generation protocols were performed and heterologous protein expression of TbMCP15, TbMCP16, TbMCP20 and TbMCP23 was assessed. Only TbMCP20 could be sufficiently expressed, purified and used to generate a specific antibody. However, the resultant antibody could not detect the TbMCP20 protein in *T. brucei* BSF449 and PCF449. This failure to detect TbMCP20 suggested it is a low-abundance protein that falls below the expression level detectable by western blotting.

The functions of TbMCP15, TbMCP16 and TbMCP20 were confirmed by successful functional yeast complementation experiments. This experiment is based on testing the growth of the interesting genes/proteins into the corresponding yeast knockout strains, and the growth

phenotypes on media containing fermentative (glucose) and non-fermentative (glycerol) carbon sources are measured. Therefore, 1) TbMCP20 restored the growth of the yeast cell line ΔSAM-5 on the non-fermentative carbon source glycerol. The successful complementation of the ΔSAM-5 growth defect strongly supported the function of TbMCP20 as a yeast SAMC (Palmieri *et al*., 2003). 2) Heterologous expression of TbMCP15, in the yeast AAC ΔJL1 2 3u cell line restored its growth on glycerol as a non-fermentative carbon source. This result indicated that TbMCP15 can rescue the activity of an AAC knockout strain and is, thus, likely an ADP/ATP transporter. TbMCP16 complementation did not restore cell growth, which indicated that TbMCP16 is not an AAC. Cell growth assays on media containing non-fermentative substrates as the sole energy and carbon sources (such as glycerol) are a convenient method for testing mitochondrial function. The lack of the growth on non-fermentable media can be due to either nuclear or mitochondrial mutations.

The mitochondrial localisation of TbMCP1, TbMCP15 and TbMCP20 was revealed by immunofluorescence microscopy using commercial anti-myc antibodies since there were no specific, selective antibodies for TbMCP15 and TbMCP1 and the anti-TbMCP20 antibody was unable to detect the protein in *T. brucei* BSF449 and PCF449. The mitochondrial localisation of TbMCP1, TbMCP15 and TbMCP20 supported their roles in mitochondrial transport.

7.2 Conclusion

The findings of this study indicated that TbMCP1 is a mitochondrial flavin carrier, TbMCP15 is an AAC, and TbMCP20 is a mitochondrial SAMC, whereas the role of TbMCP16 is not yet clear. Sequence analysis and phylogenetic construction suggested that TbMCP23 is a potential pyrimidine carrier, but its function remains to be validated through functional characterisation.

The findings in this study can be validated through additional experiments. For example, yeast complementation experiments can validate the substrate transport functions of TbMCP1 and TbMCP23. Therefore, to obtain direct evidence for TbMCP1 as a FAD carrier and TbMCP23 as RIM2 carrier, TbMCP1/TbMCP23 heterologous expression in a yeast mitochondrial FAD/Rim2-deleted strain and the growth phenotype on fermentative and non-fermentative carbon sources of these strain should be measured.

Nucleotide transport or production rate assays are needed to obtain direct evidence for the functions of the TbMCPs. To study the MCF proteins transport function, the approach is containing the isolation or purification of each metabolite transporters through affinity column

chromatography, then reconstitution into the liposomes, following by determining of its transport kinetics and substrate specificity through metabolite transport assay (Palmieri *et al*., 2010).

Gene knockout of TbMCP23 is also recommended, this method is using to generate the target gene replacement method (Voncken et al. 2003) to replace the two endogenous copies by antibiotic resistant cassettes , i.e neomycin (NEO) and blasticidin (BSD) cassettes. Moreover, the mitochondrial ATP production assays in the resulting strains to establish if ATP production from a variety of mitochondrial substrates is completely abolished.

This study used a combination of approaches to examine and characterise the mitochondrial nucleotide carriers in *T. brucei*. The findings of this study suggest the presence of a previously unknown collaborative system of mitochondrial nucleotide transporters in *T. brucei*. This means that these TbMCPs have redundant (overlapping) functions. One TbMCP could maybe transport the same substarte as another TbMCP,but with less affinity. And transport functions are connected, like for example ADP/ATP carrier and the phosphate carrier, since the phosphate required for ATP production and it will be apart of the metabolic network.

understanding the physiological role and transport function of each TbMCP will give us essential information whether these TbMCPs maybe can be used as a drug target for the much needed development of novel chemotherapeutic agents/drugs. It also gives important information about the unique metabolic pathways present in *T. brucei* and how these pathways and the flux through these pathways are controlled by these transporters. Since *T. brucei* is rather unique and different from other eukaryotes, all information is new and will increase our knowledge of these unique (and deadly) parasites. This knowledge is also transferable to other related kinetoplastid parasites, like for example Leishmania, which detrimentally affects millions of people each year. Therefore, the findings lay a solid foundation for future research into and the development of novel interventions for African sleeping sickness.

References

ADRIAN, G. S., MCCAMMON, M. T., MONTGOMERY, D. L. & DOUGLAS, M. G. 1986. Sequences required for delivery and localization of the ADP/ATP translocator to the mitochondrial inner membrane. *Mol Cell Biol,* 6**,** 626-34.

AGABIAN, N. 1990. Trans splicing of nuclear pre-mRNAs. *Cell,* 61**,** 1157-60. AGALAKOVA, N. I. & GUSEV, G. P. 2012. Fluoride induces oxidative stress andATP depletion in the rat erythrocytes in vitro. *Environ Toxicol Pharmacol,* 34**,** 334-7.

APHASIZHEV, R. & APHASIZHEVA, I. 2011. Uridine insertion/deletion editing in trypanosomes: a playground for RNA-guided information transfer. *Wiley Interdiscip Rev RNA,* 2**,** 669-85.

APTED, F. I. C. 1970. *Clinical Manifestations and Diagnosis of Sleeping Sickness. In The African Trypanosomiases.*

AQUILA, H., LINK, T. A. & KLINGENBERG, M. 1987. Solute carriers involved in energy transfer of mitochondria form a homologous protein family. *FEBS Lett,* 212**,** 1-9.

AGRIMI, G., CASTEGNA, A., SCARCIA, P., PALMIERI, L., ROTTENSTEINER, H., SPERA, I., GERMINARIO, L. & PALMIERI, F., 2014. Identification and functional characterization of a novel mitochondrial carrier for citrate and oxoglutarate in Saccharomyces cerevisiae. *The Journal of biological chemistry*, 285(23), pp.17359–70.

ARANDA, A., MAUGERI, D., UTTARO, A. D., OPPERDOES, F., CAZZULO, J. J. & NOWICKI, C. 2006. The malate dehydrogenase isoforms from *Trypanosoma brucei*: subcellular localization and differential expression in bloodstream and procyclic forms. *Int J Parasitol,* 36**,** 295-307.

ARAKAKI TL, BUCKNER FS, AND GILLESPIE JR ET AL. 2008 Characterization of Trypanosoma brucei dihydroorotate dehydrogenase as a possible drug target; structural, kinetic and RNAi studies. Mol Microbiol 68:37–50.

ALIROL E, SCHRUMPF D, AMICI HJ,.2013. Nifurtimox-eflornithine combination therapy for second-stage gambiense human African trypanosomiasis: Medecins Sans Frontieres experience in the Democratic Republic of the Congo. *Clin Infect Dis* 2013; **56:** 195–203.

ALVAR, J., VÉLEZ, I. D., BERN, C., HERRERO, M., DESJEUX, P., CANO, J., JANNIN, J., DEN BOER, M., WHO Leishmaniasis Control Team (2012). Leishmaniasis worldwide and global estimates of its incidence. PloS one, 7(5), e35671.

ARRESE, E. L. & SOULAGES, J. L. 2010. Insect fat body: energy, metabolism, and regulation. *Annu Rev Entomol,* 55**,** 207-25.

ASHLEY, J. N., BARBER, H. J., EWINS, A. J., NEWBERY, G. & SELF, A. D. H. 1942. 20. A chemotherapeutic comparison of the trypanocidal action of some aromatic diamidines. *Journal of the Chemical Society (Resumed),* 0**,** 103-116.

A. VOZZA, E. BLANCO, L. PALMIERI, F. PALMIERI, Identification of the mitochondrial GTP/GDP transporter in Saccharomyces cerevisiae, J. Biol. Chem. 279 (2004) 20850–20857.

AZZI, A., CLARK, S. A., ELLINGTON, W. R. & CHAPMAN, M. S. 2004. The role of phosphagen specificity loops in arginine kinase. *Protein Sci,* 13**,** 575-85. AZZOLIN, L., VON STOCKUM, S., BASSO, E., PETRONILLI, V., FORTE, M. A.

BERNARDI, P. 2010. The mitochondrial permeability transition from yeast to mammals. *FEBS Lett,* 584**,** 2504-9.

BABOT, M., BLANCARD, C., PELOSI, L., LAUQUIN, G. J. & TREZEGUET, V. 2012. The transmembrane prolines of the mitochondrial ADP/ATP carrier are involved in nucleotide binding and transport and its biogenesis.J Biol Chem287, 10368-78.

A. LAHAYE, H. STAHL, D. THINES-SEMPOUX, F. FOURY, PIF1: a DNA helicase in yeast mitochondria, EMBO J. 10 (1991) 997–1007.

B. AMUTHA, D. PAIN, Nucleoside diphosphate kinase of Saccharomyces cerevisiae, Ynk1p: localization to the mitochondrial intermembrane space, Biochem. J. 370 (2003) 805–815.

BARNARD, J. P. & PEDERSEN, P. L. 1994. Alteration of pyruvate metabolism in African trypanosomes during differentiation from bloodstream into insect forms. *Arch Biochem Biophys,* 313**,** 77-82.

BARRETT, F. M. 1974. Changes in the concentration of free amino acids in the haemolymph of Rhodnius prolixus during the fifth instar. *Comp Biochem Physiol B,* 48**,** 241-50.

BARRETT, M. P. 1997. The pentose phosphate pathway and parasitic protozoa. *Parasitol Today,* 13**,** 11-6.

BARRETT, M. P., BOYKIN, D. W., BRUN, R. & TIDWELL, R. R. 2007. Human African trypanosomiasis: pharmacological re-engagement with a neglected disease. *Br J Pharmacol,* 152**,** 1155-71.

BARRY, J. D. & MCCULLOCH, R. 2001. Antigenic variation in trypanosomes: enhanced phenotypic variation in a eukaryotic parasite. *Adv Parasitol,* 49**,** 1-70. BATTINI, R., FERRARI, S., KACZMAREK, L., CALABRETTA, B., CHEN, S. T.BARRY, J. D., MARCELLO, L., MORRISON, L. J., READ, A. F., LYTHGOE, K., JONES, N., CARRINGTON, M., BLANDIN, G., BOHME, U., CALER, E., HERTZ-FOWLER, C., RENAULD, H., EL-SAYED, N. & BERRIMAN, M. 2005. What the genome sequence is revealing about trypanosome antigenic variation. *Biochem Soc Trans,* 33**,** 986-9.

BASERGA, R. 1987. Molecular cloning of a cDNA for a human ADP/ATP carrier which is growth-regulated. *J Biol Chem,* 262**,** 4355-9.

BAUM, K. F., BERENS, R. L., MARR, J. J., HARRINGTON, J. A. & SPECTOR, T. 1989. Purine deoxynucleoside salvage in Giardia lamblia. *J Biol Chem,* 264**,** 21087-90.

Barrett, M.P., Burchmore, R.J., Stich, A., Lazzari, J.O., Frasch, A.C., Cazzulo, J.J. & Krishna, S., 2003. The trypanosomiases. *Lancet*, 362(9394), pp.1469–1480.

BAFUNNO, V., GIANCASPERO, T. A., BRIZIO, C., BUFANO, D., PASSARELLA, S., BOLES, E., & BARILE, M. 2004. Riboflavin Uptake and FAD Synthesis inSaccharomyces

cerevisiaeMitochondria. Journal of Biological Chemistry, 279(1), 95-102. doi:10.1074/jbc.m308230200

BENNE, R., VAN DEN BURG, J., BRAKENHOFF, J. P., SLOOF, P., VAN BOOM, J. H. & TROMP, M. C. 1986. Major transcript of the frameshifted coxII gene from trypanosome mitochondria contains four nucleotides that are not encoded in the DNA. *Cell,* 46**,** 819-26.

BERNSTEIN, B. E., WILLIAMS, D. M., BRESSI, J. C., KUHN, P., GELB, M. H., BLACKBURN, G. M. & HOL, W. G. 1998. A bisubstrate analog induces unexpected conformational changes in phosphoglycerate kinase from *Trypanosoma brucei*. *J Mol Biol,* 279**,** 1137-48.

Berriman M, Ghedin E, Hertz-Fowler C, et al. The genome of the African trypanosome BERRIMAN, M., GHEDIN, E., HERTZ-FOWLER, C., BLANDIN, G., RENAULD, H., BARTHOLOMEU, D. C., LENNARD, N. J., CALER, E., HAMLIN, N. E., HAAS, B., BOHME, U., HANNICK, L., ASLETT, M. A., SHALLOM, J., MARCELLO, L., HOU, L., WICKSTEAD, B., ALSMARK, U. C., ARROWSMITH, C., ATKIN, R. J., BARRON, A. J., BRINGAUD, F., BROOKS, K., CARRINGTON, M., CHEREVACH, I., CHILLINGWORTH, T. J., CHURCHER, C., CLARK, L. N., CORTON, C. H., CRONIN, A., DAVIES, R. M., DOGGETT, J., DJIKENG, A., FELDBLYUM, T., FIELD, M. C., FRASER, A., GOODHEAD, I., HANCE, Z., HARPER, D., HARRIS, B. R., HAUSER, H., HOSTETLER, J., IVENS, A., JAGELS, K., JOHNSON, D., JOHNSON, J., JONES, K., KERHORNOU, A. X., KOO, H., LARKE, N., LANDFEAR, S., LARKIN, C., LEECH, V., LINE, A., LORD, A., MACLEOD, A., MOONEY, P. J., MOULE, S., MARTIN, D. M., MORGAN, G. W., MUNGALL, K., NORBERTCZAK, H., ORMOND, D., PAI, G., PEACOCK, C. S., PETERSON, J., QUAIL, M. A., RABBINOWITSCH, E., RAJANDREAM, M. A., REITTER, C., SALZBERG, S. L., SANDERS, M., SCHOBEL, S., SHARP, S., SIMMONDS, M., SIMPSON, A. J., TALLON, L., TURNER, C. M., TAIT, A., TIVEY, A. R., VAN AKEN, S., WALKER, D., WANLESS, D., WANG, S., WHITE, B., WHITE, O., WHITEHEAD, S., WOODWARD, J., WORTMAN, J., ADAMS, M. D., EMBLEY, T. M., GULL, K., ULLU, E., BARRY, J. D., FAIRLAMB, A. H., OPPERDOES, F., BARRELL, B. G., DONELSON, J. E., HALL, N., FRASER, C. M., et al. 2005. The genome of the African trypanosome *Trypanosoma brucei*. *Science,* 309**,** 416-22.

BRINGAUD, F., ROBINSON, D.R., BARRADEAU, S., BITEAU, N., BALTZ, D. & BALTZ, T., 2000. Characterization and disruption of a new Trypanosoma brucei repetitive flagellum protein, using double-stranded RNA inhibition. *Molecular and biochemical parasitology*, 111(2), pp.283–97

BETINA, S., GAVURNIKOVA, G., HAVIERNIK, P., SABOVA, L. & KOLAROV, J. 1995. Expression of the AAC2 gene encoding the major mitochondrial ADP/ATP carrier in Saccharomyces cerevisiae is controlled at the transcriptional level by oxygen, heme and HAP2 factor. *European journal of biochemistry / FEBS,* 229**,** 651-7.

BEYER, K. & KLINGENBERG, M. 1985. ADP/ATP carrier protein from beef heart mitochondria has high amounts of tightly bound cardiolipin, as revealed by 31P nuclear magnetic resonance. *Biochemistry,* 24**,** 3821-6.

BIENEN, E. J., MATURI, R. K., POLLAKIS, G. & CLARKSON, A. B., JR. 1993. Non-cytochrome mediated mitochondrial ATP production in bloodstream form *Trypanosoma brucei brucei*. *Eur J Biochem,* 216**,** 75-80.

BLACKWELL, J. M., STUART, K. D., BARRELL, B., et al. 2005. The genome of the kinetoplastid parasite, *Leishmania major*. *Science,* 309**,** 436-42.

BLETHEN, S. L. & KAPLAN, N. O. 1968. Characteristics of arthropod arginine kinases. *Biochemistry,* 7**,** 2123-35.

BLUM, B., BAKALARA, N. & SIMPSON, L. 1990. A model for RNA editing in kinetoplastid mitochondria: "guide" RNA molecules transcribed from maxicircle DNA provide the edited information. *Cell,* 60**,** 189-98.*BMJ,* 325**,** 203-6.

BOCHUD-ALLEMANN, N. & SCHNEIDER, A. 2002. Mitochondrial substrate level phosphorylation is essential for growth of procyclic *Trypanosoma brucei*. *J Biol Chem,* 277**,** 32849-54.

BONEN, L. 1993. Trans-splicing of pre-mRNA in plants, animals, and protists. *FASEB J,* 7**,** 40-6.

BOUDKO DY. Molecular basis of essential amino acid transport from studies of insect nutrient amino acid transporters of the SLC6 family (NAT-SLC6). *J Insect Physiol*. 2012;58(4):433-49.

BOOTHROYD, J. C. & CROSS, G. A. 1982. Transcripts coding for variant surface glycoproteins of *Trypanosoma brucei* have a short, identical exon at their 5' end. *Gene,* 20**,** 281-9.

VIGNAIS, P. V. , BRANDOLIN, G., LE SAUX, A., TREZEGUET, V., & LAUQUIN, G. J. 1993. Biochemical characterisation of the isolated Anc2 adenine nucleotide carrier from Saccharomyces cerevisiae mitochondria. *Biochem Biophys Res Commun,* 192**,** 143-50.

BRINGAUD F, RIVIÈRE L, COUSTOU V: Energy metabolism of trypanosomatids: adaptation to available carbon sources. *Mol Biochem Parasitol.* 2006; 149(1):1–9.

BRINGAUD, F. 2005. Proline metabolism in procyclic *Trypanosoma brucei* is down-regulated in the presence of glucose. *J Biol Chem,* 280**,** 11902-10.

BRINGAUD, F., BARRETT, M. P. & ZILBERSTEIN, D. 2012. Multiple roles of proline transport and metabolism in trypanosomatids. *Front Biosci,* 17**,** 349-74.

BRINGAUD, F., RIVIERE, L. & COUSTOU, V. 2006. Energy metabolism of trypanosomatids: adaptation to available carbon sources. *Mol Biochem Parasitol,* 149**,** 1-9.

BROGNA, S. & ASHBURNER, M. 1997. The Adh-related gene of Drosophila melanogaster is expressed as a functional dicistronic messenger RNA: multigenic transcription in higher organisms. *EMBO J,* 16**,** 2023-31.

C.M.T. Marobbio, G. Agrimi, F.M. Lasorsa, F. Palmieri, Identification and functional reconstitution of yeast mitochondrial carrier for S-adenosylmethionine, EMBO J. 22 (2003) 5975–5982.

MAROBBIO, C.M.T., Di Noia, M.A. & F. Palmieri, Identification of a mitochondrial transporter for pyrimidine nucleotides in Saccharomyces cerevisiae: bacterial expression, reconstitution and functional characterization, Biochem. J. 393 (2006) 441–446.

CALLENS, M., KUNTZ, D. A. & OPPERDOES, F. R. 1991. Characterization of pyruvate kinase of *Trypanosoma brucei* and its role in the regulation of carbohydrate metabolism. *Mol Biochem Parasitol,* 47**,** 19-29.

CANEPA, G. E., CARRILLO, C., MIRANDA, M. R., SAYE, M. & PEREIRA, C. A. 2011. Arginine kinase in Phytomonas, a trypanosomatid parasite of plants. *Comp Biochem Physiol B Biochem Mol Biol,* 160**,** 40 3.

C, ALESSANDRA. (2008). Codon Bias is a Major Factor Explaining Phage Evolution in Translationally Biased Hosts. *Springer*. 66 (3), 66-212.

CANONACO, F., SCHLATTNER, U., PRUETT, P. S., WALLIMANN, T. & SAUER, U. 2002. Functional expression of phosphagen kinase systems confers resistance to transient stresses in Saccharomyces cerevisiae by buffering the ATP pool. *J Biol Chem,* 277**,** 31303-9.

CANONACO, F., SCHLATTNER, U., WALLIMANN, T. & SAUER, U. 2003. Functional expression of arginine kinase improves recovery from pH stress of Escherichia coli. *Biotechnol Lett,* 25**,** 1013-7.

CARPENTER, L. R. & ENGLUND, P. T. 1995. Kinetoplast maxicircle DNA replication in Crithidia fasciculata and *Trypanosoma brucei*. *Mol Cell Biol,* 15**,** 6794-803.

CASTRO, H., ROMAO, S., CARVALHO, S., TEIXEIRA, F., SOUSA, C. & TOMAS, A. M. 2010. Mitochondrial redox metabolism in trypanosomatids is independent of tryparedoxin activity. *PLoS One,* 5**,** e12607.

CASTILLO-ACOSTA, V. M., ESTÉVEZ, A. M., VIDAL, A. E., RUIZ-PEREZ, L. M., & GONZÁLEZ-PACANOWSKA, D. 2008. Depletion of dimeric all-α dUTPase induces DNA

strand breaks and impairs cell cycle progression in Trypanosoma brucei. The International Journal of Biochemistry & Cell Biology, 40(12), 2901-2913. doi:10.1016/j.biocel.2008.06.009

CAVALIER-SMITH, T. 1981. Eukaryote kingdoms: seven or nine? *Biosystems,* 14**,** 461-81.

VAN DER GIEZEN ., CHAN, K. W., SLOTBOOM, D. J., COX, S., EMBLEY, T. M., FABRE, O., , M., HARDING, M., HORNER, D. S., KUNJI, E. R., LEON-AVILA, G. & TOVAR, J. 2005. A novel ADP/ATP transporter in the mitosome of the microaerophilic human parasite Entamoeba histolytica. *Curr Biol,* 15**,** 737-42.

CHAUDHARY, K., DARLING, J. A., FOHL, L. M., SULLIVAN, W. J., JR., DONALD, R. G., PFEFFERKORN, E. R., ULLMAN, B. & ROOS, D. S. 2004. Purine salvage pathways in the apicomplexan parasite Toxoplasma gondii. *J Biol Chem,* 279**,** 31221-7.

CHAUDHURI, M., OTT, R. D. & HILL, G. C. 2006. Trypanosome alternative oxidase: from molecule to function. *Trends Parasitol,* 22**,** 484-91.

CHUDZIK, D. M., MICHELS, P. A., DE WALQUE, S. & HOL, W. G. 2000. Structures of type 2 peroxisomal targeting signals in two trypanosomatid aldolases. *J Mol Biol,* 300**,** 697-707.

CLEMENCON, B., REY, M., DIANOUX, A. C., TREZEGUET, V., LAUQUIN, G. J., BRANDOLIN, G. & PELOSI, L. 2008. Structure-function relationships of the C-terminal end of the Saccharomyces cerevisiae ADP/ATP carrier isoform 2. *J Biol Chem,* 283**,** 11218-25.

CLEMENCON, B., REY, M., TREZEGUET, V., FOREST, E. & PELOSI, L. 2011. Yeast ADP/ATP carrier isoform 2: conformational dynamics and role of the RRRMMM signature sequence methionines. *J Biol Chem,* 286**,** 36119-31.

Claypool SM, Boontheung P, McCaffery JM, Loo JA, Koehler CM. The cardiolipin transacylase, tafazzin, associates with two distinct respiratory components providing insight into Barth syndrome. Mol Biol Cell. 2008;19:5143–5155

COLASANTE, C., ALIBU, V. P., KIRCHBERGER, S., TJADEN, J., ELLIS, M., RUPPERT, T. & VONCKEN, F. 2006. Comparative proteomics of glycosomes from bloodstream form and procyclic culture form *Trypanosoma brucei brucei*. *Proteomics,* 6**,** 3275-93.

COLASANTE, C., PENA DIAZ, P., CLAYTON, C. & VONCKEN, F. 2009. Mitochondrial carrier family inventory of *Trypanosoma brucei brucei*: Identification, expression and subcellular localisation. *Mol Biochem Parasitol,* 167**,** 104-17.

COLASANTE, PEÑA-DIAZ, P., PELOSI, L., EBIKEME, C., GAO, F., BRINGAUD, F. & VONCKEN, F., 2012. Functional characterization of TbMCP5, a conserved and essential ADP/ATP carrier present in the mitochondrion of the human pathogen Trypanosoma brucei. *Journal of Biological Chemistry*, 287(50), pp.41861–41874.

COLASANTE, C., ZHENG, F., KEMP, C., & VONCKEN, F. 2018. A plant-like mitochondrial carrier family protein facilitates mitochondrial transport of di- and tricarboxylates in Trypanosoma brucei. *Molecular and Biochemical Parasitology, 221*, 36-51. doi:10.1016/j.molbiopara.2018.03.003.

COLEY, A. F., DODSON, H. C., MORRIS, M. T. & MORRIS, J. C. 2011. Glycolysis in the african trypanosome: targeting enzymes and their subcellular compartments for therapeutic development. *Mol Biol Int,* 2011**,** 123702.

COMINI, M. A., GUERRERO, S. A., HAILE, S., MENGE, U., LUNSDORF, H. & FLOHE, L. 2004. Validation of *Trypanosoma brucei* trypanothione synthetase as drug target. *Free Radic Biol Med,* 36**,** 1289-302.

COUSTOU, V., BESTEIRO, S., BIRAN, M., DIOLEZ, P., BOUCHAUD, V., VOISIN, P., MICHELS, P. A., CANIONI, P., BALTZ, T. & BRINGAUD, F. 2003. ATP generation in the *Trypanosoma brucei* procyclic form: cytosolic substrate level is essential, but not oxidative phosphorylation. *J Biol Chem,* 278**,** 49625-35.

COUSTOU, V., BESTEIRO, S., RIVIERE, L., BIRAN, M., BITEAU, N., FRANCONI, J. M., BOSHART, M., BALTZ, T. & BRINGAUD, F. 2005. A mitochondrial NADH-dependent

fumarate reductase involved in the production of succinate excreted by procyclic *Trypanosoma brucei*. *J Biol Chem,* 280**,** 16559-70.

DAHOUT-GONZALEZ, C., NURY, H., TREZEGUET, V., LAUQUIN, G. J., PEBAY-PEYROULA, E. & BRANDOLIN, G. 2006. Molecular, functional, and pathological aspects of the mitochondrial ADP/ATP carrier. *Physiology (Bethesda),* 21**,** 242-9.

DANIELS, J. P., GULL, K. & WICKSTEAD, B. 2010. Cell biology of the *trypanosome* genome. *Microbiol Mol Biol Rev,* 74**,** 552-69.

DAVIES, M. J., ROSS, A. M. & GUTTERIDGE, W. E. 1983. The enzymes of purine salvage in *Trypanosoma cruzi, Trypanosoma brucei* and *Leishmania mexicana*. *Parasitology,* 87 (Pt 2)**,** 211-7.

DA-RÈ, C., FRANZOLIN, E., BISCONTIN, A., PIAZZESI, A., PACCHIONI, B., GAGLIANI, M.C., MAZZOTTA, G., TACCHETTI, C., ZORDAN, M. A., ZEVIANI, M., BERNARDI, P., BIANCHI, V., DE PITTÀ, C. & COSTA, R., 2014. Functional characterization of drim2, the Drosophila melanogaster homolog of the yeast mitochondrial deoxynucleotide transporter. *Journal of Biological Chemistry*, 289(11), pp.7448–7459.

DE MARCOS LOUSA, C., TREZEGUET, V., DIANOUX, A. C., BRANDOLIN, G. DERAMCHIA K, MORAND P, BIRAN M, .Contribution of pyruvate phosphate dikinase in the maintenance of the glycosomal ATP/ADP balance in the Trypanosoma brucei procyclic form**.** *J Biol Chem.* 2014; 289(25): 17365–78.

DE KONING HP, BRIDGES DJ, BURCHMORE R.2005. Purine and pyrimidine transport in pathogenic protozoa: from biology to therapy. FEMS Microbiol Rev. 29:987–1020

DOCAMPO, R. 1995. *Antioxidant Mechanisms. In "Biochemistry and Molecular Biology of Parasites ". ,* London, Academic Press.

DOCZI, J., TURIAK, L., VAJDA, S., MANDI, M., TOROCSIK, B., GERENCSER, A. A., KISS, G., KONRAD, C., ADAM-VIZI, V. & CHINOPOULOS, C. 2011. Complex

contribution of cyclophilin D to Ca2+-induced permeability transition in brain mitochondria, with relation to the bioenergetic state. *J Biol Chem,* 286**,** 6345-53.

DOLCE, V., FIERMONTE, G., MESSINA, A. & PALMIERI, F. 1991. Nucleotide sequence of a human heart cDNA encoding the mitochondrial phosphate carrier. *DNA Seq,* 2**,** 133-5.

DOLCE, V., FIERMONTE, G., RUNSWICK, M. J., PALMIERI, F. & WALKER, J. E. 2001. The human mitochondrial deoxynucleotide carrier and its role in the toxicity of nucleoside antivirals. *Proc Natl Acad Sci U S A,* 98**,** 2284-8.

DOLCE, V., SCARCIA, P., IACOPETTA, D. & PALMIERI, F. 2005. A fourth ADP/ATP carrier isoform in man: identification, bacterial expression, functional characterization and tissue distribution. *FEBS Lett,* 579**,** 633-7.

DORMEYER, M., RECKENFELDERBAUMER, N., LUDEMANN, H. & KRAUTH-SIEGEL, R. L. 2001. Trypanothione-dependent synthesis of deoxyribonucleotides by *Trypanosoma brucei* ribonucleotide reductase. *J Biol Chem,* 276**,** 10602-6.

DRGON, T., SABOVA, L., GAVURNIKOVA, G. & KOLAROV, J. 1992. Yeast ADP/ATP carrier (AAC) proteins exhibit similar enzymatic properties but their deletion produces different phenotypes. *FEBS letters,* 304**,** 277-80.

PEÑA DIAZ, P., COLASANTE, C., CLAYTON, C. & VONCKEN, F., 2009. Mitochondrial carrier family inventory of Trypanosoma brucei brucei: Identification, expression and subcellular localisation. Molecular and Biochemical Parasitology, 167(2), pp.104– 117.

E. VAN DYCK, B. JANK, A. RAGNINI, R.J. SCHWEYEN, C. DUYCKAERTS, F. SLUSE, F. FOURY, Overexpression of a novel member of the mitochondrial carrier family rescues defects in both DNA and RNA metabolism in yeast mitochondria, Mol. Gen. Genet. 246 (1995) 426–436.

EBIKEME, C., HUBERT, J., BIRAN, M., GOUSPILLOU, G., MORAND, P., PLAZOLLES, N., GUEGAN, F., DIOLEZ, P., FRANCONI, J. M., PORTAIS, J. C. & BRINGAUD, F. 2010. Ablation of succinate production from glucose metabolism in the procyclic *trypanosomes*

induces metabolic switches to the glycerol 3-phosphate/dihydroxyacetone phosphate shuttle and to proline metabolism. *J Biol Chem,* 285**,** 32312-24.

ELLINGTON, W. R. 2001. Evolution and physiological roles of phosphagen systems.*Annu Rev Physiol,* 63**,** 289-325.

EMBLEY, T. M. & MARTIN, W. 2006. Eukaryotic evolution, changes and challenges. *Nature,* 440**,** 623-30.EMBO J. **22**, 5975–5982

ENGLUND, P. T., HAJDUK, S. L. & MARINI, J. C. 1982. The molecular biology of *trypanosomes*. *Annu Rev Biochem,* 51**,** 695-726.

ENGSTLER, M., THILO, L., WEISE, F., GRU¨NFELDER, C.G., SCHWARZ, H., BOSHART, M., AND OVERATH, P. 2004. Kinetics of endocytosis and recycling of the GPI-anchored variant surface glycoprotein in Trypanosoma brucei. J. Cell Sci. 117, 1105–1115.

FAIRLAMB, A. H., BLACKBURN, P., ULRICH, P., CHAIT, B. T. & CERAMI, A. 1985. Trypanothione: a novel bis(glutathionyl)spermidine cofactor for glutathione reductase in *trypanosomatids*. *Science,* 227**,** 1485-7.

FAROOQUI, J. Z., LEE, H. W., KIM, S. AND PAIK, W. K. (1983) Studies on compartmentation of S-adenosyl-L-methionine in Saccharomyces cerevisiae and isolated rat hepatocytes. Biochim. Biophys. Acta **757**, 342–351

FENN, K. & MATTHEWS, K. R. 2007. The cell biology of *Trypanosoma brucei* differentiation. *Curr Opin Microbiol,* 10**,** 539-46.

FERNANDEZ, P., HAOUZ, A., PEREIRA, C. A., AGUILAR, C. & ALZARI, P. M. 2007. The crystal structure of *Trypanosoma cruzi* arginine kinase. *Proteins,* 69**,** 209-12.

FERREIRA, G. C., PRATT, R. D. & PEDERSEN, P. L. 1989. Energy-linked anion transport. Cloning, sequencing, and characterization of a full length cDNA encoding the rat liver mitochondrial proton/phosphate symporter. *J Biol Chem,* 264**,** 15628-33.

FEVRE, E. M., PICOZZI, K., FYFE, J., WAISWA, C., ODIIT, M., COLEMAN, P. G. & WELBURN, S. C. 2005. A burgeoning epidemic of sleeping sickness in Uganda. *Lancet,* 366**,** 745-7.

FIERMONTE, G., DOLCE, V., ARRIGONI, R., RUNSWICK, M. J., WALKER, J. E.
FIERMONTE, G., DOLCE, V., DAVID, L., SANTORELLI, F. M., DIONISI-VICI, C., PALMIERI, F. & WALKER, J. E. 2003. The mitochondrial ornithine transporter. Bacterial expression, reconstitution, functional characterization, and tissue distribution of two human isoforms. *J Biol Chem,* 278**,** 32778-83.

FIERMONTE, G., DOLCE, V., PALMIERI, L., VENTURA, M., RUNSWICK, M. J., PALMIERI, F. & WALKER, J. E. 2001. Identification of the human mitochondrial oxodicarboxylate carrier. Bacterial expression, reconstitution, functional characterization, tissue distribution, and chromosomal location. *J Biol Chem,* 276**,** 8225-30.

FIERMONTE, G., PALMIERI, L., TODISCO, S., AGRIMI, G., PALMIERI, F. & WALKER, J. E. 2002. Identification of the mitochondrial glutamate transporter. Bacterial expression, reconstitution, functional characterization, and tissue distribution of two human isoforms. *J Biol Chem,* 277**,** 19289-94.

FROSCHAUER, E. M., SCHWEYEN, R. J. AND WIESENBERGER, G. (2009) the yeast mitochondrial carrier proteins Mrs3p/Mrs4p mediate iron transport across the inner mitochondrial membrane. Biochim. Biophys. Acta **1788**, 1044–1050.

FROSCHAUER, E.M., RIETZSCHEL, N., HASSLER, M.R., BINDER, M., SCHWEYEN, R.J., LILL, R., MÜHLENHOFF, U. & WIESENBERGER, G., 2013. The mitochondrial carrier Rim2 coimports pyrimidine nucleotides and iron. *The Biochemical journal*, 455(1), pp.57–65.

FRENCH, J. B., YATES, P. A., SOYSA, D. R., BOITZ, J. M., CARTER, N. S., CHANG, B., ULLMAN, B., EALICK, S. E. 2011. The Leishmania donovani UMP synthase is essential for promastigote viability and has an unusual tetrameric structure that exhibits substrate-controlled oligomerization. The Journal of biological chemistry, 286(23), 20930-41.

FRANZOLIN, E., DA-RÈ, C., BISCONTIN, A., PIAZZESI, A., PACCHIONI, B., GAGLIANI, M.C., MAZZOTTA, G., TACCHETTI, C., ZORDAN, M. A., ZEVIANI, M., BERNARDI, P., BIANCHI, V., DE PITTÀ, C. & COSTA, R., 2012. Functional characterization of drim2, the Drosophila melanogaster homolog of the yeast mitochondrial deoxynucleotide transporter. *Journal of Biological Chemistry*, 289(11), pp.7448–7459.

G.S. ADRIAN, M.T. MCCAMMON, D.L. MONTGOMERY, M.G. DOUGLAS, Sequences required for delivery and localization of the ADP/ATP translocator to the mitochondrial inner membrane, Mol. Cell. Biol. 6 (1986) 626–634.

GAVURNIKOVA, G., SABOVA, L., KISSOVA, I., HAVIERNIK, P. & KOLAROV, J. 1996. Transcription of the AAC1 gene encoding an isoform of mitochondrial ADP/ATP carrier in *Saccharomyces cerevisiae* is regulated by oxygen in a heme-independent manner. *European journal of biochemistry / FEBS,* 239**,** 759-63.

GAWAZ, M., DOUGLAS, M. G. & KLINGENBERG, M. 1990. Structure-function studies of adenine nucleotide transport in mitochondria. II. Biochemical analysis of distinct AAC1 and AAC2 proteins in yeast. *The Journal of biological chemistry,* 265**,** 14202-8.

GEIGENBERGER, P., STAMME, C., TJADEN, J., SCHULZ, A., QUICK, P. W., BETSCHE, T., KERSTING, H. J. & NEUHAUS, H. E. 2001. Tuber physiology and properties of starch from tubers of transgenic potato plants with altered plastidic adenylate transporter activity. *Plant Physiol,* 125**,** 1667-78.

GEBERT, N., RYAN, M. T., PFANNER, N., WIEDEMANN, N., & STOJANOVSKI, D. 2011. Mitochondrial protein import machineries and lipids: A functional connection. Biochimica Et Biophysica Acta (BBA) - Biomembranes, 1808(3), 1002-1011. doi:10.1016/j.bbamem.2010.08.003

Gebert, N., Ryan, M. T., Pfanner, N., Wiedemann, N., & Stojanovski, D. (2011). Mitochondrial protein import machineries and lipids: A functional connection. Biochimica Et Biophysica Acta (BBA) - Biomembranes, 1808(3), 1002-1011. doi:10.1016/j.bbamem.2010.08.00

GIANCASPERO, T. A., COLELLA, M., BRIZIO, C., DIFONZO, G., FIORINO, G. M., LEONE, P., BRANDSCH, R., BONOMI, F., IAMETTI, S., BARILE, M. 2015. Remaining challenges in cellular flavin cofactor homeostasis and flavoprotein biogenesis. Frontiers in chemistry, 3, 30. doi:10.3389/fchem.2015.00030

GIBSON, W. C. 1986. Will the real *Trypanosoma b. gambiense* please stand up.*Parasitol Today,* 2**,** 255-7.

Gietz, R. D. & Woods (2002). Yeast Transformation by the LiAc/SS Carrier DNA/PEG Method. Methods in Molecular Biology Yeast Genetics, 1-12. doi:10.1007/978-1-4939-1363-3_1

GILBERT, R. J. & KLEIN, R. A. 1984. Pyruvate kinase: a carnitine-regulated site of ATP production in *Trypanosoma brucei brucei*. *Comp Biochem Physiol B,* 78**,** 595-9.

GIORGIO, V., SORIANO, M. E., BASSO, E., BISETTO, E., LIPPE, G., FORTE, M. A. & BERNARDI, P. 2010. Cyclophilin D in mitochondrial pathophysiology. *Biochim Biophys Acta,* 1797**,** 1113-8.

GIANCASPERO, T. A., WAIT, R., BOLES, E., & BARILE, M. 2008. Succinate dehydrogenase flavoprotein subunit expression in Saccharomyces cerevisiae- involvement of the mitochondrial FAD transporter, Flx1p. FEBS Journal, 275(6), 1103-1117. doi:10.1111/j.1742-4658.2008.06270.

GRAHAM, B. H., WAYMIRE, K. G., COTTRELL, B., TROUNCE, I. A., MACGREGOR, G. R. & WALLACE, D. C. 1997. A mouse model for mitochondrial myopathy and cardiomyopathy resulting from a deficiency in the heart/muscle isoform of the adenine nucleotide translocator. *Nat Genet,* 16**,** 226-34.

GRAMS, J., MCMANUS, M. T. & HAJDUK, S. L. 2000. Processing of polycistronic guide RNAs is associated with RNA editing complexes in *Trypanosoma brucei. EMBO J,* 19**,** 5525-32.

GUALDRÓN-LÓPEZ M, BRENNAND A, HANNAERT V, *et al.*: When, how and why glycolysis became compartmentalised in the Kinetoplastea. A new look at an ancient organelle. *Int J Parasitol.* 2012; **42**(1): 1–20.

GUDIN S, QUASHIE NB, CANDLISH D, AL-SALABI MI, JARVIS SM, RANFORD-CARTWRIGHT LC, DE KONING HP.2006 Trypanosoma brucei: A survey of pyrimidine transport activities. Exp Parasitol. 114:118–125

GULL, K., 2003. Host-parasite interactions and trypanosome morphogenesis: a flagellar pocketful of goodies. *Curr Opin Microbiol*, 6(4), pp.365–370.

GUERIN, B., BUKUSOGLU, C., RAKOTOMANANA, F. & WOHLRAB, H. 1990. Mitochondrial phosphate transport. N-ethylmaleimide insensitivity correlates with absence of beef heart-like Cys42 from the *Saccharomyces cerevisiae* phosphate transport protein. *J Biol Chem,* 265**,** 19736-41.

H. NURY, C. DAHOUT-GONZALEZ, V. TREZEGUET, G.J. LAUQUIN, G. BRANDOLIN, E. PEBAY- PEYROULA, Relations between structure and function of the mitochondrial ADP/ATP carrier, Annu. Rev. Biochem. 75 (2006) 713–741.

HAFERKAMP, I., HACKSTEIN, J. H., VONCKEN, F. G., SCHMIT, G. & TJADEN, J. 2002. Functional integration of mitochondrial and hydrogenosomal ADP/ATP carriers in the Escherichia coli membrane reveals different biochemical characteristics for plants, mammals and anaerobic chytrids. *Eur J Biochem,* 269**,** 3172-81.

HALL, B. S., BOT, C. & WILKINSON, S. R. 2011. Nifurtimox activation by trypanosomal type I nitroreductases generates cytotoxic nitrile metabolites. *J Biol Chem,* 286**,** 13088-95.
HAMMOND, D. J. & BOWMAN, I. B. 1980. Studies on glycerol kinase and its role in ATP synthesis in *Trypanosoma brucei. Mol Biochem Parasitol,* 2**,** 77-91.

Harrison, C. J., & Langdale, J. A. (2006). A step by step guide to phylogeny reconstruction. The Plant Journal, 45(4), 561-572. doi:10.1111/j.1365-313x.2005.02611.

HANNAERT, V., BRINGAUD, F., OPPERDOES, F. R. & MICHELS, P. A. 2003.Evolution of energy metabolism and its compartmentation in Kinetoplastida.*Kinetoplastid Biol Dis,*2**,** 11.

HART, D. T., MISSET, O., EDWARDS, S. W. & OPPERDOES, F. R. 1984. A comparison of the glycosomes (microbodies) isolated from *Trypanosoma brucei* bloodstream form and cultured procyclic trypomastigotes. *Mol Biochem Parasitol,* 12**,** 25-35.

Heidkämper, D., Müller, V., Nelson, D. R., & Klingenberg, M. 1996. Probing the Role of Positive Residues in the ADP/ATP Carrier from Yeast. The Effect of Six Arginine Mutations on Transport and the Four ATP versus ADP Exchange Modes†. Biochemistry, 35(50), 16144-16152. doi:10.1021/bi960668j

HILDYARD, J. C. & HALESTRAP, A. P. 2003. Identification of the mitochondrial pyruvate carrier in Saccharomyces cerevisiae. *Biochem J,* 374**,** 607-11.

HORN D. Antigenic variation in African trypanosomes.*MolBiochemParasitol* 2014; **195:**123 29.

HORNE, D. W., HOLLOWAY, R. S. AND WAGNER, C. (1997) Transport of S-adenosylmethionine.

HORNE, D. W., HOLLOWAY, R. S. AND WAGNER, C. (1997) Transport of S-adenosylmethionine in isolated rat liver mitochondria. Arch. Biochem. Biophys. **343**, 201–206.

HOULDSWORTH, J. & ATTARDI, G. 1988. Two distinct genes for ADP/ATP translocase are expressed at the mRNA level in adult human liver. *Proc Natl Acad Sci U S A,* 85**,** 377-81.

HEINO, J., & SOININEN, J. 2005. Assembly rules and community models for unicellular organisms: Patterns in diatoms of boreal streams. Freshwater Biology, 50(4), 567-577. doi:10.1111/j.1365-2427.2005.01346.x

HOYOS, M. E., PALMIERI, L., WERTIN, T., ARRIGONI, R., POLACCO, J. C. & PALMIERI, F. 2003. Identification of a mitochondrial transporter for basic amino acids in

Arabidopsis thaliana by functional reconstitution into liposomes and complementation in yeast. *Plant J,* 33**,** 1027-35.

HUSTAD S, UELAND PM, SCHNEEDE J. 1999. Quantification of riboflavin, flavin mononucleotide, and flavin adenine dinucleotide in human plasma by capillary electrophoresis and laser-induced fluorescence detection. Clin Chem;45:862-868
HUSTAD S, UELAND PM, VOLLSET SE, ZHANG Y, BJØRKE-MONSEN AL, SCHNEEDE J. 2000. Riboflavin as a determinant of plasma total homocysteine: effect modification by the methylenetetrahydrofolate reductase C677T polymorphism. Clin Chem;46:1065-1071

IACOBAZZI, V., DE PALMA, A. & PALMIERI, F. 1996. Cloning and sequencing of the bovine cDNA encoding the mitochondrial tricarboxylate carrier protein. *Biochim Biophys Acta,* 1284**,** 9-12.

IACOBAZZI, V., PALMIERI, F., RUNSWICK, M. J. & WALKER, J. E. 1992. Sequences of the human and bovine genes for the mitochondrial 2-oxoglutarate carrier. *DNA Seq,* 3**,** 79-88. in isolated rat liver mitochondria. Arch. Biochem. Biophys. **343**, 201–206.

J. GREGAN, M. KOLISEK, R.J. SCHWEYEN, Mitochondrial Mg(2+) homeostasis is critical for group II intron splicing in vivo, Genes Dev. 15 (2001) 2229–2237.

JAMONNEAU V, ILBOUDO H, KABORÉ J, et al. Untreated human infections by Trypanosoma brucei gambiense are not 100% fatal. *PLoS Negl Trop Dis*. 2012;6(6):e1691.

KADENBACH, B., MENDE, P., KOLBE, H. V., STIPANI, I. & PALMIERI, F. 1982. The mitochondrial phosphate carrier has an essential requirement for cardiolipin. *FEBS Lett,* 139**,** 109-12.

KAUKONEN, J., JUSELIUS, J. K., TIRANTI, V., KYTTALA, A., ZEVIANI, M., COMI, G. P., KERANEN, S., PELTONEN, L. & SUOMALAINEN, A. 2000. Role of adenine nucleotide translocator 1 in mtDNA maintenance. *Science,* 289**,** 782-5.

KENNEDY, P. G. 2004. Human African trypanosomiasis of the CNS: current issues and challenges. *J Clin Invest,* 113**,** 496-504.

KENNEDY, P. G. E. 2006. Human African trypanosomiasis–neurological aspects. *Journal of neurology,* 253**,** 411-416.

KOLAROV, J., KOLAROVA, N. & NELSON, N. 1990b. A third ADP/ATP translocator gene in yeast. *J Biol Chem,* 265**,** 12711-6.

KOSLOWSKY, D. J. & YAHAMPATH, G. 1997. Mitochondrial mRNA 3' cleavage/polyadenylation and RNA editing in are independent events. *Mol Biochem Parasitol,* 90**,** 81-94.

KRAMER, R. & KLINGENBERG, M. 1985. Structural and functional asymmetry *Trypanosoma brucei* of the ADP/ATP carrier from mitochondria. *Ann N Y Acad Sci,* 456**,** 289-90.

KRAMER, R. 1996. Structural and functional aspects of the phosphate carrier from mitochondria. *Kidney Int,* 49**,** 947-52.

KRAUTH-SIEGEL, R. L., MEIERING, S. K. & SCHMIDT, H. 2003. The parasite-specific trypanothione metabolism of trypanosoma and leishmania. *Biol Chem,* 384**,** 539-49.

KUAN, J. & SAIER, M. H., JR. 1993. The mitochondrial carrier family of transport proteins: structural, functional, and evolutionary relationships. *Crit Rev Biochem Mol Biol,* 28**,** 209-33.

Kumar, A., Agarwal, S., Heyman, J. A., Matson, S., Heidtman, M., Piccirillo, S.,
Kumar, S. Agarwal, J.A. Heyman, S. Matson, M. Heidtman, S. Piccirillo, L. Umansky, A. Drawid, R. Jansen, Y. Liu, K.H. Cheung, P. Miller, M. Gerstein, G.S. Roeder, M. Snyder, Subcellular localization of the yeast proteome, Genes Dev. 16 (2002) 707–719.

KUNJI, E. R. & HARDING, M. 2003. Projection structure of the atractyloside-inhibited mitochondrial ADP/ATP carrier of *Saccharomyces cerevisiae*. *J Biol Chem,* 278**,** 36985-8.

KUNJI, E. R. & ROBINSON, A. J. 2006. The conserved substrate binding site of mitochondrial carriers. *Biochim Biophys Acta,* 1757**,** 1237-48.

KUNJI, E. R. 2004. The role and structure of mitochondrial carriers. *FEBS Lett,* 564**,** 239-44.
KUZOE, F. A. 1993. Current situation of African trypanosomiasis. *Acta Trop,* 54**,** 153-62.

KLINGENBERG, M AQUILA, H., & LINK, T.A., 2008. Solute carriers involved in energy transfer of mitochondria form a homologous protein family. *FEBS Lett*, 212(1), pp.1–9.

KRAMER, S. (2012). Developmental regulation of gene expression in the absence of transcriptional control: The case of kinetoplastids. Molecular and Biochemical Parasitology, 181(2), 61-72. doi:10.1016/j.molbiopara.2011.10.002

L. PALMIERI, H. ROTTENSTEINER, W. GIRZALSKY, P. SCARCIA, F. PALMIERI, R. ERDMANN, Identification and functional reconstitution of the yeast peroxisomal adenine nucleotide transporter, EMBO J. 20 (2001) 5049–5059.

L.M. STEINMETZ, C. SCHARFE, A.M. DEUTSCHBAUER, D. MOKRANJAC, Z.S. HERMAN, T. JONES, A.M. CHU, G. GIAEVER, H. PROKISCH, P.J. OEFNER, R.W. DAVIS, Systematic screen for human disease genes in yeast, Nat. Genet. 31 (2002) 400–404.

LAMOUR, N., RIVIERE, L., COUSTOU, V., COOMBS, G. H., BARRETT, M. P.
LAUQUIN, G. J. 2002. The human mitochondrial ADP/ATP carriers: kinetic properties and biogenesis of wild-type and mutant proteins in the yeast *S. cerevisiae*. *Biochemistry,* 41**,** 14412-20.

Laemmli, U. K. 1970. Cleavage of Structural Proteins during the Assembly of the Head of Bacteriophage T4. Nature, 227(5259), 680-685. doi:10.1038/227680a0

LAWSON, J. E. & DOUGLAS, M. G. 1988. Separate genes encode functionally equivalent ADP/ATP carrier proteins in *Saccharomyces cerevisiae*. Isolation and analysis of AAC2. *J Biol Chem,* 263**,** 14812-8.

LEIJA, C., RIJO-FERREIRA, F., KINCH, L. N., GRISHIN, N. V., NISCHAN, N., KOHLER, J. J., HU, Z., PHILLIPS, M. A. 2016. Pyrimidine Salvage Enzymes Are Essential for De Novo Biosynthesis of Deoxypyrimidine Nucleotides in Trypanosoma brucei. PLoS pathogens, 12(11), e1006010. doi:10.1371/journal.ppat.1006010

LI, E. AND ZHANG, Y. 2014. DNA Methylation in Mammals. Cold Spring Harbor Perspectives in Biology, 6(5), pp.a019133-a019133.

LORENZ, P., MAIER, A. G., BAUMGART, E., ERDMANN, R., & CLAYTON, C. 1998. Elongation and clustering of glycosomes in Trypanosoma brucei overexpressing the glycosomal Pex11p. The EMBO journal, 17(13), 3542-55.

LAWSON, J. E., GAWAZ, M., KLINGENBERG, M. & DOUGLAS, M. G. 1990. Structure-function studies of adenine nucleotide transport in mitochondria. I. Construction and genetic analysis of yeast mutants encoding the ADP/ATP carrier protein of mitochondria. *The Journal of biological chemistry,* 265**,** 14195-201.

LEROCH, M., KIRCHBERGER, S., HAFERKAMP, I., WAHL, M., NEUHAUS, H. E. & TJADEN, J. 2005. Identification and characterization of a novel plastidic adenine nucleotide uniporter from *Solanum tuberosum*. *J Biol Chem,* 280**,** 17992-8000.

LEUNG, A. W., VARANYUWATANA, P. & HALESTRAP, A. P. 2008. The mitochondrial phosphate carrier interacts with cyclophilin D and may play a key role in the permeability transition. *J Biol Chem,* 283**,** 26312-23.

LIANG, X. H., HARITAN, A., ULIEL, S. & MICHAELI, S. 2003. trans and cis splicing in trypanosomatids: mechanism, factors, and regulation. *Eukaryot Cell,* 2**,** 830-40.

LI, E., & ZHANG, Y. 2014. DNA methylation in mammals. Cold Spring Harbor perspectives in biology, 6(5), a019133. doi:10.1101/cshperspect.a019133

LOURIE, E. M. 1942. Treatment of sleeping sickness in Sierra Leone. *Trop. Med.*

LOYTYNOJA, A. & MILINKOVITCH, M. C. 2001. Molecular phylogenetic analyses of the mitochondrial ADP-ATP carriers: the Plantae/Fungi/Metazoa trichotomy revisited. *Proceedings of the National Academy of Sciences of the United States of America,* 98**,** 10202-7.

LIU, Y., & CHEN, X. J. 2013. Adenine Nucleotide Translocase, Mitochondrial Stress, and Degenerative Cell Death. Oxidative Medicine and Cellular Longevity, 2013, 1-10. doi:10.1155/2013/146860

M. D. BRAND, J. L. PAKAY, A. OCLOO ET AL., "The basal proton conductance of mitochondria depends on adenine nucleotide translocase content," *Biochemical Journal*, vol. 392, no. 2, pp.

M. ENDRES, W. NEUPERT, AND M. BRUNNER, "Transport of the ADP/ATP carrier of mitochondria from the TOM complex to the TIM22.54 complex," *EMBO Journal*, vol. 18,no. 12, pp. 3214– 3221, 1999.

MARCELLO, L. & BARRY, J. D. 2007. Analysis of the VSG gene silent archive in Trypanosoma brucei reveals that mosaic gene expression is prominent in antigenic variation and is favored by archive substructure. *Genome Res,* 17**,** 1344-52.

Moore, L., Le, T. and Fan, G. 2012. DNA Methylation and Its Basic Function. *Neuropsychopharmacology*, 38(1), pp.23-38.

MILITELLO, K., WANG, P., JAYAKAR, S., PIETRASIK, R., DUPONT, C., DODD, K., KING, A. AND VALENTI, P. 2008. African Trypanosomes Contain 5-Methylcytosine in Nuclear DNA.

MAROBBIO, C. M. T., AGRIMI, G., LASORSA, F. M. AND PALMIERI, F. (2003) Identification and functional reconstitution of yeast mitochondrial carrier for S-adenosylmethionine. *EMBO J,* 22**,** 5975-82.

MARQUET, A., BUI, B. T. AND FLORENTIN, D. MARTIN, K. L. & SMITH, T. K. 2006. The glycosylphosphatidylinositol (GPI) biosynthetic pathway of bloodstream-form *Trypanosoma brucei* is dependent on the de novo synthesis of inositol. *Mol Microbiol,* 61**,** 89-105.

MATO, J. M. AND CORRALES, F. J. (2003) Functional proteomics of non-alcoholic steatohepatitis: mitochondrial proteins as targets of S-adenosylmethionine. Proc. Natl. Acad. Sci. U.S.A. **100**, 3065–3070.

MATOVU, E., SEEBECK, T., ENYARU, J. C. & KAMINSKY, R. 2001. Drug resistance in *Trypanosoma brucei* spp., the causative agents of sleeping sickness in man and nagana in cattle. *Microbes Infect,* 3**,** 763-70.

MATTHEWS, K. R. 2005. The developmental cell biology of *Trypanosoma brucei. J Cell Sci,* 118**,** 283-90.

MATTHEWS, K. R., ELLIS, J. R. & PATEROU, A. 2004. Molecular regulation of the life cycle of African trypanosomes. *Trends Parasitol,* 20**,** 40-7.

MAYR, J. A., MERKEL, O., KOHLWEIN, S. D., GEBHARDT, B. R., BOHLES, H., FOTSCHL, U., KOCH, J., JAKSCH, M., LOCHMULLER, H., HORVATH, R., FREISINGER, P. & SPERL, W. 2007. Mitochondrial phosphate-carrier deficiency: a novel disorder of oxidative phosphorylation. *Am J Hum Genet,* 80**,** 478-84.

King, M. S., Kerr, M., Crichton, P. G., Springett, R., & Kunji, E. (2016). Formation of a cytoplasmic salt bridge network in the matrix state is a fundamental step in the transport mechanism of the mitochondrial ADP/ATP carrier. Biochimica et biophysica acta, 1857(1), 14-22.

MAYR, J. A., ZIMMERMANN, F. A., HORVATH, R., SCHNEIDER, H. C., SCHOSER, B., HOLINSKI-FEDER, E., CZERMIN, B., FREISINGER, P. & SPERL, W. 2011. Deficiency of the mitochondrial phosphate carrier presenting as myopathy and cardiomyopathy in a family with three affected children. *Neuromuscul Disord,* 21**,** 803-8.

MENDE, P., HUTHER, F. J. & KADENBACH, B. 1983. Specific and reversible activation and inactivation of the mitochondrial phosphate carrier by cardiolipin and nonionic detergents, respectively. *FEBS Lett,* 158**,** 331-4.

MICHELS, P. A., BRINGAUD, F., HERMAN, M. & HANNAERT, V. 2006. Metabolic functions of glycosomes in trypanosomatids. *Biochimica et biophysica acta,* 1763**,** 1463-77.
MICHELS, P. A., HANNAERT, V. & BRINGAUD, F. 2000. Metabolic aspects of glycosomes in trypanosomatidae - new data and views. *Parasitol Today,* 16**,** 482-9.

MILLAR, A. H. & HEAZLEWOOD, J. L. 2003. Genomic and proteomic analysis of mitochondrial carrier proteins in Arabidopsis. *Plant Physiol,* 131**,** 443-53.

MIRANDA, M. R., BOUVIER, L. A., CANEPA, G. E. & PEREIRA, C. A. 2009. Subcellular localization of *Trypanosoma cruzi* arginine kinase. *Parasitology,* 136**,** 1201-7.

MIRANDA, M. R., CANEPA, G. E., BOUVIER, L. A. & PEREIRA, C. A. 2006. *Trypanosoma cruzi:* Oxidative stress induces arginine kinase expression. *Exp Parasitol,* 114**,** 341-4.

MADEO, M., CARRISI, C., IACOPETTA, D., CAPOBIANCO, L., CAPPELLO, A. R., BUCCI, C., DOLCE, V. 2009. Abundant expression and purification of biologically active mitochondrial citrate carrier in baculovirus-infected insect cells. Journal of Bioenergetics and Biomembranes, 41(3), 289-297. doi:10.1007/s10863-009-9226-6

MIROUX, B. & WALKER, J. E. 1996. Over-production of proteins in *Escherichia coli*: mutant hosts that allow synthesis of some membrane proteins and globular proteins at high levels. *J Mol Biol,* 260**,** 289-98.

MOHLMANN, T., TJADEN, J., SCHWOPPE, C., WINKLER, H. H., KAMPFENKEL, K. & NEUHAUS, H. E. 1998. Occurrence of two plastidic ATP/ADP transporters in *Arabidopsis thaliana L.*--molecular characterisation and comparative structural analysis of similar ATP/ADP translocators from plastids and Rickettsia prowazekii. *Eur J Biochem,* 252**,** 353-9.
Morikawa, T., Yasuno, R. and Wada, H. (2001) Do mammalian cells synthesize lipoic acid? Identification of a mouse cDNA encoding a lipoic acid synthase located in mitochondria. FEBS Lett. **498**, 16–21.

Moreira D, López-García P, Vickerman K. An updated view of kinetoplastid phylogeny using environmental sequences and a closer outgroup: proposal for a new classification of the class Kinetoplastea. Int J Syst Evol Microbiol. 2004;54:1861–1875

NAPOLI, L., BORDONI, A., ZEVIANI, M., HADJIGEORGIOU, G. M., SCIACCO, M., TIRANTI, V., TERENTIOU, A., MOGGIO, M., PAPADIMITRIOU, A., SCARLATO, G. &

COMI, G. P. 2001. A novel missense adenine nucleotide translocator-1 gene mutation in a Greek adPEO family. *Neurology,* 57**,** 2295-8.

NELSON, D. R., FELIX, C. M. & SWANSON, J. M. 1998. Highly conserved charge-pair networks in the mitochondrial carrier family. *J Mol Biol,* 277**,** 285-308.

NEUFELD, D. S. & LEADER, J. P. 1998. Cold inhibition of cell volume regulation during the freezing of insect malpighian tubules. *J Exp Biol,* 201**,** 2195-204.

NIGHTINGALE, S. 1991. Drug for sleeping sickness approved. *JAMA,* 265**,** 1229. NJOGU, R. M., WHITTAKER, C. J. & HILL, G. C. 1980. Evidence for a branched electron transport chain in *Trypanosoma brucei. Mol Biochem Parasitol,* 1**,** 13-29.

NADIA LAMOU, LOI¨C RIVIE`RE, VIRGINIE COUSTOU, GRAHAM H. COOMBS, MICHAEL P. BARRETT,, 2005. Proline Metabolism in Procyclic Trypanosoma brucei Is. *Vol. 280, No. 12, Issue of March 25, pp. 11902–11910, 2005*, Vol. 280, No. 12, Issue of March 25, pp. 11902–11910, 2005, 11910.

NOGOCEKE, E., GOMMEL, D. U., KIESS, M., KALISZ, H. M. & FLOHE, L. 1997. A unique cascade of oxidoreductases catalyses trypanothione-mediated peroxide metabolism in *Crithidia fasciculata*. *Biol Chem,* 378**,** 827-36.

NGÔ, H., TSCHUDI, C., GULL, K. & ULLU, E., 1998. Double-stranded RNA induces mRNA degradation in Trypanosoma brucei. Proceedings of the National Academy of Sciences of the United States of America, 95(25), pp.14687–92.

NURY, H., DAHOUT-GONZALEZ, C., TREZEGUET, V., LAUQUIN, G. J., BRANDOLIN, G. & PEBAY-PEYROULA, E. 2006. Relations between structure and function of the mitochondrial ADP/ATP carrier. *Annu Rev Biochem,* 75**,** 713-41.

OPPERDOES, F. R. & BORST, P. 1977. Localization of nine glycolytic enzymes in a microbody-like organelle in *Trypanosoma brucei*: the glycosome. *FEBS Lett,* 80**,** 360-4.

OPPERDOES, F. R. & SZIKORA, J. P. 2006. In silico prediction of the glycosomal enzymes of *Leishmania major* and *trypanosomes. Mol Biochem Parasitol,* 147**,** 193-206.

OPPERDOES, F. R. 1984. Localization of the initial steps in alkoxyphospholipid biosynthesis in glycosomes (microbodies) of *Trypanosoma brucei*. *FEBS Lett,* 169**,** 35-9.

OPPERDOES, F. R. 1987. Compartmentation of carbohydrate metabolism in trypanosomes. *Annu Rev Microbiol,* 41**,** 127-51.

OVERATH, P. & ENGSTLER, M. 2004. Endocytosis, membrane recycling and sorting of GPI-anchored proteins: *Trypanosoma brucei* as a model system. *Mol Microbiol,* 53**,** 735-44.

OZENS, A. L., RUNSWICK, M. J. & WALKER, J. E. 1989. DNA sequences of two expressed nuclear genes for human mitochondrial ADP/ATP translocase. *J Mol Biol,* 206**,** 261-80.

PALMIERI, F. 1999. Organization and sequence of the gene for the human mitochondrial dicarboxylate carrier: evolution of the carrier family. *Biochem J,* 344 Pt 3**,** 953-60.

PALMIERI, F. 2004. The mitochondrial transporter family (SLC25): physiological and pathological implications. *Pflugers Arch,* 447**,** 689-709.

PALMIERI, F., AGRIMI, G., BLANCO, E., CASTEGNA, A., DI NOIA, M. A., IACOBAZZI, V., LASORSA, F. M., MAROBBIO, C. M., PALMIERI, L., SCARCIA, P., TODISCO, S., VOZZA, A. & WALKER, J. 2006. Identification of mitochondrial carriers in *Saccharomyces cerevisiae* by transport assay of reconstituted recombinant proteins. *Biochim Biophys Acta,* 1757**,** 1249-62.

PALMIERI, F., PIERRI, C. L., DE GRASSI, A., NUNES-NESI, A. & FERNIE, A. R. 2011. Evolution, structure and function of mitochondrial carriers: a review with new insights. *Plant J,* 66**,** 161-81.

PALMIERI, L., ARRIGONI, R., BLANCO, E., CARRARI, F., ZANOR, M. I., STUDART-GUIMARAES, C., FERNIE, A. R. & PALMIERI, F. 2006. Molecular identification of an Arabidopsis S-adenosylmethionine transporter. Analysis of organ distribution, bacterial

expression, reconstitution into liposomes, and functional characterization. *Plant Physiol,* 142**,** 855-65.

PALMIERI, L., PARDO, B., LASORSA, F. M., DEL ARCO, A., KOBAYASHI, K., IIJIMA, M., RUNSWICK, M. J., WALKER, J. E., SAHEKI, T., SATRUSTEGUI, J. & PALMIERI, F. 2001. Citrin and aralar1 are Ca(2+)-stimulated aspartate/glutamate transporters in mitochondria. *EMBO J,* 20**,** 5060-9.

PALMIERI, L., RUNSWICK, M. J., FIERMONTE, G., WALKER, J. E. & PALMIERI, F. 2000. Yeast mitochondrial carriers: bacterial expression, biochemical identification and metabolic significance. *J Bioenerg Biomembr,* 32**,** 67-77.

PANIGRAHI, A. K., OGATA, Y., ZIKOVA, A., ANUPAMA, A., DALLEY, R. A., ACESTOR, N., MYLER, P. J. & STUART, K. D. 2009. A comprehensive analysis of *Trypanosoma brucei* mitochondrial proteome. *Proteomics,* 9**,** 434-50.

PANIGRAHI, A. K., SCHNAUFER, A., ERNST, N. L., WANG, B., CARMEAN, N., SALAVATI, R. & STUART, K. 2003. Identification of novel components of *Trypanosoma brucei* editosomes. *RNA,* 9**,** 484-92.

PANIGRAHI, A. K., ZIKOVA, A., DALLEY, R. A., ACESTOR, N., OGATA, Y., ANUPAMA, A., MYLER, P. J. & STUART, K. D. 2008. Mitochondrial complexes in *Trypanosoma brucei*: a novel complex and a unique oxidoreductase complex. *Mol Cell Proteomics,* 7**,** 534-45.

PARADIES, G. & RUGGIERO, F. M. 1990. Stimulation of phosphate transport in rat-liver mitochondria by thyroid hormones. *Biochim Biophys Acta,* 1019**,** 133-6.
Parasitol, 36**,** 113-131.

PARSONS, M. 2004. Glycosomes: parasites and the divergence of peroxisomal purpose. *Mol Microbiol,* 53**,** 717-24.

PARSONS, M., FURUYA, T., PAL, S. & KESSLER, P. 2001. Biogenesis and function of peroxisomes and glycosomes. *Mol Biochem Parasitol,* 115**,** 19-28. PAYS, E., TEBABI, P., PAYS, A., COQUELET, H., REVELARD, P., SALMON, D.
PEBAY-PEYROULA, E., DAHOUT-GONZALEZ, C., KAHN, R., TREZEGUET, V., LAUQUIN, G. J. & BRANDOLIN, G. 2003. Structure of mitochondrial ADP/ATP carrier in complex with carboxyatractyloside. *Nature,* 426**,** 39-44.

PEREIRA, C. A., ALONSO, G. D., IVALDI, S., SILBER, A. M., ALVES, M. J., TORRES, H. N. & FLAWIA, M. M. 2003. Arginine kinase overexpression improves *Trypanosoma cruzi* survival capability. *FEBS Lett,* 554**,** 201-5.

PEREIRA, C. A., ALONSO, G. D., PAVETO, M. C., IRIBARREN, A., CABANAS, M. L., TORRES, H. N. & FLAWIA, M. M. 2000. *Trypanosoma cruzi* arginine kinase characterization and cloning. A novel energetic pathway in protozoan parasites. *J Biol Chem,* 275**,** 1495-501.

PEREIRA, C. A., ALONSO, G. D., TORRES, H. N. & FLAWIA, M. M. 2002. Arginine kinase: a common feature for management of energy reserves in African and American flagellated trypanosomatids. *J Eukaryot Microbiol,* 49**,** 82-5.

PEREIRA, C. A., BOUVIER, L. A., CAMARA MDE, L. & MIRANDA, M. R. 2011. Singular features of trypanosomatids' phosphotransferases involved in cell energy management. *Enzyme Res,* 2011**,** 576483.

PHELPS, A. & WOHLRAB, H. 1991. Mitochondrial phosphate transport. *The Saccharomyces cerevisiae* (threonine 43 to cysteine) mutant protein explicitly identifies transport with genomic sequence. *J Biol Chem,* 266**,** 19882-5.

PHELPS, A., SCHOBERT, C. T. & WOHLRAB, H. 1991. Cloning and characterization of the mitochondrial phosphate transport protein gene from the yeast *Saccharomyces cerevisiae*. *Biochemistry,* 30**,** 248-52.

PI, H., LEE, L. W. & LO, S. J. 2009. New insights into polycistronic transcripts in eukaryotes. *Chang Gung Med J,* 32**,** 494-8.

PICAULT, N., HODGES, M., PALMIERI, L. & PALMIERI, F. 2004. The growing family of mitochondrial carriers in *Arabidopsis*. *Trends Plant Sci,* 9**,** 138-46.
PICAULT, N., PALMIERI, L., PISANO, I., HODGES, M. & PALMIERI, F. 2002. Identification of a novel transporter for dicarboxylates and tricarboxylates in plant mitochondria. Bacterial expression, reconstitution, functional characterization, and tissue distribution. *J Biol Chem,* 277**,** 24204-11.

POLLARD, V. W., HARRIS, M. E. & HAJDUK, S. L. 1992. Native mRNA editing complexes from *Trypanosoma brucei* mitochondria. *EMBO J,* 11**,** 4429-38.

POWELL, S. J., MEDD, S. M., RUNSWICK, M. J. & WALKER, J. E. 1989. Two bovine genes for mitochondrial ADP/ATP translocase expressed differences in various tissues. *Biochemistry,* 28**,** 866-73.

Purohit, V., Gao, B., & Song, B. J. 2008. Molecular mechanisms of alcoholic fatty liver. Alcoholism, clinical and experimental research, 33(2), 191-205.

PRIOTTO, G., KASPARIAN, S., NGOUAMA, D., GHORASHIAN, S., ARNOLD, U., GHABRI, S. & KARUNAKARA, U. 2007. Nifurtimox-eflornithine combination therapy for second-stage *Trypanosoma brucei* gambiense sleeping sickness: a randomized clinical trial in Congo. *Clin Infect Dis,* 45**,** 1435-42.

PRUETT, P. S., AZZI, A., CLARK, S. A., YOUSEF, M. S., GATTIS, J. L., SOMASUNDARAM, T., ELLINGTON, W. R. & CHAPMAN, M. S. 2003. The putative catalytic bases have, at most, an accessory role in the mechanism of arginine kinase. *J Biol Chem,* 278**,** 26952-7.

R. YAO, Z. ZHANG, X. AN, B. BUCCI, D.L. PERLSTEIN, J. STUBBE, M. HUANG, Subcellular localization of yeast ribonucleotide reductase regulated by the DNA replication and damage checkpoint pathways, Proc. Natl. Acad. Sci. U. S. A. 100 (2003) 6628–6633.

RAY, D. S. 1987. Kinetoplast DNA minicircles: high-copy-number mitochondrial plasmids. *Plasmid,* 17**,** 177-90.

RIGAUD, J. L. 2002. Membrane proteins: functional and structural studies using reconstituted proteoliposomes and 2-D crystals. *Braz J Med Biol Res,* 35**,** 753-66.

RIGAUD, J. L., PITARD, B. & LEVY, D. 1995. Reconstitution of membrane proteins into liposomes: application to energy-transducing membrane proteins. *Biochim Biophys Acta,* 1231**,** 223-46.

ROBINSON, A. J. & KUNJI, E. R. 2006. Mitochondrial carriers in the cytoplasmic state have a common substrate binding site. *Proc Natl Acad Sci U S A,* 103**,** 2617-22.

RODGERS, J. 2009. Human African trypanosomiasis, chemotherapy and CNS disease. *J Neuroimmunol,* 211**,** 16-22.

ROSEMEYER, H. 2004. The chemodiversity of purine as a constituent of natural products. *Chem Biodivers,* 1**,** 361-401.

ROSANO, G.L. & CECCARELLI, E.A., 2014. Recombinant protein expression in Escherichia coli: advances and challenges. Frontiers in microbiology, 5, p.172.

RUNSWICK, M. J., POWELL, S. J., NYREN, P. & WALKER, J. E. 1987. Sequence of the bovine mitochondrial phosphate carrier protein: structural relationship to ADP/ATP translocase and the brown fat mitochondria uncoupling protein.*EMBO J,* 6**,** 1367-73.
S A, 82**,** 5695-9.

SABOVA, L., GAVURNIKOVA, G. & KOLAROV, J. 1996. Regulation of AAC isogenes encoding mitochondrial ADP/ATP translocator in the yeast *Saccharomyces cerevisiae. Folia microbiologica,* 41**,** 124-6.

SABOVA, L., ZEMAN, I., SUPEK, F. & KOLAROV, J. 1993. Transcriptional control of AAC3 gene encoding mitochondrial ADP/ATP translocator in *Saccharomyces cerevisiae* by oxygen, heme and ROX1 factor. *European journal of biochemistry / FEBS,* 213**,** 547-53.

Santamaria, E., Avila, M. A., Latasa, M. U., Rubio, A., Martin-Duce, A., Lu, S. C.,

SARASTE, M. & WALKER, J. E. 1982. Internal sequence repeats and the path of polypeptide in mitochondrial ADP/ATP translocase. *FEBS Lett,* 144**,** 250-4.

SATHER, S. & AGABIAN, N. 1985. A 5' spliced leader is added in trans to both alpha- and beta-tubulin transcripts in *Trypanosoma brucei*. *Proc Natl Acad Sci*
SCHNAUFER, A., CLARK-WALKER, G. D., STEINBERG, A. G. & STUART, K. 2005. The F1-ATP synthase complex in bloodstream stage trypanosomes has an unusual and essential function. *EMBO J,* 24**,** 4029-40.

SCHNEIDER, A. 2001. Unique aspects of mitochondrial biogenesis in trypanosomatids. *Int J Parasitol,* 31**,** 1403-15.

SCHNEIDER, A., BOUZAIDI-TIALI, N., CHANEZ, A. L. & BULLIARD, L. 2007. ATP production in isolated mitochondria of procyclic *Trypanosoma brucei. Methods Mol Biol,* 372**,** 379-87.

SCHROERS, A., KRAMER, R. & WOHLRAB, H. 1997. The reversible antiport-uniport conversion of the phosphate carrier from yeast mitochondria depends on the presence of a single cysteine. *J Biol Chem,* 272**,** 10558-64.

SEGREST, J. P., GULIK-KRZYWICKI, T. & SARDET, C. 1974. Association of the membrane-penetrating polypeptide segment of the human erythrocyte MN-glycoprotein with phospholipid bilayers. I. Formation of freeze-etch intramembranous particles. *Proc Natl Acad Sci U S A,* 71**,** 3294-8.

SEDDON, A. M., CURNOW, P. & BOOTH, P. J. 2004. Membrane proteins, lipids and detergents: not just a soap opera. Biochim Biophys Acta, 1666, 105-17.

SHABNAM, N., TRIPATHI, I., SHARMILA, P. & PARDHA-SARADHI, P., 2015. A rapid, ideal, and eco-friendlier protocol for quantifying proline. *Protoplasma*.

SHARP, P. M. & LI, W. H. 1987. The codon Adaptation Index--a measure of directional synonymous codon usage bias, and its potential applications. Nucleic Acids Res, 15, 1281-95.

Schoneck, R., Billaut-Mulot, O., Numrich, P., Ouaissi, M. A., & Krauth-Siegel, R. L. 1997. Cloning, Sequencing and Functional Expression of Dihydrolipoamide Dehydrogenase from the Human Pathogen Trypanosoma Cruzi. European Journal of Biochemistry, 243(3), 739-747. doi:10.1111/j.1432-1033.1997.00739.x

SIMARRO PP, CECCHI G, FRANCO JR, PAONE M, DIARRA A, ET AL. (2012) Estimating and mapping the population at risk of sleeping sickness. PLoS Negl Trop Dis 6: e1859

SIMPSON, L. 1973. Structure and function of kinetoplast DNA. *J Protozool,* 20**,** 2-8.

SIMPSON, L., SIMPSON, A. M., KIDANE, G., LIVINGSTON, L. & SPITHILL, T.W. 1980. The kinetoplast DNA of the hemoflagellate protozoa. *Am J Trop Med Hyg,* 29**,** 1053-63.
SMITH, T. K. & BUTIKOFER, P. 2010. Lipid metabolism in *Trypanosoma brucei.Mol Biochem Parasitol,* 172**,** 66-79.

SILVESTER E, MCWILLIAM KR, MATTHEWS KR. The Cytological Events and Molecular Control of Life Cycle Development of Trypanosoma brucei in the Mammalian Bloodstream. Pathog (Basel, Switzerland). 2017;6. pmid:28657594

SIENKIEWICZ, N., JAROSŁAWSKI, S., WYLLIE, S., & FAIRLAMB, A. H. 2008. Chemical and genetic validation of dihydrofolate reductase-thymidylate synthase as a drug target in African trypanosomes. Molecular microbiology, 69(2), 520-33.

SPINKS, D., SHANKS, E. J., CLEGHORN, L. A., MCELROY, S., JONES, D., JAMES, D., FAIRLAMB, A. H., FREARSON, J. A., WYATT, P. G. & GILBERT, I. H. 2009. Investigation of trypanothione reductase as a drug target in *Trypanosoma brucei ChemMedChem,*4**,** 2060-9.
STAPPEN, R. & KRAMER, R. 1993. Functional properties of the reconstituted phosphate carrier from bovine heart mitochondria: evidence for asymmetric orientation and characterization of three different transport modes. *Biochim Biophys Acta,* 1149**,** 40-8.

STEINERT, M. 1989. The genes and transcripts of an antigen gene expression site from T. brucei. *Cell,* 57**,** 835-45.

TURCOTTE, B., LIANG, X. B., ROBERT, F., & SOONTORNGUN, N. 2009. Transcriptional regulation of nonfermentable carbon utilization in budding yeast. FEMS yeast research, 10(1), 2-13.

STEPHENS, J. L., LEE, S. H., PAUL, K. S. & ENGLUND, P. T. 2007. Mitochondrial fatty acid synthesis in *Trypanosoma brucei*. *J Biol Chem,* 282**,** 4427-36.

STEPIEN, G., TORRONI, A., CHUNG, A. B., HODGE, J. A. & WALLACE, D. C. 1992. Differential expression of adenine nucleotide translocator isoforms in mammalian tissues and during muscle cell differentiation. *J Biol Chem,* 267**,** 14592-7.
TAIT, STEPHEN W G AND DOUGLAS R GREEN. "Mitochondria and cell signalling" *Journal of cell science* vol. 125,Pt 4 (2012): 807-15.

STEVERDING, D. 2010. The development of drugs for treatment of sleeping sickness: a historical review. *Parasit Vectors,* 3**,** 15.

STICH, A., ABEL, P. M. & KRISHNA, S. 2002. Human African trypanosomiasis.

STOCKDALE, C., SWIDERSKI, M. R., BARRY, J. D. & MCCULLOCH, R. 2008. Antigenic variation in *Trypanosoma brucei:* joining the DOTs. *PLoS Biol,* 6**,** e185.

STUART, K. 1993. The RNA editing process in Trypanosoma brucei. *Semin Cell Biol,* 4**,** 251-60.

STUART, K., BRUN, R., CROFT, S., FAIRLAMB, A., GURTLER, R.E., MCKERROW, J., REED, S. & TARLETON, R., 2008. Kinetoplastids: related protozoan pathogens, different diseases. *J Clin Invest*, 118(4), pp.1301–1310.

STURM, N. R. & SIMPSON, L. 1990. Partially edited mRNAs for cytochrome b and subunit III of cytochrome oxidase from *Leishmania tarentolae* mitochondria: RNA editing intermediates. *Cell,* 61**,** 871-8.

SULO, P. AND MARTIN, N. C. (1993) Isolation and characterization of LIP5. A lipoate biosynthetic locus of Saccharomyces cerevisiae. J. Biol. Chem. **268**, 17634–17639 23 Kang,

D., FUJIWARA, T. AND TAKESHINGE, K. (1992) Ubiquinone biosynthesis by mitochondria, sonicated mitochondria and mitoplasts of rat liver. J. Biochem. (Tokyo).

STEVERDING, D. 2010. The development of drugs for treatment of sleeping sickness: A historical review. Parasites & Vectors, 3(1), 15. doi:10.1186/1756-3305-3-15

SUTHERLAND, C. S., YUKICH, J., GOEREE, R., & TEDIOSI, F. (2015). A literature review of economic evaluations for a neglected tropical disease: human African trypanosomiasis ("sleeping sickness"). PLoS neglected tropical diseases, 9(2), e0003397. doi:10.1371/journal.pntd.0003397

SUZUKI, T., FUKUTA, H., NAGATO, H. & UMEKAWA, M. 2000. Arginine kinase from Nautilus pompilius, a living fossil. Site-directed mutagenesis studies on the role of amino acid residues in the Guanidino specificity region. *J Biol Chem,* 275**,** 23884-90.

TAKAHASHI, T., & KAKEHI, J. 2010. Polyamines: ubiquitous polycations with unique roles in growth and stress responses. Annals of botany, 105(1), 1-6.

TER KULLE, B. H. 1993. Glucose and proline transport in kinetoplastids. *Parasitol Today,* 9**,** 206-10.

THIMMAPURAM, J., DUAN, H., LIU, L. & SCHULER, M. A. 2005. Bicistronic and fused monocistronic transcripts are derived from adjacent loci in the *Arabidopsis* genome. *RNA,* 11**,** 128-38.

THOMPSON CB: Rethinking the regulation of cellular metabolism**.** *Cold Spring Harb Symp Quant Biol.* 2011; **76**: 23–9.

TIELENS, A. G. & VAN HELLEMOND, J. J. 1998. Differences in energy metabolism between trypanosomatidae. *Parasitol Today,* 14**,** 265-72.

TIWARI, B. S., BELENGHI, B. & LEVINE, A. 2002. Oxidative stress increased respiration and generation of reactive oxygen species, resulting in ATP depletion, opening of

mitochondrial permeability transition, and programmed cell death. *Plant Physiol,* 128**,** 1271-81.

TJADEN, J., HAFERKAMP, I., BOXMA, B., TIELENS, A. G., HUYNEN, M. & HACKSTEIN, J. H. 2004. A divergent ADP/ATP carrier in the hydrogenosomes of *Trichomonas gallinae* argues for an independent origin of these organelles. *Mol Microbiol,* 51**,** 1439-46.

TJADEN, J., SCHWOPPE, C., MOHLMANN, T., QUICK, P. W. & NEUHAUS, H. E. 1998. Expression of a plastidic ATP/ADP transporter gene in Escherichia coli leads to a functional adenine nucleotide transport system in the bacterial cytoplasmic membrane. *J Biol Chem,* 273**,** 9630-6.

TRABA, J., SATRUSTEGUI, J. & DEL ARCO, A. 2011. Adenine nucleotide transporters in organelles: novel genes and functions. *Cellular and molecular life sciences : CMLS,* 68**,** 1183-206.

TREZEGUET, V., PELOSI, L., LAUQUIN, G. J. & BRANDOLIN, G. 2008. The mitochondrial ADP/ATP carrier: functional and structural studies in the route of elucidating pathophysiological aspects. *J Bioenerg Biomembr,* 40**,** 435-43.

TRUMPOWER, B. L., HOUSER, R. M. AND OLSON, R. E. (1974) Studies on ubiquinone. Demonstration of the total biosynthesis of ubiquinone-9 in rat liver mitochondria. J. Biol. Chem. **249**, 3041–3048

TRINDADE, D., PEREIRA, C., CHAVES, S. R., MANON, S., CÔRTE-REAL, M., & SOUSA, M. J. 2016. VDAC regulates AAC-mediated apoptosis and cytochrome c release in yeast. Microbial cell (Graz, Austria), 3(10), 500-510. doi:10.15698/mic2016.10.533

TURRENS, J. F. 2004. Oxidative stress and antioxidant defenses: a target for the treatment of diseases caused by parasitic protozoa. *Mol Aspects Med,* 25**,** 211-20.

TYLER, K. M., MATTHEWS, K. R. & GULL, K. 1997. The bloodstream differentiation-division of *Trypanosoma brucei* studied using mitochondrial markers. *Proc Biol Sci,* 264**,** 1481-90.

UMANSKY, L., DRAWID, A., JANSEN, R., LIU, Y. ET AL. (2002) Subcellular localization of theV. Desquiret, D. Loiseau, C. Jacques, O. Douay, Y. Malthiery, P. Ritz, D. Roussel, Dinitrophenolinduced mitochondrial uncoupling in vivo triggers respiratory adaptation in HepG2 cells, Biochim. Biophys. Acta 1757 (2006) 21–30.

VAGO, A. R., MACEDO, A. M., OLIVEIRA, R. P., ANDRADE, L. O., CHIARI, E., GALVAO, L. M., REIS, D., PEREIRA, M. E., SIMPSON, A. J., TOSTES, S. & PENA, S. D. 1996. Kinetoplast DNA signatures of *Trypanosoma cruzi* strains obtained directly from infected tissues. *Am J Pathol,* 149**,** 2153-9.

VAN HELLEMOND, J. J., OPPERDOES, F. R. & TIELENS, A. G. 2005. The extraordinary mitochondrion and unusual citric acid cycle in *Trypanosoma brucei. Biochem Soc Trans,* 33**,** 967-71.

VAN WEELDEN, S. W., FAST, B., VOGT, A., VAN DER MEER, P., SAAS, J., VAN HELLEMOND, J. J., TIELENS, A. G. & BOSHART, M. 2003. Procyclic *Trypanosoma brucei* do not use Krebs cycle activity for energy generation. *J Biol Chem,* 278**,** 12854-63.

VAN LEEUWEN, F., KIEFT, R., CROSS, M. and BORST, P. (2000). Tandemly repeated DNA is a target for the partial replacement of thymine by β-d-glucosyl-hydroxymethyluracil in Trypanosoma brucei. Molecular and Biochemical Parasitology, 109(2), pp.133-145.

VAN HELLEMOND, J. J., OPPERDOES, F. R. & TIELENS, A. G. 1998. Trypanosomatidae produce acetate via a mitochondrial acetate:succinate CoA transferase. *Proc Natl Acad Sci U S A,* 95**,** 3036-41.

VAN HELLEMONDT, G. G., SONNEVELD, H., SCHREUDER, M. H., KOOIJMAN, M. A. & DE KLEUVER, M. 2005. Triple osteotomy of the pelvis for acetabular dysplasia: results at a mean follow-up of 15 years. *J Bone Joint Surg Br,* 87**,** 911-5.

VAN WILPE, S., BOUMANS, H., LOBO-HAJDU, G., GRIVELL, L. A. & BERDEN, J. A. 1999. Functional complementation analysis of yeast bc1 mutants. A study of the mitochondrial import of heterologous and hybrid proteins. *Eur J Biochem,* 264**,** 825-32.

Vander Heiden MG, Cantley LC, Thompson CB: Understanding the Warburg effect: the metabolic requirements of cell proliferation. *Science.* 2009; 324(5930): 1029–33.

VARANYUWATANA, P. & HALESTRAP, A. P. 2012. The roles of phosphate and the phosphate carrier in the mitochondrial permeability transition pore. *Mitochondrion,* 12**,** 120-5.

VASSELLA, E., STRAESSER, K. & BOSHART, M. 1997. A mitochondrion-specific dye for multicolour fluorescent imaging of *Trypanosoma brucei*. *Mol Biochem Parasitol,* 90**,** 381-5.

VICKERMAN, K. & LUCKINS, A. G. 1969. Localization of variable antigens in the surface coat of *Trypanosoma brucei* using ferritin conjugated antibody. *Nature,* 224**,** 1125-6.

VICKERMAN, K. 1985. Developmental cycles and biology of pathogenic trypanosomes. *Br Med Bull,* 41**,** 105-14.

Vickerman, K. Antigenic variation in trypanosomes. Nature 1978, 273, 613–617.

Fenn, K. Matthews, K.R. The cell biology of Trypanosomabrucei differentiation. Curr. Opin. Microbiol. 2007, 10, 539–546.

VONCKEN, F. 2006a. Characterization and developmentally regulated localization of the mitochondrial carrier protein homologue MCP6 from*Trypanosoma brucei*. *Eukaryot Cell,* 5**,** 1194-205.

WALLIMANN, T., WYSS, M., BRDICZKA, D., NICOLAY, K. & EPPENBERGER, H. M. 1992. Intracellular compartmentation, structure and function of creatine kinase isoenzymes in tissues with high and fluctuating energy demands: the'phosphocreatine circuit' for cellular energy homeostasis. *Biochem J,* 281 (Pt 1)**,** 21-40.

WEHRLE, J. P. & PEDERSEN, P. L. 1982. Characteristics of phosphate uptake by Ehrlich ascites tumor cells. *J Biol Chem,* 257**,** 9698-703.

WEHRLE, J. P. & PEDERSEN, P. L. 1982. Characteristics of phosphate uptake by Ehrlich ascites tumor cells. *J Biol Chem,* 257**,** 9698-703.

KÜHLBRANDT W. 2015. Structure and function of mitochondrial membrane protein complexes. BMC biology, 13, 89. doi:10.1186/s12915-015-0201-x

WERR, M., CRAMER, J. & ILG, T. 2009. Identification and characterization of two arginine kinases from the parasitic insect *Ctenocephalides felis*. *Insect Biochem Mol Biol,* 39**,** 634-45.

WERR, M., CRAMER, J. & ILG, T. 2009. Identification and characterization of two arginine kinases from the parasitic insect *Ctenocephalides felis*. *Insect Biochem Mol Biol,* 39**,** 634-45.

WHO. 2017. *Africantrypanosomiasis (sleeping sickness)* [Online]. Available: http://www.who.int/mediacentre/factsheets/fs259/en/index.html.

WIEMER, E. A., L, I. J., VAN ROY, J., WANDERS, R. J. & OPPERDOES, F. R. 1996. Identification of 2-enoyl coenzyme A hydratase and NADP(+)-dependent 3-hydroxyacyl-CoA dehydrogenase activity in glycosomes of procyclic *Trypanosoma brucei*. *Mol Biochem Parasitol,* 82**,** 107-11.

WIERENGA, R. K., NOBLE, M. E., VRIEND, G., NAUCHE, S. & HOL, W. G. 1991. Refined 1.83 A structure of trypanosomal triosephosphate isomerase crystallized in the presence of 2.4 M-ammonium sulphate. A comparison with the structure of the trypanosomal triosephosphate isomerase-glycerol-3-phosphate complex. *J Mol Biol,* 220**,** 995-1015.

WILLIAMS, B. A., HAFERKAMP, I. & KEELING, P. J. 2008. An ADP/ATP-specific mitochondrial carrier protein in the microsporidian *Antonospora locustae*. *J Mol Biol,* 375**,** 1249-57.

Wingfield, P. T., Palmer, I., & Liang, S. 2001. Folding and Purification of Insoluble (Inclusion Body) Proteins fromEscherichia coli. Current Protocols in Protein Science. doi:10.1002/0471140864.ps0605s78

WOHLRAB, H. & BRIGGS, C. 1994. Yeast mitochondrial phosphate transport protein expressed in *Escherichia coli.* Site-directed mutations at threonine-43 and at a similar location in the second tandem repeat (isoleucine-141). *Biochemistry,* 33**,** 9371-5.

WOHLRAB, H. 1986. Molecular aspects of inorganic phosphate transport in mitochondria. *Biochim Biophys Acta,* 853**,** 115-34.

WOHLRAB, H. 2006. The human mitochondrial transport/carrier protein family. Nonsynonymous single nucleotide polymorphisms (nsSNPs) and mutations that lead to human diseases. *Biochim Biophys Acta,* 1757**,** 1263-70.

YOUSEF, M. S., CLARK, S. A., PRUETT, P. K., SOMASUNDARAM, T., ELLINGTON, W. R. & CHAPMAN, M. S. 2003. Induced fit in guanidino kinases--comparison of substrate-free and transition state analog structures of arginine kinase. *Protein Sci,* 12**,** 103-11.

YOUSEF, M. S., FABIOLA, F., GATTIS, J. L., SOMASUNDARAM, T. & CHAPMAN, M. S. 2002. Refinement of the arginine kinase transition-state analogue complex at 1.2 A resolution: mechanistic insights. *Acta Crystallogr D Biol Crystallogr,* 58**,** 2009-17.

ZHOU, G., SOMASUNDARAM, T., BLANC, E., PARTHASARATHY, G., ELLINGTON, W. R. & CHAPMAN, M. S. 1998. Transition state structure of arginine kinase: implications for catalysis of bimolecular reactions. *Proc Natl Acad Sci U S A,* 95**,** 8449-54.

YOON, H., ZHANG, Y., PAIN, J., LYVER, E.R., LESUISSE, E., PAIN, D. & DANCIS, A., 2011. Rim2,a pyrimidine nucleotide exchanger, is needed for iron utilization in mitochondria. *Biochemical Journal*, 440(1), pp.137–146.

Appendix

Appendix 1: illustrated the different components of MEM-pros media

Ingredients	Quantities: gram/ 10L
KCl	4.0
$CaCL_2 \times 2H_2O$	2.65
$MgSO_4 \times 7H_2O$	2.0
$NaH_2PO4 \times H_2O$	1.40
NaCl	68.0
HEPES	71.40
L-CYs-Cys	0.24
L-Arg-HCl	1.26
L-His-HCl × H_2O	0.42
L-Gln	2.92
L-Lys	0.73
L-Leu	0.52
L-lle	0.52
L-Thr	0.48
L-Met	0.15
L-Phe	1.0
L-Try	0.10
L-Val	0.46
L-Tyr	1.0
L-Pro	6.0
Adenosin	0.12
Ornithin-HCl	0.10
Phenol red (pH indicuter)	0.1
MEM non-essential amino acids (Sigma)	100 ml
MEM vitamins (Sigma)	100 ml

HEPES is used to prepare a salt solution in 4L of water and NaOH is used as a buffer to maintain the pH at 7.4. In the prepared solution, solid materials were added for dissolution. The final volume is made up to 10 litters using ultra-pure water. Then the media was stored at 4 ºC in 450 ml aliquots.

A2 Protocols A3-1 SDM-79 media

	mM	MW	gram	vol. (ml)	product code
Dulbecco's modified Eagle medium (DMEM) powder	**Custom-made : pyridoxal, <u>not</u> pyridoxine**		3.50		**Gibco 23800** <u>NOT</u> 31600-083
Medium 199, Hank salt			1.00		Gibco 10012-037
Glucose□H_2O	5.5	198	0.55		Riedel de Haën 16301
HEPES	33.6	238.3	4.00		Gibco 11344-033
MOPS	23.9	209.3	2.50		Duchefa M1502
$NaHCO_3$	23.8	84.0	1.00		Sigma S-5761
Adenosine	0.037	267.2	0.005		Sigma A9251
Guanosine	0.035	283.2	0.005		Sigma G6752
D(+)-glucosamine HCl	0.23	215.6	0.025		Sigma G4875
Folic acid	0.009	441.4	0.002		Sigma F7876
p-Aminobenzoic acid	0.011	175.2	0.001		Sigma A0254
D(+)-biotin	0.82 µM	244.3	0.1 mg		Merck 124514
Amino-acids					
L-alanine	2.24	89.1	0.10		Merck 101007
L-arginine HCl	0.47	210.7	0.050		Sigma A5131
L-methionine	0.47	149.2	0.035		Sigma M9625
L-phenylalanine	0.48	165.2	0.040		Aldrich P1 700-8
L-proline	5.21	115.1	0.30		Sigma P0380
L-serine	0.57	105.1	0.030		Aldrich S260-0
Taurine	1.28	125.1	0.080		Sigma T0625
L-threonine	2.94	119.1	0.175		Sigma T8625
L-tyrosine	0.55	181.2	0.05 500		Sigma T3754

Dissolve in ca. ½ of final volume, then add following solutions:

	mM	MW gram	volume (ml)	product code
MEM amino acid solution 50X			4.0	Gibco 11130-036
MEM non-essent. AA solution 100X			3.0	Gibco 11140-035

Adjust to pH 7.3 using NaOH, adjust to final volume and stir for 2-3 h. Filter sterilise (use a 0.2 m cellulose acetate membrane-filter) and dispense in sterile flasks in usable portions (generally 5×100 ml) and store these at 4 °C. Prior to use, add to 100 ml medium the following compounds:

	mM	MW gram	volum (ml)	product code
Foetal bovine serum (□10%) 10270-106			11.1	Gibco-BRL (lot. nr. 40q2021k)
Hemin stock solution			0.22	
Penicillin/Streptomycin solution (500×)			0.22	Roche 1074440

Prepare the Hemin stock solution by dissolving 0.10 g Hemin in 40 ml NaOH, 50 mM. Stirr at least 30 minutes, filter sterilise (use a 0.2 □m cellulose acetate membrane-filter), and make aliquots of 1.1 ml in sterile eppendorfs. Store at -20 °C.

Appendix3. Illustrated the genbank associated to the different TbMCPs in this study.

Genbank (gb), EMBL (emb) or Swissprotein (sp) accession numbers for TbMCP1 were: HsapGDC, *Homo sapiens* sp_P16260; BtauGDC, *Bos taurus* sp_Q01888; ScerLEU5, *Saccharomyces cerevisiae* NP_011865; CeleGDC, *Caenorhabditis elegans* NP_492333; ScerADT1, *S. cerevisiae* emb_CAA89766; TbruAAC, *Trypanosoma brucei* gb_AAC23561; HsapADT1, *H. sapiens* sp_P12235; HsapADT2, *H. sapiens* sp_P05141; ScerMRS4, *S. cerevisiae* sp_P23500; ScerMRS3, *S. cerevisiae* sp_P10566; ScerSAM5, *S. cerevisiae* NP_014395; BtauMPCP, *B. Taurus* sp_P12234; HsapMPCP, *H. sapiens* sp_Q00325; ScerPic2, *S. cerevisiae* NP_010973; ScerMir1, *S. cerevisiae* NP_012611; HsapCMC2, *H. sapiens* sp_Q9UJS0; HsapCMC1, *H. sapiens* sp_O075746; HsapGHC1, *H. sapiens* sp_Q9H936; ScerTXTP, *S. cerevisiae* NP_014914; SpomTXTP, *Schizosaccharomyces pombe* NP_594262; RnorTXTP, *R. norvegicus* sp_P32089; HsapTXTP, *H. sapiens* sp_P53007; ScerACR1, *S. cerevisiae* sp_P33303; ScerODC1, *S. cerevisiae* NP_015191; HsapODC, *H. sapiens* sp_Q9BQT8; HsapORN1, *H. sapiens* NP_055067; HsapORT2, *H. sapiens* sp_Q9BXI2; RnorMCAT, *R. norvegicus* sp_P97521; HsapMCAT, *H. sapiens* sp_O43772; CeleDIF1, *C. elegans* sp_Q27257; NcraspARG1, *N. crassa* sp_Q01356; HsapUCP1, *H. sapiens* sp_P25874; BtauUCP1, *B. taurus* sp_P10861; RnorDIC, *R. norvegicus* NP_596909; HsapDIC, *H. sapiens* sp_Q9UBX; HsapM2OM, *H. sapiens* NP_003553; BtauM2OM, *B. taurus* sp_P22292; NtabDIC-TX, *Nicotiana tabacum* emb_CAC84545; ScerPMT, *S. cerevisiae* NP_012802; ScerGGT1, *S. cerevisiae* sp_P38988; SpomFLX, *S. cerevisiae* NP_595541; ScerFLX1, *S. cerevisiae* sp_P40464; MmusPMP34, *Mus musculus* sp_O70579; HsapPMP34, *H. sapiens* sp_O43808; XlaePMP34, *Xenopus laevis* emb_CAC21237; CboiPMP47A, *Candida boidinii* sp_P21245; HsapAPC, *H. sapiens* NP_077008; OcunMCSC, *Oryctolagus cuniculus* gb_AAB69156; HsapMCSC, *H. sapiens* NP_443133; AthaMCSC, *Arabidopsis thaliana* emb_CAB8792; ZmayBT1, *Zea mays* sp_P29518; TvagHMP31, *Trichomonas vaginalis* gb_AAF27626; MCP1, *T. brucei* Tb09.211.3200.

Genbank (gb), EMBL (emb) or Swissprotein (sp) accession numbers for TbMCP20 were TbMCP20 NP_10612510 Leishmania donovani XP_003863430.1,Danio reri NP_001025314.1, Caenorhabditis elegans NP_501552.1,Mus musculus NP_080531.2, Saccharomyces cerevisiae S288c NP_014395.3, Homo sapiens NP_775742.4, Drosophila melanogaster NP_651415.1, Glycine max chloroplastic isoform X1 XP_014618821.1 , Arabidopsis thaliana NP_001328265.1, Glycine maxchloroplastic/mitochondrial-like isoform X2 XP_006580311.1, Homo sapiens mitochondrial carrier protein isoform X1 XP_016861160.1, Arabidopsis thaliana S-adenosylmethionine carrier 2 NP_564436.4, Homo sapiens mitochondrial carrier protein isoform X2 XP_006713019.1, Mus musculus mitochondrial carrier protein isoform X4 XP_006506583.1, Homo sapiensmitochondrial carrier protein isoform X6 XP_011531630.1.

Genbank (gb), EMBL (emb) or Swissprotein (sp) accession numbers for TbMCP15 were Trypanosoma brucei MCP15 gb|AAZ12901.1; Trypanosoma cruzi mitochondrial carrier protein (putative) gb|EAN87637.1; Leishmania infantum ADP/ATP carrier-like protein emb|CAM65622.1; Leishmania major ADP/ATP carrier-like protein emb|CAJ07014.1; Leishmania braziliensis ADP/ATP carrier-like protein emb|CAM41671.1; Ajellomyces dermatitidis gb|EEQ78320.1; Tetrahymena thermophila ADP/ATP carrier protein 1 gb|EEQ78320.1; Arthroderma gypseum gb|EFQ98049.1; Zygosaccharomyces rouxii emb|CAR29621.1; Neocallimastix frontalis hydrogenosomal ATP/ADP carrier gb|AAN04660.1; Drosophila melanogaster ANT2A gb|AAF47956.1; Drosophila melanogaster ANT2B gb|AAO41648.1; Schizosaccharomyces japonicus Anc1 gb|EEB06978.1; Toxoplasma gondii gb|EEB04619.1; Bos taurus 25 member 6 sp|P32007.3; Ovis aries SLC25A6 gb|ACC93605.1; Lepeophtheirus salmonis ADP/ATP carrier protein 3 gb|ACO12488.1; Homo sapiens SLC25A5 gb|AAH68199.1; Saccharomyces cerevisiae Aac3p tpg|DAA07205.1; Arabidopsis thaliana AAC3 NP_194568.1.

Genbank (gb), EMBL (emb) or Swissprotein (sp) accession numbers for TbMCP16 were Oikopleura dioica emb|CBY13776.1; Neocallimastix frontalis gb|AAN04660.1; Drosophila melanogaster stress-sensitive B, isoform A NP_511109.1; Drosophila melanogaster stress-sensitive B, isoform B NP_727450.1; Drosophila melanogaster stress-sensitive B, isoform C NP_727448.1; Drosophila melanogaster stress sensitive B, isoform D NP_727449.1; Callithrix jacchus ADP/ATP translocase 4 XP_002745417.1; Rana rugosa dbj|BAA36507.1; Xenopus tropicalis SLC25A5 emb|CAJ82932.1; Bos taurus 25 member 31 sp|Q2YDD9.1; Ixodes scapularis gb|EEC13826.1; Talaromyces stipitatus gb|EED20116.1; Trypanosoma cruzi ADP/ATP carrier putative 1 gb|EAN90730.1; Trypanosoma cruzi ADP/ATP translocase putative 2 gb|EAN90731.1; Leishmania infantum ADP/ATP mitochondrial carrier-like emb|CAM66663.1; Leishmania major ADP/ATP mitochondrial carrier-like emb|CAJ03149.1; Leishmania braziliensis ADP/ATP mitochondrial carrier-like emb|CAM37567.1; Neurospora crassa gb|EAA33965.1; Candida dubliniensis emb|CAX41441.1; Leishmania major 1 emb|CAJ07106.1; Tetrahymena thermophila ADP/ATP carrier protein 1 gb|EAR94678.1; Lepeophtheirus salmonis ADP/ATP carrier protein 3 gb|ACO12488.1; Schistosoma japonicum emb|CAX78321.1; Arabidopsis thaliana ADP/ATP translocase-like gb|AAM65037.1

The GenBank (gb), EMBL (emb) and Swissprotein (sp) accession numbers for TbMCP23 (Tb927.5.1550) alignments were as follows: TbMCP23 (gb_AAX70434.1); T.b.gambiense, *Trypanosoma brucei gambiense* XP_011773360.1; T.congolense, *Trypanosoma congolense* emb_CCC90444.1; T.cruzi, *Trypanosoma cruzi* gb_EKG06478.1; Lpanamensis, *Leishmania panamensis* gb_AIN96737.1; L.major, *Leishmania major* emb_CAJ03236.1; Bos taurus SLC25A33, *Bos taurus* XP_010821400.1; Sus scrofa SLC25A33, *Sus scrofa* XP_003127586.4; Homo sapiens PNC1, *Homo sapiens* NP_115691.1; Ailuropoda melanoleuca SLC25A33, *Ailuropoda melanoleuca* XP_015676906.1; Mus musculus SLC25A33, *Mus musculus* NP_081736.2; Rattus norvegicus SLC25A33, *Rattus norvegicus* gb_EDL81173.1; S.cerevisiae Rim2, *Saccharomyces cerevisiae* gb_EGA76005.1; S.cerevisiae Yia6p NAD+ transporter, *Saccharomyces cerevisiae* gb_EGA86348.1; Z.mays YEL006W,

Zea mays gb_ACN33438.1; A.thaliana folate transporter, *Arabidopsis thaliana* emb_CAH65737.1; H.sapiens folate transporter, *Homo sapiens* gb_AAG37834.1; C.glabrata FAD carrier, *Candida glabrata* gb_KTA96224.1; A.nidulans folate carrier, *Aspergillus nidulans* tpe_CBF70867.1; C.immitis deoxynucleotide carrier, *Coccidioides immitis* gb_KMU78566.1; C.posadasii folate/deoxynucleotide carrier, *Coccidioides posadasii* gb_EER29041.1; M.gypseum FAD carrier, *Microsporum gypseum* XP_003171754.1; T.tonsurans folate carrier, *Trichophyton tonsurans* gb_EGD96496.1; T.rubrum folate carrier, *Trichophyton rubrum* gb_KMQ42387.1; T.errucosum folate carrier, *Trichophyton verrucosum* gb_OAL68854.1; H.sapiens PNC1, Homo sapiens NP_115691.1; H.sapiens thiamine pyrophosphate carrier, *Homo sapiens* NP_068380.3; A.thaliana ATP-Mg/Pi transporter, *Arabidopsis thaliana* emb_CAB87921.1; H.sapiens graves disease carrier protein, *Homo sapiens* NP_001311242.1; H.sapiens calcium-binding mitochondrial carrier SCaMC-3, *Homo sapiens* NP_077008.2; H.sapiens calcium-binding mitochondrial carrier protein SCaMC-1, *Homo sapiens* NP_037518.3.

Appendix 4. . Illustrated the different primers used in this study.

Primer Name	Sequence	Annealing Temp. used
MCP5EcoFor	ggcGAATTCatgacgcggataaaaagcgggaaccgg	55°C
MCP5StopBamRev	gcGGATCCttaattcgatctgcgccactccacataaatgg	68°C
MCP15EcoFor	ggcGAATTCatggttggtggcatggtgaggagc	55°C
MCP15StopBamRev	gccGGATCCttaggcagccggtaaaaaccacatatagagtac	68°C
MCP16EcoFor	ggcGAATTCatggatcacgatcaactatacgactctccc	55°C
MCP16StopBamRev	cgcGGATCCttaaacggcccagaaatggcgatgcagttccag	55°C
MCP15SForH	ggAAGCTTacatatcggtgcagtccctc	55°C
MCP15SRevXH	caCTCGAGcgcgctaaaggagatgtggagc	55°C
MCP15ASForB	caGGATCCacatatacggtgcagtccctc	55°C
MCP15ASRevXH	cgAAGCTTccctcgagggtagtcgcgagagagaacctg	68°C
MCP16SForH	ggAAGCTTaacgttactggccaccgtag	55°C
MCP16SRevXH	caCTCGAGccacgtagttcgtcactattgtg	55°C
MCP16ASForH	caggatccAAGCTTactggccaccgtag	68°C
MCP16ASRevXH	cgaagctttccCTCGAGtttcaccgtcatccttgtca	68°C
MCPExpXHFor	ggcCTCGAGgttggtggcgatggtgaggagc	55°C
MCP15ExpEcoRev	gctGAATTCtcaggcagccggtaaaaaccacatatagagtgac	68°C
MCP16ExpBamFor	ggcGGATCCgatcacgatcaactatacgactctccc	55°C
MCP16ExpEcoRev	cgcGAATTCtcaaacggcccagaaatggcgatgcagttccag	55°C
MCP15ClaFor	ggaTCGATAtggttggtggcgatggtgag	55°C
MCP15NotRev	gagcggccgctcaggcagccggtaaaaaccatatag	55°C
MCP16BamFor	gcGGATCCatggatcacgatcaactatcgactctc	55°C
MCP16NotRev	gcgcggccgctcaaacggcccagaaatggcgatg	55°C
MCP15partCForXH	cttCTCGAGagtccgtgtgatctttatgattatcgt	68°C
MCP15partNRevEco	caagaattcttcaataatcataaagatcacacggactacg	68°C
MCP16partCForBam	cttGGATCCaagtccaaaaatcctgacaaggatga	55°C
MCP16partNRevEco	caagaattcttagtcatccttgtcaggatttttggacttc	55°C
MCP20stopBamRev	ggacggaagcttatggactcgtttgtggcaggtgcggcg	55°C
MCP20StHinFor	ggacggAAGCTTatggactgtttgtggcaggtgcggcg	55°C

MCP20ASForBam	ggtGGATCCatgcagggagaaaacagtgg	55°C
MCP20SForHin	ggtAAGCTTatgcagggagaaaacagttgg	55°C
MCP20ASRevApa	gttgggcccggtacttcagtgaagtaactc	55°C
MCP20SRevApa	ctcgggcccctcacctgtccaagcataatg	55°C
NtSaANC2BamFor	gGGATCCatgtcttccaaacgcccaagt	55°C
NtScANC2ClaRev	ggatcgataatcaaaaagttagattccttctttg	55°C
MCP15ShClaFor	ggatcgatatggagtctctgaggcacccaacg	55°C
MCP15ShwoNtClaF	GTATCGATTGTGTTCAGAAGTGTTGCTTATG	55°C
MCP5woNtEcoF	ggaattcttaattggtggtgtcgctgccggtttatc	55°C
MCP15ShEcoFor	ggaattcatggagtctgaggcacccaacg	55°C
MCP15ShwoNtEcoF	ggaattcttatgtgttcagaagtgttgcttatg	55°C
MCP15StoClaRev	gatcgatttaggcagccggtaaaaaccacatatagagtg	55°C
MCP16woNtEcoF	GGAATTCTTATTGATCGTAACGTTTGCGCAG	55°C
NtScANC2EcoRev	cgaattcaatcaaaaagttagattccttctttg	55°C
NtScANC2HinFor	gcAAGCTTatgtcttccaacgcccaagt	55°C
NtScANC2stEcoFor	gagaattcatgtcttccaacgcccaagtcaaac	55°C
NtScANC2StopBamR	gaGGATCCttatttgaacttcttaccaaacaagatc	55°C
ScSAM5StaEcoFor	cgaattcatgaatacttttttctttccttgctaagtgg	68°C
ScSAM5stopBamRev	gggatccttacgctctcatttctGGATCCgttgg	68°C
MCP20staBamFor	caggatGGATCCactcgtttgtggcaggtgcggcg	55°C
MCP20StoHinRev	gcaAAGCTTttatttttcatggaaacgataacaactacaataacgac	55°C
SAM5BamFor	caggatccatgaatacttttttttctttcttgctaagaagtggcg	68°C
SAM5stopHinRev	gcaAAGCTTttacgctctcatttctccagccgttggggaaacttttcg	68°C
MCP20HinRev	gcaAAGCTTtttcatggaaacgataacaactacaataac	55°C
MCP20BamFor	caggatccGGATCCgtttgtggcaggtgcggcg	55°C
MCP23AS5B	accagaaGGATCCacctgccattgcggcttgtg	68°C
MCP23ASRevAp	catGGGCCCgttgtaaggataagagacggtg	68°C
MCP23S5H	accagAAGCTTcaacctgccattgcggcttgtg	68°C
MCP23SRevApa	catGGGCCCgttgtaaggataagagacggtg	68°C

MCP23BamFor	ggacggGGATCCaccatggcactcccgacatcgcatgt	68°C
MCP23HindRev	gcgAAGCTTttatgcgggagcgcaagaaacaacgg	68°C
MCP23qPCRFor	ccaatattgtgggtcggttc	55°C
MCP23qPCRRev	ctaccgcgacagatgtcaga	55°C
TERTqPCRFor	gagcgtgtgacttccgaagg	55°C
TERTqPCRRev	aggaactgtcacggagtttgc	55°C
MCP15qPCRFor	attcgtagtttctggcgtgg	55°C
MCP15qPCRRev	attgatgcatatgtggcggc	55°C
MCP16qPCRFor	aacgttactggcaccgtag	55°C
MCP16qPCRRev	cacagcgtcagttaaaagacc	55°C
MCP20qPCRFor	atgcagggaaaacagtgg	55°C
MCP20qPCRRev	ctgcgcaggttcctgtgttg	55°C

Appendix 5. Plasmid maps and cloning strategies

5.1 Plasmid map of pHD676

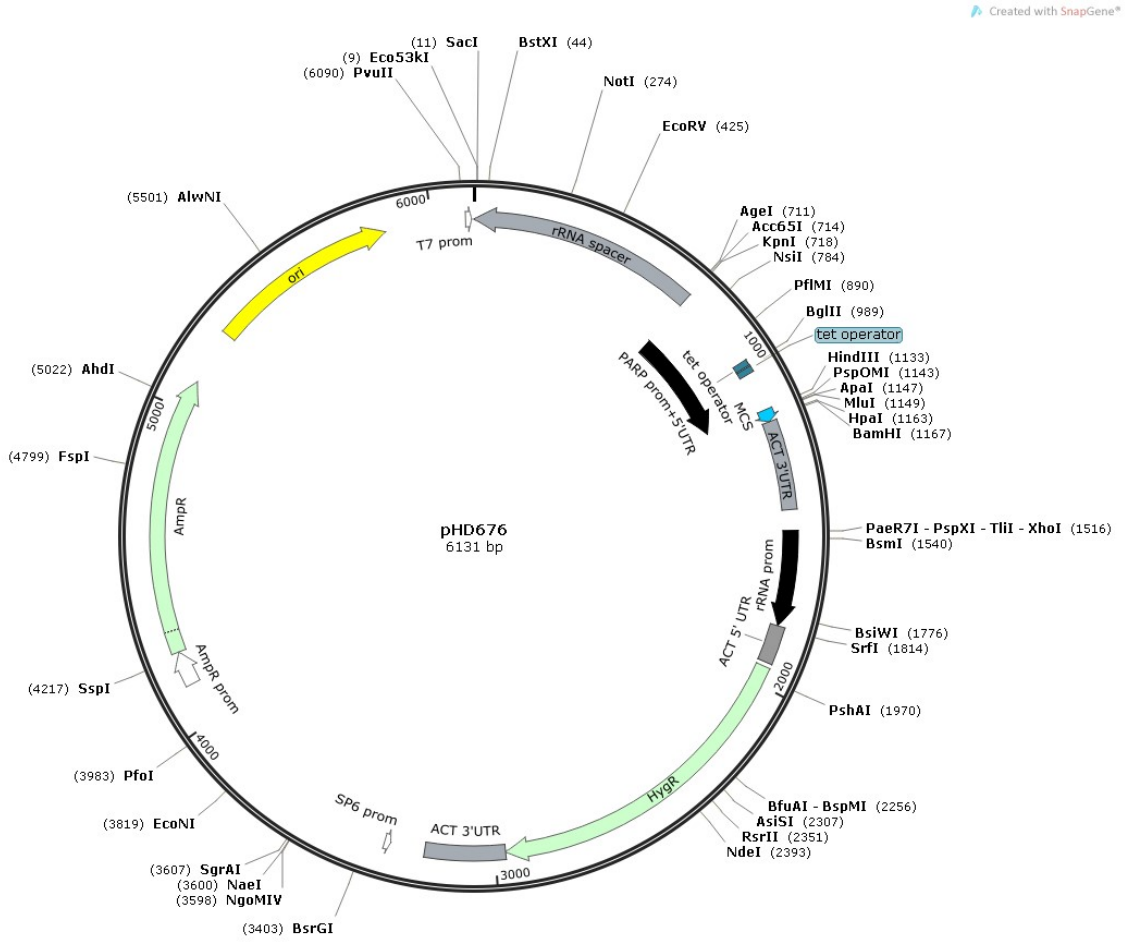

5.4 Plasmid map of pET28a

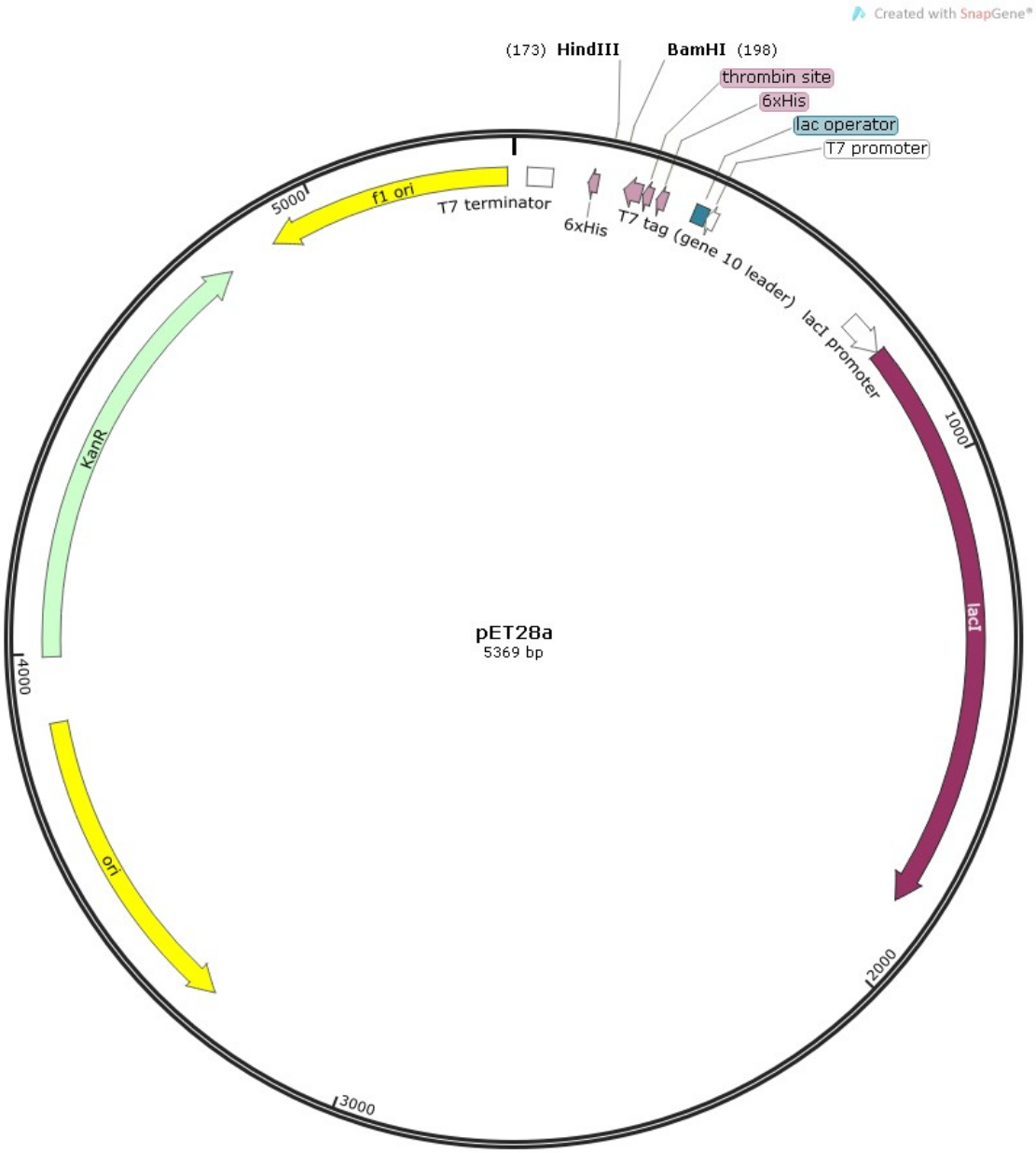

5.5 Plasmid map of pGEM-T- EASY

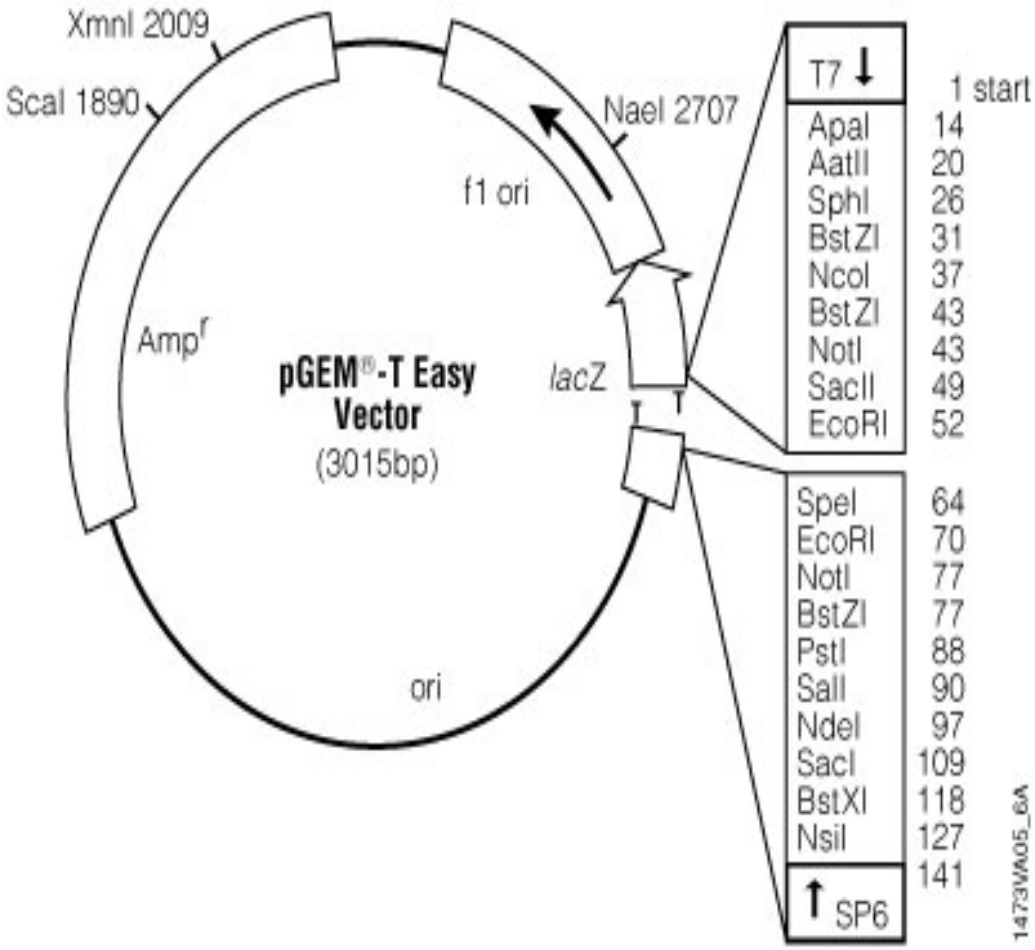

5.6 Plasmid map of pCM190

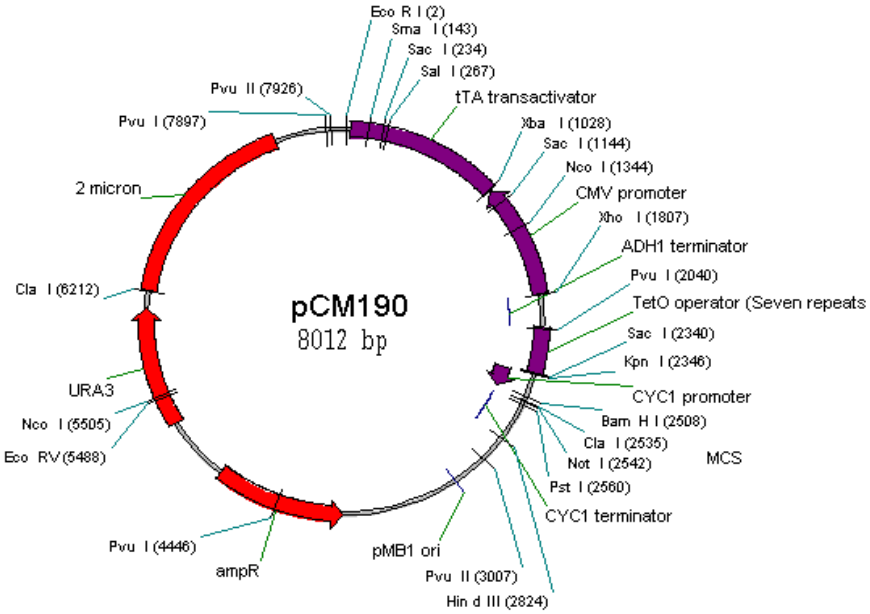

Appendix 6. ZPFM and Cytomix protocol

ZPFM (Zimmerman's Post Fusion Medium): 132 mM NaCl, 8 mM KCl, 8 mM Na_2HPO_4, 1.5 mM KH_2PO_4,1.5 mM $MgAc \cdot 4H_2O$, 90 μM $Ca(OAc)_2$; pH 7.0, filter-sterilized and stored at 4 °C.

Cytomix:

EGTA p.H. 7.6	2 mM
KCl	120 mM
$CaCl_2$	0.15 mM
[1]K_2HPO_4/KH_2PO_4 p.H 7.6	10 mM
HEPES p.H 7.6	25 mM
$MgCl_2 \cdot 6H_2O$	5 mM
Glucose (Dextrose)	0.5%
BSA	100 ug/ml
[2]Hypoxanthine	1 mM

[1] Prepare 10× K_2HPO_4/KH_2PO_4 p.H 7.6 by mixing 8.66 ml 1 M K_2HPO_4 with 1.34 ml 1 M KH_2PO_4 in 90 mls H_2O.

[2] Same 100× as for HMI-9 (13.6 mg/ml in 0.1 M NaOH).

Appendix 7. Sequences of genes related to this study

TbMCP1

MDATLHDKSTRQNTAPTCLSKAETKPSIHAAAGLLGASISTAMFYPLDALRTQMHV
CKGGDVNQLSSLRQVVRQKGLRRLYAGFAVSVTSYGIGWGAYMAVFKSVQQNLSA
YVSSNQIGGGSGSAKSGSVTAGCNVLSGCAAAITTGTVVTPLCVIRTRQQLFDGSNG
AKPQNCWQGFKAIVENEGCGALMRGMIPQILIMGNTIIQMAIYEELRHYIVEQKIQPT
SFDVALISSVSKAVASALFNPIEVVRTRLQDKRNCTSPEYRSMTVGLRTIWRTEGIRG
LYRGVWVNLCRVVPTTSVSFILYEKFLAILSHHNARRAACLPLVAD

TbMCP15

MVGGDGEEPGLQRQAKRALGDPLPLDNEMESEAPNDFSNDPSDNISVQSLQVACVQ
KCCLCTIVAPLDRIKFVMQCQKELQRTGVLDRTFRSSWHCFRCIHSIEGIRSFWRGNL
VQVGSLLPVTAAHMLLGGPMQMWVYNNFPRGFPFGHSAATYASILCGALAVSAVS
YPLEFARFRLAVDLRRSPCDLYDYRHSLAFFAQSVFSEAPHLLYAGFGLYVTGSIIYG
VMYTGLTQQVLSRLPSEPGGYTATVVQVGAGVGVSAVSTLGLHPLDTMRRRMMIA
VTMDGLRYASARHCFHHILSTEGIAGFYRGAAFTMVRMVYISSLYMWFLPAA

TbMCP16

MDHDQLYDSPQSAKDSLLDMTALLIVTFAQRAVMAPSYRVTLLATVEGELVREGRL
PPKGFGGVFGCIKRLYVKEGVRSFFRGLLTDAVLSLPATVVENISSTLVSFALQVAIPV
RLVESMNPWTYLTLSLSSTSAAVLLATPATGLHSTIVTNYVADIVAPVPSEKSKNPDK
DDGENNKEIKEGEKGGEESYRYATATEAVASIFRRWGFSGFYRCIGADAIAVFLYRG
TYYYGLQLLPSTLHNRFPYGISRCLAVVAGFLTQPFEVVSRRMQLTASSTTGRRYKG
MLHCARTIVAEEGYTALWAGMQARLLVTCVGVAVLELHRHFWAV

TbMCP20

MDSFVAGAAAGLVVDFTLYPIDTIKTRLQSRDGFRRAGGFVGVYRGLSAVAIGSVPS
GAAFFVGYDLTKRALLGEDDGQSDVTYAGRKQWQLASQATAAVVGETTASCIRVPI
EMLKQRLQAGQHRNLRSALVHITHGVTPGVATDTAPTSMRVRGIPNLLSGIPVMLLR
DVPFAVIQMLCYEALKVALHTDRRPHYLPLCGALGGATAAFITTPLDLLKTRIMLGQ
VSSPRAGRPKKLSVVCGALQELLHEVPRPTDRWGPMQRFFRGAVPRVTWISIGGSVF
FTTYEVVRRYCSCYRFHEK

TbMCP23

MALPTSHVVQTPKRQEYLASCLSGCVAGVCSTCVINPLDTVRVRLSVSRSATGKAHR
SLLYTVRDLFEGGIVHAFSRGLSANLMASLPSNGIYLPTYRCIKDQLSSAGVNQNVQP
AIAACGAVCVTNTILGPIFLVRTRVQVNEKLTVRQTFRDVLKHEGFSGFYRGTMTNI
VGRFVEEGLFWSIYELLKRLSNEASFKGSSNFFLTSVAVASLSAVAKIAATTVSYPYN
VVMNHMRSVSYVTGKPEYERIMPTIRHIYYQDGIPGFYKGLAPQLLRSTLSKAVQIYS
FELAMFIYFSTVQRPVVSCAPA